

# **Development of Sustainable Asphalt Mix Solution for use in Approach Intersection Pavements in Southern Ontario**

by

Mehran Kafi Farashah

A thesis  
presented to the University of Waterloo  
in fulfillment of the  
thesis requirement for the degree of  
Doctor of Philosophy  
in  
Civil Engineering

Waterloo, Ontario, Canada, 2023

©Mehran Kafi Farashah 2023

## **Examining Committee Membership**

The following served on the Examining Committee for this thesis. The decision of the Examining Committee is by majority vote.

### **External Examiner**

Professor Ahmed Shalaby      Civil Engineering, University of Manitoba

### **Supervisor**

Professor Susan Tighe      Civil and Environmental Engineering, University of Waterloo

### **Supervisor**

Professor Hassan Baaj      Civil and Environmental Engineering, University of Waterloo

### **Internal-external Member**

Professor Hamid Jahed      Mechanical & Mechatronics Engineering, University of Waterloo

### **Internal Member**

Professor Sina Varamini      Civil and Environmental Engineering, University of Waterloo

### **Internal Member**

Professor Vimy Henderson      Civil and Environmental Engineering, University of Waterloo

## **Author's Declaration**

I hereby declare that I am the sole author of this thesis. This is a true copy of the thesis, including any required final revisions, as accepted by my examiners.

I understand that my thesis may be made electronically available to the public.

## Abstract

Due to the continuous rise in heavy truck traffic and the impacts of climate change, York Region is facing premature pavement failure at many of its heavy truck traffic intersections, primarily in the form of deformation or rutting. This implies that the pavement materials commonly used in the York Region for heavy truck traffic volume intersections may not meet desired resilience. As a result, the York Region selected six approach intersections for examination to assess their in-service performance and determine any need for material improvement. The findings from the field investigation revealed that rutting damage was only present in the asphalt surface layer, suggesting that the pavement structures were structurally sound, and the rutting was possibly caused by inadequate asphalt mix stability. In addition, three (3) currently specified plant-produced asphalt surface mixes by York Region were investigated to evaluate their rutting resistance: HMA-SP12.5 FC1 PG64-28, HMA-SP12.5 FC1 PG70-28, and WMA-SP12.5 FC2 PG70-28. The research used HWTT, Flow Number, IDEAL-RT, and a modified Uniaxial Shear Tester. Although the WMA-SP12.5 FC2 provided the best results, the conclusion was that the current asphalt mixes are not suitable for intersections with high traffic volume due to inadequate rutting resistance. The results from both field investigation and laboratory tests on plant-produced asphalt surface mixes indicated that relying solely on volumetric design may not fully reflect the mix's performance under heavy traffic. It is advised to incorporate performance testing in the design stage for a more comprehensive understanding of the mix's rutting resistance and desired reliability.

The intent of this research was to propose a sustainable asphalt surface mix for the heavy truck traffic approach intersections in Southern Ontario, aimed at improving its resilience to rutting and cracking through performance testing. Therefore, a total of seven lab-produced asphalt surface mixes including six SMA and one EME asphalt mixes were investigated. The SMA mixes were produced by using two Nominal Maximum Aggregate Sizes (NMAS), 9.5mm and 12.5mm, and three polymer-modified asphalt binders, namely PG70-28, PG76-28, and PG82-28. The EME mix was produced with a 12.5mm NMAS and PG82-28 asphalt binder. In addition, HWTT, IDEAL-RT, Flow Number, and Dynamic Modulus tests were conducted to evaluate the shear resistance of asphalt mixes. Moreover, I-FIT and IDEAL-CT tests were applied to determine the intermediate temperature cracking resistance. While the DC(T) test was employed to evaluate the low-temperature cracking resistance. Furthermore, BPT and TSR

tests were conducted to investigate the friction and moisture susceptibility of asphalt mixes, respectively.

To establish performance specifications for evaluating the resistance of asphalt surface mixes to rutting and cracking at approach intersections with high truck volume in Southern Ontario, the results of the HWTT, IDEAL-CT, I-FIT, and DC(T) tests on seven proposed heavy-duty asphalt mixes were analyzed. The proposed preliminary specifications stated that the HWTT test should be performed at a temperature of 58°C and with 40,000 wheel-track passes. Furthermore, it was suggested that the rut depth acceptance threshold be reduced from 12.5mm to 6mm to address safety concerns at approach intersections. Based on the study data, a pre-determined threshold DC(T) fracture energy value of 900 J/m<sup>2</sup> can be used. Additionally, it was recommended that the Flexibility Index (FI) value be set at 20 and the CT Index value at 500 for the heavy-duty asphalt mixes. The overall ranking based on the results of the HWTT, I-FIT, DC(T), and IDEAL-CT tests indicated that the best performing lab-produced asphalt mix was SMA12.5-PG76-28. The results of the life cycle analysis demonstrated a substantial increase in the service life of the pavement, leading to both material and cost savings when using the SMA12.5-PG76-28 asphalt mix in comparison to a currently specified asphalt mix in the York Region.

## Acknowledgements

I would like to express my sincere gratitude to my supervisors, Professor Tighe and Professor Baaj, for their unwavering support, guidance, and their expertise through my PhD research. I would also like to thank Professor Jahed, Professor Varamini, Professor Henderson, and my external examiner, Professor Shalaby, who honored me by accepting to be part of my committee. I benefitted greatly from their guidance and feedback.

My gratitude also goes to the following individuals namely:

- The Transportation and Infrastructure Planning Director, Brian Titherington at Regional Municipality of York.
- The Transportation Asset Management team at Regional Municipality of York; especially Thomas MacPherson, Agnieszka Bevan, John Zhu, Gary Crone, Kent Hougham, Lisa Stoltz, Bryan Bingham, Nirouz AlChanaa, Tara Marshal, Vivian Yu, Goby Jeyagoby, and Connie Jia.
- The Civil and Environmental Engineering Department's technical staff: Richard Morrison, Peter Volcic, and Doug Hirst
- The McAsphalt Industries Research Centre in Toronto; especially Michael Esenwa, Anton (Tony) Kucharek, and all laboratory technicians.
- The PSI Technologies in Guelph; especially Dan Pickel and Mathias Cawthra
- The Engtec Consulting Inc.; especially Salman Bhutta, and all field technicians.
- The Miller Group; especially Justin Baxter at the Miller's Markham plant.
- Special thanks to Dr. Saied Salehi-Ashani for his time and technical guidance at the University of Waterloo
- All my friends, colleagues, and co-op students at the University of Waterloo who contributed their time and effort during my research work; especially Tyler Allan Camarda, Taher Baghaee Moghadam, Pejoochan Tavassoti, Luke Zhao, Ata Nahidi, Abdulrahman Hamid, Dandi Zho, Daniel Zhao, Frank Liu, Ali Qabur, Rob Aurilio, Basel Shoueb, Shenglin Wang, and many others whose names are not mentioned here.

Appreciation is extended to the Regional Municipality of York for financial support. Complimentary technical support and material donation from the McAsphalt Industries Ltd. and the Miller Group is greatly appreciated. Appreciation is also extended to the Norman W McLeod Chair in Sustainable Engineering at the University of Waterloo.

I would like to gratefully thank my family, particularly my parents, Mehdi and Mahnaz, and my brother Amir for their unconditional love, support, and unwavering belief in me.

Finally, I would like to thank my lovely wife Sharareh whose continuous love and support cannot go unmentioned.

## **Dedication**

To my beloved grandfathers, Akbar and Abbas, whose love is always with me – Rest in Peace.

# Table of Contents

|   |      |
|---|------|
| List of Figures.....  | xii  |
| List of Tables .....  | xvii |
| List of Abbreviations .....   | xx   |
| Chapter 1 Introduction.....   | 1    |
| 1.1. Background.....  | 1    |
| 1.2. Research Hypotheses.....   | 2    |
| 1.3. Research Objectives and Motivations .....                        | 3    |
| 1.4. Research Methodology.....  | 4    |
| 1.5. Thesis Organization.....   | 4    |
| Chapter 2 Literature Review .....                                     | 6    |
| 2.1. Asphalt Pavement.....  | 6    |
| 2.2. Pavement Deformation.....  | 7    |
| 2.2.1. Factors Affecting Pavement Deformation.....                    | 9    |
| 2.2.1.1. Asphalt Binder.....  | 9    |
| 2.2.1.2. Aggregates .....   | 10   |
| 2.2.2. External Factors Influencing Permanent Deformation.....        | 12   |
| 2.2.2.1. Temperature.....   | 12   |
| 2.2.2.2. Traffic Load.....  | 13   |
| 2.3. Fatigue and Low-Temperature Cracking.....                        | 13   |
| 2.3.1. Fatigue Cracking .....   | 13   |
| 2.3.2. Low Temperature Cracking.....                                  | 14   |
| 2.4. Asphalt Mix Design.....  | 15   |
| 2.4.1. Hveem Mix Design Method .....                                  | 16   |
| 2.4.2. Marshall Mix Design Method .....                               | 16   |
| 2.4.3. Superpave Mix Design Method.....                               | 16   |
| 2.5. Performance Tests for Evaluating Rutting in an Asphalt Mix ..... | 22   |
| 2.6. Asphalt Mix Classification .....                                 | 25   |



|           |  |    |
|-----------|--|----|
| 2.6.1.    | Dense-Graded Asphalt Mixes.....  | 25 |
| 2.6.2.    | Open-Graded Asphalt Mixes.....   | 25 |
| 2.6.3.    | Gap-Graded Asphalt Mixes.....  | 25 |
| 2.7.      | Balanced Mix-Design.....   | 27 |
| 2.8.      | Pavement Design.....   | 32 |
| 2.8.1.    | Empirical Design Methods.....  | 33 |
| 2.8.2.    | Mechanistic-Empirical Design Methods.....                                | 34 |
| 2.9.      | Summary of Challenges, Research Gaps and Opportunity for Innovation..... | 35 |
| Chapter 3 | Research Methodology and Materials.....                                  | 36 |
| 3.1.      | Design of Experiments (DOEs).....  | 37 |
| 3.2.      | Experimental Materials.....  | 42 |
| 3.2.1.    | Plant-produced Asphalt Mixes.....  | 42 |
| 3.2.2.    | Lab-produced Asphalt Mixes.....  | 42 |
| 3.3.      | Characterization of Asphalt Binders.....                                 | 45 |
| 3.4.      | Asphalt Mixture Characterization.....                                    | 45 |
| 3.4.1.    | Specimen Fabrication.....  | 45 |
| 3.4.2.    | Hamburg Wheel Tracking Test (AASHTO T324).....                           | 45 |
| 3.4.4.    | IDEAL Rutting Test (ASTM WK71466).....                                   | 47 |
| 3.4.5.    | Uniaxial Shear Tester (AASHTO T320-07).....                              | 49 |
| 3.4.6.    | Dynamic Modulus Test (AASHTO T 342).....                                 | 50 |
| 3.4.7.    | IDEAL-CT (ASTM D8225).....   | 51 |
| 3.4.8.    | Illinois Flexibility Index Test (I-FIT) Test (AASHTO TP124).....         | 53 |
| 3.4.9.    | Disk-Shaped Compact Tension DC(T)Test (ASTM D7313).....                  | 54 |
| 3.4.10.   | British Pendulum Friction Testing (ASTM E 303-93).....                   | 55 |
| 3.5.      | Preliminary Specification for performance Tests.....                     | 57 |
| 3.6.      | Life cycle Cost Assessment.....  | 57 |
| 3.7.      | Summary.....   | 58 |
| Chapter 4 | Field and Laboratory Methods of Evaluating Rutting.....                  | 59 |

|   |   |     |
|---|---|-----|
| 4.1.  | Field Investigation .....                                   | 59  |
| 4.1.1.  | Site Information.....                                       | 59  |
| 4.2.1.  | Ranking Method 1 .....                                      | 60  |
| 4.1.3.  | Ranking Method 2 .....                                      | 62  |
| 4.2.  | Performance Evaluation of Plant-Produced Asphalt Mixes..... | 63  |
| 4.2.1.  | Hamburg Wheel Tracking Test .....                           | 64  |
| 4.2.2.  | Flow Number (FN) Test .....                                 | 66  |
| 4.2.3.  | Uniaxial Shear Tester .....                                 | 67  |
| 4.2.4.  | IDEAL-RT Test.....  | 69  |
| 4.3.  | Summary and Conclusions .....                               | 70  |
| Chapter 5 Permanent Deformation Evaluation of Stone Mastic Asphalts (SMA) and High-Modulus Asphalt Mix (EME)..... |   | 72  |
| 5.1.  | Asphalt Binder Characterization Results.....                | 72  |
| 5.2.  | Asphalt Mix Characterization Results.....                   | 73  |
| 5.2.1.  | Hamburg Wheel Tracking Test Results .....                   | 73  |
| 5.2.2.  | Flow Number Test Results .....                              | 77  |
| 5.2.3.  | IDEAL-RT Test Results .....                                 | 81  |
| 5.2.4.  | Dynamic Modulus Test Results.....                           | 86  |
| 5.2.5.  | Relationship Between Test Results .....                     | 89  |
| 5.2.6.  | Asphalt Mixes Ranking .....                                 | 94  |
| 5.3.  | Summary and Conclusions .....                               | 95  |
| Chapter 6 Development of Performance-based Specifications for Heavy-Duty Asphalt Mixes in Southern Ontario .....  |   | 98  |
| 6.1.  | Asphalt Binder Characterization Results.....                | 99  |
| 6.2.  | Asphalt Mix Characterization Results.....                   | 100 |
| 6.2.1.  | Disk-Shaped Compact Tension DC(T)Test.....                  | 100 |
| 6.2.2.  | Indirect Tensile Asphalt Cracking Test (IDEAL-CT).....      | 104 |
| 6.2.3.  | Illinois Flexibility Index Test (I-FIT).....                | 106 |
| 6.2.4.  | Hamburg Wheel Tracking Test (HWTT) Results .....            | 109 |
| 6.2.5.  | British Pendulum Friction Test .....                        | 109 |

|   |     |
|---|-----|
| 6.2.6. Relationship Between Cracking Resistance Test Results .....                              | 112 |
| 6.2.7. Asphalt Mixes Ranking .....  | 115 |
| 6.2.8. Interaction Plots Between HWTT Rut Depth, DC(T) Failure Energy, CT Index,<br>and FI..... | 116 |
| 6.2.9. Predicted Life Cycle Cost Analysis.....  | 120 |
| 6.3. Summary and Conclusions .....  | 126 |
| Chapter 7 Conclusions, Recommendations, and Future research .....                               | 128 |
| 7.1. General Summary .....  | 128 |
| 7.2. Major Findings and Conclusions.....  | 129 |
| 7.3. Contributions .....  | 131 |
| 7.4. Future Research Opportunities .....  | 131 |
| Bibliography .....  | 133 |
| Appendix A .....  | 140 |

## List of Figures

|  |    |
|--|----|
| Figure 1-1: York Region Location (Kafi Farashah et al., 2021b) .....   | 2  |
| Figure 2-1: Sections Schematic Representation of Stress/Strain Distribution in a Typical Asphalt Concrete Structure (Baghaee Moghaddam, 2019)..... | 6  |
| Figure 2-2: Rutting in Approach Intersection at Heavy Truck Traffic Road in York Region 2018 .....   | 7  |
| Figure 2-3: Rutting from Weak Subgrade Left (Asphalt Institute, 2014), Rutting from Inadequate Mix Stability (Faruk et al., 2015).....             | 8  |
| Figure 2-4: Asphalt Mix Permanent Strain and Permanent Strain Rate vs. Loading Cycles (Witczak, 2002) .....  | 8  |
| Figure 2-5: Viscoelastic Behavior of Asphalt Binder (Superpave Fundamentals, 2000) .....   | 9  |
| Figure 2-6: Aggregate Stone Skeleton (Asphalt Institute, 2014) .....   | 10 |
| Figure 2-7: Effect of Aggregate and Mortar on the Failure Behaviour of Asphalt Mixtures (Hafeez, 2009) .....                                       | 12 |
| Figure 2-8: Fatigue (Alligator) Cracking – York Region 2018.....   | 14 |
| Figure 2-9: Low-Temperature Cracking - York Region 2018 .....  | 14 |
| Figure 2-10: Asphalt Binder Performance Grade Selection for Different Reliabilities (Asphalt Institute, 2008).....                                 | 18 |
| Figure 2-11: Superpave Grade-Bumping Chart (NRC, 2003).....  | 18 |
| Figure 2-12: Schematic View of Binder Tests Set up (Superpave Fundamentals, 2000) .....  | 19 |
| Figure 2-13: Dynamic Shear Rheometer (DSR) Equipment.....  | 20 |
| Figure 2-14: Superpave Gyrotory Compactor (SGC) (Baghaee Moghaddam, 2019) .....  | 21 |
| Figure 2-15: A Graphic Representation of SMA (Left) and Dense-Graded Asphalt Mix (Right) (NAPA, 2002) .....  | 26 |
| Figure 2-16: Schematic Illustration of Three BMD Approaches (NCHRP, 2016) .....  | 28 |
| Figure 2-17: Principle of Empirical Pavement Design (Dore & Zubeck, 2009).....   | 33 |
| Figure 2-18: Principle of Mechanistic-Empirical Pavement Design (Dore & Zubeck, 2009).....   | 34 |

|   |    |
|---|----|
| Figure 3-1: Research Plan Methodology .....   | 41 |
| Figure 3-2: Laboratory Procedure for SMA and EME Asphalt Mixes Production in CPATT<br>Laboratory .....  | 44 |
| Figure 3-3: Hamburg Wheel Track Device Setup (left) and Test Specimens Before and After<br>(Right).....   | 46 |
| Figure 3-4: Typical Results from Hamburg Wheel Tracking Test (NCHRP, 2011).....   | 46 |
| Figure 3-5: Flow Number Test Specimens Before (Left) and After (Right).....   | 47 |
| Figure 3-6: IDEAL-RT Test Fixture with Test Specimen Before (Left) and After Test (Right)<br>.....  | 48 |
| Figure 3-7: Uniaxial Shear Tester (Top Right), Hollow Cylindrical Specimen (Bottom Right),<br>and Uniaxial Shear Tester Setup (Left) (Zak et al., 2017) ..... | 49 |
| Figure 3-8: Uniaxial Shear Tester Monotonic Setup, and Test Specimens Before and After<br>Testing .....   | 50 |
| Figure 3-9: Specimen Preparation (a) and (b) and Specimen Test Setup (c) .....  | 51 |
| Figure 3-10: IDEAL-CT Test Loading Fixture .....  | 52 |
| Figure 3-11: IDEAL-CT Load-Displacement Curve and Test Parameter (Chen et al., 2021).53   |    |
| Figure 3-12: Specimen Preparation for I-FIT Test.....   | 54 |
| Figure 3-13: I-FIT Test Loading Fixture (Left) After Test (Right).....  | 54 |
| Figure 3-14: DC(T) Test Loading Fixture (Left) After Test (Right).....  | 55 |
| Figure 3-15: British Pendulum Skid Resistance Tester Fixture (Left) Rubber Slider (Right).56  |    |
| Figure 3-16: Indirect Tensile Strength Testing Equipment.....   | 57 |
| Figure 3-17: Conceptual Framework of Pavement Management (TAC, 2014).....   | 58 |
| Figure 4-1: Hamburg Wheel Tracking Test Results for Plant-Produced Asphalt Mixes.....   | 65 |
| Figure 4-2: Flow Number Test Results @ 58°C Testing Temperature .....   | 67 |
| Figure 4-3: Uniaxial Shear Tester Results at 50°C Testing Temperature .....   | 68 |
| Figure 4-4: Uniaxial Shear Tester Results at 58°C Testing Temperature .....   | 68 |

|   |    |
|---|----|
| Figure 4-5: IDEAL-RT Test Results .....   | 69 |
| Figure 5-1: HWTT Test Results @ 44°C .....  | 75 |
| Figure 5-2: HWTT Test Results @ 50°C .....  | 75 |
| Figure 5-3: HWTT Test Results @ 58°C .....  | 76 |
| Figure 5-4: HWTT Test Results for All Temperatures .....  | 77 |
| Figure 5-5: Flow Number Test Results for All Testing Temperatures .....                                 | 78 |
| Figure 5-6: Main Effects Plots for FN Test for SMA Mixes .....  | 80 |
| Figure 5-7: IDEAL-RT Index Results at Three Testing Temperatures.....                                   | 82 |
| Figure 5-8: Main Effects Plots for IDEAL-RT Index for SMA Mixes .....                                   | 83 |
| Figure 5-9: Dynamic Modulus Results at -10°C Testing Temperature.....                                   | 86 |
| Figure 5-10: Dynamic Modulus Results at 4°C Testing Temperature .....                                   | 86 |
| Figure 5-11: Dynamic Modulus Results at 21.1°C Testing Temperature .....                                | 87 |
| Figure 5-12: Dynamic Modulus Results at 37.8°C Testing Temperature .....                                | 87 |
| Figure 5-13: Dynamic Modulus Results at 54.4°C Testing Temperature .....                                | 88 |
| Figure 5-14: Master Curve Results for All Asphalt Mixes .....   | 89 |
| Figure 5-15: Low Frequency Zone Master Curve Results for All Asphalt Mixes .....                        | 89 |
| Figure 5-16: Flow Number at 50°C vs. Dynamic Modulus  E*  at 54.4°C at 1Hz for Group A<br>.....         | 91 |
| Figure 5-17: IDEAL-RT Index at 50°C vs. Dynamic Modulus  E*  at 54.4°C at 1Hz for Group<br>A .....      | 91 |
| Figure 5-18: HWTT at 20,000 pass at 50°C vs. Dynamic Modulus  E*  at 54.4°C at 1Hz for<br>Group A ..... | 91 |
| Figure 5-19: FN at 50°C vs. IDEAL-RT Index at 50°C for Group A .....                                    | 92 |
| Figure 5-20: FN at 50°C vs. HWTT at 20,000 pass at 50°C for Group A .....                               | 92 |
| Figure 5-21: IDEAL-RT Index at 50°C vs. HWTT at 20,000 pass at 50°C for Group A.....                    | 92 |

|  |     |
|--|-----|
| Figure 6-1: DC(T) Fracture Energy Results at -18°C Testing Temperatures .....  | 101 |
| Figure 6-2: Main Effects Plots for Average DC(T) Fracture Energy for SMA Mixes .....   | 102 |
| Figure 6-3: Average CT Index Results at 25°C Testing Temperatures.....   | 104 |
| Figure 6-4: Main Effects Plots for Average CT Index for SMA Mixes.....   | 105 |
| Figure 6-5: Average FI Results at 25°C Testing Temperatures .....  | 107 |
| Figure 6-6: Main Effects Plots for Average FI for SMA Mixes .....  | 108 |
| Figure 6-7: Average BPN Results at Various Testing Temperatures in Dry Condition .....   | 110 |
| Figure 6-8: Average BPN Results at Various Testing Temperatures in Wet Condition.....  | 111 |
| Figure 6-9: Main Effects Plots for BPN Values for SMA Mixes.....   | 112 |
| Figure 6-10: FI vs. CT Index for Group A .....   | 113 |
| Figure 6-11: FI vs. CT Index for Group B .....   | 113 |
| Figure 6-12: DC(T) Fracture Energy vs. CT Index for Group A .....  | 114 |
| Figure 6-13: DC(T) Fracture Energy vs. CT Index for Group B .....  | 114 |
| Figure 6-14: DC(T) Fracture Energy vs. FI for Group A.....   | 114 |
| Figure 6-15: DC(T) Fracture Energy vs. FI for Group B.....   | 115 |
| Figure 6-16: Performance Space Diagram of DC(T) Fracture Energy vs. Rut Depth with<br>Preliminary Threshold Criteria.....                  | 118 |
| Figure 6-17: Performance Space Diagram of FI vs. Rut Depth with Preliminary Threshold<br>Criteria.....                                     | 118 |
| Figure 6-18: Performance Space Diagram of IDEAL-CT vs. Rut Depth with Preliminary<br>Threshold Criteria.....                               | 119 |
| Figure 6-19: Results for SP12.5 FC2-PG70-28 for both a) Average FI and b) Average DC(T)<br>Fracture Energy .....                           | 120 |
| Figure 6-20: Deterioration Curves for SP12.5 FC2-PG70-28 and SMA 12.5-PG76-28 Asphalt<br>Mixes with No Life Cycle Treatment.....           | 122 |
| Figure 6-21: Deterioration Curves for SP12.5 FC2-PG70-28 Asphalt Mix (No Life Cycle<br>Treatment vs. Including Life Cycle Treatment) ..... | 123 |

Figure 6-22: Deterioration Curves for SMA 12.5-PG76-28 Asphalt Mix (No Life Cycle Treatment vs. Including Life Cycle Treatment) ..... 123



## List of Tables

|   |    |
|---|----|
| Table 2-1: Asphalt Mix Design Methods Practiced in Some Countries (Grobler et al., 2018).   | 15 |
| Table 2-2: Aggregate Consensus Property Requirements (Asphalt Institute, 2014).....   | 21 |
| Table 2-3: Recommended Superpave Source Property Tests and Typical Requirements<br>(Asphalt Institute, 2014).....   | 21 |
| Table 2-4: An Overview of Asphalt Mixture Performance Tests for Rutting Resistance<br>Evaluation (NCHRP 20-07/Task 406, 2018), (EvothermWMA, 2020), (Aschenbreber,<br>1992), (Brosseaud et al., 1993), (Kafi Farashah et al., 2021c)..... | 23 |
| Table 2-5: Performance Specifications Set up by Some DOTs for Quality Assurance and<br>BMD Activities .....   | 29 |
| Table 3-1: DOE used for Plant-Produced Mixes to Determine Rutting Resistance.....   | 37 |
| Table 3-2: DOE used for Plant-Produced Mixes to Determine Intermediate Temperature<br>Cracking Resistance .....   | 38 |
| Table 3-3: DOE used for Plant-Produced Mixes to Determine Low Temperature Cracking<br>Resistance .....  | 38 |
| Table 3-4: DOE used for Lab-Produced Mixes to Determine Rutting Resistance.....   | 38 |
| Table 3-5: DOE used for Lab-Produced Mixes to Determine Intermediate Temperature<br>Cracking Resistance .....   | 39 |
| Table 3-6: DOE used to Determine the Dynamic Modulus Values of Lab-Produced Mixes ..  | 39 |
| Table 3-7: DOE used for Lab-Produced Mixes to Determine Low Temperature Cracking<br>Resistance .....  | 39 |
| Table 3-9: DOE used to Determine Surface Frictional Property of Lab-Produced Mixes .....  | 40 |
| Table 3-8: DOE used to Determine Moisture Susceptibility of Lab-Produced Mixes using<br>TSR Test.....   | 40 |
| Table 3-10: Properties of Coarse and Fine Aggregates.....   | 42 |
| Table 3-11: Physical Properties of Lab-Produced Asphalt Surface Mixes .....   | 43 |
| Table 4-1: Site Location Information .....  | 60 |
| Table 4-2: Method 1 - Ranking Score .....   | 61 |

|   |    |
|---|----|
| Table 4-3: Method 1 - Total Ranking Score.....  | 62 |
| Table 4-4: Rate of Rutting at Test Sites .....  | 62 |
| Table 4-5: Physical Properties of Plant-Produced Asphalt Surface Mix .....  | 64 |
| Table 4-6: Hamburg Wheel Tracking Test Results for Plant-Produced Asphalt Mixes .....   | 66 |
| Table 4-7: Uniaxial Shear Test Results .....  | 69 |
| Table 4-8: IDEAL-RT Test Results .....  | 70 |
| Table 5-1: Asphalt Binder Properties at High Testing Temperatures .....   | 73 |
| Table 5-2: Summarized Analysis of Variance (ANOVA) for FN test for SMA Mixes.....   | 79 |
| Table 5-3: Statistical Analysis for FN Test (EME vs. SMA mixes) .....   | 80 |
| Table 5-4: Summarized Analysis of Tukey’s HSD Ranking Based on Average FN at 44°C<br>Testing Temperature.....   | 81 |
| Table 5-5: Summarized Analysis of Tukey’s HSD Ranking Based on Average FN at 50°C<br>Testing Temperature.....   | 81 |
| Table 5-6: Summarized Analysis of Tukey’s HSD Ranking Based on Average FN at 58°C<br>Testing Temperature.....   | 81 |
| Table 5-7: Summarized Analysis of Variance (ANOVA) for IDEAL-RT Index for SMA<br>Mixes .....  | 83 |
| Table 5-8: Statistical Analysis for IDEAL-RT Index (EME vs. SMA mixes).....   | 84 |
| Table 5-9: Summarized Analysis of Tukey’s HSD Ranking Based on Average IDEAL-RT<br>Index at 44°C Testing Temperature .....  | 85 |
| Table 5-10: Summarized Analysis of Tukey’s HSD Ranking Based on Average IDEAL-RT<br>Index at 50°C Testing Temperature .....   | 85 |
| Table 5-11: Summarized Analysis of Tukey’s HSD Ranking Based on Average IDEAL-RT<br>Index at 58°C Testing Temperature .....   | 85 |
| Table 5-12: Correlation Summary Between FN, IDEAL-RT Index, HWTT, and Dynamic<br>Modulus (54.4°C@ 1Hz and 0.1Hz) for Both Groups A and B at 50°C and 58°C<br>Testing Temperatures ..... | 93 |
| Table 5-13: Rankings of Asphalt Mixes’ Rutting Resistance Based on HWTT, FN, and<br>IDEAL-RT Tests at 58°C Testing Temperature.....   | 95 |

|  |     |
|--|-----|
| Table 6-1: Asphalt Binder Properties .....   | 100 |
| Table 6-2: Summarized Analysis of Variance (ANOVA) for DC(T) Fracture Energy for SMA Mixes .....                                     | 102 |
| Table 6-3: Statistical Analysis for Average DC(T) Fracture Energy for PG Asphalt Binder  | 103 |
| Table 6-4: Statistical Analysis for Average DC(T) Fracture Energy (EME vs. SMA mixes)  | 103 |
| Table 6-5: Summarized Analysis of Tukey’s HSD Ranking Based on Average DC(T) Fracture Energy.....                                    | 103 |
| Table 6-6: Summarized Analysis of Variance (ANOVA) for CT Index for SMA Mixes .....  | 105 |
| Table 6-7: Statistical Analysis for CT Index (EME vs. SMA mixes) .....   | 106 |
| Table 6-8: Summarized Analysis of Tukey’s HSD Ranking Based on Average CT-Index ..   | 106 |
| Table 6-9: Summarized Analysis of Variance (ANOVA) for FI for SMA Mixes.....   | 108 |
| Table 6-10: Statistical Analysis for FI Index (EME vs. SMA mixes).....   | 108 |
| Table 6-11: Summarized Analysis of Tukey’s HSD Ranking Based on Average FI .....   | 109 |
| Table 6-12: Summarized Analysis of Variance (ANOVA) for BPN for SMA Mixes.....   | 112 |
| Table 6-13: Rankings of Asphalt Mixes’ Cracking and Rutting Resistance Based on HWTT, IDEAL-CT, I-FIT, and DC(T) Tests .....         | 116 |
| Table 6-14: Performance Comparison SMA12.5-PG76-28 vs. SP12.5FC2-PG70-28 .....   | 121 |
| Table 6-15: Typical Life Cycle Activities for Heavy Traffic Volume Roads in York Region .....  | 122 |
| Table 6-16: Life Cycle Net Present Worth for Maintaining Heavy Traffic Roads with SMA 12.5-PG76-28 Asphalt Mix Surface Course.....   | 125 |
| Table 6-17: Life Cycle Net Present Worth for Maintaining Heavy Traffic Roads with SP12.5 FC2-PG70-28 Asphalt Mix Surface Course..... | 125 |

## List of Abbreviations

|                 |  |
|-----------------|--|
| AASHTO          | American Association of State Highway and Transportation Officials |
| AI              | Asphalt Institute  |
| ALF             | Accelerated Loading Facility                                       |
| ANOVA           | Analysis of Variance   |
| APA             | Asphalt Pavement Analyzer  |
| ASTM            | American Society for Testing and Materials                         |
| BMD             | Balance-Mix Design   |
| BPN             | British Pendulum Number  |
| BPT             | British Pendulum Tester  |
| CA              | Coarse Aggregates  |
| CMA             | Cold Mix Asphalt   |
| CMOD            | Crack Mouth Opening Displacement                                   |
| COV             | Coefficient of Variation   |
| CPATT           | Centre for Pavement and Transportation Technology                  |
| CT Index        | Cracking Tolerance Index   |
| DC(T)           | Disc-Shaped Compact Tension Test                                   |
| DOE             | Design of Experiment   |
| DOT             | Department of Transportation                                       |
| DSM             | Designated Sources for Materials                                   |
| DSR             | Dynamic Shear Rheometer  |
| E*              | Complex Modulus  |
| EME             | Enrobé à Module Élevé  |
| ESALs           | Equivalent Single Axle Loads                                       |
| FA              | Fine Aggregates  |
| FC              | Friction Course  |
| FE              | Fracture Energy  |
| FI              | Flexibility Index  |
| FN              | Flow Number  |
| G*              | Complex Shear Modulus  |
| G <sub>mb</sub> | Bulk Specific Gravity  |
| G <sub>mm</sub> | Theoretical Maximum Specific Gravity                               |
| GPR             | Ground Penetration Radar   |
| HMA             | Hot Mix Asphalt  |
| HWTT            | Hamburg Wheel-Tracking Test  |
| IDEAL-CT        | Indirect Tensile Asphalt Cracking Test                             |
| IDEAL-RT        | IDEAL Rutting Test   |
| IDT             | Indirect Tensile Strength  |
| I-FIT           | Illinois Flexibility Index Test                                    |
| J <sub>nr</sub> | Non-Recoverable Creep Compliance                                   |
| LVDT            | Low Voltage Displacement Transducer                                |
| MEPDG           | Mechanistic-Empirical Pavement Design Guide                        |
| MSCR            | Multiple Stress Creep Recovery                                     |
| MTO             | Ministry of Transportation Ontario                                 |

|             |   |
|-------------|---|
| NAPA        | National Asphalt Pavement Association             |
| NCHRP       | National Cooperative Highway Research Program     |
| $N_{des}$   | Design Number of Gyration                         |
| $N_{ini}$   | Initial Number of Gyration                        |
| NPV         | Net Present Worth                                 |
| NMAS        | Nominal Maximum Aggregate Size                    |
| $N_{max}$   | Maximum Number of Gyration                        |
| OPSS        | Ontario Provincial Standard Specification         |
| PAV         | Pressure Aging Vessel                             |
| PCI         | Pavement Condition Index                          |
| PG          | Performance Grading                               |
| RAP         | Reclaimed Asphalt Pavement                        |
| RAS         | Recycled Asphalt Shingles                         |
| $R_e$       | Percent Recovery                                  |
| RSCH        | Repeated Shear at Constant Height                 |
| RTFO        | Rolling Thin Film Oven                            |
| RT-Index    | Rutting Tolerance Index                           |
| RV          | Rotational Viscometer                             |
| SGC         | Superpave Gyrotory Compactor                      |
| SIP         | Stripping Inflection Point                        |
| SHRP        | Strategic Highway Research Program                |
| SMA         | Stone Mastic (Matrix) Asphalt                     |
| SP          | Superpave   |
| TAC         | Transportation Association of Canada              |
| TSR         | Tensile Strength Ratio                            |
| UST         | Uniaxial Shear Tester                             |
| $V_a$       | Air Voids   |
| VCA         | Voids in Coarse Aggregate                         |
| $VCA_{DRC}$ | Voids in Coarse Aggregate in Dry-Rodded Condition |
| VFA         | Voids Filled with Asphalt                         |
| VMA         | Voids in Mineral Aggregate                        |
| WMA         | Warm Mix Asphalt                                  |

# Chapter 1 Introduction

## 1.1. Background

The Transportation Association of Canada states that 90% of all goods and services in Canada are transported by truck over a vast and diverse landscape with challenging conditions (TAC, 2013). As a result, transportation agencies have a crucial role in ensuring that roads are designed to perform optimally during their service life while prioritizing user safety. In addition, it is crucial for transportation agencies to use pavement materials that are both cost-effective and environmentally sustainable. It is also essential to consider the impact of future population growth, which will increase traffic volume and loading, and the effects of climate change when designing pavement materials.

The increase in traffic volume, particularly the rise in heavy trucks with high axle loads and harsh environmental conditions, is a major challenge for transportation agencies in Southern Ontario. This can significantly reduce the pavement's expected service life. *"Human influence has driven Canada's warming climate and it will continue to warm in the future"* (Canada, 2019). Therefore, it is imperative to adopt innovative pavement designs to improve pavement performance and address these challenges in Southern Ontario.

When designing a road, a standard pavement design is typically applied to the entire road segment. However, areas such as approach intersections, turning lanes, and bus stops face unique loading scenarios, making them more susceptible to pavement failure such as permanent deformation or rutting. These areas are affected by the high shear stresses generated by vehicle turning, stopping, accelerating, and slow traffic movement (NCAT, 1998). As a result, approach intersections require more frequent maintenance, which is both costly and time-consuming.

The use of thicker asphalt layers to resolve pavement permanent deformation is an expensive solution for government agencies and taxpayers. Thus, this research aimed to explore cost-effective and sustainable asphalt surface mixes using local aggregates for use in heavy truck traffic intersections in Southern Ontario.

The Regional Municipality of York (York Region) is recognized as a large and rapidly growing municipality in Canada. It is the third largest in Ontario and the seventh largest in Canada. Located in the Greater Toronto Area, York Region covers approximately 1,776 km<sup>2</sup> and comprises nine local municipalities. York Region is bounded to the south by the City of Toronto, to the east by

the Region of Durham, to the west by the Region of Peel, and to the north by Simcoe County and Lake Simcoe, as shown in Figure 1-1 (Kafi Farashah et al., 2021b).



Figure 1-1: York Region Location (Kafi Farashah et al., 2021b)

York Region serves over 1.2 million residents and 52,000 businesses across nine cities and towns. Its population is projected to reach 1.8 million by 2051. The 2019 Transportation State of Infrastructure Report Card shows that the majority of York Region's transportation assets are in good condition (Kafi Farashah et al., 2021b). However, due to aging and the region's population growth, York Region needs to invest over \$1.1 billion in the next 20 years to maintain its roads infrastructure (Kafi Farashah et al., 2021b). With the growing population and increased number of vehicles, including trucks, and changing temperature patterns, York Region is facing premature pavement failure, such as rutting, at its high truck traffic approach intersections (Kafi Farashah et al., 2021b). It was evident that the conventional asphalt surface mixes used for these intersections are not able to meet their expected design service life (Kafi Farashah et al., 2021b). Hence, this research aims to propose a sustainable asphalt surface mix for use in high truck traffic volume approach intersections in Southern Ontario to address the rutting issue. The research involves collaboration with the Centre for Pavement and Transportation Technology (CPATT) at the University of Waterloo and the York Region.

## 1.2. Research Hypotheses

The main hypotheses for this research are as follows:

- Only adjustment to asphalt binder performance grading (PG) or “grade-bumping” may enhance the rutting resistance of asphalt mixes without compromising other properties of asphalt mixes such as fatigue and low-temperature cracking.
- Only adjustment to aggregate gradation may enhance the rutting resistivity asphalt mixes without compromising other properties of asphalt mixes such as fatigue and low-temperature cracking.
- Combination of change in both asphalt binder performance grading and aggregate gradation may enhance the rutting resistance of asphalt mixes without compromising other properties of asphalt mixes such as fatigue and low-temperature cracking.

### **1.3. Research Objectives and Motivations**

It is evident that the conventional asphalt surface mixes and volumetric-based mix design approach have not provided sufficient performance for heavy truck volume approach intersections in York Region, a fast-growing municipality in Canada. This research aims to explore asphalt surface mixes that can produce durable surface layers through a balanced mix design and performance testing, resulting in the creation of rutting and cracking resistant mixes for specific traffic and climatic conditions. The overall objectives of this research are:

- 1) To propose a sustainable asphalt surface mix for heavy truck traffic approach intersections in Southern Ontario, with the aim of improving its resilience to rutting and cracking through performance testing.
- 2) To identify appropriate and practical asphalt surface mix performance tests for use in quality assurance and quality control activities, with the aim of evaluating the rutting and cracking resistance of asphalt mixes in heavy truck traffic approach intersections in Southern Ontario.
- 3) To implement performance specifications for evaluating the rutting and cracking resistance of asphalt surface mixes used in heavy truck traffic approach intersections in Southern Ontario.
- 4) To predict the service life and associated life cycle costs of the proposed asphalt surface mix for use in heavy truck traffic approach intersections in Southern Ontario.



## **1.4. Research Methodology**

The objectives of this thesis are achieved through a field inspection and laboratory testing on both plant-produced and lab-produced asphalt surface course mixes. Laboratory asphalt binder and asphalt mix performance testing were conducted at the Centre for Pavement and Transportation Technology (CPATT) located at the University of Waterloo and at the laboratory of McAsphalt Industries in Toronto. Also, material donation was provided by McAsphalt Industries and Miller Paving in Toronto. Chapter three of this thesis provides more details on the research methodology.

## **1.5. Thesis Organization**

This thesis is organized into seven chapters as follows:

**Chapter 1: Introduction** – This chapter provides the scope and overall objectives of this research project.

**Chapter 2: Literature Review** – This chapter summarizes the asphalt mix design, factors effecting permanent deformation, performance testing to evaluate rutting, overview of balanced mix design, and performance specifications.

**Chapter 3: Research Methodology and Materials** – This chapter explains methodology employed to evaluate both plant-produced and lab-produced asphalt mixes which includes material characteristics, sample fabrication, and asphalt performance testing,

**Chapter 4: Field and Laboratory Methods of Evaluating Rutting** – This chapter summarizes the field evaluation and rutting resistance evaluation of three plant-produced asphalt surface mixes from York Region.

**Chapter 5: Permanent Deformation Evaluation of Stone Mastic Asphalts (SMA) and High-Modulus Asphalt Mix (EME)** – This chapter involves rutting resistance evaluation of the seven lab-produced asphalt surface mixes by means of rutting resistance performance tests as well as statistical analysis.

**Chapter 6: Development of Performance-based Specifications for Heavy-Duty Asphalt Mix in Southern Ontario** – This chapter analyzed the low-temperature cracking resistance, intermediate temperature cracking resistance, shear resistance, and surface friction of the seven lab-produced asphalt mixes. In addition, a preliminary performance-based specification was developed for

heavy-duty asphalt surface mixes used in Southern Ontario. Moreover, a life cycle cost analysis was performed to evaluate the potential benefits of using a heavy-duty asphalt surface mix compared to a currently specified asphalt surface mix used at a high traffic volume approach intersection in York Region.

***Chapter 7: Conclusions, recommendations, and future research***

## Chapter 2 Literature Review

*Parts of this chapter have been published in a paper submitted to the Transportation Association of Canada (TAC) conference in 2021 (Kafi Farashah, 2021a).*

### 2.1. Asphalt Pavement

Asphalt pavement is widely used for roads and airport pavements, with around 90% of Canadian roads constructed using it (Baghaee Moghaddam, 2019). Flexible pavements consist of layers of asphalt and granular materials on top of the subgrade. As the name suggests, flexible pavement bends under traffic load. The goal of flexible pavements is to transfer and distribute traffic loads and stresses safely to the ground without compromising its stability (Baghaee Moghaddam, 2019). The strongest material is typically used as the top layer and the weakest as the bottom layer. Figure 2-1 illustrates the load distribution in flexible pavement. The mixing temperature determines the type of bound layer, including hot mix asphalt (HMA), warm mix asphalt (WMA), and cold mix asphalt (CMA) (Varamini, 2013). HMA is the most common surface type used for medium to high traffic volume roads and is produced at temperatures ranging from 145°C to 165°C. WMA is produced and placed at temperatures 20°C to 50°C lower than HMA (Politano, 2012).

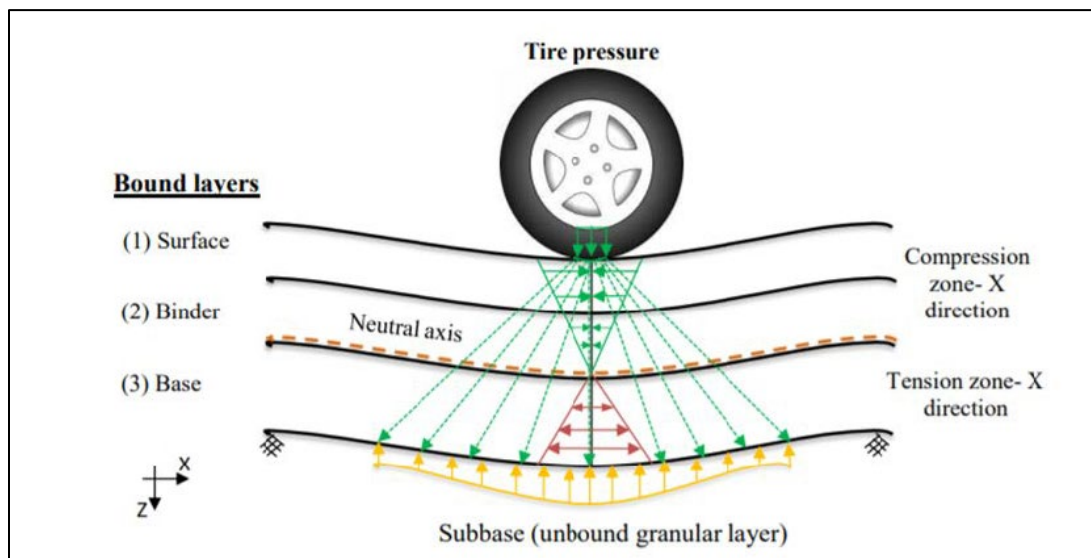


**Figure 2-1: Sections Schematic Representation of Stress/Strain Distribution in a Typical Asphalt Concrete Structure (Baghaee Moghaddam, 2019)**

## 2.2. Pavement Deformation

Pavement deformation, or rutting, as shown in Figure 2-2, is one of the most serious asphalt pavement distresses. It manifests itself as surface depression in wheel paths under heavy traffic loads, static loading, and frequent vehicle braking and accelerating, particularly in areas such as bus stops and approach intersections. rutting poses a significant threat to road safety. Asphalt, being an impervious material, traps water in rutted areas, leading to a reduction in surface friction and the risk of hydroplaning. Deeper ruts also complicate vehicle handling and increase the hazards associated with driving (Al-Mosawe, 2016). Hence, it is vital to accurately predict and assess the rutting susceptibility of asphalt mixes in order to ensure their safe and effective use.



**Figure 2-2: Rutting in Approach Intersection at Heavy Truck Traffic Road in York Region 2018**

There are two main forms of rutting. The first type is the structural rutting that occurs due to deformation in the subgrade or underlying layers, such as the base or sub-base, and results in deformation of the pavement structure as a whole as shown in Figure 2-3 (Asphalt Institute, 2014). The second type of rutting is due to inadequate asphalt mix stability which occurs when the asphalt mix lacks shear strength, leading to the accumulation of unrecoverable strain from applied wheel loads. (Faruk et al., 2015). This results in the densification and/or lateral movement of the asphalt layer under traffic, as shown in Figure 2-3. The focus of this thesis is on the rutting which occurs on the asphalt surface layer due to asphalt mix's inadequate shear strength

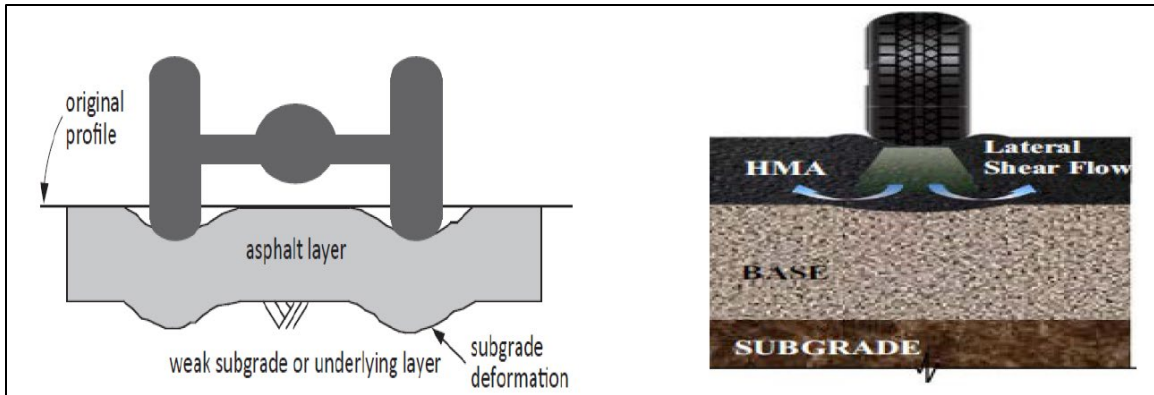


**Figure 2-3: Rutting from Weak Subgrade Left (Asphalt Institute, 2014), Rutting from Inadequate Mix Stability (Faruk et al., 2015)**

Rutting can occur in three (3) different stages, as shown in Figure 2-4, namely: a) decelerating (primary), b) stationary (secondary), and c) accelerating (tertiary) stages. In the primary stage, the accumulated permanent strain increases rapidly and the strain rate drops. In this stage, densification generally occurs. As indicated by many researchers, the initial deformation usually occurs in the first or two years of a pavement’s service life which could be due to inadequate compaction during construction (Said, et al., 2016). Typically, roads with higher air voids are susceptible to higher densification related rutting (Du et.al, 2018). The most critical rutting stage in asphalt pavement is lateral plastic flow deformation, or “shear-related deformation,” which is a result of an inability to resist the shear stresses imparted from frequent repetitions of heavy axle vehicles, braking, and turning (Du et.al, 2018).

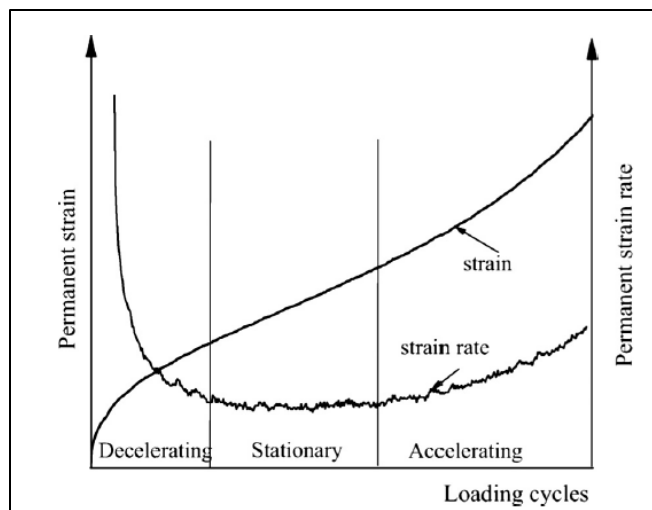


**Figure 2-4: Asphalt Mix Permanent Strain and Permanent Strain Rate vs. Loading Cycles (Witczak, 2002)**

### 2.2.1. Factors Affecting Pavement Deformation

Factors such as asphalt binder, aggregate's physical properties and skeleton, temperature, air voids (%), traffic load, and traffic speed are some of the factors affecting an asphalt mix's shear strength.

#### 2.2.1.1. Asphalt Binder

According to a study by Sybilski et al., the asphalt binder can contribute up to 40% of the rutting resistance of asphalt mixtures (Sybilski et al., 2013). Asphalt binder is a viscoelastic material that behaves elastically at lower temperatures and like a viscous fluid at higher temperatures, as shown in Figure 2-5 (Superpave Fundamentals, 2000). When subjected to loading, the binder deforms, with the portion that recovers after the load is removed exhibiting elastic behavior and the portion that remains deformed, referred to as permanent deformation, displaying plastic behavior (Baghaee Moghaddam, 2019). In addition, temperature plays a crucial role as the viscosity and stiffness of the asphalt binder decrease at high temperatures, making it more prone to deformation. Thus, it is essential to enhance the rheological properties of the asphalt binder at high temperatures, such as increasing its stiffness, to improve the resistance of the asphalt mix to shear failure caused by repetitive loading at elevated temperatures (Sybilski et al., 2013).

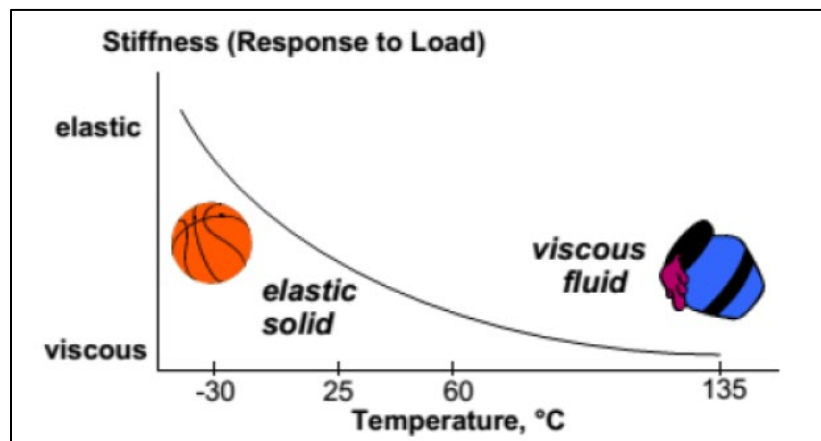


Figure 2-5: Viscoelastic Behavior of Asphalt Binder (Superpave Fundamentals, 2000)

The research conducted by Mahboub and Little suggested that asphalt mixes containing less viscous asphalt binder have low stiffness and are more susceptible to rutting (Mahboub and Little, 1988).

The study performed by Monismith and Tayebali found that polymer modified asphalt binder displayed greater resistance to rutting compared to unmodified asphalt binder when subjected to

high temperatures. They also concluded that the addition of polymer to the asphalt binder results in an increase in its viscosity at high temperatures, thereby enhancing its resistance to rutting without any negative impact on its performance at low temperatures. (Monismith and Tayebali 1988).

The investigation conducted by Robert aimed to evaluate the rutting resistance of the asphalt binder through the use of a Dynamic Shear Rheometer (DSR) test. The results showed that higher values of the shear complex modulus ( $G^*$ ) and lower values of the phase angle ( $\delta$ ) correlated with improved rutting resistance in asphalt mixes (Robert, 2000).

### 2.2.1.2. Aggregates

The Strategic Highway Research Program (SHRP) found that aggregate properties and gradation are the major factors affecting the rutting resistance of asphalt mixes (SHRP, 1990). To improve the shear strength of the mixture, it is crucial to use angular and rough-textured aggregates, as they offer higher inter-particle friction and result in a more rut-resistant asphalt mix (Figure 2-6) (Asphalt Institute, 2014). In contrast, smooth and rounded aggregates are more prone to sliding which make the asphalt mix susceptible to rutting (McGennis et. al, 1994).

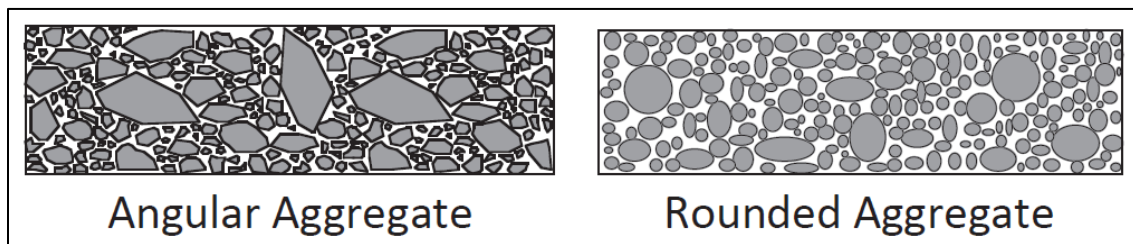


Figure 2-6: Aggregate Stone Skeleton (Asphalt Institute, 2014)

The research carried out by Crawford showed that the shape of particles and the proportion of aggregate passing the No. 4 sieve (4.75 mm) have a significant impact on the susceptibility of asphalt mix to rutting. The study revealed that asphalt mixes containing rounded, uncrushed aggregates are more prone to rutting, particularly when the amount of uncrushed material passing the No. 4 sieve increases (Crawford, 1989).

The study conducted by Kennedy et al. concluded that the use of aggregates with angular particles leads to increased interlock, internal friction, and mechanical stability.

The research conducted by Kalcheff and Tunnicliff demonstrated the effect of aggregate surface texture on permanent deformation. They found that asphalt mixes composed of crushed coarse and fine aggregates demonstrate high resistance to rutting (Kalcheff and Tunnicliff, 1982).

The study investigated by Kim et al. suggested that aggregate gradation only is not a significant factor causing rutting in asphalt mix. However, the research found that the interaction of aggregate type with gradation and other factors such as temperature and air voids are significant in rutting susceptibility of asphalt mix (Kim et al., 1992).

The National Centre for Asphalt Technology of Auburn University investigated the effect of five different nominal maximum aggregate sizes (NMASs) on rutting resistance of the asphalt mixes. The results revealed that asphalt mixes with larger aggregate size are generally stronger and more resistance to rutting (Brown and Bassett 1989).

The study by Chen and Liao looked into the influence of fine aggregate percentage on the rutting resistance of asphalt mix. The findings indicated that having an appropriate range of fine aggregate percentage would improve the rutting resistance of the asphalt mixture. (Chen and Liao, 2002).

The general consensus among various studies is that asphalt mixes with aggregates having a high degree of angularity and surface roughness exhibit a high level of rutting resistance (Button et al. 1990, Sousa et al. 1991, Brown and Bassett 1990, Kandhal and Mallick 2001).

The shear strength of asphalt mixes can be presented using Mohr–Coulomb failure theory as presented in Equation 2-1 (Du et.al, 2018).

$$\tau = c + \sigma \tan\phi \quad (2-1)$$

Where:

- $\tau$  = shear strength,
- $c$  = cohesion,
- $\sigma$  = normal stress,
- $\Phi$  = angle of internal friction.

According to the Equation (2-1), an increase in the cohesive strength of the asphalt binder and the internal friction angle of the aggregate can enhance the shear strength of the asphalt mixture, making it more resistant to rutting, as depicted in Figure 2-7 (Hafeez, 2009). Since aggregate has limited cohesion, its shear strength mainly depends on the resistance to movement or inter-particle



friction offered by the aggregate. Hence, the use of angular and rough-textured aggregates is important to achieve higher interlock among the aggregates, which results in a mixture that is resistant to rutting (Asphalt Institute, 2014).

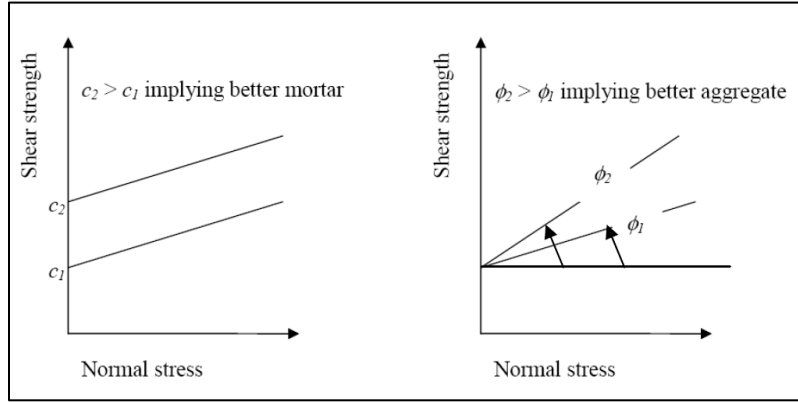


**Figure 2-7: Effect of Aggregate and Mortar on the Failure Behaviour of Asphalt Mixtures (Hafeez, 2009)**

The percentage of air voids in the asphalt mix also plays a role in the durability of the pavement in terms of rutting. A specific percentage of air voids is necessary to accommodate the expansion of the asphalt due to temperature increases and additional compaction under traffic loads (Asphalt Institute, 2014).

## 2.2.2. External Factors Influencing Permanent Deformation

### 2.2.2.1. Temperature

The study conducted by the University of Waterloo in partnership with Environment Canada found that changing weather patterns, due to climate change, will result in more frequent freeze-thaw cycles, changes in precipitation regimes, and increases in temperature extremes. The study also indicated that heat waves will occur more frequently and with longer duration each year. These changes in weather, especially temperature changes, will negatively affect transportation infrastructure, including pavements, as it reduces their longevity.

Temperature plays a critical role in rutting formation as higher temperatures cause asphalt to become less viscous and more susceptible to deformation. A study by Al-Bayati found that by increasing the hamburger wheel track testing temperature from 40°C to 50°C, the permanent deformation increased by 57.6% to reach the 10mm target level.

### 2.2.2.2. Traffic Load

The traffic pattern has a significant effect on the resilience of asphalt binder mix to rutting and early failure. Slow traffic movement, high repetitive loading, and high tire pressure increase the susceptibility of asphalt mix to deformation, particularly in areas with heavy truck trafficking and high shear stress, such as intersections. Agencies determine traffic load using Equivalent Single Axle Loads (ESALs), with the most accurate method being weight-in-motion (WIM) devices. However, due to the cost of WIM equipment, the total ESALs during the design period can be determined using Equation 2-2 (Huang 2004, TAC 2013).

$$ESAL = (ADT0)*(T)*(T1)*(G)*(D)*(L)*(365)*(Y) \quad (2-2)$$

where:

- ADT0 = Average daily traffic at the start of the design period;
- T = Percentage of Trucks in ADT;
- T1 = Number of 80kN single axle load applications per truck (Truck factor);
- G = Growth factor;
- D = Directional distribution factor;
- L = Lane distribution factor;
- Y = Design period in years.

The growth factor (G) can be calculated using the following formula (Equation 2-3) (Huang 2004, TAC 2013):

$$G = [(1 + r)^Y - 1] / r \quad (2-3)$$

Where:

- r = Annual rate of traffic growth;
- Y = Design period in years.

## 2.3. Fatigue and Low-Temperature Cracking

In addition to rutting, asphalt pavement can also suffer from fatigue cracking and low-temperature cracking, leading to a loss of performance. Thus, the resistance of the asphalt concrete mixture to cracking must also be evaluated.

### 2.3.1. Fatigue Cracking

Fatigue cracking in pavements is caused by repetitive traffic loading, which stresses the pavement to its limit. s shown in Figure 2-8. It typically occurs at intermediate pavement service temperatures

and is initiated at the bottom of the asphalt layer where maximum tensile strains occur. (Roberts et al., 1991), (McGennis et al., 1994).



**Figure 2-8: Fatigue (Alligator) Cracking – York Region 2018**

### **2.3.2. Low Temperature Cracking**

Low-temperature cracking, as shown in Figure 2-9, is a form of pavement distress that mainly occurs in regions with cold climates (Das et al., 2013). At low temperatures, the asphalt mix contracts and creates induced tensile thermal stress in the asphalt layer (Baghaee Moghaddam, 2019). When the amount of induced tensile stress exceeds the tensile strength of the material, it fractures, causing transverse cracks to appear on the surface of the pavement (Baghaee Moghaddam, 2019).



**Figure 2-9: Low-Temperature Cracking - York Region 2018**

## 2.4. Asphalt Mix Design

Asphalt mix design has been developed over the past 80 years to ensure that asphalt pavements have desirable properties throughout their service life. Asphalt mix design aims to determine the optimal proportions of aggregate, asphalt binder, additives, and supplementary materials to prevent pavement distresses like rutting and cracking and ensure desirable properties during the pavement's service life. Asphalt mixes must be designed, produced, laid down, and compacted such that the durability and stability of the mix are met during the pavement's service life. Asphalt mix durability refers to the pavement's ability to preserve its structural integrity under climate and traffic loading, while stability refers to its resistance to permanent deformation. (Bonaquist, 2014). Overall, the asphalt mix designs developed across the world can be divided into six categories: recipe, empirical testing, analytical computations, volumetric method, performance-related testing, and fundamental testing (Francken, 1998). The two most widely adopted methods globally are the Marshall mix design and the Superpave mix design, with the latter being volumetric and the former empirical as presented in Table 2-1.

**Table 2-1: Asphalt Mix Design Methods Practiced in Some Countries (Grobler et al., 2018)**

| <b>Country/Province or State</b> | <b>Mix Design Method</b>        | <b>Performance Tests</b>  |
|----------------------------------|---------------------------------|---|
| Ontario-Canada                   | Superpave                       | Moisture Sensitivity  |
| Quebec-Canada                    | A modified version of Superpave | Moisture Sensitivity and Hamburg Wheel Tracking (HWT)   |
| Alberta-Canada                   | Marshall                        | Hamburg Wheel Tracking (HWT)  |
| U.S.A.                           | Superpave                       | Hamburg Wheel Tracking (HWT), Asphalt Pavement Analyzer (APA), Complex Modulus and Uniaxial Cyclic, Flexural Beam Fatigue, Disc-Shaped Compact Tension (DC(T)), Semi-Circular Bend (SCB), Texas Overlay (OT) and Superpave Shear Tester (SST) |
| France                           | French                          | Moisture Sensitivity, Wheel Tracking, Stiffness Modulus and Fatigue   |
| Germany/Central Europe           | Marshall                        | Moisture Sensitivity and Hamburg Wheel Tracking   |
| United Kingdom                   | Marshall                        | Moisture Sensitivity, Resistant to Permanent Deformation, Modulus and Fatigue   |
| South Africa                     | Marshall and Superpave          | Moisture Sensitivity, Complex Modulus, Hamburg Wheel Tracking and Flexural Beam Fatigue   |
| Australia and New Zealand        | Marshall and Superpave          | Moisture Sensitivity, Resilient Modulus, Hamburg Wheel Tracking and Flexural Beam Fatigue   |

#### **2.4.1. Hveem Mix Design Method**

In the early 1930s, Francis Hveem, an engineer from California, developed the Hveem mix design, which emphasized the optimum asphalt binder content as the key element (Huber, 2017). Hveem believed that a sufficient amount of asphalt binder in the mix would provide a minimum asphalt film thickness on the surface of the aggregates, which affects stability. The concept of air voids ( $V_a$ ) in the mix was not included in the Hveem mix design until the 1980s and 1990s (Huber, 2017).

#### **2.4.2. Marshall Mix Design Method**

In the late 1930s to early 1940s, Bruce Marshall, an engineer in the Mississippi Department of Highways, developed the Marshall mix design which took into account both air voids ( $V_a$ ) and voids filled with asphalt (VFA) as key elements (Huber, 2017). In the 1950s, Norman McLeod added voids in the mineral aggregate (VMA), which was supported by the Asphalt Institute (AI) in the US. However, the problem of excessive asphalt surface rutting in the 1980s and 1990s emerged as the primary pavement distress (Huber, 2017).

#### **2.4.3. Superpave Mix Design Method**

The Superpave mix design method was developed by the Strategic Highway Research Program (SHRP) from 1987 to 1993 to be a more appropriate asphalt mix design method compared to previous methods, the Hveem and Marshall methods. The main objectives of SHRP were to develop and implement a mix design system, performance-based asphalt binder specifications, and performance-based asphalt mix specifications. Although SHRP was successful in implementing the first and second objectives, the third objective was not successfully implemented due to complexities. As a result, the Superpave mix design system did not provide a simple test to measure the stability of asphalt mixes as the Hveem and Marshall methods provided. (Huber, 2017). Therefore, the Departments of Transportation in the US and Canada only use mix design and asphalt binder specifications for the construction of asphalt pavements. The failure to implement appropriate performance-based asphalt mix specifications has put the Superpave mix design on the same level of effectiveness as previous methods like Hveem and Marshall, as it cannot predict and measure the expected performance of asphalt pavements against distresses such as rutting. According to the Superpave mix design method, the proportioning of aggregate and asphalt binder in a mix design is based on two factors: the characteristics of the aggregate and asphalt binder, and

the volumetric properties of the mix, such as air voids, voids in the mineral aggregate, and voids filled with asphalt.

For the performance-based asphalt binder specifications the SHRP introduced an asphalt-grading system called Performance Grading (PG) with intention of matching the physical binder properties to the desired level of resistance to rutting, fatigue and low-temperature cracking, subjected to local climate and environmental conditions (Varamini, 2016). PG consists of two parts or performance temperatures (PG HH-LL). The first two digits from the left shows the highest temperature at which physical property requirements need to be met which is optioned at a depth of 20 mm below the pavement surface using the seven-day average high air temperature. The second two digits the lowest pavement surface temperature is considered.

The Performance Grading (PG) system, introduced by the Strategic Highway Research Program (SHRP) for asphalt binder specifications, aims to match the physical properties of the asphalt binder to the desired level of resistance to distresses such as rutting, fatigue, and low-temperature cracking. The PG system consists of two parts, the performance temperatures (PG HH-LL), which are determined by the highest and lowest temperatures at the pavement surface. The first two digits (HH) indicate the highest temperature at which the physical property requirements need to be met, determined using the seven-day average high air temperature at 20mm below the pavement surface, while the second two digits (LL) show the lowest pavement surface temperature considered.

The design reliability level is an important factor in determining the pavement service temperatures in the selection process. A sample calculation for determining the PG based on different reliability levels is shown in Figure 2-10.

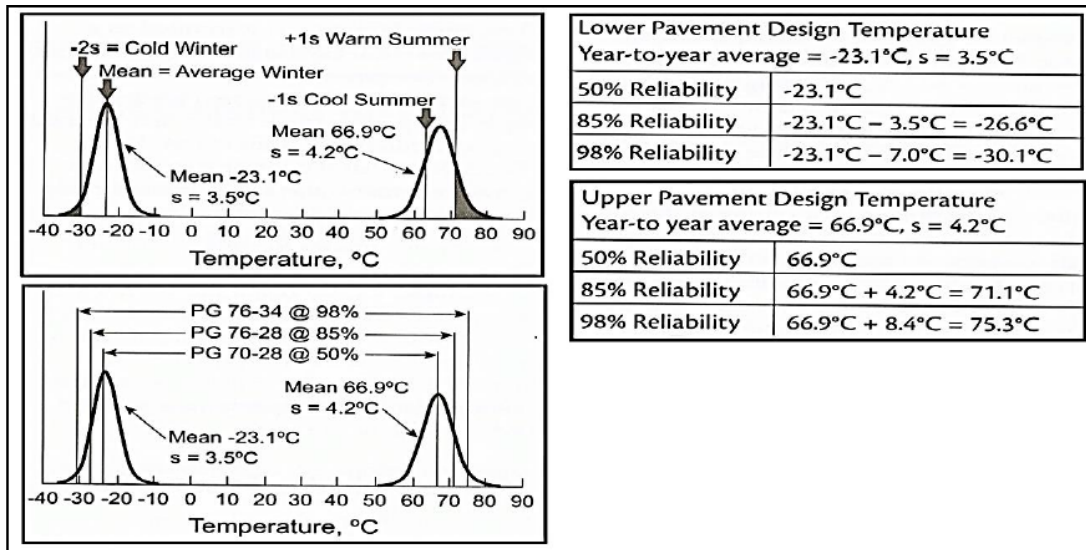


Figure 2-10: Asphalt Binder Performance Grade Selection for Different Reliabilities (Asphalt Institute, 2008)

In areas subjected to high stress loading and slow-moving traffic, such as approach intersections, it may be necessary to select a higher performance grade, known as "grade-bumping", to prevent permanent deformation. Figure 2-11 provides a summary of the Superpave grade-bumping chart. A set of testing procedures are recommended to not only simulate short-term and long-term aging of the asphalt binder, but also to evaluate its resiliency to climate conditions. Figure 2-12 presents the temperatures at which the tests are conducted and the properties that can be evaluated using each test method. The Rolling Thin Film Oven (RTFO) is used to simulate the hardening (aging) characteristics of asphalt binder during production at an asphalt mix plant. The Paving Aging Vessel (PAV) is used to simulate the in-service aging of the asphalt binder.

| Design ESALs million | High Temperature Grade Increase in 6°C Grade Equivalents |                     |                    |
|----------------------|--|---------------------|--------------------|
|                      | Heavy Traffic (Trucks and/or Buses) Loading Rate (Speed) |                     |                    |
|                      | Standing < 20 km/hr                                      | Slow 20 to 70 km/hr | Standard > 70 k/hr |
| < 0.3                | –  | –                   | –                  |
| 0.3 – < 3            | 2  | 1                   | –                  |
| 3 – 10               | 2  | 1                   | –                  |
| 10 – < 30            | 2  | 1                   | –                  |
| ≥ 30                 | 2  | 1                   | 1                  |

Figure 2-11: Superpave Grade-Bumping Chart (NRC, 2003)

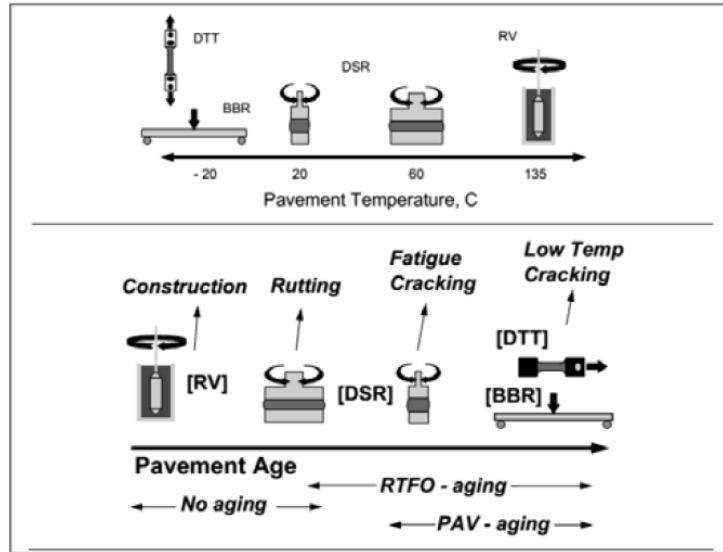


Figure 2-12: Schematic View of Binder Tests Set up (Superpave Fundamentals, 2000)

The Dynamic Shear Rheometer (DSR) is used to measure the physical properties of asphalt binder at high and intermediate pavement temperatures to ensure resistance to rutting and fatigue cracking, respectively. The Bending Beam Rheometer (BBR) measures the physical properties of asphalt binder at low temperatures to ensure adequate resistance to low-temperature cracking. The Rotational Viscometer (RV) measures the viscosity of the asphalt binder at various temperatures to determine the optimal mixing and compaction temperatures (Varamini, 2016).

The Superpave mixture design method uses the Dynamic Shear Rheometer (DSR) test to measure the shear resistivity of asphalt binder (Figure 2-13). The DSR test captures the complex shear modulus ( $G^*$ ) and phase angle ( $\delta$ ) of the binder, which provide crucial information about its rheological properties during the shearing process. These parameters are important indicators of the binder's resistance to rutting. The complex shear modulus ( $G^*$ ) measures the sample's overall resistance to deformation when subjected to shear, while the phase angle ( $\delta$ ) represents the time delay between the applied shear stress and the resulting shear strain (PI, 2021). The DSR test calculates the rutting parameter as  $G^*/\sin\delta$ . However, studies have shown that the rutting parameter determined by the DSR test in the Superpave mixture design is not a reliable indicator of the actual conditions in the field. This is because the test results are based on only one (1) cycle and only take into account the linear visco-elastic region of the material (Asphalt Institute, 2014).





**Figure 2-13: Dynamic Shear Rheometer (DSR) Equipment**

More recently, the Multiple Stress Creep Recovery (MSCR) test was introduced to better simulate rutting by applying multiple cycles to the binder to better demonstrate rutting as a non-linear failure. The MSCR test investigates the creep recovery behaviour of asphalt binder by considering two parameters: non-recoverable creep compliance ( $J_{nr}$ ) and percent recovery ( $Re$ ). A prescribed stress is applied for one (1) second and then removed (rest period) for nine (9) seconds. This is repeated for a number of 10 cycles and the residual strain after the last load application is recorded (Du et al., 2018). The MSCR test is considered a superior test method compared to the Dynamic Shear Rheometer (DSR) test. The MSCR test provides a more accurate representation of what occurs in actual pavements because it applies higher levels of stress and strain to the binder during the test, which better simulates real-world conditions. (Witzak, 2005). According to the study conducted by the Federal Highway Administrative (FHWA) at its Accelerated Loading Facility (ALF), the  $J_{nr}$  parameter from the MSCR test provides an excellent correlation with rutting (FHWA, 2011).

The SHRP has established limits and requirements for various aggregate properties to ensure the rutting resistance of asphalt mixes. These properties include toughness, soundness, the presence of deleterious materials, coarse and fine aggregate angularity, and the levels of flat and elongated particles. By meeting these standards, the asphalt mix can provide adequate resistance to rutting. (Asphalt Institute, 2014). These aggregate properties are divided into two categories: consensus properties and source properties and are varied depending on traffic in terms of equivalent single axle loads, as shown in Table 2-2 and Table 2-3 (Asphalt Institute, 2014).

**Table 2-2: Aggregate Consensus Property Requirements (Asphalt Institute, 2014)**

| Design ESALs<br>(In Millions) | Coarse Aggregate Angularity<br>(CAA) (Percent), minimum |          | Uncompacted Void<br>Content of Fine<br>Aggregate Angularity<br>(FAA) (Percent), minimum |          | Sand<br>Equivalent<br>(SE)<br>(Percent),<br>minimum | Flat and<br>Elongated<br>(F&E)<br>(Percent),<br>maximum |
|-------------------------------|---|----------|---|----------|---|---|
|                               | ≤ 100 mm  | > 100 mm | ≤ 100 mm  | > 100 mm |   |   |
| < 0.3                         | 55/-  | -/-      | -   | -        | 40  | -   |
| 0.3 to < 3                    | 75/-  | 50/-     | 40  | 40       | 40  | 10  |
| 3 to < 10                     | 85/80   | 60/-     | 45  | 40       | 45  | 10  |
| 10 to < 30                    | 95/90   | 80/75    | 45  | 40       | 45  | 10  |
| ≥ 30                          | 100/100   | 100/100  | 45  | 45       | 50  | 10  |

**Table 2-3: Recommended Superpave Source Property Tests and Typical Requirements (Asphalt Institute, 2014)**

| 20-Year Design<br>Equivalent Single<br>Axle Loads<br>(ESALs in millions) | Los Angeles<br>Abrasion<br>(Max. %)<br>AASHTO T 96 | Sodium or Magnesium<br>Sulfate Soundness<br>(Max. %)<br>AASHTO T 104 | Deleterious materials*                           |  |
|--|--|--|--|--|
|  |  |  | Clay Lumps/<br>Friable Particles<br>AASHTO T 112 | Lightweight<br>Particles<br>AASHTO T 113 |
| < 0.3  | 45   | 25   | <5   | <5                                       |
| 0.3 to < 3   | 40   | 20   | <4   | <4                                       |
| 3 to < 10  | 30   | 15   | <3   | <3                                       |
| 10 to < 30   | 30   | 15   | <2   | <2                                       |
| ≥ 30   | 25   | <10  | <1   | <1                                       |

\*Specific tests and property requirements to be determined locally

After selection of aggregate structure, the materials then go through compaction process using superpave gyratory compactor (SGC) as shown in Figure 2-14.

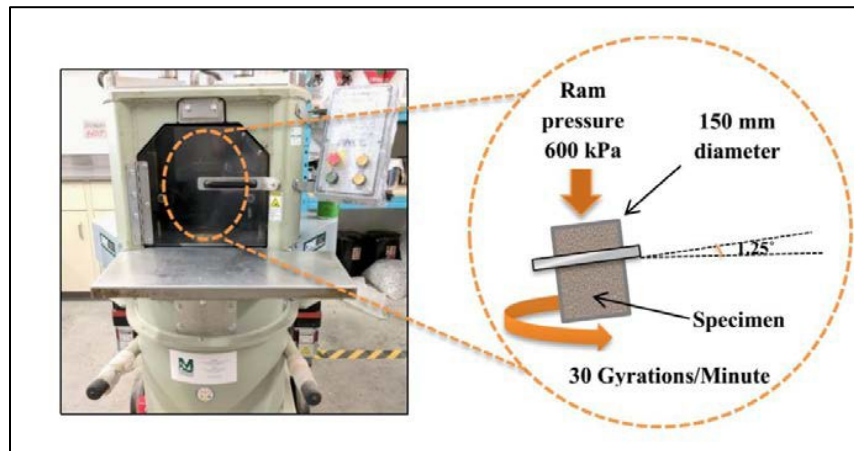


**Figure 2-14: Superpave Gyratory Compactor (SGC) (Baghaee Moghaddam, 2019)**

The design number of gyrations ( $N_{des}$ ) is determined accordance to traffic level. It means at higher traffic level more compactive effort is required to achieve higher asphalt mix density. Initial number of gyrations ( $N_{ini}$ ) is also used to measure the compatibility of asphalt mix. In addition, the  $N_{max}$ , which represents the maximum number of gyrations, provides an indication of the highest asphalt mix density that should not be exceeded during actual construction. This value helps ensure

that the asphalt mixture is compacted to the proper density and has adequate resistance to rutting (Baghaee Moghaddam, 2019). The use of gyratory compaction results in specimens that are more representative of the as-constructed pavement in terms of aggregate orientation and compaction. This method provides a more accurate simulation of the compaction process that occurs during construction, ensuring that the final asphalt mixture has the desired properties and will perform well in the field (TAC, 2013).

## **2.5. Performance Tests for Evaluating Rutting in an Asphalt Mix**



As mentioned earlier, the Superpave asphalt mix design has limitations in accurately predicting and measuring the performance of asphalt pavements against rutting because it does not incorporate appropriate performance-based specifications that account for the interaction between the binder and aggregate and its impact on rutting. This lack of consideration has resulted in the inability of the Superpave method to effectively predict and measure the expected performance of asphalt pavements against rutting.



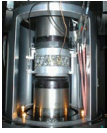



The limitations of recipe-based and volumetric asphalt mixture design in considering rutting and shear resistance are clear. To ensure the durability of asphalt mixes against rutting and to provide higher reliability, it is necessary to include performance tests in the design process. This will provide a deeper understanding of the rutting and shear resistance of the asphalt mix, ensuring that the final product meets the required performance standards. (Kafi Farashah et al., 2021c).


Table 2-4 provides information on various tests that can be used to capture the durability of asphalt mixes at higher temperatures and improve the level of reliability. The Table 2-4 lists the cost of equipment, specimen fabrication, complexity of test results and data analysis, practicality for design and quality assurance, correlation to field performance, and test variability for each test. This information can be used to determine which tests are best suited for a given project based on factors such as cost, feasibility, and accuracy (Kafi Farashah et al., 2021c). The tests listed in Table 2-4 aim to improve the understanding of the performance of volumetric designs at high temperatures. Most of these test methods are qualitative and are intended to provide an indexed performance threshold. This means that they provide a general indication of the performance of the asphalt mix, rather than detailed quantitative results. These tests can be used to assess the overall performance of the mix and to make adjustments to the design as needed to meet the desired performance criteria.

Generally speaking, testing can be categorized into three testing types a) monotonic, b) dynamic, and c) simulative types of loading (Kafi Farashah et al., 2021c). The simulative tests are relatively straightforward tests that simulate the impact of traffic on asphalt mix samples. They do this by applying a wheel load to the samples and tracking the amount of deformation that occurs after each cycle including Hamburg Wheel Tracking test, Asphalt Pavement Analyzer test, and French Rutting Tester. In dynamic loading mode, a number of sinusoidal loading cycles are applied on the asphalt mix specimen. The results can then be translated to deformation. The test results present the level of resistance of an asphalt mix to rutting and shear. The dynamic tests include Flow Number Test, Superpave Shear Tester, and the Uniaxial Shear Tester. A monotonic loading mode is used to apply a high level of strain to the asphalt mix to capture the asphalt mixes' resistance to high temperature permanent deformation. In addition, a constant strain rate is applied until the peak load is reached. The monotonic tests include Marshall Stability Test, Hveem Stabilometer, and IDEAL-RT test.

**Table 2-4: An Overview of Asphalt Mixture Performance Tests for Rutting Resistance Evaluation (NCHRP 20-07/Task 406, 2018), (EvothermWMA, 2020), (Aschenbreber, 1992), (Brosseaud et al., 1993), (Kafi Farashah et al., 2021c)**

| Laboratory tests for Rutting   | Equipment and Cost   | Test Analysis Complexity | Practicality for Mix Design and QA | Correlation to Field Performance   | Test Variability    |
|--|--|--------------------------|------------------------------------|--|---------------------|
| Hamburg Wheel Tracking Test (AASHTO T324)<br> | Hamburg Wheel-Tracking device and saw for cutting specimens<br>\$ 40,000-70,000 US | Simple                   | Good                               | Good correlation to pavement sections in Colorado and Texas                                      | Medium (COV=10-30%) |
| Asphalt Pavement Analyzer (AASHTO T340)<br>   | Asphalt Pavement Analyzer<br>\$ 120,000 US   | Simple                   | Good                               | Good correlation to pavement sections on FHWA ALF, WesTrack, NCAT Test Track, MnRoad, and Nevada | Medium (COV=20%)    |

| Laboratory tests for Rutting   | Equipment and Cost  | Test Analysis Complexity | Practicality for Mix Design and QA | Correlation to Field Performance   | Test Variability  |
|--|---|--------------------------|------------------------------------|--|-------------------|
| French Rutting Tester (LC26-410)<br>                    | French Rutting Tester<br>\$ 85,000 US   | Simple                   | Good                               | Good correlation to Field in Colorado  | Medium (COV<=20%) |
| Flow Number Test (AASHTO T378)<br>                      | Asphalt Mixture Performance Tester, Core drill, environmental chamber, saw for cutting specimens<br>\$ 112,000 US | Fair                     | Fair                               | Good correlation to pavement sections on FHWA ALF, WesTrack, NCAT Test Track, MnRoad | High (COV>30%)    |
| Superpave Shear Tester (AASHTO T320)<br>               | Superpave Shear Tester, Environmental chamber, saw for cutting specimens. The cost of testing device is unknown   | Fair                     | Fair                               | Good correlation to pavement sections on FHWA ALF, WesTrack, and MnRoad              | Unknown           |
| Uniaxial Shear Tester<br>                             | Testing Frame, Core drill, environmental chamber, saw for cutting specimens<br>\$100,000 US                       | Fair                     | Fair                               | Unknown  | Unknown           |
| Marshall Stability Test ASTM D6926 and ASTM D6927<br> | Marshall Apparatus<br>\$ 10,000 US  | Simple                   | Good                               | Unknown  | Medium (COV<=16)  |
| Hveem Stabilometer Test ASTM D1561 and ASTM D1560<br> | Hveem Stabilometer<br>\$ 10,000 US  | Simple                   | Good                               | Unknown  | Medium (COV<=20%) |

| Laboratory tests for Rutting   | Equipment and Cost  | Test Analysis Complexity | Practicality for Mix Design and QA | Correlation to Field Performance | Test Variability  |
|--|---|--------------------------|------------------------------------|----------------------------------|-------------------|
| IDEAL Rutting Test (ASTM WK71466)<br> | Testing Frame (Same as SCB and Ideal CT),<br>Ideal RT Jig<br><br>\$ 10,000 US | Simple                   | Good                               | Unknown                          | Medium (COV<15 %) |

## 2.6. Asphalt Mix Classification

Asphalt mix is a mixture of aggregate particles and asphalt cement, typically in a 95:5 weight ratio. The specific combination of aggregate used can vary depending on the intended construction use.

### 2.6.1. Dense-Graded Asphalt Mixes

In dense-graded asphalt mix the entire range of sieve is used, and mix has a well-distributed aggregate gradation (Asphalt Institute, 2014). The dense-graded asphalt mix is the most common type of asphalt mix used today in North America.

The “Enrobé à Module Élevé- (EME)” or “High-Modulus Asphalt Mix” EME is one of the examples of the dense-graded asphalt mixes which it was first developed in France in 1980’s using French method mix design (Baghaee Moghaddam & Baaj, 2018). The EME is a durable mix and provides high rutting and fatigue resistance (Baghaee Moghaddam & Baaj, 2018). The thesis research conducted at the University of Waterloo resulted in development of EME mix design for Southern Ontario (Baghaee Moghaddam, 2019).

### 2.6.2. Open-Graded Asphalt Mixes

An open-graded asphalt mix typically contains a large volume of air voids, ranging from 18 to 22 percent, due to its limited small aggregate particles filling the spaces between larger particles. The aim of this gap-graded asphalt mix is to facilitate easy water drainage through the pavement layer (Asphalt Institute, 2014).

### 2.6.3. Gap-Graded Asphalt Mixes

Gap gradation means a lack or minimal share of specified fractions of intermediate aggregates. In gap-graded asphalt mix, certain aggregate particles of certain sizes are partially missing. Typically,

gap-graded asphalt mixes contain only a small percentage of aggregate particles in the mid-size range. One of the commonly used gap-graded asphalt mixes today is the Stone Matrix (Mastic) Asphalt (SMA) mix the Stone Matrix (Mastic) Asphalt (SMA) mix. SMA mixes have a gap-graded aggregate structure, with a high content of coarse aggregate fractions, filler, asphalt binder, and a stabilizing additive to prevent the asphalt binder from draining away from the aggregates (Figure 2-15).

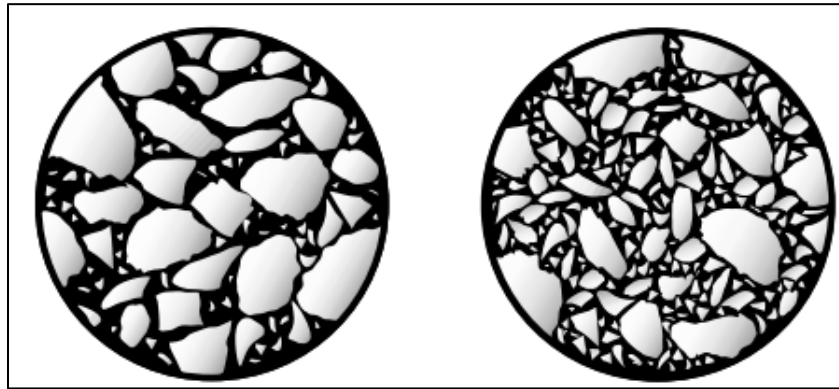


**Figure 2-15: A Graphic Representation of SMA (Left) and Dense-Graded Asphalt Mix (Right) (NAPA, 2002)**

The SMA mix was first invented by Dr. Zichner, a German engineer and manager of the Central Laboratory for Road Construction at Strabag Bau AG, to mitigate the harm caused by studded tires on asphalt pavement. The mix consisted of a robust aggregate skeleton of coarse aggregates (excluding those between 2mm and 5mm) and mastic, such as asphalt binder, filler, and sand, to fill the gaps between the aggregates (Blazejowski, 2011).

Over the years, the SMA mix gained popularity and was modified from its original design in North America. In addition to the design parameters used in the Superpave asphalt mix design, such as VMA, other parameters like Voids in Coarse Aggregate (VCA) were used to ensure proper stone-on-stone contact. The VCA has two components:  $VCA_{DRC}$  (dry rodded condition), which represents the volume between coarse aggregate particles after compaction in accordance with AASHTO T 19, and  $VCA_{MIX}$ , which represents the volume of SMA mix components excluding coarse aggregate (Blazejowski, 2011). Typically, if  $VCA_{MIX}$  value is less than  $VCA_{DRC}$  value, the SMA mix is considered to have adequate stone-on-stone contact and a suitable aggregate structure (Blazejowski, 2011). The drain down effect, which is the separation of asphalt binder or mastic from the SMA mix at high temperatures due to an intentional excess of binder to coat the aggregate, must also be taken into account to guarantee the stability of the mix. The drain down test procedure is based on AASHTO T 305.

SMA asphalt mixes, due to their stone-to-stone aggregate structure, have been demonstrated to be a strong option for resisting rutting. (NAPA, 2002). However, they require a higher asphalt binder content and use of premium aggregate, making them generally more expensive compared to other asphalt mixes. Although SMA mixes have been used in the past, there are no specific performance tests, conditions, and criteria to evaluate their rutting and cracking performance and distinguish between different SMA mixes.

## **2.7. Balanced Mix-Design**

Pavement distresses such as rutting have demonstrated that the recipe and volumetric approach used in Superpave may not accurately capture the durability of the asphalt mix in the short- and long-term, nor provide insight into its resistance to rutting and shear. Furthermore, the current asphalt mix design methods used in North America may not be adequate in predicting the performance of asphalt pavements in the field. These limitations have become increasingly complex with the addition of components such as Reclaimed Asphalt Pavement (RAP), Recycled Asphalt Shingles (RAS), warm-mix asphalt additives, rejuvenators, polymers, and fibres in asphalt mixes (NCHRP 9-57, 2016). Thus, it is essential to introduce testing that can assess an asphalt mix's durability and increase the level of reliability in its resistance to rutting and shear (NCHRP 9-57, 2016).

The balanced mix design (BMD) is defined as “asphalt mix design using performance tests on appropriately conditioned specimens that address multiple modes of distress taking into consideration mix aging, traffic, climate and location within the pavement structure” (NCHRP, 2018). The BMD comprises of two or more performance tests, such as rutting and cracking tests, to evaluate the asphalt mixes' resilience to pavement distresses Overall, there are three main methods in BMD that are currently being used in some states in the United States, including Texas, Illinois, Louisiana, and New Jersey, as shown in Figure 2-16. (Bennert, 2018), (Zhou F. , 2017), (Cooper & Mohammad, 2018), (Ozer & Al-Qadi, 2018), (Newcomb & Zhou, 2018). In addition, these performance tests could be done as part of a) performance-verified volumetric design, b) performance-modified volumetric design, or c) only considering performance design, targeting asphalt mix durability. In the performance-verified volumetric design, performance tests are performed to confirm the resistance to a particular distress, such as rutting, in the asphalt mix. In the performance-modified volumetric design, performance tests are conducted to alter the mix



proportions, such as adjusting the asphalt concrete content, to improve its resistance to rutting. The last method, the volumetric properties are not mandatory and the design is based solely on performance response (Newcomb & Zhou 2018). Table 2-5 presents a list of some of the performance tests and their specifications that have been established or are under development by some Departments of Transportation (DOTs) in the US (West, 2018).

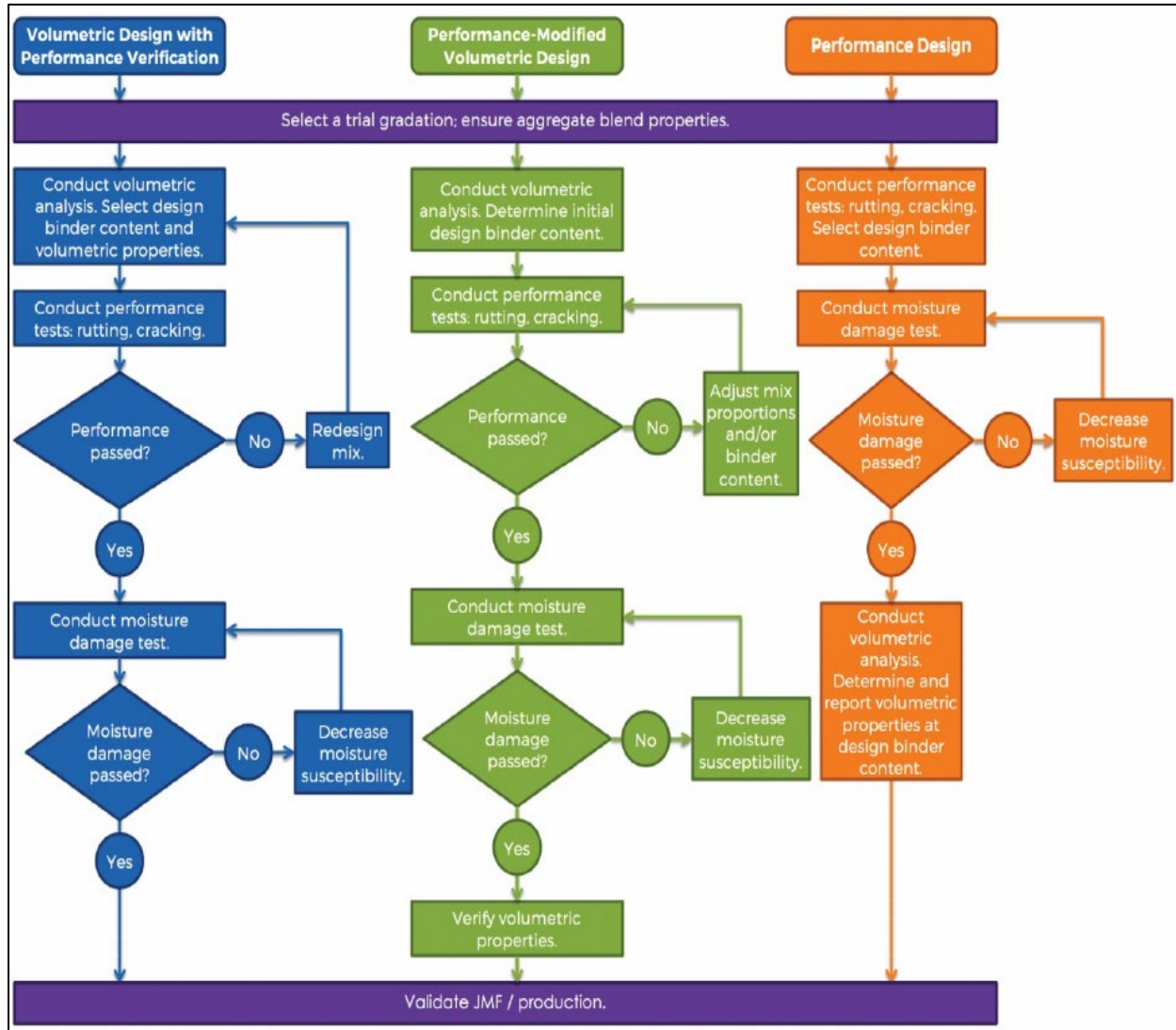


Figure 2-16: Schematic Illustration of Three BMD Approaches (NCHRP, 2016)

**Table 2-5: Performance Specifications Set up by Some DOTs for Quality Assurance and BMD Activities (West, 2018)**

| State      | Description  | Cracking Criteria  | Rutting Criteria  |
|------------|--|--|---|
| California | Performance-Based Specifications (PBSs) and the CalME (Caltrans' Mechanistic Empirical Design Program) | Bending Beam Fatigue Test (AASHTO T 321)   | Determining the Permanent Shear Strain and Stiffness of Asphalt Mixtures Using the Superpave Shear Tester (SST) (AASHTO T 320)<br>Hamburg Wheel Track Test (AASHTO T324)  |
| Florida    | Research is in progress  | IDT Energy Ratio<br>Texas Overlay  | Flow Number<br>Hamburg Wheel Track (HWT) Test (AASHTO T324)<br>Rutting and Moisture Damage Asphalt Pavement Analyzer (APA) Test @64°C (AASHTO T340)<br><b>Acceptance Criteria:<br/>Maximum rut depth of 4.5 mm at 8000 cycles</b>   |
| Georgia    | Research is in progress  | _____  | Hamburg Wheel Track (HWT) Test (AASHTO T324)<br>Rutting and Moisture Damage Asphalt Pavement Analyzer (APA) Test (AASHTO T340)  |
| Iowa       | Research is in progress  | Bending Beam Fatigue Test (AASHTO T 321)<br><b>Minimum threshold of 100,000 cycles to failure at 2,000 micro strain</b><br>For High Performance Thin Overlay (HPTO)<br>Disk-shaped compact tension (DC(T)) test (ASTM 7313)  | Hamburg Wheel Track (HWT) Test (AASHTO T324) @40°C for PG 58-xx asphalt binders and 50°C for higher binder grades<br><b>Acceptance Criteria:<br/>Maximum 8 mm rut depth at 8,000 passes<br/>Minimum HWTT stripping inflection point (SIP) of 10,000 for plant produced mixtures with traffic designation Standard (S), and 14,000 for mixtures with traffic designations High (H) and Very High (V)</b> |
| Minnesota  | Research is in progress  | Disk-shaped compact tension (DC(T)) test (ASTM 7313)<br><b>Acceptance Criteria:<br/>ESALs&gt;30M<br/>FE=690J/m<sup>2</sup><br/>30M&gt;ESALs&gt;10M<br/>FE=460J/m<sup>2</sup><br/>ESALs&lt;10M<br/>FE=400J/ m<sup>2</sup></b> | _____   |

| State                     | Description             | Cracking Criteria  | Rutting Criteria   |                           |                  |                |                |                |                |                |                |                 |                |                 |                |
|---------------------------|-------------------------|--|--|---------------------------|------------------|----------------|----------------|----------------|----------------|----------------|----------------|-----------------|----------------|-----------------|----------------|
| New Mexico                | Research is in progress | _____  | Hamburg Wheel Track (HWT) Test<br>AASHTO T324<br>@40°C, 50°C and 60°C  |                           |                  |                |                |                |                |                |                |                 |                |                 |                |
| Ohio                      | Research is in progress | Bending Beam Fatigue Test<br>(AASHTO T321)<br><br><b>Acceptance Criteria:</b><br><br><b>Minimum of 100,000 cycles at 1500micro strain for Bridge deck waterproofing surface course</b> | Asphalt Pavement Analyzer (APA) Test<br>(AASHTO T340)<br>48.9°C for non-polymer asphalt binder mixes and 54.4°C for all heavy surface and high stress area mixes<br><b>Acceptance Criteria:</b><br><b>The maximum APA rut depth is 5.0 mm at 8,000 cycles for most mixes, and 3.0 mm for high stress mixes</b>   |                           |                  |                |                |                |                |                |                |                 |                |                 |                |
| Oklahoma                  | Research is in progress | IFIT and Cantabro  | Hamburg Wheel Track (HWT) Test<br>AASHTO T324<br>@50°C<br><b>Acceptance Criteria:</b><br><b>Minimum passes at 12.5 mm rut depth</b><br><br><table border="0"> <tr> <td><b>Binder Pass</b></td> <td><b>Number of</b></td> </tr> <tr> <td><b>PG64-XX</b></td> <td><b>10000</b></td> </tr> <tr> <td><b>PG70-XX</b></td> <td><b>15000</b></td> </tr> <tr> <td><b>PG76-XX</b></td> <td><b>20000</b></td> </tr> </table>   | <b>Binder Pass</b>        | <b>Number of</b> | <b>PG64-XX</b> | <b>10000</b>   | <b>PG70-XX</b> | <b>15000</b>   | <b>PG76-XX</b> | <b>20000</b>   |                 |                |                 |                |
| <b>Binder Pass</b>        | <b>Number of</b>        |  |  |                           |                  |                |                |                |                |                |                |                 |                |                 |                |
| <b>PG64-XX</b>            | <b>10000</b>            |  |  |                           |                  |                |                |                |                |                |                |                 |                |                 |                |
| <b>PG70-XX</b>            | <b>15000</b>            |  |  |                           |                  |                |                |                |                |                |                |                 |                |                 |                |
| <b>PG76-XX</b>            | <b>20000</b>            |  |  |                           |                  |                |                |                |                |                |                |                 |                |                 |                |
| South Dakota              | Research is in progress | Disk-shaped compact tension (DC(T)) test<br>(ASTM 7313)<br><br>SCB Low Temperature<br>(AASHTO TP105)   | Asphalt Pavement Analyzer (APA) Test<br>(AASHTO T340)<br><br>@ Binder's high temperature PG<br><b>Acceptance Criteria:</b><br><b>Maximum Rut Depth at 8000 Cycles</b><br><br><table border="0"> <tr> <td><b>Truck ADT Depth</b></td> <td><b>Rut</b></td> </tr> <tr> <td><b>&lt;75</b></td> <td><b>&lt;8mm</b></td> </tr> <tr> <td><b>76-250</b></td> <td><b>&lt;7mm</b></td> </tr> <tr> <td><b>251-650</b></td> <td><b>&lt;6mm</b></td> </tr> <tr> <td><b>651-1200</b></td> <td><b>&lt;5mm</b></td> </tr> <tr> <td><b>&gt;1200</b></td> <td><b>&lt;5mm</b></td> </tr> </table> | <b>Truck ADT Depth</b>    | <b>Rut</b>       | <b>&lt;75</b>  | <b>&lt;8mm</b> | <b>76-250</b>  | <b>&lt;7mm</b> | <b>251-650</b> | <b>&lt;6mm</b> | <b>651-1200</b> | <b>&lt;5mm</b> | <b>&gt;1200</b> | <b>&lt;5mm</b> |
| <b>Truck ADT Depth</b>    | <b>Rut</b>              |  |  |                           |                  |                |                |                |                |                |                |                 |                |                 |                |
| <b>&lt;75</b>             | <b>&lt;8mm</b>          |  |  |                           |                  |                |                |                |                |                |                |                 |                |                 |                |
| <b>76-250</b>             | <b>&lt;7mm</b>          |  |  |                           |                  |                |                |                |                |                |                |                 |                |                 |                |
| <b>251-650</b>            | <b>&lt;6mm</b>          |  |  |                           |                  |                |                |                |                |                |                |                 |                |                 |                |
| <b>651-1200</b>           | <b>&lt;5mm</b>          |  |  |                           |                  |                |                |                |                |                |                |                 |                |                 |                |
| <b>&gt;1200</b>           | <b>&lt;5mm</b>          |  |  |                           |                  |                |                |                |                |                |                |                 |                |                 |                |
| Utah                      | Research is in progress | IFIT Test<br>(AASHTO TP124)<br><br>Bending Beam Rheometer<br>(AASHTO TP125)  | Hamburg Wheel Track (HWT) Test<br>AASHTO T324<br><b>Acceptance Criteria:</b><br><b>Maximum 10mm rut depth @20000 cycles</b><br><br><table border="0"> <tr> <td><b>Binder Temperature</b></td> <td></td> </tr> <tr> <td><b>PG58-XX</b></td> <td><b>46°C</b></td> </tr> <tr> <td><b>PG64-XX</b></td> <td><b>50°C</b></td> </tr> <tr> <td><b>PG70-XX</b></td> <td><b>54°C</b></td> </tr> </table>   | <b>Binder Temperature</b> |                  | <b>PG58-XX</b> | <b>46°C</b>    | <b>PG64-XX</b> | <b>50°C</b>    | <b>PG70-XX</b> | <b>54°C</b>    |                 |                |                 |                |
| <b>Binder Temperature</b> |                         |  |  |                           |                  |                |                |                |                |                |                |                 |                |                 |                |
| <b>PG58-XX</b>            | <b>46°C</b>             |  |  |                           |                  |                |                |                |                |                |                |                 |                |                 |                |
| <b>PG64-XX</b>            | <b>50°C</b>             |  |  |                           |                  |                |                |                |                |                |                |                 |                |                 |                |
| <b>PG70-XX</b>            | <b>54°C</b>             |  |  |                           |                  |                |                |                |                |                |                |                 |                |                 |                |

| State                  | Description   | Cracking Criteria  | Rutting Criteria  |              |                           |                        |       |         |         |                        |       |   |             |                        |                |              |              |              |
|------------------------|---|--|---|--------------|---------------------------|------------------------|-------|---------|---------|------------------------|-------|---|-------------|------------------------|----------------|--------------|--------------|--------------|
| Texas                  | <p>BMD-Volumetric Design with Performance Verifications</p> <p>A space diagram including both rut depth of HWT test and minimum number of cycles of OT test is used during mix design and acceptance</p>                | <p>Texas Overlay Test (Tex-248-F)</p> <p><b>Acceptance Criteria:</b><br/> <b>Asphalt Mix Number of Cycles</b><br/> <b>Porous Friction Course &gt;200</b><br/> <b>SMA &gt;200</b><br/> <b>Thin Overlay (PG70-XX) &gt;300</b><br/> <b>Thin Overlay (PG76-XX) &gt;300</b><br/> <b>Hot-in-place recycling &gt;150</b></p>  | <p>Hamburg Wheel Track (HWT) Test AASHTO T324 @50°C</p> <p><b>Acceptance Criteria:</b><br/> <b>Minimum passes at 12.5mm rut depth</b></p> <table> <thead> <tr> <th>Asphalt Mix</th> <th>Minimum Passes</th> </tr> </thead> <tbody> <tr> <td>Porous Friction Course</td> <td>10000</td> </tr> <tr> <td>SMA</td> <td>20000</td> </tr> <tr> <td>Thin Overlay (PG70-XX)</td> <td>15000</td> </tr> <tr> <td>Thin Overlay (PG76-XX)</td> <td>20000</td> </tr> <tr> <td>Hot-in-place recycling</td> <td>10000</td> </tr> </tbody> </table> | Asphalt Mix  | Minimum Passes            | Porous Friction Course | 10000 | SMA     | 20000   | Thin Overlay (PG70-XX) | 15000 | Thin Overlay (PG76-XX)  | 20000       | Hot-in-place recycling | 10000          |              |              |              |
| Asphalt Mix            | Minimum Passes  |  |   |              |                           |                        |       |         |         |                        |       |   |             |                        |                |              |              |              |
| Porous Friction Course | 10000   |  |   |              |                           |                        |       |         |         |                        |       |   |             |                        |                |              |              |              |
| SMA                    | 20000   |  |   |              |                           |                        |       |         |         |                        |       |   |             |                        |                |              |              |              |
| Thin Overlay (PG70-XX) | 15000   |  |   |              |                           |                        |       |         |         |                        |       |   |             |                        |                |              |              |              |
| Thin Overlay (PG76-XX) | 20000   |  |   |              |                           |                        |       |         |         |                        |       |   |             |                        |                |              |              |              |
| Hot-in-place recycling | 10000   |  |   |              |                           |                        |       |         |         |                        |       |   |             |                        |                |              |              |              |
| Louisiana              | <p>BMD-Volumetric Design with Performance Verifications</p> <p>A space diagram including both rut depth of HWT test and minimum critical strain energy release of SCB test is used during mix design and acceptance</p> | <p>ASTM D8044</p> <p>Minimum critical strain energy release (<math>J_c</math>) <math>\text{kJ/m}^2</math></p> <p><b>Acceptance Criteria:</b><br/> <b>Minimum of 0.6 and 0.5 <math>\text{kJ/m}^2</math> of critical strain energy released for level 1 and 2 of traffic respectively</b></p>  | <p>Hamburg Wheel Track (HWT) Test AASHTO T324 @50°C</p> <p><b>Acceptance Criteria:</b><br/> <b>Minimum number of passes at 12 mm rut depth</b></p> <table> <thead> <tr> <th>Binder Pass</th> <th>Number of Pass</th> </tr> </thead> <tbody> <tr> <td>PG58-XX</td> <td>12000</td> </tr> <tr> <td>PG64-XX</td> <td>20000</td> </tr> <tr> <td>PG70-XX (OGFC)</td> <td>7500</td> </tr> </tbody> </table>  | Binder Pass  | Number of Pass            | PG58-XX                | 12000 | PG64-XX | 20000   | PG70-XX (OGFC)         | 7500  |   |             |                        |                |              |              |              |
| Binder Pass            | Number of Pass  |  |   |              |                           |                        |       |         |         |                        |       |   |             |                        |                |              |              |              |
| PG58-XX                | 12000   |  |   |              |                           |                        |       |         |         |                        |       |   |             |                        |                |              |              |              |
| PG64-XX                | 20000   |  |   |              |                           |                        |       |         |         |                        |       |   |             |                        |                |              |              |              |
| PG70-XX (OGFC)         | 7500  |  |   |              |                           |                        |       |         |         |                        |       |   |             |                        |                |              |              |              |
| Illinois               | <p>BMD-Volumetric Design with Performance Verifications</p> <p>A space diagram including both rut depth of HWT test and minimum Flexibility Index (FI) of SCB test is used during mix design and acceptance</p>         | <p>I-FIT AASHTO TP124</p> <p>Flexibility Index (FI)</p> <p><b>Acceptance Criteria:</b><br/> <b>FI<math>\geq</math>8</b></p>  | <p>Hamburg Wheel Track (HWT) Test AASHTO T324 @50°C</p> <p><b>Acceptance Criteria:</b><br/> <b>Maximum rut depth 12.5mm</b></p> <table> <thead> <tr> <th>Binder Pass</th> <th>Number of Pass</th> </tr> </thead> <tbody> <tr> <td>PG58-XX</td> <td>5000</td> </tr> <tr> <td>PG64-XX</td> <td>7500</td> </tr> <tr> <td>PG70-XX (OGFC)</td> <td>15000</td> </tr> <tr> <td>PG76-XX</td> <td>20000</td> </tr> </tbody> </table>   | Binder Pass  | Number of Pass            | PG58-XX                | 5000  | PG64-XX | 7500    | PG70-XX (OGFC)         | 15000 | PG76-XX   | 20000       |                        |                |              |              |              |
| Binder Pass            | Number of Pass  |  |   |              |                           |                        |       |         |         |                        |       |   |             |                        |                |              |              |              |
| PG58-XX                | 5000  |  |   |              |                           |                        |       |         |         |                        |       |   |             |                        |                |              |              |              |
| PG64-XX                | 7500  |  |   |              |                           |                        |       |         |         |                        |       |   |             |                        |                |              |              |              |
| PG70-XX (OGFC)         | 15000   |  |   |              |                           |                        |       |         |         |                        |       |   |             |                        |                |              |              |              |
| PG76-XX                | 20000   |  |   |              |                           |                        |       |         |         |                        |       |   |             |                        |                |              |              |              |
| Wisconsin              | <p>Research in Progress</p>   | <p>Disk-shaped compact tension (DC(T)) test (ASTM 7313)</p> <p>Low-temperature semi-circular bend test (AASHTO TP105)</p> <p>Extracted Binder (<math>\Delta T_c</math>)</p> <table> <thead> <tr> <th>Binder</th> <th><math>\Delta T_c</math></th> <th>DC(T)FE(<math>\text{J/m}^2</math>)</th> </tr> </thead> <tbody> <tr> <td>PG58-XX</td> <td>&lt;5°C</td> <td>&gt;400</td> </tr> <tr> <td>PG64-XX</td> <td>&lt;5°C</td> <td>&gt;400</td> </tr> </tbody> </table> | Binder  | $\Delta T_c$ | DC(T)FE( $\text{J/m}^2$ ) | PG58-XX                | <5°C  | >400    | PG64-XX | <5°C                   | >400  | <p>Hamburg Wheel Track (HWT) Test (AASHTO T324)</p> <p><b>Acceptance Criteria:</b><br/> <b>@45°C</b><br/> <b>Minimum passes to 12.5 mm</b></p> <table> <tbody> <tr> <td>Low traffic</td> <td>7500 passes</td> </tr> <tr> <td>Medium traffic</td> <td>11250 passes</td> </tr> <tr> <td>High traffic</td> <td>15000 passes</td> </tr> </tbody> </table> | Low traffic | 7500 passes            | Medium traffic | 11250 passes | High traffic | 15000 passes |
| Binder                 | $\Delta T_c$  | DC(T)FE( $\text{J/m}^2$ )  |   |              |                           |                        |       |         |         |                        |       |   |             |                        |                |              |              |              |
| PG58-XX                | <5°C  | >400   |   |              |                           |                        |       |         |         |                        |       |   |             |                        |                |              |              |              |
| PG64-XX                | <5°C  | >400   |   |              |                           |                        |       |         |         |                        |       |   |             |                        |                |              |              |              |
| Low traffic            | 7500 passes   |  |   |              |                           |                        |       |         |         |                        |       |   |             |                        |                |              |              |              |
| Medium traffic         | 11250 passes  |  |   |              |                           |                        |       |         |         |                        |       |   |             |                        |                |              |              |              |
| High traffic           | 15000 passes  |  |   |              |                           |                        |       |         |         |                        |       |   |             |                        |                |              |              |              |

| State          | Description   | Cracking Criteria   | Rutting Criteria  |
|----------------|---|---|---|
| New Jersey     | Flexural beam test is used if the mode of cracking is dependent on the flexural properties of the pavement and OT test is used if the expansion-contraction of concrete slab underlying asphalt mix is causing the cracking | <p>Texas Overlay (OT) test (TX-248-F)</p> <p><b>Acceptance Criteria:</b><br/> <b>Minimum of 700 cycles for Binder-rich intermediate course and 170 cycles for High RAP mixes</b></p> <p>and</p> <p>Flexural Beam Fatigue Test (AASHTO T321)<br/> <b>Acceptance Criteria:</b><br/> <b>Minimum of 100,000 cycles @15°C and 1500micro strain for Bridge deck waterproofing surface course</b><br/> and<br/> <b>Minimum of 100,000,000 cycles @15°C and 100micro strain for Bottom rich base course</b></p> | <p>Rutting and Moisture Damage Asphalt Pavement Analyzer (APA) Test (AASHTO T340) @64°C 100-psi hose pressure, 100-lb wheel loads and 8000 cycles</p> <p><b>Acceptance Criteria:</b></p> <p><b>Maximum of 4mm rut depth for High-performance thin overlay</b></p> <p><b>Maximum of 6mm rut depth for Binder-rich intermediate course</b></p> <p><b>Maximum of 3mm rut depth for Bridge deck waterproofing surface course</b></p> <p><b>Maximum of 5mm rut depth for Bottom-rich base course</b></p> <p><b>Minimum of 4mm for High RAP mix with PG70-22 and minimum of 7mm for High RAP mix with PG64-22</b></p> |
| Alabama        | Research in Progress  | _____   | <p>Asphalt Pavement Analyzer (APA) Test (AASHTO T340)<br/> <b>Acceptance Criteria:</b><br/> <b>Rut depth @ 8000 cycles</b></p> <p><b>Traffic Depth</b>                      <b>Max Rut</b><br/> <b>30M&gt;ESALs&gt;10M</b>      <b>4.5 mm @67°C</b></p>   |
| South Carolina | Research in Progress  | _____   | <p>Asphalt Pavement Analyzer (APA) Test (AASHTO T340)<br/> <b>Acceptance Criteria:</b><br/> <b>Rut depth @ 8000 cycles</b></p> <p><b>Binder Max Rut Depth</b><br/> <b>PG76-22</b>                      <b>3mm @64°C</b><br/> <b>PG64-22</b>                      <b>5mm @64°C</b></p>   |

## 2.8. Pavement Design

The objective of pavement design is to create a cost-effective road structure that can withstand anticipated traffic and environmental loading over its expected service life (MTO, 2013). The flexible pavement structure is composed of asphalt layers, granular base and subbase layers, and the subgrade, which must be designed to provide sufficient strength to support expected traffic loads and distribute it to the subgrade (MTO, 2013). Pavement design is a complex process that

considers factors such as available materials, anticipated traffic, environment, local contractors, resources, expected level of service, cost, agency policies, established practices, and sustainability (TAC, 2013). There are several pavement design methods used for road infrastructure, including empirical and mechanistic-empirical methods, which are the most commonly used.

### 2.8.1. Empirical Design Methods

The empirical design methods rely on the results of measured pavement responses, such as pavement deflection, to determine the optimal thickness for different traffic levels and subgrade structural capacities (TAC 2013; Varamini 2016). These methods are based on extrapolating past experience to predict future conditions (TAC, 2013). The principal of the empirical pavement design is shown in Figure 2-17. The American State Highway and Transportation Officials (AASHTO) conducted a significant research program in Ottawa and Illinois in the late 1950s to improve understanding of pavement performance and develop more durable and cost-effective pavement structures. This research led to the creation of a pavement design guideline, which has undergone multiple revisions, with the latest revision being in 1993. The AASHTO 1993 Guide for Design of Pavement Structures is widely used for designing pavements in Canada and the associated design software, DARWin, is the preferred method used by most road agencies in the country. This design guide has undergone multiple revisions and is considered an authoritative resource for pavement design. (AASHTO, 1993; TAC, 2013).

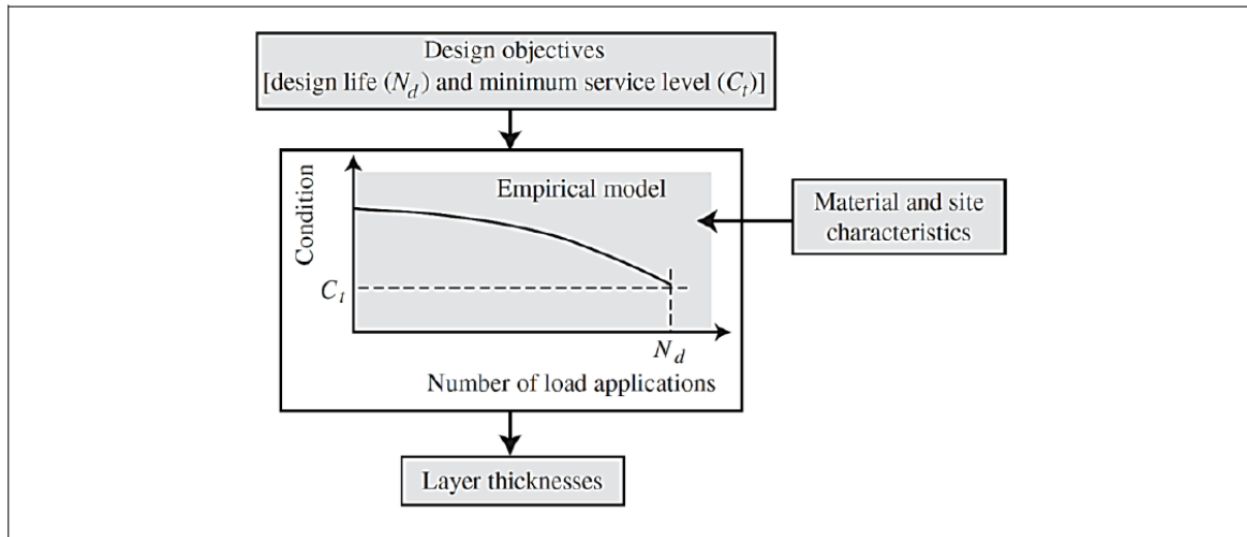


Figure 2-17: Principle of Empirical Pavement Design (Dore & Zubeck, 2009)

### 2.8.2. Mechanistic-Empirical Design Methods

The AASHTO design method was a significant improvement but still had empirical limitations. The mechanistic-empirical design method uses laboratory-derived input parameters to inform the mechanistic portion of the design, but these inputs must be adjusted for in-service variations. The correction in the mechanistic-empirical design method is based on observations of previous pavement performance. Hence, it is referred to as a mechanistic-empirical method. The principle of the mechanistic-empirical pavement design is shown in Figure 2-18. One of the most comprehensive and widely used mechanistic-empirical methods is known as the Mechanistic-Empirical Pavement Design Guide (MEPDG). The MEPDG was developed in 2002 under the National Cooperative Highway Research Program (NCHRP) Project 1-37A (NCHRP, 2004, Varamini 2016). In 2011, due to technical deficiencies in the accuracy of predicting pavement performance, a revised version of the mechanistic-empirical pavement design guide (MEPDG) was introduced under the name of AASHTOWare DARWin-ME. (Varamini, 2016).

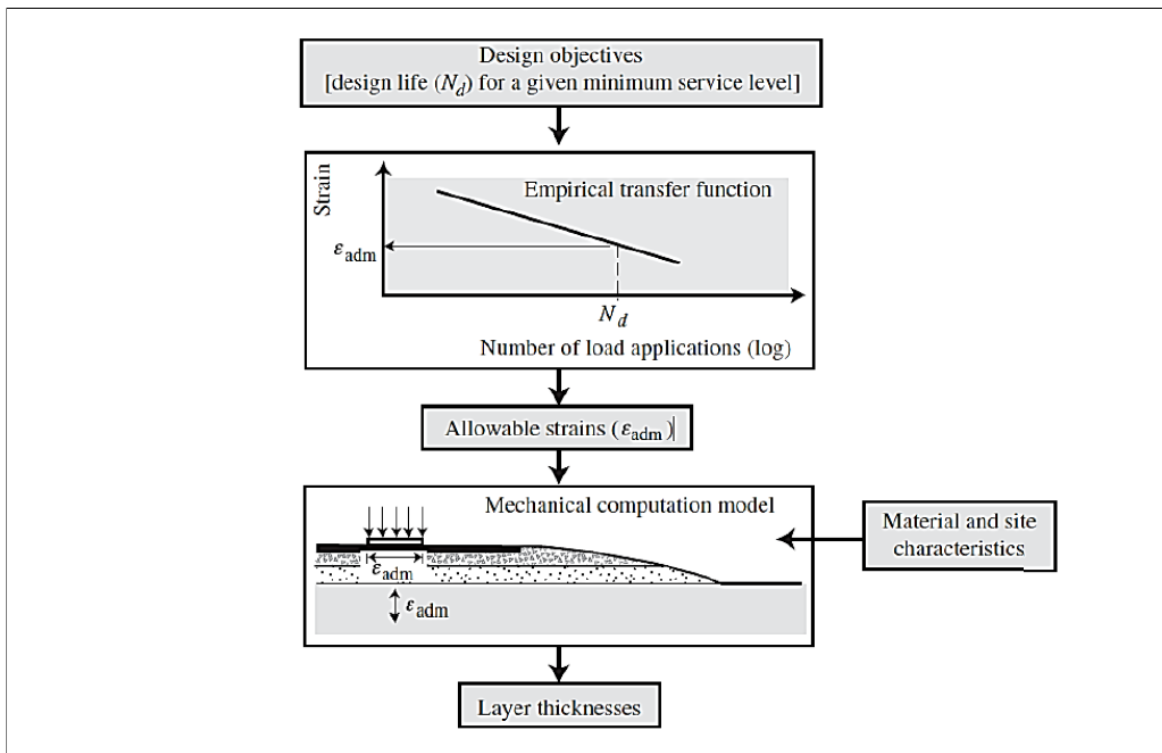


Figure 2-18: Principle of Mechanistic-Empirical Pavement Design (Dore & Zubeck, 2009)

## **2.9. Summary of Challenges, Research Gaps and Opportunity for Innovation**

Rutting remains a significant problem in areas such as approach intersections, turning lanes, and bus stops due to their different loading scenarios compared to other road sections. This results in pavement premature failures, which pose safety concerns and expenses to municipalities.

Research shows that stiffer asphalt binders are more resistant to rutting. Approach intersections require stiffer binders due to slow-moving traffic causing excessive shear stress. Low traffic loading frequencies make the asphalt binder more prone to plastic deformation, leading to the need for a heavy-duty asphalt mix design in these areas compared to other road sections.

In addition, there have been no specific studies conducted in Canada regarding mix design for approach intersections using very stiff asphalt binders like PG76-28 and PG82-28. Additionally, no literature in Canada has evaluated performance testing and specimen conditioning to differentiate heavy-duty asphalt mixes with high resistance to rutting and cracking. Therefore, the primary aim of this thesis is to develop a durable asphalt surface mix for approach intersections with high truck traffic in Southern Ontario.



## Chapter 3 Research Methodology and Materials

The goal of this study was to design a durable asphalt surface mix for approach intersections with high traffic volume in Ontario, providing resistance to rutting and other pavement performance issues such as fatigue and low-temperature cracking. The aim was also to establish a foundation for implementing performance specifications for heavy-duty asphalt mix resistance to rutting and cracking in Southern Ontario.

To achieve the goals of the study, the experimental work started with a field examination of six intersections with high traffic volume in York Region. These six locations were chosen to represent the asphalt mixes specified by York Region in the past decade. The conclusion of the study was that areas near the intersection had significantly deeper ruts, especially in areas where truck acceleration and deceleration occurred (Kafi Farashah et al., 2021b). Additionally, the study looked into three plant-produced asphalt mixes currently specified by York Region including two Hot Mix Asphalts (HMA) HMA-SP12.5 FC1 PG64-28 and HMA-SP12.5 FC1 PG70-28, and a Warm Mix Asphalt (WMA) WMA-SP12.5 FC2 PG70-28. "FC" stands for "friction course," and the aggregate for these asphalt mixes must come from pre-approved sources listed on the Ministry of Transportation Ontario's (MTO) Designated Sources for Materials (DSM). The investigation focused on evaluating the rutting resistance of the three asphalt mixes using various established and under-development test methods, including the Hamburg Wheel Tracking Test (HWTT), Flow Number Test, IDEAL Rutting Test (IDEAL-RT), and a modified version of the Uniaxial Shear Tester. The conclusion was that the conventional asphalt mixes used in York Region are inadequate in providing acceptable rutting resistance for high truck traffic approach intersections. To address the aforementioned issue, a total of seven lab-produced asphalt surface mixes including six SMA and an EME asphalt mixes were investigated. The SMA mixes were produced by using two Nominal Maximum Aggregate Sizes (NMAS), 9.5mm and 12.5mm, and three polymer-modified asphalt binders, namely PG70-28, PG76-28, and PG82-28. The EME mix was produced with a 12.5mm NMAS and PG82-28 asphalt binder. The SMA asphalt mixes included SMA9.5-PG70-28, SMA9.5-PG76-28, SMA9.5-PG82-28, SMA12.5-PG70-28, SMA12.5-PG76-28, and SMA12.5-PG82-28. The EME asphalt mix was EME12.5-PG82-28 which developed in 2019 by Baghaee Moghadam as part of his Ph.D. research at the University of Waterloo.

To investigate the asphalt binders' rheological properties, Dynamic Shear Rheometer (DSR), Multiple Stress Creep and Recovery (MSCR), Rotational Viscometers (RV), and Bending Beam Rheometer (BBR) tests were performed. To evaluate the response of the asphalt mixes to cracking and rutting resistance, friction, and moisture damage, the following tests were carried out: (1) Hamburg Wheel Tracking Test (HWTT), (2) IDEAL Rutting Test (IDEAL-RT), (3) Flow Number test, (4) Illinois Flexibility Index (I-FIT), (5) Indirect Tensile Asphalt Cracking Test (IDEAL-CT), (6) Dynamic Modulus, (7) Disc-Shaped Compact Tension Test (DC(T)), (8) British Pendulum Friction Test (BPT), and (9) Tensile Strength Ratio (TSR). The results of these tests were then analyzed. The statistical analysis of the test results was performed using Minitab© software and included analysis of variance (ANOVA), Tukey's HSD (Honestly Significant Difference) test, and pairwise t-test. The results also led to recommendations for preliminary specifications for the HWTT, I-FIT, IDEAL-CT, and DC(T) tests for the heavy-duty asphalt mixes studied. Additionally, a life cycle cost analysis was carried out to estimate the service life and associated maintenance/rehabilitation costs for the proposed heavy-duty asphalt surface mix.

### 3.1. Design of Experiments (DOEs)

The research conducted for plant-produced asphalt mixes used DOEs from Table 3-1 to Table 3-3, while the DOEs used for lab-produced asphalt mixes are presented in Table 3-4 to Table 3-9. The research plan methodology is shown in Figure 3-1.

**Table 3-1: DOE used for Plant-Produced Mixes to Determine Rutting Resistance**

| Research Variable        | Number of levels | Levels [Number of specimens per experiment]                                    |
|--------------------------|------------------|--|
| Performance-related test | 4                | HWTT [4]<br>IDEAL-RT [3]<br>Flow Number [3]<br>Uniaxial Shear Tester [3]       |
| Asphalt Mix              | 3                | HMA SP12.5 FC1 PG 64-28,<br>HMA SP12.5 FC1 PG 70-28<br>WMA-SP12.5 FC2 PG 70-28 |
| Temperature              | 3                | 44°C, 50°C, 58°C (Flow Number Test Conducted only at 58°C)                     |

**Table 3-2: DOE used for Plant-Produced Mixes to Determine Intermediate Temperature Cracking Resistance**

| <b>Research Variable</b> | <b>Number of levels</b> | <b>Levels [Number of specimens per experiment]</b>                             |
|--------------------------|-------------------------|--|
| Performance-related test | 1                       | I-FIT [3]  |
| Asphalt Mix              | 3                       | HMA SP12.5 FC1 PG 64-28,<br>HMA SP12.5 FC1 PG 70-28<br>WMA-SP12.5 FC2 PG 70-28 |
| Temperature              | 1                       | 25°C   |

**Table 3-3: DOE used for Plant-Produced Mixes to Determine Low Temperature Cracking Resistance**

| <b>Research Variable</b> | <b>Number of levels</b> | <b>Levels [Number of specimens per experiment]</b>                             |
|--------------------------|-------------------------|--|
| Performance-related test | 1                       | DC(T) [3]  |
| Asphalt Mix              | 3                       | HMA SP12.5 FC1 PG 64-28,<br>HMA SP12.5 FC1 PG 70-28<br>WMA-SP12.5 FC2 PG 70-28 |
| Temperature              | 1                       | -18°C  |

**Table 3-4: DOE used for Lab-Produced Mixes to Determine Rutting Resistance**

| <b>Research Variable</b> | <b>Number of levels</b> | <b>Levels [Number of specimens per experiment]</b>  |
|--------------------------|-------------------------|---|
| Performance-related test | 3                       | HWTT [4]<br>IDEAL-RT [3]<br>Flow Number [3]   |
| Asphalt Mix              | 7                       | SMA 9.5 PG70-28<br>SMA 9.5 PG76-28<br>SMA 9.5 PG82-28<br>SMA 12.5 PG70-28<br>SMA 12.5 PG76-28<br>SMA 12.5 PG82-28<br>EME 12.5 PG82-28 |
| Temperature              | 3                       | 44°C, 50°C, 58°C  |

**Table 3-5: DOE used for Lab-Produced Mixes to Determine Intermediate Temperature Cracking Resistance**

| <b>Research Variable</b> | <b>Number of levels</b> | <b>Levels [Number of specimens per experiment]</b>  |
|--------------------------|-------------------------|---|
| Performance-related test | 2                       | IDEAL-CT [3]<br>I-FIT [3]   |
| Asphalt Mix              | 7                       | SMA 9.5 PG70-28<br>SMA 9.5 PG76-28<br>SMA 9.5 PG82-28<br>SMA 12.5 PG70-28<br>SMA 12.5 PG76-28<br>SMA 12.5 PG82-28<br>EME 12.5 PG82-28 |
| Temperature              | 1                       | 25°C  |

**Table 3-6: DOE used to Determine the Dynamic Modulus Values of Lab-Produced Mixes**

| <b>Research Variable</b> | <b>Number of levels</b> | <b>Levels [Number of specimens per experiment]</b>  |
|--------------------------|-------------------------|---|
| Performance-related test | 1                       | Dynamic Modulus [2]   |
| Asphalt Mix              | 7                       | SMA 9.5 PG70-28<br>SMA 9.5 PG76-28<br>SMA 9.5 PG82-28<br>SMA 12.5 PG70-28<br>SMA 12.5 PG76-28<br>SMA 12.5 PG82-28<br>EME 12.5 PG82-28 |
| Temperature              | 5                       | -10°C, 4.4°C, 21.1°C, 37.8°C, 54.4°C  |
| Test Loading Frequency   | 6                       | 25, 10, 5, 1, 0.5, 0.1 Hz   |

**Table 3-7: DOE used for Lab-Produced Mixes to Determine Low Temperature Cracking Resistance**

| <b>Research Variable</b> | <b>Number of levels</b> | <b>Levels [Number of specimens per experiment]</b>  |
|--------------------------|-------------------------|---|
| Performance-related test | 1                       | DC(T) [3]   |
| Asphalt Mix              | 7                       | SMA 9.5 PG70-28<br>SMA 9.5 PG76-28<br>SMA 9.5 PG82-28<br>SMA 12.5 PG70-28<br>SMA 12.5 PG76-28<br>SMA 12.5 PG82-28<br>EME 12.5 PG82-28 |
| Temperature              | 1                       | -18°C   |

**Table 3-8: DOE used to Determine Surface Frictional Property of Lab-Produced Mixes**

| Research Variable        | Number of levels | Levels [Number of specimens per experiment]   |
|--------------------------|------------------|---|
| Performance-related test | 1                | Friction Test [2]   |
| Asphalt Mix              | 7                | SMA 9.5 PG70-28<br>SMA 9.5 PG76-28<br>SMA 9.5 PG82-28<br>SMA 12.5 PG70-28<br>SMA 12.5 PG76-28<br>SMA 12.5 PG82-28<br>EME 12.5 PG82-28 |
| Temperature              | 5                | 0°C, 10°C, 23°C, 37°C, 58°C   |
| Testing Condition        | 2                | Dry and Wet   |

**Table 3-9: DOE used to Determine Moisture Susceptibility of Lab-Produced Mixes using TSR Test**

| Research Variable        | Number of levels | Levels [Number of specimens per experiment]   |
|--------------------------|------------------|---|
| Performance-related test | 1                | TSR Test [6]  |
| Asphalt Mix              | 7                | SMA 9.5 PG70-28<br>SMA 9.5 PG76-28<br>SMA 9.5 PG82-28<br>SMA 12.5 PG70-28<br>SMA 12.5 PG76-28<br>SMA 12.5 PG82-28<br>EME 12.5 PG82-28   |
| Temperature              | 1                | 25°C  |
| Testing Condition        | 2                | Conditioned <ul style="list-style-type: none"> <li>• Saturation Level of 75%</li> <li>• 16 hours at -20°C</li> <li>• 24 hours at 60°C</li> <li>• 2 hours at 25°C</li> </ul> Unconditioned <ul style="list-style-type: none"> <li>• 2 hours at 25°C</li> </ul> |

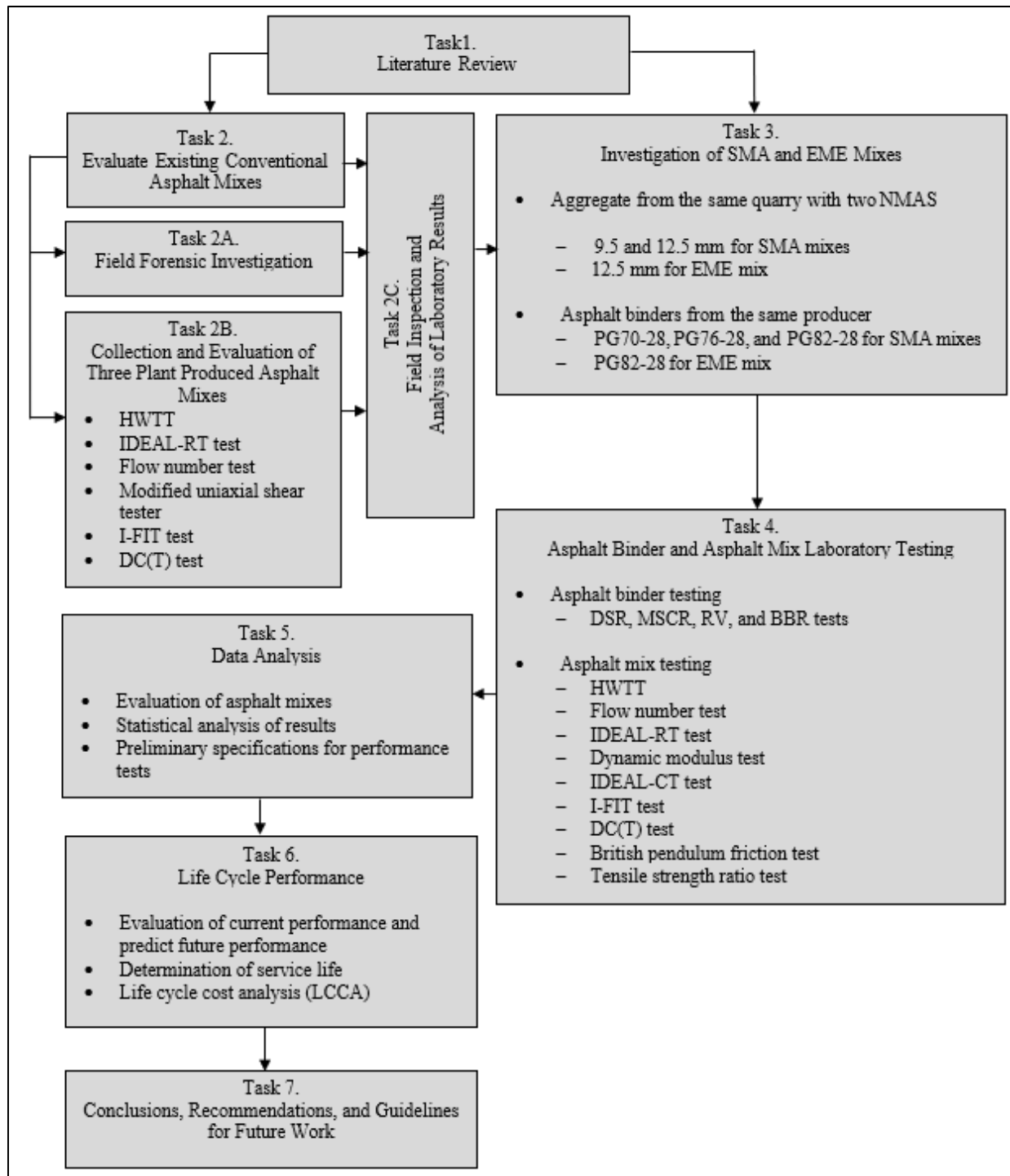


Figure 3-1: Research Plan Methodology

### 3.2. Experimental Materials

An evaluation was carried out on a variety of materials, including those produced in a controlled laboratory environment and those collected during plant production. Detailed descriptions of each material are given in subsequent sections.

#### 3.2.1. Plant-produced Asphalt Mixes

Physical properties of the plant-produced asphalt surface mixes are presented in Chapter 4.0.

#### 3.2.2. Lab-produced Asphalt Mixes

The aggregates used in this study were sourced from the same quarry to ensure consistency, while the asphalt binders came from the same producer. The type of aggregate used to produce the asphalt mixes was Gabbro, which is listed in the MTO's Designated Sources for Material (DSM). The properties of the aggregates are shown in Table 3-10.

**Table 3-10: Properties of Coarse and Fine Aggregates**

| <b>Fraction Retained on 4.75mm Sieve (Coarse Aggregates)</b> |  |   |                |
|--|--|---|----------------|
| <b>Standards</b>   | <b>Laboratory Test</b>                             | <b>Requirement</b>  | <b>Results</b> |
|  |  | <b>Traffic Level E (Design ESALs <math>\geq</math> 30 Millions)</b> |                |
| ASTM D5821   | Fractured Particles in Coarse Aggregates % minimum | <i>100/100</i>  | 100/100        |
| ASTM D4791   | Flat and Elongated Particles (5:1), % maximum      | <i>10</i>   | 0.4            |
| <b>Fraction Passing the 4.75mm Sieve (Fine Aggregates)</b>   |  |   |                |
| <b>Standards</b>   | <b>Laboratory Test</b>                             | <b>Requirement</b>  | <b>Results</b> |
|  |  | <b>Traffic Level E (Design ESALs <math>\geq</math> 30 Millions)</b> |                |
| LS-629   | Uncompacted Voids, % minimum                       | <i>45</i>   | 48.9           |
| ASSHTO T176  | Sand Equivalent, minimum                           | <i>50</i>   | 78.3           |

The asphalt binders used in the study were polymer-modified and included PG70-28, PG76-28, and PG82-28. The SMA mixes consisted of two Nominal Maximum Aggregate Sizes (NMAS), 9.5mm and 12.5mm, while the EME mix only used NMAS 12.5mm. Information regarding the aggregate gradation, asphalt binder content, specific bulk gravity of aggregate, and volumetric properties (such as VMA and VFA) of the asphalt mix design can be found in Table 3-11. Figure 3-2 displays the procedure used to produce the asphalt mixes in the CPATT laboratory at the

University of Waterloo. The mixes were subjected to a 4-hour short-term aging process at 135°C, in accordance with AASHTO R30, using an air-forced oven.

**Table 3-11: Physical Properties of Lab-Produced Asphalt Surface Mixes**

| Property  |                       |  | SMA 9.5<br>Aggregate<br>Gradation<br>(PG-70-28,<br>PG-76-28,<br>and<br>PG-82-28) | <i>OPSS 1151<br/>Requirement<br/>for SMA<br/>12.5</i> | SMA 12.5<br>Aggregate<br>Gradation<br>(PG-70-28,<br>PG-76-28,<br>and<br>PG-82-28) | <i>Taher Baghaee<br/>Moghaddam –<br/>EME 12.5</i>                      | EME<br>12.5<br>PG82-<br>28   |
|---|-----------------------|--|--|---|---|--|------------------------------|
| Aggregate<br>Gradation<br>(%<br>Passing)          | Sieve<br>Size<br>(mm) | <i>OPSS 1151<br/>Requirement<br/>for SMA 9.5</i> |  |   |   |  |                              |
|   | 25                    | 100  | 100  | 100   | 100   | 100  | 100                          |
|   | 19                    | 100  | 100  | 100   | 100   | 100  | 100                          |
|   | 12.5                  | 100  | 100  | 90-100  | 93.1  | 94-100   | 94.5                         |
|   | 9.5                   | 70-95  | 83.7   | 50-80   | 70.7  | 78-88  | 82.5                         |
|   | 6.7                   | -  | 46.2   | -   | 44.6  | 60-75  | N/A                          |
|   | 4.75                  | 30-50  | 32   | 20-35   | 26.1  | 42-60  | 51.5                         |
|   | 2.36                  | 20-30  | 22.1   | 16-24   | 18.4  | 25-38  | 31.4                         |
|   | 1.18                  | max. 21  | 17.6   | -   | 15.4  | 18-25  | 21.3                         |
|   | 0.6                   | max. 18  | 14.7   | -   | 13.5  | 12-19  | 15.1                         |
|   | 0.3                   | max. 15  | 12.6   | -   | 12.2  | 9-12   | 10.7                         |
| 0.15  | -                     | 10.5   | -  | 10.3  | 7-9   | 7.6  |                              |
| 0.075   | 8-12                  | 8.6  | 8-11   | 8.7   | 4-6   | 4.9  |                              |
| Additive<br>(Cellulose Fibre)                     |                       | -  | 0.3% of Mix  | -   | 0.3% of Mix   | -  | N/A                          |
| Property  |                       | <i>OPSS 1151 -<br/>2021</i>                      | SMA 9.5<br>(PG-70-28,<br>PG-76-28,<br>and<br>PG-82-28)                           | <i>OPSS 1151 -<br/>2021</i>                           | SMA 12.5<br>(PG-70-28,<br>PG-76-28,<br>PG-82-28)                                  | <i>Conventional<br/>Mix<br/>(Gouvernement<br/>du Quebec,<br/>2003)</i> | EME<br>12.5 -<br>PG82-<br>28 |
| N <sub>des</sub>                                  |                       | -  | 100  | -   | 100   |  | 100                          |
| N <sub>ini</sub>                                  |                       | -  | 8  | -   | 8   |  | 10                           |
| N <sub>max</sub>                                  |                       | -  | 160  | -   | 160   |  | 200                          |
| Air Voids (%) at<br>N <sub>des</sub>              |                       | 4.0  | 4.0  | 4.0   | 4.0   | 4.0-7.0  | 3.7                          |
| Voids in Mineral<br>Aggregate, VMA<br>(% minimum) |                       | 17.0   | 17.9   | 17.0  | 17.6  | 14   | 15.1                         |
| Asphalt Binder<br>Performance<br>Grade            |                       | -  | PG-70-28,<br>PG-76-28 and<br>PG-82-28  | -   | PG-70-28,<br>PG-76-28,<br>and<br>PG-82-28   | -  | PG 82-<br>28                 |
| Voids Filled with<br>Asphalt, VFA (%)             |                       | -  | 77.9   | -   | 78.3  | 65-75  | 75.4                         |
| Bulk Specific<br>Gravity (G <sub>mb</sub> )       |                       | -  | 2.892  | -   | 2.924   | 2.924  | 2.924                        |
| Dust Proportion,<br>DP                            |                       | -  | 1.5  | -   | 1.6   | 0.6-1.2  | 1.08                         |



| Property                               | OPSS 1151 Requirement for SMA 9.5 | SMA 9.5 Aggregate Gradation (PG-70-28, PG-76-28, and PG-82-28) | OPSS 1151 Requirement for SMA 12.5 | SMA 12.5 Aggregate Gradation (PG-70-28, PG-76-28, and PG-82-28) | Conventional Mix (Gouvernement du Quebec, 2003) | EME 12.5 PG82-28 |
|--|-----------------------------------|--|------------------------------------|---|---|------------------|
| Tensile Strength Ratio, TSR (%)        | 70                                | PG70-28 = 91.9<br>PG-76-28 = 93.1<br>PG-82-28 = 95.2           | 70                                 | PG-70-28 = 83.5<br>PG-76-28 = 85.1<br>PG-82-28 = 87.3           | 70  | 93.5             |
| Asphalt Cement Content (%)             | -                                 | 5.7  | -                                  | 5.7   | -   | 5                |
| Voids in Coarse Aggregate, $VCA_{mix}$ | $<VCA_{DRC}$                      | 38.5<42.1  | $<VCA_{DRC}$                       | 38.9<42.6   | -   | -                |
| Drain Down (%)                         | Max 0.3                           | 0.1  | Max 0.3                            | 0.1   | -   | -                |

Notes: OPSS is Ontario Provincial Standard Specification,  $N_{des}$ ,  $N_{ini}$ ,  $N_{max}$  are number of gyrations at different compaction levels (design, initial, and maximum), and  $G_{mb}$  is bulk specific gravity.



Figure 3-2: Laboratory Procedure for SMA and EME Asphalt Mixes Production in CPATT Laboratory

### **3.3. Characterization of Asphalt Binders**

The Dynamic Shear Rheometer (DSR) and Multiple Stress Creep and Recovery (MSCR) tests, according to AASHTO T315 and AASHTO T350 test methods, respectively, were conducted to characterize the asphalt binders. The DSR test was used to verify the PG (performance grade) of the asphalt binder and to determine its high and intermediate temperature grades. The MSCR test was employed to calculate the average percent recovery (Re) at 3.2 kPa and non-recoverable creep compliance (Jnr) at 3.2 kPa. In addition, the viscosity of the asphalt binders was determined using Rotational Viscometers (RV) in accordance with AASHTO T316. To assess performance at low temperature, the Bending Beam Rheometer (BBR) test was performed on the long-term aged asphalt binder, in accordance with AASHTO T313, to determine its low temperature grades, creep stiffness (S), and the rate of change of creep stiffness (m) at 60 seconds in the linear viscoelastic region.

### **3.4. Asphalt Mixture Characterization**

This section outlines the test methods used to evaluate both plant-produced and lab-produced asphalt mixes in the state-of-the-art pavement laboratory at CPATT, located at the University of Waterloo. The methods used to create specimens for the tests are also detailed in this section.

#### **3.4.1. Specimen Fabrication**

The CPATT Superpave Gyratory Compactor (SGC) was used to fabricate compacted specimens (as shown in Figure 2-14). The specimens had a diameter of 150mm and height of 178mm (for I-FIT, DC(T), Flow Number, and Dynamic Modulus tests), a height of 62mm (for HWTT, IDEAL-RT, IDEAL-CT, and BPT tests), and a height of 94mm (for TSR). They were compacted with a pressure of 600 kPa in accordance with AASHTO PP 60-13 and were compacted to achieve a target air void of  $7 \pm 0.5$  percent.

#### **3.4.2. Hamburg Wheel Tracking Test (AASHTO T324)**

The Hamburg Wheel Tracking Device (HWTD) was used to evaluate the rutting resistance of the asphalt mixes (as shown in Figure 3-3). The test, performed in accordance with AASHTO T324 (AASHTO, 2016), was capable of evaluating the moisture sensitivity of compacted asphalt mixes by tracking a 158-lb (705-N) load steel wheel across the surface of a gyratory-compacted specimen (150mm in diameter and 62mm high) in a hot water bath maintained at 50°C. This allowed for the

evaluation of the sample's performance in high in-service temperatures and in the presence of moisture (Brown et al., 2009). The Hamburg Wheel Tracking test was performed at additional test temperatures of 44°C and 58°C to assess the effect of temperature on the rutting resistance and moisture damage of the asphalt mixes in this study. By using Low Voltage Displacement Transducers (LVDTs), the accumulated permanent deformation was measured to determine the rutting susceptibility of the asphalt mixes. Figure 3-3 also shows a typical specimen before and after testing. The moisture susceptibility was evaluated by computing the Stripping Inflection Point (SIP), which is defined as the intersection of the slopes of stripping and rutting. SIP is reported as the number of passes at which there was a sudden increase in rut depth. Figure 3-4 illustrates SIP and its relation to overall behaviour of a mix susceptible to moisture damage (NCHRP, 2011). The test was terminated either when the specimen reached a total rut depth of 12.5mm or after 20,000 wheel-track passes, whichever happened first.

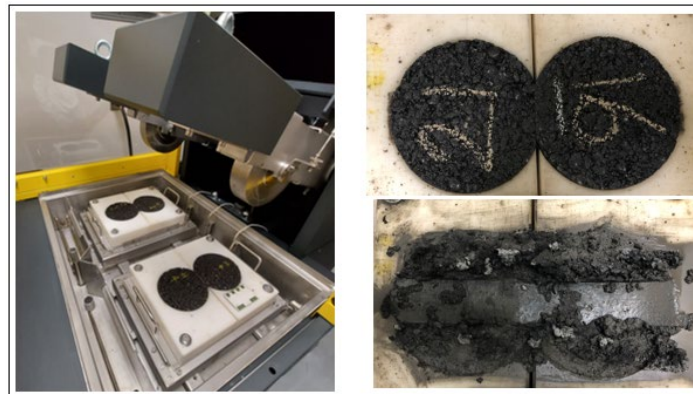


**Figure 3-3: Hamburg Wheel Track Device Setup (left) and Test Specimens Before and After (Right)**

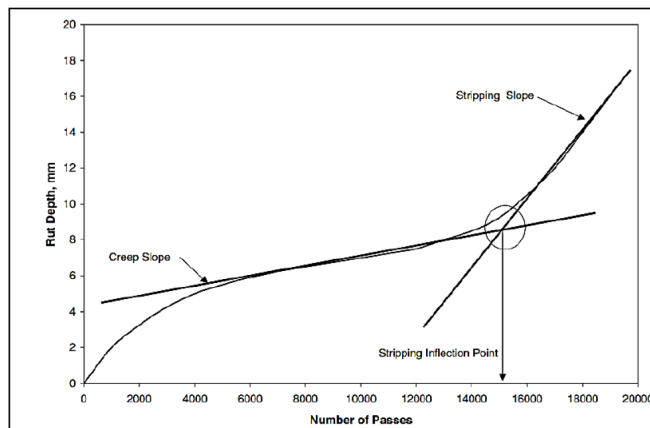


**Figure 3-4: Typical Results from Hamburg Wheel Tracking Test (NCHRP, 2011)**

### 3.4.3. Flow Number (FN) Test (AASHTO T378)

The Repeated Load Permanent Deformation test or Flow Number (FN) test was developed to predict the rutting behavior of asphalt mixes. The FN test is conducted according to the AASHTO T 378 specification (AASHTO, 2017) and involves repeated compressive loading cycles. Each cycle consists of a 0.1 second loading time and 0.9 second resting time. The test measures the vertical accumulated permanent strains as a function of the number of loading cycles. The test involves applying compressive load to a specimen with a 100-mm diameter and a height of 150 mm. The FN test was conducted at three temperatures (44°C, 50°C, and 58°C). The cyclic loading was applied using an unconfined pressure load of 600 kPa. The test is terminated either when the asphalt mix specimen fails or when 10,000 loading cycles have been reached, whichever occurs first. The Flow Number is defined as the loading cycle at which the minimum strain rate occurs. Figure 3-5 shows a typical specimen before and after testing.



Figure 3-5: Flow Number Test Specimens Before (Left) and After (Right)

### 3.4.4. IDEAL Rutting Test (ASTM WK71466)

The IDEAL Rutting Test (IDEAL-RT), developed by Fujie Zhou at Texas A&M University. The test evaluates the shear resistivity of an asphalt mixture (Cooper, 2021). The test involves applying compressive load to a cylindrical specimen with a diameter of 150 mm and height of 62 mm. The specimen is constrained by a rigid fixture and the compressive load is applied at a rate of 50 mm/min. The test temperature can vary, but it is typically performed at 50°C to match the Hamburg Wheel Tracking Test. However, in this specific research, the tests were conducted at three different temperatures (44°C, 50°C, and 58°C).

As shown in Figure 3-6, two separate shear planes are developed in the specimen when compressive load is applied. The test provides a measure of the maximum shear resistivity of the asphalt mix, referred to as RT-Index (Cooper, 2021). A higher RT-Index value indicates a greater resistance to shear deformation. The test determines the maximum vertical displacement at peak load, which is the result of both non-damage stage deformation and damage stage deformation. The study conducted by Fujie Zhou showed that the IDEAL-RT test had a good correlation with both HWTT and Asphalt Pavement Analyzer (APA) tests (Cooper, 2021). Shear strength of asphalt mix is calculated from the measured maximum load as indicated in Equation 3-1 (ASTM, 2021)

$$\tau_f = 0.356 \times \frac{P_{max}}{t \times w} \quad (3-1)$$

Where:  $\tau_f$  is the shear strength (Pa);  
 $P_{max}$  is the maximum load (N);  
 $t$  is the specimen thickness (m); and  
 $w$  is the width of upper loading strip (=0.0191 m).

Rutting tolerance index ( $RT_{Index}$ ) is calculated from the shear strength, as per Equation 3-2 (ASTM, 2021).

$$RT_{Index} = 6.618 \times 10^{-5} \times \frac{\tau_f}{1Pa} \quad (3-2)$$

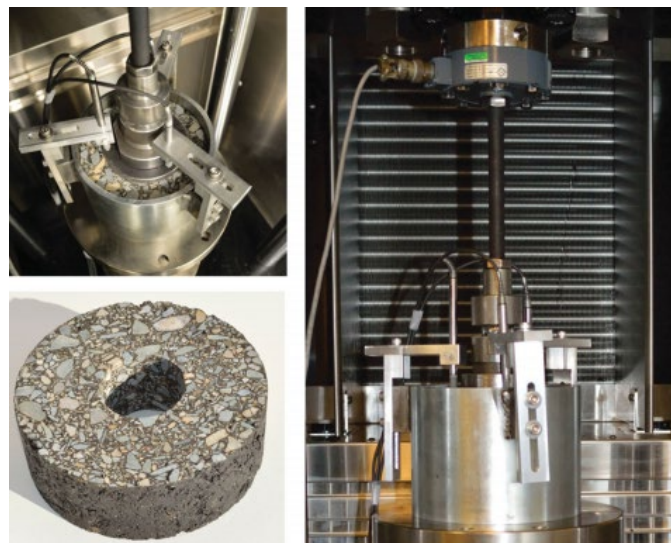
Where:  $RT_{Index}$  is the rutting tolerance index; and  
 $\tau_f$  is the shear strength calculated from Equation 3-1 (Pa).



Figure 3-6: IDEAL-RT Test Fixture with Test Specimen Before (Left) and After Test (Right)

### 3.4.5. Uniaxial Shear Tester (AASHTO T320-07)

The Uniaxial Shear Tester (UST) was developed through a collaboration between the University of California Pavement Research Centre and the Czech Technical University in Prague. The test measures the shear resistance of cylindrical specimens that are 150 mm in diameter and 50 mm in height. A 50-mm diameter hole is cored through the center of the specimen to accommodate a cylindrical steel cylinder. Shear loading is then applied through a knee joint on the steel insert (as shown in Figure 3-7), and the vertical deflection of the steel insert is measured during loading (Zak et al., 2017). To understand the correlation between the UST and the Repeated Shear at Constant Height (RSCH) tests, 30,000 cycles of haversine shear pulses (69 kPa for 0.1 second followed by 0.6 seconds of rest periods) were applied at a test temperature of 50°C (Zak et al., 2017). The study concluded that the shear values obtained from the UST test have a good correlation with the RSCH test. If there are limitations in the loading frame, monotonic loading can also be adopted for the UST test.



**Figure 3-7: Uniaxial Shear Tester (Top Right), Hollow Cylindrical Specimen (Bottom Right), and Uniaxial Shear Tester Setup (Left) (Zak et al., 2017)**

The UST test was performed in a monotonic mode due to test frame availability, instead of the cyclic mode described by Zak et al. The test specimen dimensions were the same as the HWTT test (150 mm in diameter and 62 mm in height) with a 50-mm diameter hole is cored through the center of the specimen to accommodate a cylindrical steel cylinder. Figure 3-8 shows the monotonic test setup and the specimens before and after the shear testing. The test was conducted at 50°C and 58°C, with loading rates of 50, 25, and 12.5 mm/min to determine the shear resistance

of the asphalt mixes. It should be noted that testing at 44°C was attempted, but the 50kN load cell was maxed out during the test.



Figure 3-8: Uniaxial Shear Tester Monotonic Setup, and Test Specimens Before and After Testing

### 3.4.6. Dynamic Modulus Test (AASHTO T 342)

The Dynamic Modulus test was conducted to determine the linear viscoelastic characteristics of asphalt mixes. The test was performed on cylindrical specimens that measured 100mm in diameter and 150mm in height, which were cored and cut from a larger compacted specimen measured 150mm in diameter and 180mm in height as shown in Figure 3-9. The test also performed at five temperatures (-10°C, 4.4°C, 21.1°C, 37.8°C, 54.4°C) and six frequencies (25, 10, 5, 1, 0.5, 0.1 Hz) by applying sinusoidal loading and measuring the deformations. Dynamic modulus, abbreviated as  $E^*$  (pronounced as E-star), is used to relate stress to describe the relationship between stress and strain for viscoelastic materials like asphalt mixes (NCHRP, 2011).

This relationship is determined by performing a laboratory test in which the stress applied is given by Equation 3-3:

$$\sigma = \sigma_o \sin(\omega t) \quad (3-3)$$

Where:

- $\sigma_o$  = peak (maximum) stress (kPa)
- $\omega$  = angular velocity (Hz)
- $t$  = time (seconds)

The corresponding strain is expressed by Equation 3-4:

$$\varepsilon = \varepsilon_o \sin(\omega t + \phi) \quad (3-4)$$

Where:

- $\varepsilon_o$  = peak (maximum) strain

$\phi$  = phase angle (degrees)

Asphalt mixes behave both viscous and elastic, and the relationship between the maximum stress and strain is commonly used in terms of dynamic modulus  $|E^*|$  to quantify such behavior as shown in Equation 3-5.

$$|E^*| = \sigma_o / \epsilon_o \quad (3-5)$$

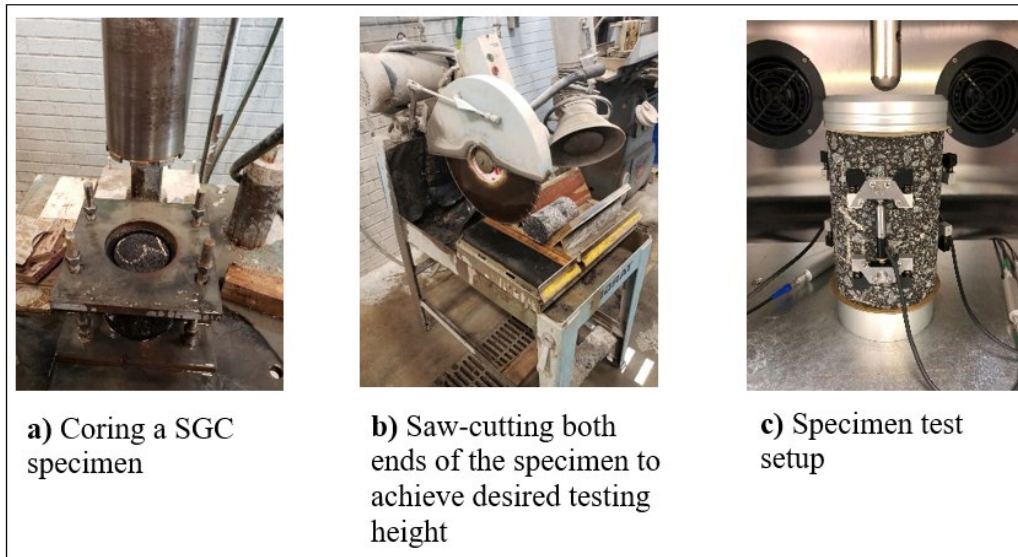


**Figure 3-9: Specimen Preparation (a) and (b) and Specimen Test Setup (c)**

The master curve represents the behavior of the asphalt mix at various temperatures and is used to predict the viscoelastic response of the mix under different loading conditions. The master curve is created by fitting the dynamic modulus results obtained at different temperatures to a reference temperature of 21.1°C using a second-order polynomial fit (Equation 3-6). The fitting process is performed using the "Solver" analysis tool in Microsoft Excel© (Witczack, 2005). The AASHTO PP62-09 procedure provides guidelines for the creation of the master curve.

$$\log|E^*| = \delta + \frac{\alpha}{1 + e^{(\beta + \gamma \log(tr))}} \quad (3-6)$$

Where :

- $\delta$  = minimum value of  $E^*$  (MPa)
- $\alpha$  = span of modulus values
- $\beta, \gamma$  = shape factors
- $t_r$  = time of loading at reference temperature 21.1°C

### 3.4.7. IDEAL-CT (ASTM D8225)

The Indirect Tensile Asphalt Cracking Test (IDEAL-CT) is a test that evaluates the resistance of asphalt mixtures to intermediate crack propagation. It is performed on cylindrical specimens with



a diameter of 150 mm and height of 62±1 mm at a temperature of 25 °C and a loading rate of 50 mm/min as shown in Figure 3-10. The CT-index, which is a measure of the resistance of the asphalt mixture, is determined from the load-displacement curve obtained from the test (as shown in Figure 3-11) and is calculated using Equation 3-7. A larger CT-index value indicates a higher resistance to intermediate crack propagation.



**Figure 3-10: IDEAL-CT Test Loading Fixture**

$$CT_{\text{index}} = \frac{G_f}{|m_{75}|} \times \left( \frac{L_{75}}{D} \right) \times \left( \frac{t}{62} \right) \quad (3-7)$$

Where:

- $G_f$  =Fracture energy (AREA under the curve normalized by the area fractured)
- AREA =Area under the load-displacement curve, until a terminal load of 0.1 kN is reached
- $m_{75}$  =Absolute value of slope at 75% of post peak load
- $L_{75}$  =Vertical displacement when load is reduced to 75% of post peak load
- $D$  =Specimen diameter
- $t$  =Specimen Thickness

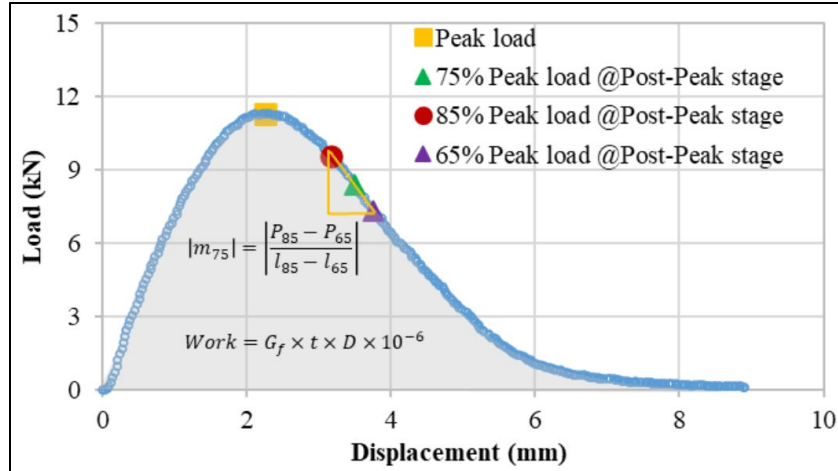


Figure 3-11: IDEAL-CT Load-Displacement Curve and Test Parameter (Chen et al., 2021)

### 3.4.8. Illinois Flexibility Index Test (I-FIT) Test (AASHTO TP124)

The I-FIT test is a test method used to evaluate the resistance of asphalt mixes to intermediate temperature cracking. It follows the AASHTO TP124 test method as described in AASHTO TP124 (2016). To perform the test, a SGC compacted specimen with a diameter of 150 mm and height of 180 mm is cut into two discs with a height of 50 mm. These discs are then cut in half using a tile-saw to create two test specimen replicates. A notch with a length of  $15 \pm 0.5$  mm and width of  $1.5 \pm 0.5$  mm is then cut in the middle of the flat side of each half-disc as shown in Figure 3-12. The I-FIT test samples must be conditioned at  $25 \pm 0.5^\circ\text{C}$  for 2 hours  $\pm$  10 minutes in an environmental chamber or water bath before the test starts. The specimen is mounted on its flat side on two roller supports on the testing frame and tested at  $25^\circ\text{C}$ , as shown in Figure 3-13. During the test, a monotonic load is applied by the testing machine at a rate of 50 mm/min until a crack initiates at the tip of the notch and propagates upwards. The test stops as soon as the post-peak load reaches 0.1 kN. The I-FIT test provides parameters such as fracture energy, post-peak load slope, strength, and the flexibility index (FI). FI is an empirical index that is computed as shown in Equation 3-8.

$$FI = \frac{G_f}{|m|} (0.01) \quad (3-8)$$

Where:

- FI = Flexibility Index
- $G_f$  = work of fracture, calculated as the area under the load-displacement curve ( $\text{J}/\text{m}^2$ ) by dividing  $W_f$  (work of fracture) by the ligament area.
- $m$  = slope of post-peak softening curve

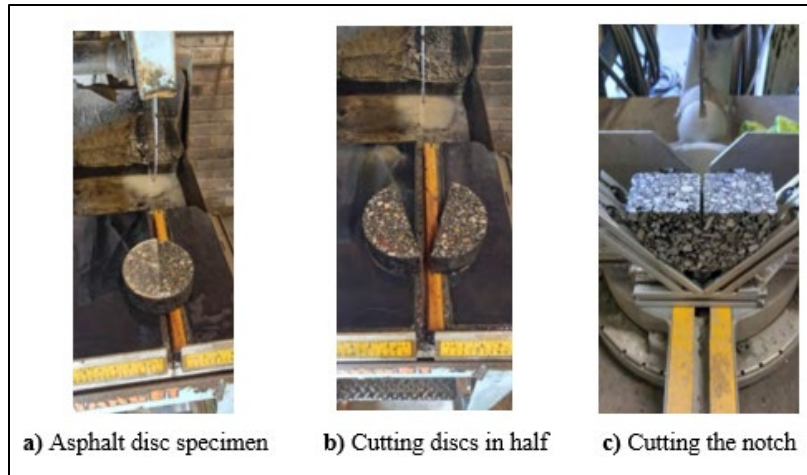


Figure 3-12: Specimen Preparation for I-FIT Test

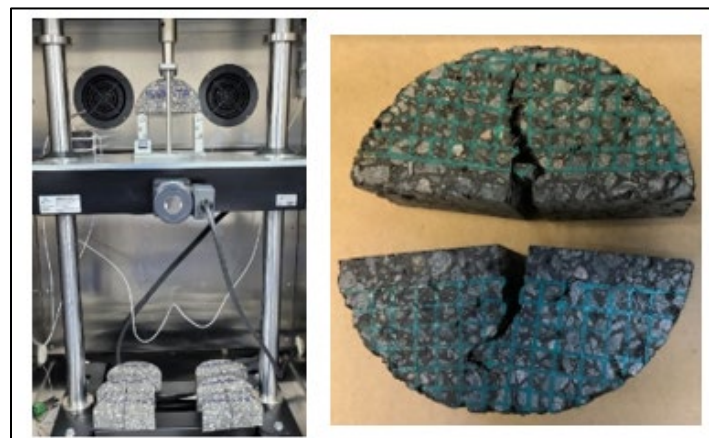


Figure 3-13: I-FIT Test Loading Fixture (Left) After Test (Right)

### 3.4.9. Disk-Shaped Compact Tension DC(T)Test (ASTM D7313)

The DC(T) test is designed to evaluate the fracture behavior of asphalt mixes at low temperatures. The test specimens must have a diameter of  $150 \pm 10$  mm, a thickness of  $50 \pm 5$  mm, a notch depth of  $62 \pm 3$  mm, and a notch width of  $1.5 \pm 0.5$  mm. The specimens must be conditioned for 8-16 hours in a freezer at a temperature  $10$  °C higher than the low temperature grade of the PG asphalt binder used in the asphalt mix. During the test, as shown in Figure 3-14, the specimen is pulled apart from the loading holes in a Crack Mouth Opening Displacement (CMOD) controlled mode with a displacement rate of 1 mm/min. The test ends when a crack has propagated such that the post-peak load level has been reduced to 0.1 kN. The fracture energy ( $G_f$ ) ( $J/m^2$ ) is calculated by determining the area under the Load-CMOD displacement curve, which is then normalized by the

product of the ligament length and thickness (fractured area) of the specimen, as shown in Equation 3-9. The larger the  $G_f$  value, the more resistant the asphalt mix is to low-temperature cracking.

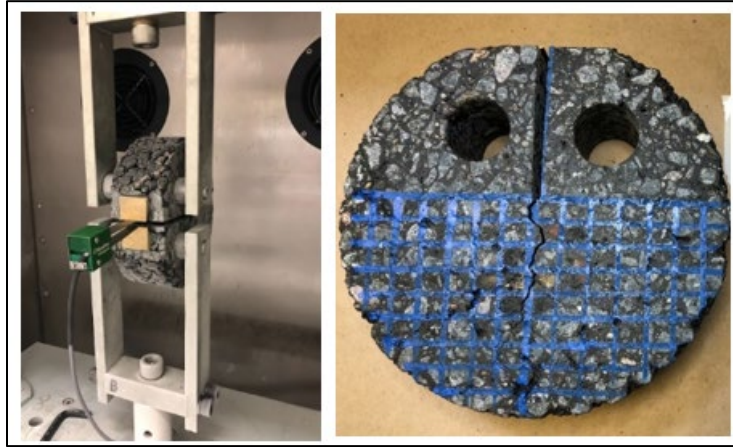


Figure 3-14: DC(T) Test Loading Fixture (Left) After Test (Right)

$$G_f = \frac{\text{Area}}{B \cdot L} \quad (3-9)$$

Where:

- $G_f$  = Fracture energy in  $\text{J/m}^2$ ,
- Area = Area under the load–CMODFIT curve until the terminal load of 0.1 kN is reached,
- B = Specimen thickness in m, 0.050 m
- L = Ligament length, usually around 0.083 m.

#### 3.4.10. British Pendulum Friction Testing (ASTM E 303-93)

The surface friction of the asphalt mixes was determined using the British Pendulum Skid Resistance Tester, in accordance with the ASTM E 303-93 Standard Test Method. The specimens were prepared using the CPATT SGC and measured 150 mm in diameter. The test was conducted at five different temperatures (0, 10, 23, 37, and 58°C) under both dry and wet conditions. The surface friction was measured as the amount of energy loss during the contact between the rubber slider and the test surface, and was expressed in terms of a British Pendulum Number (BPN) as shown in Figure 3-15. The greater the friction between the slider and the test surface, the larger the BPN reading. In the wet condition, approximately 45 mL of distilled water was sprayed across the specimen at the start of each swing and 5 mL of water was sprayed on the specimen surface between swings to replace the lost water.

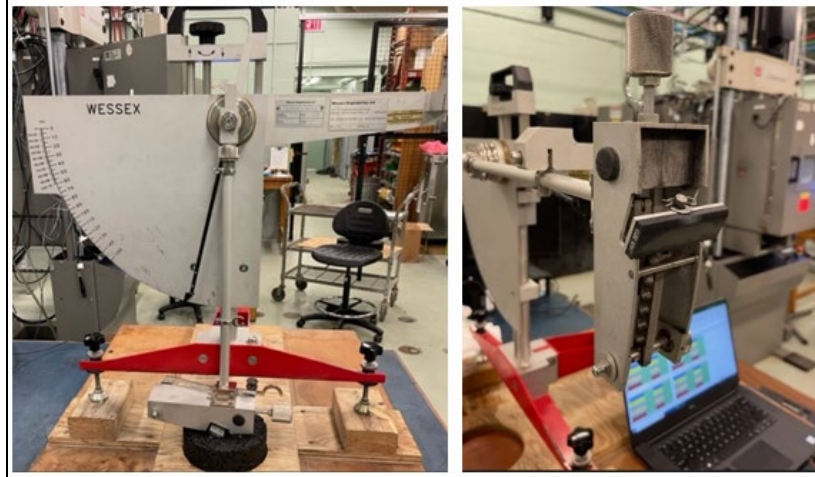


Figure 3-15: British Pendulum Skid Resistance Tester Fixture (Left) Rubber Slider (Right)

### 3.4.11. Tensile Strength Ratio Test (TSR) (ASTM D6931)

To determine the moisture sensitivity of asphalt mixes the TSR test employed using Indirect Tensile Strength (IDT) (Figure 3-16) apparatus in accordance with ASTM D6931-12, “Standard Test Method for Indirect Tensile Strength of Bituminous Mixtures” (ASTM, 2012). Six specimens each measuring 150 mm in diameter and  $100 \pm 5$  mm in height and target air voids of  $7.0\% \pm 0.5\%$  were prepared and were divided in two groups a) conditioned and b) unconditioned. The three specimens (unconditioned) were placed in an environmental chamber at  $25^{\circ}\text{C}$  for 2hrs to measure the tensile strength. The second group of specimens was subjected to a saturation process and a freeze-thaw cycle before being conditioned at  $25^{\circ}\text{C}$  for 2 hours. The saturation process involved vacuuming the specimens to  $75 \pm 3\%$  saturation and then subjecting them to a freeze-cycle of 16 hours at  $-20^{\circ}\text{C}$  followed by a thaw-cycle in a water bath for 24 hours at  $60^{\circ}\text{C}$ . The level of saturated air voids in the specimens was adjusted by applying a vacuum partial pressure of 13 to 67 kPa for 3 to 10 minutes. The Indirect Tensile Strength (IDT) of the specimens was determined by conducting IDT tests at a displacement rate of 50 mm/min on both conditioned and unconditioned specimens. The IDT strength was calculated using Equation 3-10.

$$S_t = \frac{2000P}{\pi t D} \quad (3-10)$$

Where:

- $S_t$  = IDT strength, kPa
- $P$  = Maximum load, N
- $t$  = sample thickness immediately before test, mm
- $D$  = sample diameter, mm; and
- $\pi$  = 3.14

The tensile strength ratio (TSR) was then calculated as follow (Equation 3-11)

$$\text{TSR} = \frac{S_t \text{ Conditioned}}{S_t \text{ Unconditioned}} \quad (3-11)$$

where  $S_t$  Conditioned is the indirect tensile strength at wet condition (kPa), and  $S_t$  Unconditioned is the indirect tensile strength at dry condition (kPa).



**Figure 3-16: Indirect Tensile Strength Testing Equipment**

### **3.5. Preliminary Specification for performance Tests**

The use of efficient and practical performance-related specifications is important in the mix design process and in the Quality Control and Quality Assurance of asphalt mixes. The performance-verified volumetric design was used to develop preliminary specifications for selected performance tests to address the various types of distress that can occur in high-traffic volume approach intersections, considering both traffic and climate conditions.

### **3.6. Life cycle Cost Assessment**

The purpose of a life cycle assessment is to identify a set of planned actions that can provide the desired level of service in a sustainable manner at the lowest life cycle cost. The conceptual framework for pavement management, as shown in Figure 3-17, shows that performance prediction models, desired level of service, treatment type, cost, and benefit, as well as budget, are

crucial elements in the life cycle cost assessment. The life cycle cost analysis was performed to compare the benefits of using heavy-duty asphalt mixes as a surface course to those of the asphalt mixes currently specified by the York Region.

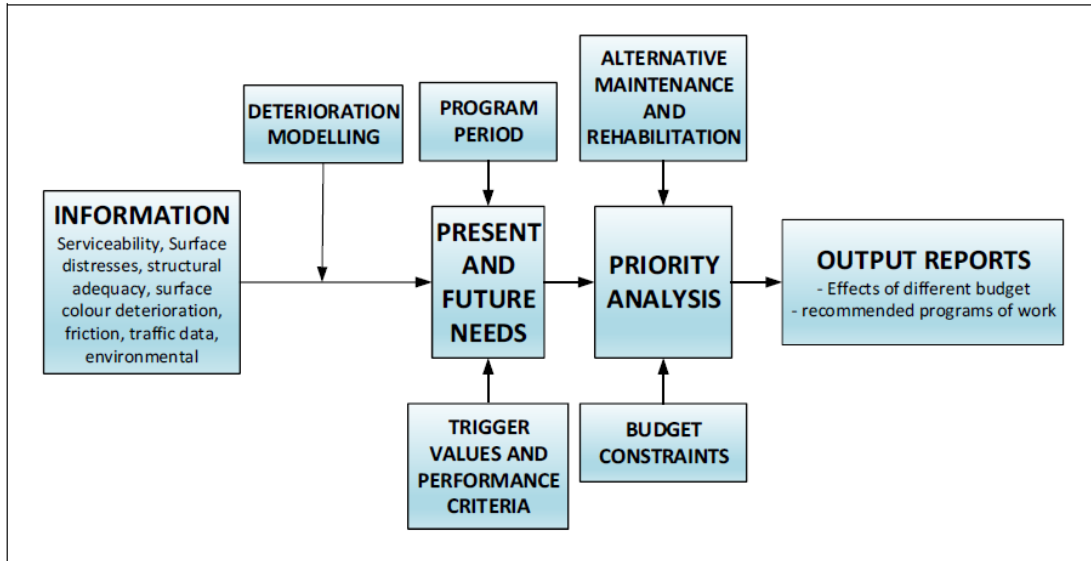


Figure 3-17: Conceptual Framework of Pavement Management (TAC, 2014)

### 3.7. Summary

This chapter presented the research methodology and its corresponding tasks used in this study to achieve its two main objectives. These objectives include 1) the development of a sustainable surface course asphalt mix for heavy truck traffic approach intersections in Southern Ontario and 2) the development of preliminary specifications for performance tests to address the resistance to rutting and cracking of heavy-duty asphalt mixes in high-traffic volume approach intersections.

## **Chapter 4 Field and Laboratory Methods of Evaluating Rutting**

*Parts of this chapter have been published in a paper submitted to the Canadian Technical Asphalt Association (CTAA) conference in 2021 (Kafi Farashah, 2021c).*

Six approach intersections were selected by York Region's Transportation Asset Management staff to investigate the in-service performance and identify any need for material improvement. The selected approach intersections were investigated by field work, which included manual rut depth measurement and geotechnical investigation, such as extracting core specimens, boreholes, and conducting transverse Ground Penetration Radar (GPR) surveys. In addition, three (3) currently specified plant-produced asphalt surface mixes by York Region were investigated to evaluate their rutting resistance: HMA-SP12.5 FC1 PG64-28, HMA-SP12.5 FC1 PG70-28, and WMA-SP12.5 FC2 PG70-28. The research used HWTT, Flow Number, IDEAL-RT, and modified Uniaxial Shear Tester tests to measure the shear properties of the asphalt mixes.

### **4.1. Field Investigation**

#### **4.1.1. Site Information**

To study the in-service performance and root cause of the rutting at York Region, six (6) approach intersections were selected in this research. The research consists of conducting field measurement of rutting depth and geotechnical investigation, such as extracting core specimens, boreholes, and conducting transverse Ground Penetration Radar (GPR) surveys. The goal was to cover the three most used conventional asphalt mixes for the surface course layer in the York Region over the past decade. Table 4-1 lists the main attributes of selected approach intersections. As presented in Table 4-1, the asphalt surface layer of all approach intersections except for Site "A" constructed using modified asphalt binder. Site A experienced the least Equivalent Single Axle Loads (ESALs) and was in-service relatively in shorter period of time compared to all other sections. A detailed field measurements of rut depth including the lanes (through lanes, turning lanes, etc.) where the geotechnical investigation such as extracting core specimens, boreholes, and transverse Ground Penetration Radar (GPR) conducted can be found in the Canadian Society of Civil Engineering (CSCE) 2021 annual conference proceedings (Kafi Farashah et al., 2021b).



**Table 4-1: Site Location Information**

| Site ID | Intersection Location               | Number of Lanes <sup>(1)</sup> | Surface Layer Mix Type          | Surface Layer Thickness (mm) | Base Layer Thickness (mm) | Truck % | ESALs <sup>(2)</sup> | Last Rehabilitation Year | Surface Layer Age |
|---------|-------------------------------------|--------------------------------|---------------------------------|------------------------------|---------------------------|---------|----------------------|--------------------------|-------------------|
| A       | Kennedy Road & Elgin Mills Road E   | 3                              | SP12.5 PG58-28 Category 'C'     | 55                           | 80                        | 2.9     | 517,740              | 2014                     | 6                 |
| B       | Highway 27 and Dr. Kay Drive        | 4                              | SP12.5 FC2 PG64-28 Category 'D' | 50                           | 100                       | 3.9     | 903,519              | 2011                     | 9                 |
| C       | York Durham Line & Bloomington Road | 1                              | SP12.5 PG64-28 Category 'C'     | 65                           | 50                        | 4.9     | 1,412,829            | 2009                     | 11                |
| D       | Davis Drive and Warden Avenue       | 3                              | SP12.5FC1 PG64-28 Category 'C'  | 90                           | 90                        | 8.2     | 6,284,832            | 2008                     | 12                |
| E       | Weston Road and Aviva Park          | 4                              | SP12.5 FC1 PG64-28 Category 'D' | 45                           | 60                        | 1.5     | 715,680              | 2010                     | 10                |
| F       | Pine Valley Drive and Vinyl         | 4                              | SP12.5 FC1 PG64-28 Category 'D' | 55                           | 60                        | 1.4     | 876,240              | 2010                     | 10                |

Notes: (1) Number of lanes per direction including turning lanes, and (2) Equivalent Single Axle Load based on surface layer age. FC<sub>1</sub> and FC<sub>2</sub> are Friction Coarse type 1 and type 2; respectively. Traffic Category 'C' means Traffic is between 3 million ESALs to 10 million ESALs and for Category 'D' traffic is between 10 million ESALs to 30 million ESALs.

The study found that rutting only occurred within the surface layer and all sections were found to be structurally sound. The highest rutting was observed in areas closer to intersections. The field evaluation was completed after ranking all the under-study sites based on two ranking methods. This was to ensure key site attributes such as traffic parameters, in-service life, and thickness of asphalt surface layer were considered in the comparison of in-situ performance. Due to difference attributes such as traffic parameters and surface layer's age and thickness, it was vital to normalize the site condition to compare the susceptibility of asphalt layer mixes to rutting. The results of the study and the use of the ranking systems are described in sections 4.1.2 and 4.1.3 of the research.

#### 4.2.1. Ranking Method 1

The first ranking system used five different categories to evaluate the sites, including truck percentage, number of lanes, thickness of the asphalt surface layer in millimeters, service life (referred to as "age"), and maximum rut depth of the asphalt surface layer in millimeters. Each

category was ranked between 1 (best scenario) and 6 (worst scenario) as shown in Table 4-2. In case of duplicates in values for each criterion, each site received the same score for that criterion. The use of this ranking system allowed for a comprehensive evaluation and comparison of the sites based on key attributes affecting rutting.

The following assumptions were made for ranking each criterion:

- Site with the highest truck percentage received ranking no.1;
- Site with the lowest number of lanes received ranking no.1;
- Site with the lowest asphalt surface layer thickness received ranking no.1;
- Site with the lowest average asphalt surface layer rut depth received ranking no.1; and
- Site with the highest asphalt surface layer age received ranking no.1.

**Table 4-2: Method 1 - Ranking Score**

| Site ID | Truck % | Ranking Score | Number of Lanes | Ranking Score | Surface Layer Thickness (mm) | Ranking Score | Surface Average Layer Rut Depth (mm) | Ranking Score | Treatment Age | Ranking Score |
|---------|---------|---------------|-----------------|---------------|------------------------------|---------------|--------------------------------------|---------------|---------------|---------------|
| A       | 2.9     | 4             | 3               | 2             | 55                           | 3             | 19                                   | 4             | 6             | 5             |
| B       | 3.9     | 3             | 4               | 3             | 50                           | 2             | 10                                   | 3             | 9             | 4             |
| C       | 4.9     | 2             | 1               | 1             | 65                           | 4             | 31                                   | 6             | 11            | 2             |
| D       | 8.2     | 1             | 3               | 2             | 90                           | 5             | 20                                   | 5             | 12            | 1             |
| E       | 1.5     | 5             | 4               | 3             | 45                           | 1             | 9                                    | 2             | 10            | 3             |
| F       | 1.4     | 6             | 4               | 3             | 55                           | 3             | 7                                    | 1             | 10            | 3             |

The total ranking scores were calculated and presented in Table 4-3. The results indicated that the asphalt surface mix with unmodified asphalt binder (PG58-28) had the highest total score, indicating the worst mix. The results also showed that there were no significant changes in the ranking score when comparing PG64-28 asphalt binders. This suggests that the use of unmodified asphalt binder was a significant factor in the performance of the surface layer with regards to rutting.

**Table 4-3: Method 1 - Total Ranking Score**

| Site ID | Total Score | Surface Asphalt Layer Mix Type  |
|---------|-------------|---------------------------------|
| A       | 18          | SP12.5 PG58-28 Category 'C'     |
| F       | 16          | SP12.5 FC1 PG64-28 Category 'D' |
| B       | 15          | SP12.5 FC2 PG64-28 Category 'D' |
| C       | 15          | SP12.5 PG64-28 Category 'C'     |
| D       | 14          | SP12.5FC1 PG64-28 Category 'C'  |
| E       | 14          | SP12.5 FC1 PG64-28 Category 'D' |

#### 4.1.3. Ranking Method 2

The second ranking method used was a calculation of the rate of rutting as the ratio of rutting depth over the square root of accumulated ESALs in million, as described in Equation 4-1 (Brown et al., 1989, Thiessen et al., 2000). The results of this method were shown in Table 4-4 and provided a ranking of the six approach intersections based on the rate of rutting.

$$\text{Rate of Rutting} = \frac{\text{Rut Depth (mm)}}{\sqrt{\text{MESALS}}} \quad (4-1)$$

where: MESALS is the number of Equivalent Single Axial Load in millions.

**Table 4-4: Rate of Rutting at Test Sites**

| Intersection ID | Average Rut Depth (mm) | Total ESALs in Million | Rate of Rutting (mm/ $\sqrt{\text{MESALS}}$ ) | Surface Asphalt Layer Mix Type  |
|-----------------|------------------------|------------------------|---|---------------------------------|
| A               | 19                     | 0.52                   | 26.41   | SP12.5 PG58-28 Category 'C'     |
| C               | 31                     | 1.41                   | 26.08   | SP12.5 PG64-28 Category 'C'     |
| E               | 9                      | 0.72                   | 10.64   | SP12.5 FC1 PG64-28 Category 'D' |
| B               | 10                     | 0.90                   | 10.52   | SP12.5 FC2 PG64-28 Category 'D' |
| D               | 20                     | 6.28                   | 7.98  | SP12.5FC1 PG64-28 Category 'C'  |
| F               | 7                      | 0.88                   | 7.48  | SP12.5 FC1 PG64-28 Category 'D' |

According to Table 4-4, the unmodified asphalt binder (PG58-28) had the highest rate of rutting (26.41 mm/ $\sqrt{\text{MESALS}}$ ), indicating the worst-case scenario. Site C, which had all traffic passing through only one lane, was ranked the highest among the PG64-28 asphalt binders with a rutting rate of 26.08 mm/ $\sqrt{\text{MESALS}}$ . This suggests that the use of unmodified asphalt binder was a

significant factor in the performance of the surface layer with regards to rutting, and that lane configuration also played a role in the rutting rate.

In conclusion, the results of the two ranking methods in the study suggested that the use of modified asphalt binder would provide a higher level of resistance to rutting. The study also found that changes in traffic category from C to D did not necessarily make the asphalt mix more resistant to rutting. This highlights the importance of benchmarking the current asphalt mixes specified by the York Region and using performance thresholds as key parameters in improving the design of asphalt mixes for heavily loaded intersections. This study is a significant step for the York Region in understanding performance-based mix design and moving towards full adoption of this concept for other mixes.

#### **4.2. Performance Evaluation of Plant-Produced Asphalt Mixes**

The literature review identified several test methods, both established and under development, that could evaluate the rutting resistance of asphalt mixes. The evaluation was completed on the currently specified asphalt mixes by the York Region for use at intersections, as follows:

- Mix 1: HMA-SP12.5 FC1 PG64-28
- Mix 2: HMA-SP12.5 FC1 PG70-28
- Mix 3: WMA-SP12.5 FC2 PG70-28

Table 4-5 provides key physical properties of the mixes. It should be noted that asphalt surface Mix 3 (a Warm Mix Asphalt) was produced using foaming technique. In foaming technique, a small amount of cold water is added to the hot asphalt binder as it is mixed with aggregate particles during asphalt mix production process. The testing program included: (1) HWTT, (2) FN (3) IDEAL-RT, and (4) modified UST tests. The specimens were prepared by heating up the loose plant-produced asphalt mix to the specified compaction temperature using an air-forced oven, then immediately compacting the material using a SGC to achieve  $7 \pm 0.5$  percent air voids. These tests were used to evaluate the rutting resistance of the asphalt mixes.

**Table 4-5: Physical Properties of Plant-Produced Asphalt Surface Mix**

| Property                                       |                             | Mix 1 -<br>SP12.5 PG64-<br>28          | Mix 2 - SP12.5<br>FC1 PG70-28         | Mix 3 -<br>SP12.5 FC2<br>PG70-28          |
|--|-----------------------------|--|---------------------------------------|---|
| <b>Gradation<br/>(% Passing)</b>               | <b>Sieve Size<br/>(mm)</b>  |  |                                       |   |
|  | 19                          | 100                                    | 100                                   | 100                                       |
|  | 12.5                        | 98.5                                   | 98.6                                  | 99.4                                      |
|  | 9.5                         | 82.5                                   | 82.5                                  | 83.3                                      |
|  | 4.75                        | 57.9                                   | 54.6                                  | 57.3                                      |
|  | 2.36                        | 50.3                                   | 43.6                                  | 48.9                                      |
|  | 1.18                        | 33.6                                   | 27.2                                  | 33.1                                      |
|  | 0.6                         | 24.2                                   | 18.6                                  | 21.5                                      |
|  | 0.3                         | 11.1                                   | 10.8                                  | 13.3                                      |
|  | 0.15                        | 4.3                                    | 6.3                                   | 8.2                                       |
|  | 0.075                       | 3.1                                    | 4.3                                   | 5.1                                       |
| <b>Property</b>                                | <b>OPSS 1151<br/>- 2021</b> | <b>Mix 1 -<br/>SP12.5 PG64-<br/>28</b> | <b>Mix 2 - SP12.5<br/>FC1 PG70-28</b> | <b>Mix 3 -<br/>SP12.5 FC2<br/>PG70-28</b> |
| Ndes (% G <sub>mm</sub> )                      | 96                          | 96                                     | 96                                    | 96  |
| Nini (% G <sub>mm</sub> )                      | ≤ 89.0                      | 88.5                                   | 86.7                                  | 86.9                                      |
| Nmax (% G <sub>mm</sub> )                      | ≤ 98.0                      | 97.2                                   | 97.1                                  | 96.7                                      |
| Air Voids (%) at Ndes                          | 4                           | 4                                      | 4                                     | 4   |
| Voids in Mineral Aggregate,<br>VMA (% minimum) | 14                          | 14.8                                   | 14.9                                  | 16  |
| Asphalt Binder Performance<br>Grade            | -                           | PG64-28                                | PG70-28                               | PG70-28                                   |
| Voids Filled with Asphalt,<br>VFA (%)          | 65 – 75                     | 73                                     | 73.2                                  | 75  |
| Bulk Specific Gravity (G <sub>mb</sub> )       | -                           | 2.710                                  | 2.834                                 | 2.909                                     |
| Dust Proportion, DP                            | 0.6 – 1.2                   | 0.69                                   | 1                                     | 1.08                                      |
| Tensile Strength Ratio, TSR<br>(%)             | 80                          | 87.2                                   | 91.3                                  | 88.2                                      |
| Asphalt Film Thickness<br>(µm)                 | -                           | 11.3                                   | -                                     | 9.9                                       |
| Asphalt Cement Content<br>(%)                  | -                           | 5                                      | 5                                     | 5   |

Notes: Foam technique was used for Mix 3, OPSS is Ontario Provincial Standard Specification,  $N_{des}$ ,  $N_{ini}$ ,  $N_{max}$  are number of gyrations at different compaction levels (design, initial, and maximum), and  $G_{mm}$  is theoretical maximum specific gravity.  $FC_1$  and  $FC_2$  are Friction Coarse type 1 and type 2; respectively.

#### 4.2.1. Hamburg Wheel Tracking Test

According to AASHTO T324, cylindrical test specimens are required to be tested while submerged in a 50°C water bath. However, in this study, additional test temperatures of 44°C and 58°C were considered to capture the effect of temperature change on rutting resistance and moisture damage.

The testing temperature of 58°C was selected as it represents the Southern Ontario’s climatic high PG temperature. Also, the testing temperature of 44°C was chosen based on the research conducted by the Ministry of Transportation Ontario (MTO) recommendation (Salehi-Ashani, 2019; Bashir et al., 2020). The results of the test indicate that Mix 1 with a softer binder (PG64-28) had lower resistance to rutting compared to the other mixes at all test temperatures. The results showed that all three mixes reached the maximum allowable rut depth of 12.5mm before 20,000 wheel passes at 58°C, which may indicate that the 58°C temperature was too severe. Mixes 2 and 3 did not reach the 12.5mm rut depth limit after 20,000 wheel passes at 44°C and 50°C. Mix 3 provided better resistance to permanent deformation than Mix 2. Testing at 58°C differentiated the durability of the mixes relative to extreme temperature changes, as Mixes 2 and 3 with stiffer binders exhibited more than 2 times more resistance to rutting compared to Mix 1. The 58°C testing temperature (or climatic base PG temperature) may have been too severe, but it did provide insight into the mix's resiliency to extreme temperature changes. Such temperature changes should be considered when testing materials for climatic resiliency.

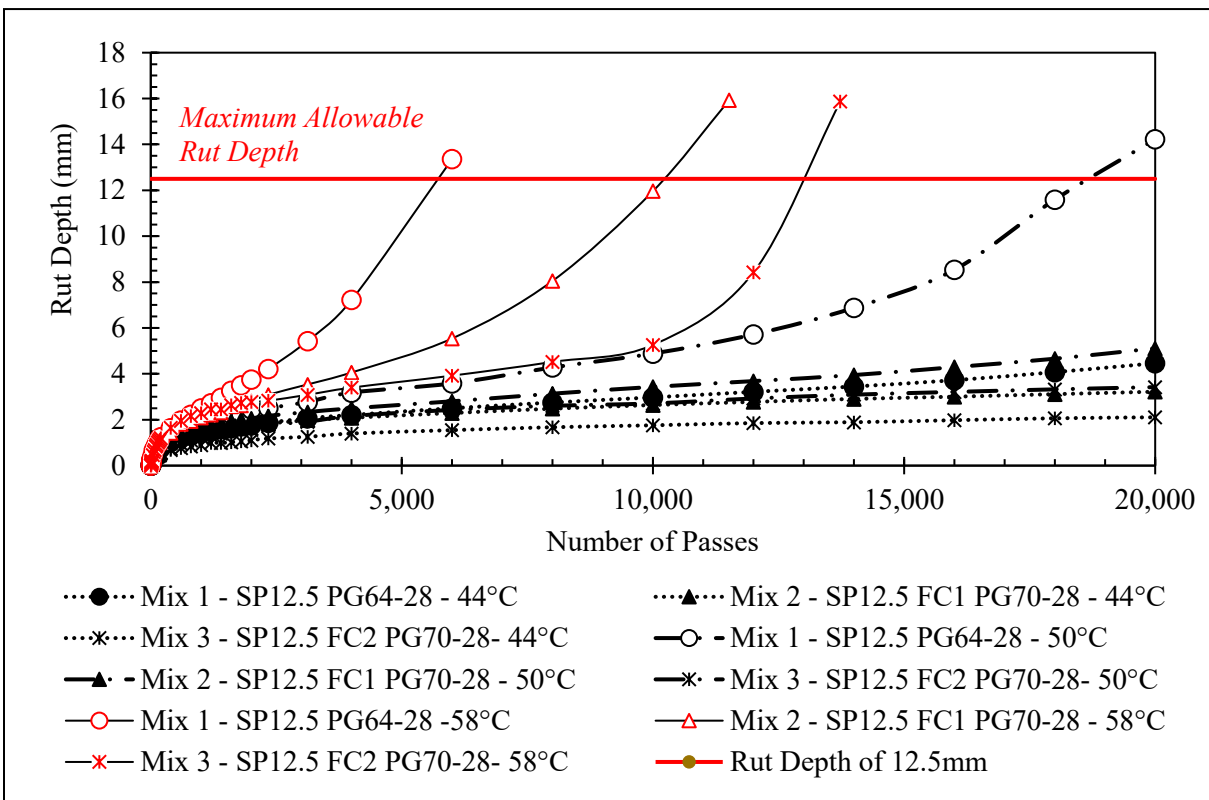


Figure 4-1: Hamburg Wheel Tracking Test Results for Plant-Produced Asphalt Mixes

Table 4-6 summarizes the accumulated rut depth of all asphalt mixes at different test temperatures and the number of wheel passes. Table 4-6 also presents the accumulated rut depth and wheel pass at the SIP. The results showed that SIP was not observed for any of the mixes at 44°C as the accumulated deformation did not reach the tertiary zone after 20,000 wheel passes. However, SIP was observed at 50°C and 58°C. This highlights the importance of selecting the testing temperature relative to the asphalt mix's base PG temperature. If this is not properly considered, the recommended testing temperature of 50°C by the AASHTO method could potentially introduce bias into the performance evaluation.

**Table 4-6: Hamburg Wheel Tracking Test Results for Plant-Produced Asphalt Mixes**

| Mix Type                   | Rut Depth (mm)<br>As Function of Passes |     |     |     |      | Stripping<br>Inflection Point    |                       | Number<br>of<br>Passes at<br>12.5mm<br>Rut<br>Depth |
|----------------------------|---|-----|-----|-----|------|----------------------------------|-----------------------|---|
|                            | 1k                                      | 5k  | 10k | 15k | 20k  | Number<br>of<br>Passes to<br>SIP | Ruth<br>Depth<br>(mm) |   |
| <b>Testing Temperature</b> | <b>44°C</b>                             |     |     |     |      |                                  |                       |   |
| Mix 1 - SP12.5 PG64-28     | 1.5                                     | 2.2 | 3   | 3.6 | 4.5  | -                                | -                     | -   |
| Mix 2 - SP12.5 FC1 PG70-28 | 1.6                                     | 2.3 | 2.6 | 2.9 | 3.5  | -                                | -                     | -   |
| Mix 3 - SP12.5 FC2 PG70-28 | 0.9                                     | 1.5 | 1.7 | 1.9 | 2.1  | -                                | -                     | -   |
|                            | <b>50°C</b>                             |     |     |     |      |                                  |                       |   |
| Mix 1 - SP12.5 PG64-28     | 2                                       | 3.5 | 5.0 | 7.6 | 14.3 | 14,500                           | 6.2                   | 18,200  |
| Mix 2 - SP12.5 FC1 PG70-28 | 1.7                                     | 2.6 | 3.5 | 4.1 | 5.2  | -                                | -                     | -   |
| Mix 3 - SP12.5 FC2 PG70-28 | 1.3                                     | 2.3 | 2.7 | 3.1 | 3.4  | -                                | -                     | -   |
|                            | <b>58°C</b>                             |     |     |     |      |                                  |                       |   |
| Mix 1 - SP12.5 PG64-28     | 2.5                                     | 11  | N/A | N/A | N/A  | 3,800                            | 3.8                   | 5,700   |
| Mix 2 - SP12.5 FC1 PG70-28 | 2.1                                     | 4.7 | 12  | N/A | N/A  | 7,100                            | 6.0                   | 10,200  |
| Mix 3 - SP12.5 FC2 PG70-28 | 2.3                                     | 3.6 | 5.3 | N/A | N/A  | 11,500                           | 5.5                   | 13,000  |

*Note: SIP is Stripping Inflection Point and HWTT is Hamburg Wheel Tracking Test.*

#### 4.2.2. Flow Number (FN) Test

To assess the rutting response of the asphalt mixes, the FN test was performed at 58°C with an unconfined pressure load of 200 kPa instead of the 600 kPa specified in AASHTO T378 to determine the difference in FN under lower pressure. The test was terminated when either the asphalt mix test specimen failed or 10,000 loading cycles were reached, whichever happened first. As shown in Figure 4.2, Mix 1 had the lowest FN values, indicating the lowest resistance to rutting among the selected asphalt mix types

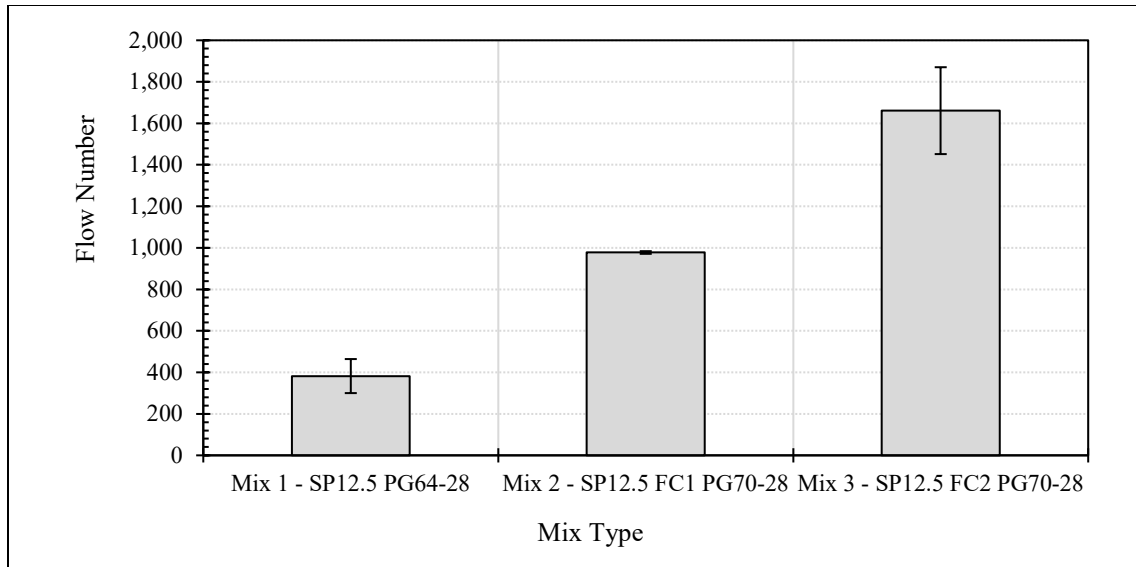


**Figure 4-2: Flow Number Test Results @ 58°C Testing Temperature**

The higher the FN, the better resistance to rutting. The results also indicated that Mix 3 had higher FN compared to Mix 2; therefore, it provided higher resistance to permanent deformation.

#### **4.2.3. Uniaxial Shear Tester**

Due to test frame limitations, the test was performed in monotonic mode rather than the cyclic mode described by Zak et al. in 2017. The same test specimen dimensions as those of the HWTT test were used, after gyrating to the targeted height. The test was performed at 50°C and 58°C with loading rates of 50, 25, and 12.5 mm/min. It should be noted that a 44°C testing temperature was attempted, but the 50kN load cell was maxed out during the test. The uniaxial shear tester test results for test temperatures of 50°C and 58°C are presented in Figures 4-3 and 4-4, respectively. As the temperature increases, the results show that the peak load required to cause lateral plastic flow decreases, indicating a reduction in the shear resistance of the asphalt mixtures. In addition to testing at different temperatures, three different loading rates were applied at each temperature to examine the effect of traffic speed on the asphalt mixture's shear resistance.



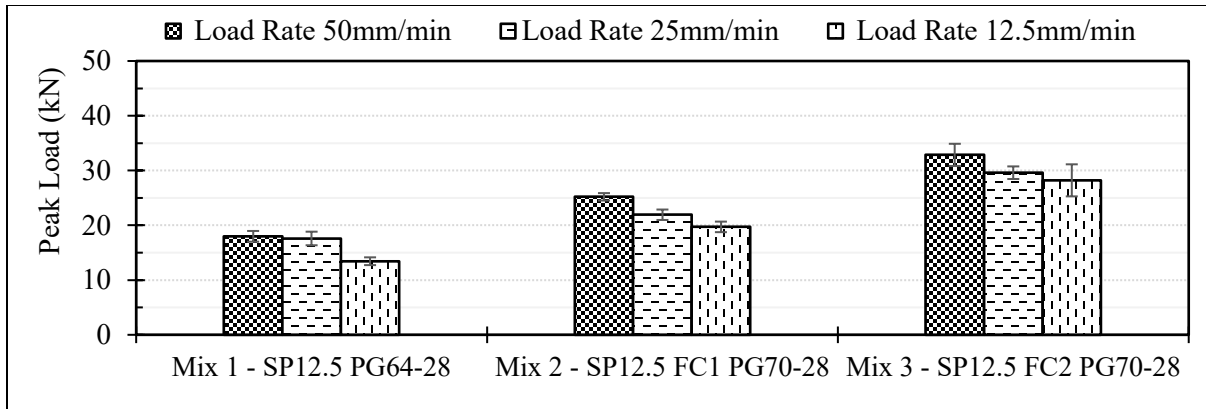


**Figure 4-3: Uniaxial Shear Tester Results at 50°C Testing Temperature**

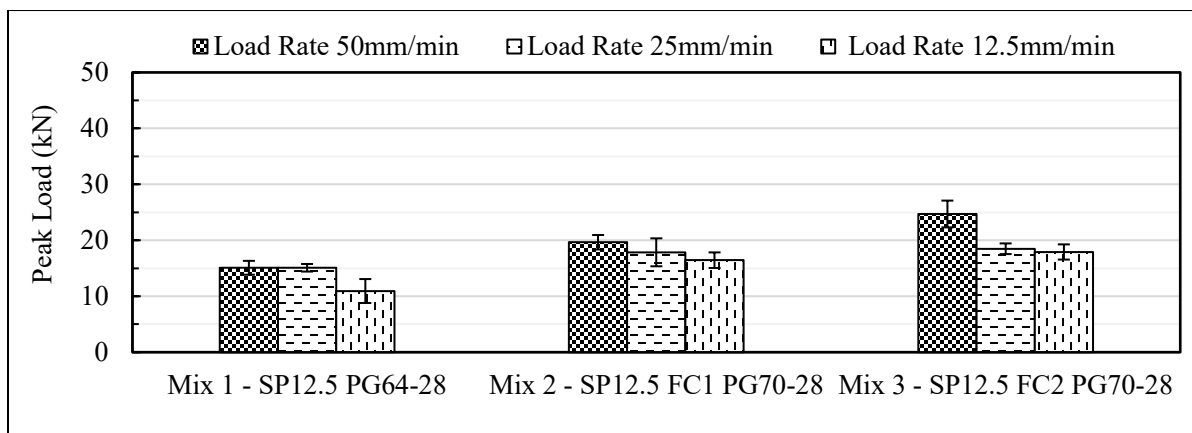


**Figure 4-4: Uniaxial Shear Tester Results at 58°C Testing Temperature**

As noted in Figures 4-3 and 4-4, for all test temperatures, the asphalt mix peak load decreased as the loading rate was reduced. The results suggest that the asphalt mixes performed better at higher loading rates, which might indicate that lower traffic speeds make the asphalt mix more susceptible to rutting damage. Additionally, similar to the HWTT and FN tests, the results indicate that Mix 1 with the softer binder (PG64-28) had less resistance to rutting damage compared to the other two mixes with stiffer asphalt binder (PG70-28). It was also observed that Mix 3 had better rutting resistance than Mix 2. Table 4-7 provides the average, standard deviation, and coefficient of variation of the peak load results for the tested asphalt specimens. According to the Table 4-7, uniaxial shear tester provided medium coefficient of variation of less than 20 percent for 3 replicates.

**Table 4-7: Uniaxial Shear Test Results**

| Uniaxial Shear Test        | Test Temperature at 50°C |          |     |                      |          |      |                        |          |      |
|----------------------------|--------------------------|----------|-----|----------------------|----------|------|------------------------|----------|------|
|                            | Load Rate (50mm/min)     |          |     | Load Rate (25mm/min) |          |      | Load Rate (12.5mm/min) |          |      |
|                            | APL (kN)                 | St. Dev. | COV | APL (kN)             | St. Dev. | COV  | APL (kN)               | St. Dev. | COV  |
| Mix 1 - SP12.5 PG64-28     | 17.98                    | 0.98     | 5.4 | 17.59                | 1.24     | 7.1  | 13.44                  | 0.71     | 5.3  |
| Mix 2 - SP12.5 FC1 PG70-28 | 25.20                    | 0.68     | 2.7 | 21.92                | 0.95     | 4.3  | 19.71                  | 0.96     | 4.9  |
| Mix 3 - SP12.5 FC2 PG70-28 | 32.85                    | 2.03     | 6.2 | 29.60                | 1.15     | 3.9  | 28.21                  | 2.93     | 10.4 |
| Asphalt Mixture            | Test Temperature at 58°C |          |     |                      |          |      |                        |          |      |
|                            | Load Rate (50mm/min)     |          |     | Load Rate (25mm/min) |          |      | Load Rate (12.5mm/min) |          |      |
|                            | APL (kN)                 | St. Dev. | COV | APL (kN)             | St. Dev. | COV  | APL (kN)               | St. Dev. | COV  |
| Mix 1 - SP12.5 PG64-28     | 15.09                    | 1.24     | 8.2 | 15.09                | 0.68     | 4.5  | 10.93                  | 2.14     | 19.5 |
| Mix 2 - SP12.5 FC1 PG70-28 | 19.65                    | 1.29     | 6.6 | 17.85                | 2.50     | 14.0 | 16.44                  | 1.39     | 8.5  |
| Mix 3 - SP12.5 FC2 PG70-28 | 24.70                    | 2.39     | 9.7 | 18.49                | 0.95     | 5.2  | 17.91                  | 1.36     | 7.6  |

Note: APL is Average Peak Load, COV is Coefficient of Variation, and St. Dev. is Standard Deviation.

**4.2.4. IDEAL-RT Test**

To capture the temperate impact on the asphalt mix’s shear resistance, the test was performed at three different temperatures (44, 50, and 58°C). The results of the uniaxial shear test showed that as the temperature increased, the shear resistance of the asphalt mixes decreased, as seen in Figure 4-5. The Figure 4-5 illustrates that a lower peak load was required to cause lateral plastic flow at higher temperatures, which is consistent with the observation that higher temperatures can result in lower shear resistance. Additionally, the results indicate that Mix 1, which has a softer binder (PG64-28), had lower shear resistance compared to the other two mixes with stiffer asphalt binders (PG70-28).

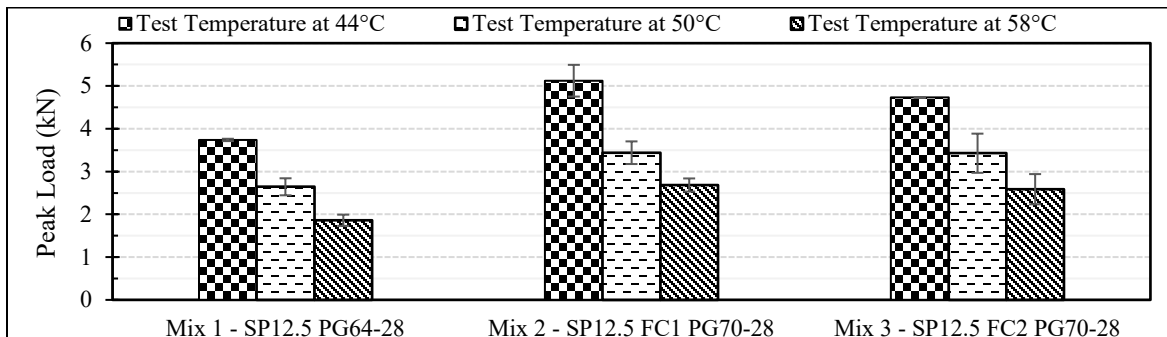


**Figure 4-5: IDEAL-RT Test Results**

Table 4-8 provides the average, standard deviation, and coefficient of variation of IDEAL-RT’s peak load results for the tested asphalt specimens. According to Table 4-8, the results indicate a medium coefficient of variation of less than 15 percent for the 3 replicates, which suggests that the

test results are relatively consistent. The Table 4-8 also includes the shear strength and the RT-index., which is the maximum shear resistivity of the asphalt mix. As indicated by Zhou et al. the RT-Index should meet the following ranges (Zhou et al., 2021)

- For mixtures with PG64-XX (or lower) with 95 percent confidence: RT-Index  $\geq 60$ .
- For mixtures with PG70-XX with 95 percent confidence: RT-Index  $\geq 65$ .

As provided in Table 4-8, all asphalt mixes failed to meet the specified RT-Index requirement at the test temperature of 58°C. In addition, Mix 1 also did not meet the RT-Index requirement at the test temperature of 50°C.

**Table 4-8: IDEAL-RT Test Results**

| IDEAL-RT Test              | Test Temperature at 44°C |          |      |              |          |
|----------------------------|--------------------------|----------|------|--------------|----------|
|                            | APL (kN)                 | St. Dev. | COV  | $\tau_f$     | RT-Index |
| Asphalt Mix                |                          |          |      |              |          |
| Mix 1 - SP12.5 PG64-28     | 3.7                      | 0.0      | 0.7  | 1.1          | 74.4     |
| Mix 2 - SP12.5 FC1 PG70-28 | 5.1                      | 0.4      | 7.2  | 1.5          | 101.9    |
| Mix 3 - SP12.5 FC2 PG70-28 | 4.7                      | 0.0      | 0.0  | 1.4          | 94.1     |
| Asphalt Mix                | Test Temperature at 50°C |          |      |              |          |
|                            | APL (kN)                 | St. Dev. | COV  | $\tau_f$     | RT-Index |
| Mix 1 - SP12.5 PG64-28     | 2.6                      | 0.2      | 7.5  | 0.8          | 52.6     |
| Mix 2 - SP12.5 FC1 PG70-28 | 3.4                      | 0.3      | 7.7  | 1.0          | 68.4     |
| Mix 3 - SP12.5 FC2 PG70-28 | 3.4                      | 0.5      | 13.4 | 1.0          | 68.2     |
| Asphalt Mix                | Test Temperature at 58°C |          |      |              |          |
|                            | APL (kN)                 | St. Dev. | COV  | $\tau_{max}$ | RT-Index |
| Mix 1 - SP12.5 PG64-28     | 1.9                      | 0.1      | 7.1  | 0.6          | 37.0     |
| Mix 2 - SP12.5 FC1 PG70-28 | 2.7                      | 0.2      | 5.7  | 0.8          | 53.4     |
| Mix 3 - SP12.5 FC2 PG70-28 | 2.6                      | 0.4      | 13.6 | 0.8          | 51.5     |

*Note: APL is Average Peak Load, COV is Coefficient of Variation, and St. Dev. is Standard Deviation.*

### 4.3. Summary and Conclusions

The results of the field investigation showed that rutting damage only appeared on the top layer of the asphalt pavement, suggesting that the underlying structure was strong enough, but the rutting may have been caused by insufficient stability in the asphalt mix. Previous research and these findings suggest that relying solely on volumetric design methods may not provide a complete understanding of the mix's performance under heavy traffic loads. To ensure adequate rutting resistance with a desired level of reliability, performance testing should be incorporated into the design stage. As a result, HWTT, IDEAL-RT, Flow Number, and modified UST tests were conducted to evaluate rutting resistance of three asphalt mixes placed at the York Region's intersections. The results suggest that as temperature increases, the asphalt binder becomes softer, reducing binder stiffness and resulting in lower resistance to permanent deformation. Mix 1, with

its softer binder (PG64-28), showed less resistance to rutting compared to Mixes 2 and 3, which used a stiffer binder (PG70-28). With the exception of IDEAL-RT at both 44°C and 58°C testing temperatures, all results indicated that Mix 3 had higher shear resistance than Mix 2. The results from the uniaxial shear tester also indicated that the asphalt mixes showed higher shear resistance at higher loading rates, suggesting that lower loading rates or lower traffic speeds make the asphalt mixes more vulnerable to rutting damage. The results of the laboratory tests showed that the SP12.5 FC2 PG70-28 asphalt mix had the best rutting resistance compared to the other two mixes. Knowledge gained through this step of the study provided an insight into proper selection of testing temperature in optimizing or balancing performance toward higher rutting resistance. This information can help in setting performance standards for accepting innovative asphalt mixes and materials for use at approach intersections with heavy traffic loads in Southern Ontario.

## **Chapter 5 Permanent Deformation Evaluation of Stone Mastic Asphalts (SMA) and High-Modulus Asphalt Mix (EME)**

*Parts of this chapter have been submitted to the Journal of Construction and Building Materials (Kafi Farashah, 2023a).*

A total of seven surface course asphalt mixes were evaluated for their rutting susceptibility through laboratory testing. These mixes included six Stone Mastic Asphalt (SMA) mixes and one High-Modulus Asphalt Mix (EME). The SMA mixes had three PG asphalt binders (PG70-28, PG76-28, and PG82-28) and two nominal maximum aggregate sizes (NMAS) of 9.5mm and 12.5mm. The EME had NMAS of 12.5mm and asphalt binder of PG82-28. The shear resistance of the asphalt binders was characterized through the Dynamic Shear Rheometer (DSR) and Multiple Stress Creep and Recovery (MSCR) tests. The rutting resistance of the asphalt mixes was determined through the HWTT, IDAEL-RT, and Flow number tests.

The results of the asphalt mix performance tests were analyzed through Analysis of variance (ANOVA) and Tukey's HSD (Honestly Significant Difference) tests using Minitab© software to compare the rutting resistance of the asphalt mixes. A t-test was also conducted to determine any statistical difference between the rutting resistance of the EME mix and the six SMA mixes. The dynamic modulus test was performed on the asphalt mixes at five temperatures (-10, 4, 21.1, 37.8, and 54.4°C) and six frequencies (25, 10, 5, 1, 0.5, and 0.1 Hz) to determine their stiffness and construct the corresponding master curves at 21.1°C.

### **5.1. Asphalt Binder Characterization Results**

The DSR test and MSCR test were performed to evaluate the shear resistance of three asphalt binders in accordance with AASHTO T315 and AASHTO T350, respectively. The  $|G^*|/\sin(\delta)$  parameter was obtained from the DSR test for both unaged and short-term aged asphalt binders. The short-term aging was done using the Rolling Thin-Film Oven (RTFO) following AASHTO T240-09. The short-term aging process simulates the aging of asphalt binders due to exposure to air during mixing, transportation, and paving. The DSR test results must meet the stiffness limit requirements set by AASHTO T315, which are 1.0 kPa for unaged binders and 2.2 kPa for RTFO-aged binders. The MSCR test, as per AASHTO T350, was also performed to evaluate the creep recovery behavior of RTFO-aged asphalt binders. Two parameters were considered in this test: non-recoverable creep compliance ( $J_{nr}$ ) with an upper limit of 4.5 1/kPa and percent recovery ( $Re$ )

at a shear stress of 3.2 kPa. Table 5-1 presents the high temperature rheological properties of three asphalt binders used in the research. The results showed that asphalt binder PG82-28 had the lowest non-recoverable creep compliance ( $J_{nr}= 0.05$ ) while asphalt binder PG76-28 had the highest percent recovery ( $Re=92.3\%$ ).

**Table 5-1: Asphalt Binder Properties at High Testing Temperatures**

| <b>Tests on Original Asphalt Binders</b>     | <b>PGAC 70-28</b>                 | <b>PGAC 76-28</b>                 | <b>PGAC 82-28</b>                 | <b>Specification Limits</b> |
|--|-----------------------------------|-----------------------------------|-----------------------------------|-----------------------------|
| G*/sin( $\delta$ ) (kPa) (70°C)              | 1.870                             | 3.28                              | 6.98                              | 1.0 min                     |
| <b>Tests on RTFO Residue Asphalt Binders</b> |                                   |                                   |                                   |                             |
| G*/sin( $\delta$ ) (kPa)                     | 2.52 (70°C)<br>and 1.26<br>(76°C) | 2.43 (76°C)<br>and 1.21<br>(82°C) | 2.83 (82°C)<br>and 1.41<br>(88°C) | 2.2 min                     |
| MSCR $J_{nr}$ (1/kPa) (58°C and 3.2 kPa)     | 0.18                              | 0.09                              | 0.05                              | 4.5 max                     |
| MSCR Percent Recovery (%) (58°C and 3.2 kPa) | 83.50                             | 92.3                              | 81.5                              | -                           |
| Continuous High PG Grade (°C)                | 71.5                              | 77.1                              | 84.7                              | -                           |

## 5.2. Asphalt Mix Characterization Results

### 5.2.1. Hamburg Wheel Tracking Test Results

The HWTT was performed to evaluate both rutting resistance and moisture susceptibility of the lab-produced asphalt mixes in accordance with AASHTO T324. Typically, HWTT is conducted with asphalt mix specimens submerged in water at the temperature of 50°C and the test ends when the total rut depth of the specimens reaches 12.5mm or the specimens receive 20,000 passes, whichever occurs first. The AASHTO T324 standard does not specify a specific total rut depth tolerance for different asphalt mix types. Hence, in this study, a tolerable total rut depth of 6mm was chosen due to safety concerns related to hydroplaning and skidding at approach intersections. This trigger level aligns with the recommendation of ASTM 1989, which states that a rut depth below 6mm does not require pavement treatment (ASTM, 1989). Furthermore, the number of wheel-track passes was increased to 40,000 to study the behavior of each mix under harsh conditions and to identify high-rut resistant asphalt mixes. Additionally, to determine the sensitivity of the asphalt mixes to testing temperature in terms of rutting resistance, the HWTT was also conducted at 44°C and 58°C, in addition to the standard temperature of 50°C specified in AASHTO T324. The testing temperature of 58°C was selected as it represents the Southern

Ontario's climatic high PG temperature. Also, the testing temperature of 44°C was chosen based on the research conducted by the Ministry of Transportation Ontario (MTO) recommendation (Salehi-Ashani, 2019; Bashir et al., 2020).

The results of the HWTT for the seven lab-produced asphalt mixes are displayed in Figures 5-1, 5-2, and 5-3 for the testing temperatures of 44°C, 50°C, and 58°C, respectively. As shown in Figures 5-1, all of the asphalt mixes displayed excellent rutting resistance at a testing temperature of 44°C, as none of the mixes reached the maximum permissible rut depth of 6mm after 40,000 wheel-track passes. This suggests that the 44°C testing temperature may not be adequate for distinguishing between heavy-duty asphalt mixes. The results of a study show that the SMA mix with greater NMAS has higher resistance to rutting. The study also shows that the higher the asphalt binder PG, the higher the resistance to rutting. For example, SMA9.5-PG76-28 had a total rut depth of 2.92mm while SMA12.5-PG76-28 had a lower total rut depth of 2.36mm at 44°C testing temperature. The highest total rut depth was shown by SMA9.5-PG70-28 and SMA12.5-PG70-28 at 4.29mm and 4.21mm, respectively. The lowest total rut depth was shown by SMA12.5-PG82-28, SMA9.5-PG82-28 and EME mixes with values of 1.78mm, 2.11mm, and 2.16mm, respectively. The results also suggested that the higher the asphalt binder PG the higher the asphalt mix resistance to rutting when comparing across the mixes with same NMAS.

As presented in Figure 5-2, all asphalt mixes except SMA9.5-PG70-28 had great resistance to rutting at a testing temperature of 50°C and 40,000 wheel-track passes. SMA9.5-PG70-28 reached 6mm total rut depth at 33,500 passes. The results also suggest that the SMA mixes with greater NMAS and higher PG asphalt binder provide higher rutting resistance at 50°C. The highest resistance was shown by EME, SMA12.5-PG82-28, and SMA9.5-PG82-28 with total rut depths of 2.44mm, 2.55mm, and 3.59mm respectively. The study indicates that 50°C is not a sufficient testing temperature to distinguish high rut-resistant asphalt mixes. As shown in Figure 5-3, all asphalt mixes except SMA12.5-PG76-28 and SMA12.5-PG82-28 failed to provide sufficient resistance to rutting (maximum rutting depth of 6mm) at 40,000 wheel-track passes. The highest total rut depth was shown by SMA9.5-PG70-28 (22mm), followed by EME mix (16mm), SMA12.5-PG70-28 (9.61mm), SMA9.5-PG76-28 (9.40mm), and SMA9.5-PG82-28 (7.45mm). The results suggest that the asphalt mixes with NMAS of 12.5 provide better resistance compared to 9.5mm NMAS when using the same PG asphalt binder. The 58°C testing temperature was able to distinguish high rut-resistant asphalt mixes.

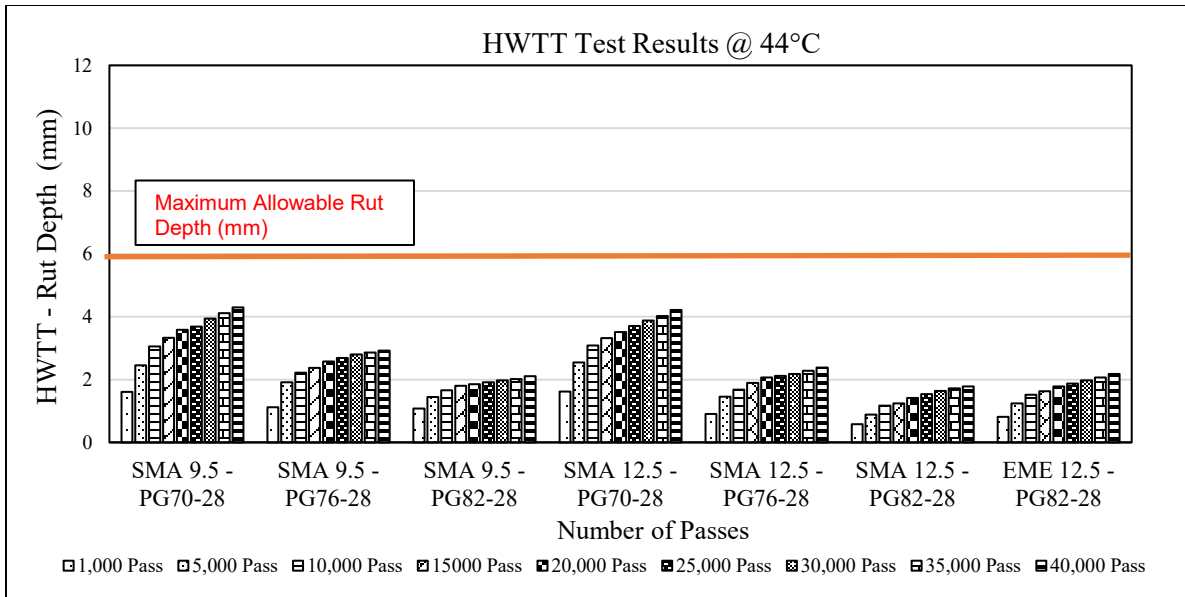


**Figure 5-1: HWTT Test Results @ 44°C**

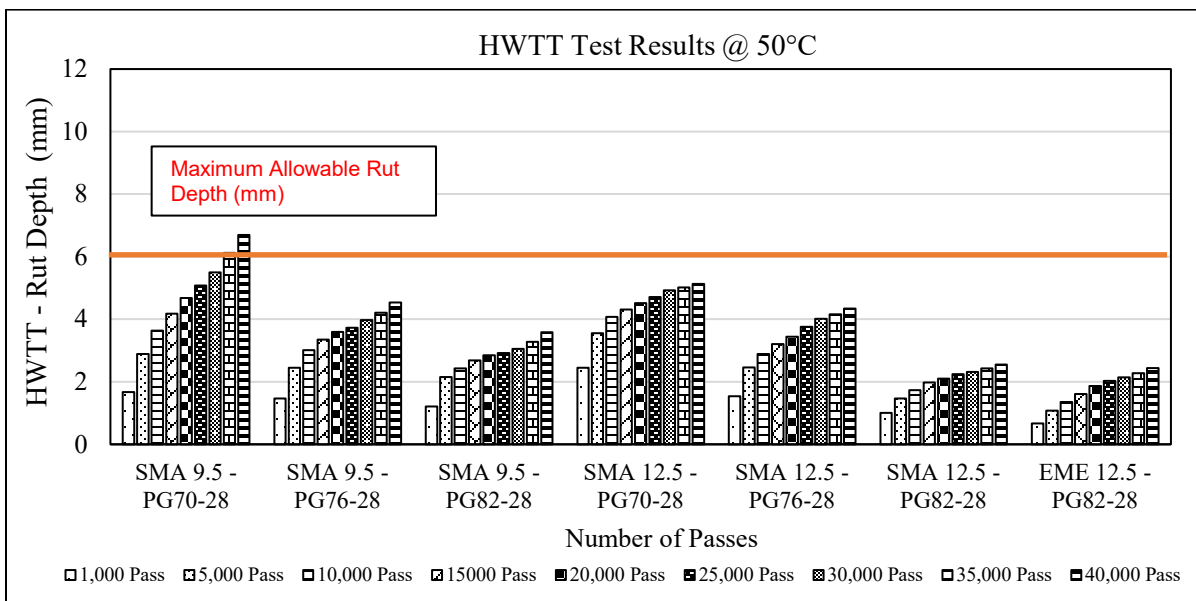


**Figure 5-2: HWTT Test Results @ 50°C**



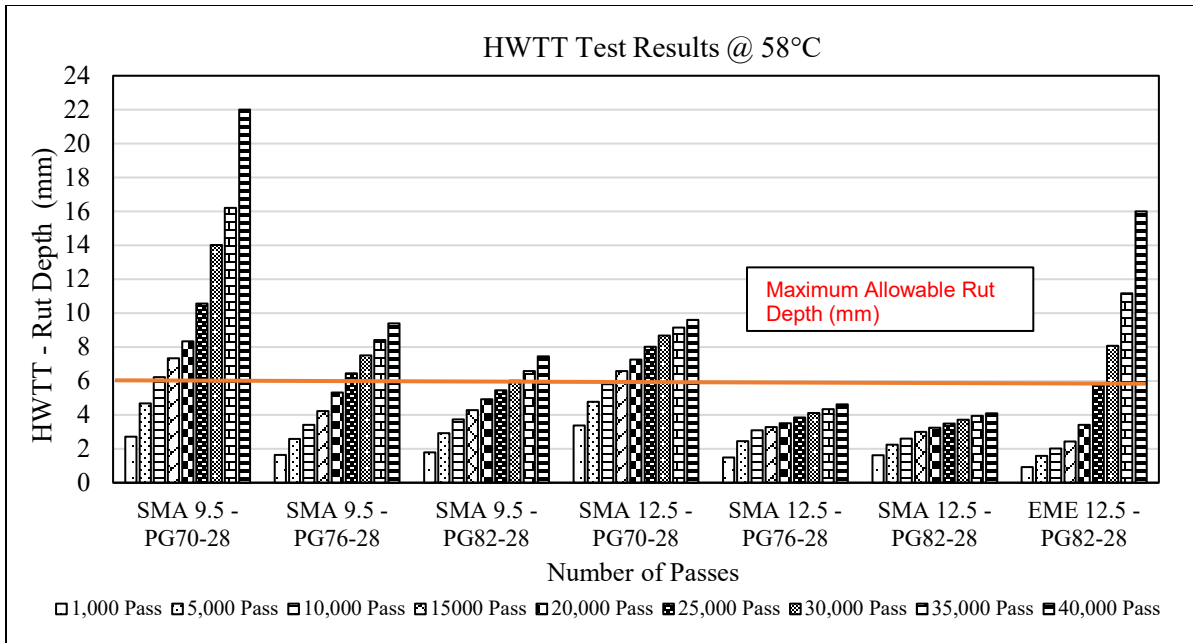


**Figure 5-3: HWTT Test Results @ 58°C**

The line graph is employed as shown in Figure 5-4, which is combined results of Figures 5-1 to 5-3, to illustrate both rut resistance and possible moisture susceptibility of the asphalt mixes. Each curve in Figure 5-4 demonstrates the correspondence total rut depth of each asphalt mix for a specific wheel-track passes and testing temperature. As illustrated in Figure 5-4, no potential moisture damage observed for the asphalt mixes tested at the testing temperature of 44°C and 50°C. This suggests that the water bath testing temperature was not high enough to weaken or break the bond between the asphalt binder and the aggregate, leading to no observed moisture damage. On the other hand, SIP occurred at 58°C testing temperature for SMA9.5-PG70-28 and EME mixes when the wheel-track passes reached 21,900 and 19,800, respectively. In addition, the total rut depth of SMA9.5-PG70-28, SMA12.5-PG70-28, SMA9.5-PG76-28, EME, and SMA9.5-PG82-28 mixes were 6mm at 8,500, 12,200, 23,150, 25,200, and 30,000 wheel-track passes, respectively. Comparing the results from different testing temperatures showed that the average total rut depth increased by 48.6% from 44°C to 50°C and 164.9% from 50°C to 58°C at 40,000 wheel-track passes. Therefore, it is recommended to conduct HWTT at 58°C testing temperature and increase the wheel-track passes to 40,000 to effectively distinguish heavy-duty asphalt mixes.

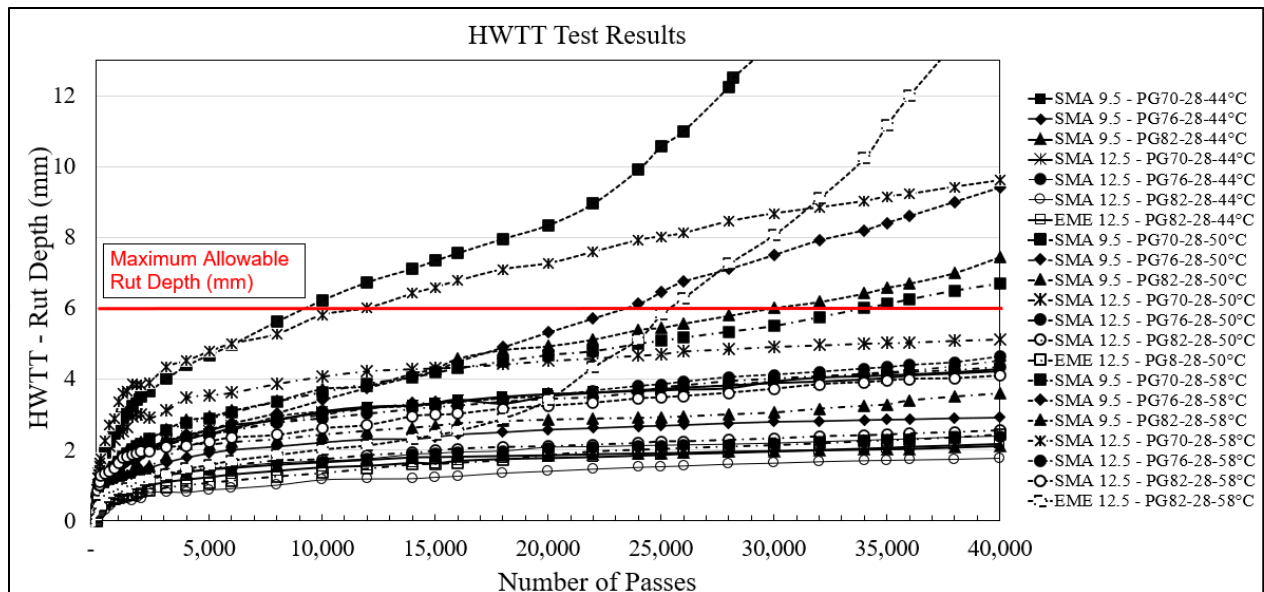
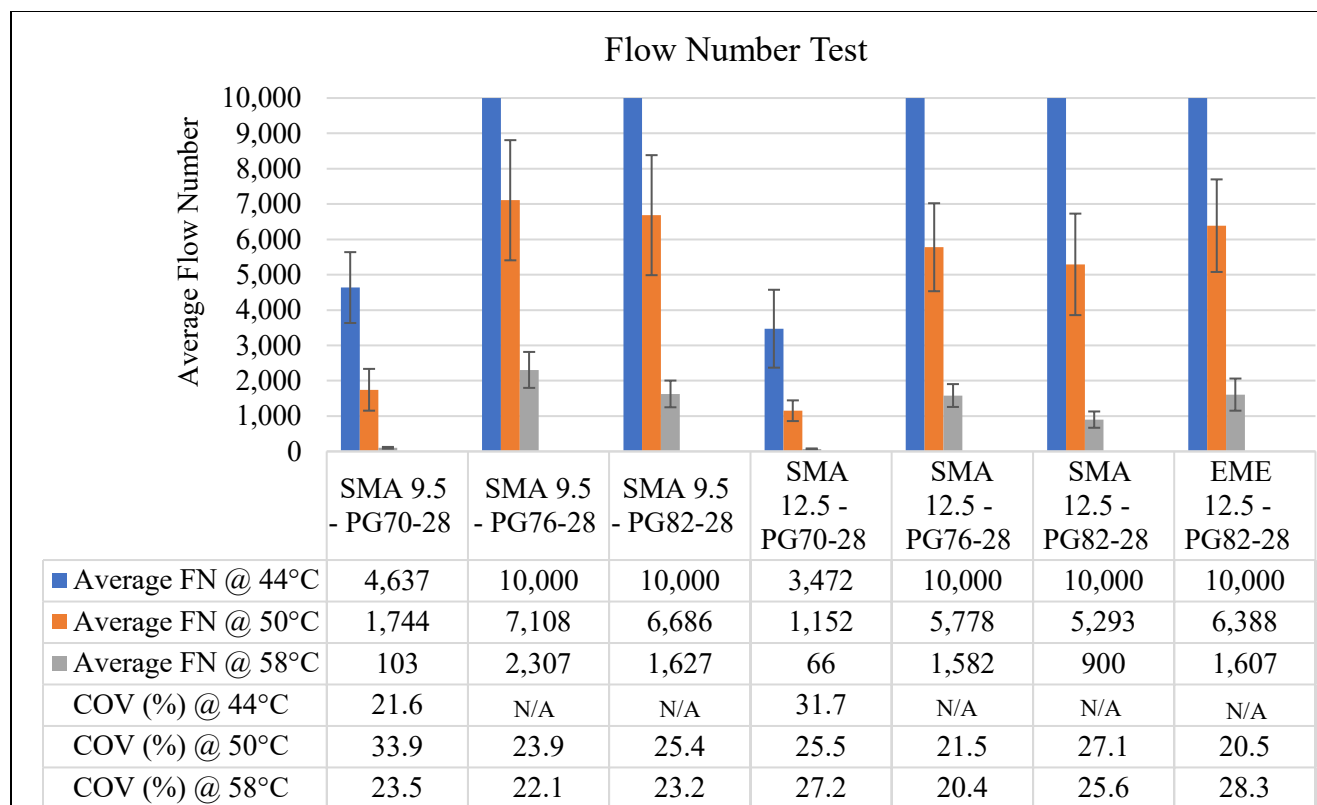


Figure 5-4: HWTT Test Results for All Temperatures

### 5.2.2. Flow Number Test Results

The FN test was conducted on triplicates to evaluate the rutting resistance of lab-produced asphalt mixes by applying repeated compressive loading cycles according to AASHTO T 378. Three testing temperatures (44°C, 50°C, and 58°C) were used, with the test performed at a 600 kPa unconfined pressure load. The test was ended either when the specimen failed or when 10,000 loading cycles were reached, whichever occurred first. FN was defined as the cycle at which the minimum strain rate occurred.

Figure 5-5 displays the average FN for each lab-produced asphalt mix, along with the standard deviation error bar and Coefficient of Variation (COV) for each temperature (44°C, 50°C, and 58°C). The results at 44°C showed that all mixes except for SMA12.5-PG70-28 (FN=3,472) and SMA9.5-PG70-28 (FN=4,637) had good rutting resistance as no samples failed at the maximum 10,000 loading cycles. However, the results at 44°C suggest that this temperature may not be appropriate for distinguishing the rutting resistance of high shear resistance mixes.



**Figure 5-5: Flow Number Test Results for All Testing Temperatures**

As indicated in Figure 5-5, the FN was observed for all asphalt mixes at the testing temperature of 50°C. The results indicated that among the SMA mixes, the smaller the NMAS, the higher the FN for mixes with the same PG binder. SMA12.5-PG70-28 showed the lowest rutting resistance (FN=1,152) followed by SMA9.5-PG70-28 (FN=1,744) at the 50°C testing temperature. Conversely, SMA9.5-PG76-28 showed the highest rutting resistance (FN=7,108) followed by SMA9.5-PG82-28 and EME mix with FN values of 6,686 and 6,388, respectively.

As seen in Figure 5-5, the FN values were much lower for the asphalt mixes when testing was conducted at 58°C. A similar trend was observed as at 50°C, with SMA12.5-PG70-28 and SMA9.5-PG70-28 showing the lowest rutting resistance on average (FN=66 and FN=103, respectively). SMA9.5-PG76-28 (FN=2,307) showed the highest rutting resistance, followed by SMA9.5-PG82-28 (FN=1,627) and EME mix (FN=1,607). The results indicate that a smaller NMAS leads to a higher FN for mixes with the same PG binder.

Overall, as shown in Figure 5-5, the COV of the FN was found to range from 20.4% to 33.9%, with an average of 25.1%, which is considered a high COV level. The FN value on average decreased by 45.2% as the testing temperature increased from 44°C to 50°C, with SMA12.5-PG70-

28 and SMA9.5-PG70-28 showing the highest average reduction of 66.8% and 62.4%, respectively. Furthermore, the FN value on average dropped by 80.3% as the testing temperature increased from 58°C to 50°C, with SMA12.5-PG70-28 and SMA9.5-PG70-28 showing the highest average reduction of 94.2% and 94.1%, respectively. SMA9.5-PG76-28, SMA12.5-PG76-28, and EME showed the lowest average FN value reduction of 67.5%, 72.6%, and 74.8%, respectively. Generally, the Flow Number test results showed that the SMA mixes with PG70-28 asphalt binder had the lowest rutting resistance (low FN values). This was attributed to the high softness of PG70-28 asphalt binder at high testing temperatures, which led to low cohesion and low adhesion between the binder and aggregate. The statistical analysis conducted using ANOVA showed that NMAS, PG binder, and testing temperature were significant sources of variation in the rutting resistance of the SMA mixes, with the interaction between asphalt binder PG grade and testing temperature also being statistically significant (as shown in Table 5-2). However, the effect of NMAS was found to be less important than the other factors, as shown by the low F statistics value

**Table 5-2: Summarized Analysis of Variance (ANOVA) for FN test for SMA Mixes**

| Source                | DF <sup>1</sup> | Adjusted SS <sup>2</sup> | Adjusted MS <sup>3</sup> | F-Value <sup>4</sup> | P-Value <sup>5</sup> | Statistically Significant |
|-----------------------|-----------------|--------------------------|--------------------------|----------------------|----------------------|---------------------------|
| NMAS                  | 1               | 5935508                  | 5935508                  | 8.48                 | 0.006                | Yes                       |
| PG Binder             | 2               | 200823631                | 100411815                | 143.40               | 0.000                | Yes                       |
| Temperature           | 2               | 431131894                | 215565947                | 307.86               | 0.000                | Yes                       |
| NMAS*PG Binder        | 2               | 29814                    | 14907                    | 0.02                 | 0.979                | No                        |
| NMAS*Temperature      | 2               | 1344509                  | 672255                   | 0.96                 | 0.392                | No                        |
| PG Binder*Temperature | 4               | 42764751                 | 10691188                 | 15.27                | 0.000                | Yes                       |
| Error                 | 36              | 25207780                 | 700216                   |                      |                      |                           |
| Total                 | 53              | 709632894                |                          |                      |                      |                           |

Note: <sup>1</sup>Degree of Freedom, <sup>2</sup>Adjusted Sum of Square, <sup>3</sup>Adjusted Mean of Squares, <sup>4</sup>Ratio of explained variance to unexplained variance, <sup>5</sup>P-Value is the probability  $|T_{observed}| > t_{critical}$  at significance level of 5% ( $\alpha=0.05$ )

The ANOVA analysis showed that 9.5mm NMAS had greater rutting resistance than 12.5mm NMAS based on the average of 27 test specimens. Additionally, PG76-28 asphalt binder produced higher average FN compared to PG82-28 and PG70-28 asphalt binders based on the average of 18 test specimens. Testing temperature of 44°C also showed higher average FN than 50°C and 58°C based on the average of 18 specimens. Figure 5-6 shows the main effect plots of FN test for SMA mixes using ANOVA analysis.

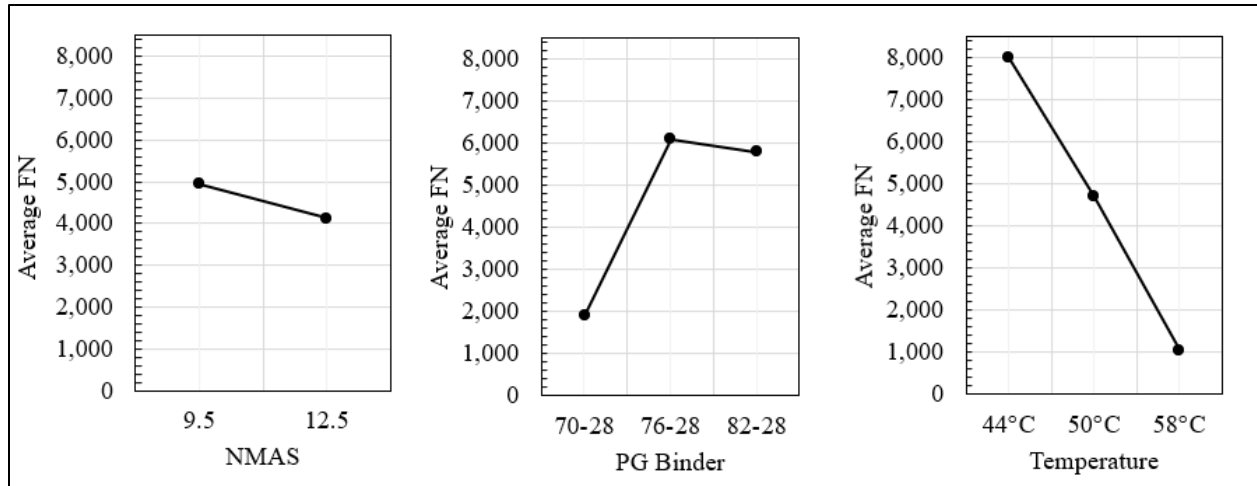


Figure 5-6: Main Effects Plots for FN Test for SMA Mixes

In addition, a paired t-test was performed on FN values to compare the SMA and EME asphalt mixes at 50°C and 58°C. The results in Table 5-3 showed that there was no significant difference between the FN values except between EME asphalt mix and both SMA9.5-PG70-28 and SMA12.5-PG70-28 mixes.

Table 5-3: Statistical Analysis for FN Test (EME vs. SMA mixes)

| Paired Mixes     |                  | Testing Temperature 50°C |                           | Testing Temperature 58°C |                           |
|------------------|------------------|--------------------------|---------------------------|--------------------------|---------------------------|
|                  |                  | P-Value                  | Statistically Significant | P-Value                  | Statistically Significant |
| SMA 9.5 PG70-28  | EME 12.5 PG82-28 | 0.005                    | Yes                       | 0.004                    | Yes                       |
| SMA 9.5 PG76-28  | EME 12.5 PG82-28 | 0.592                    | No                        | 0.150                    | No                        |
| SMA 9.5 PG82-28  | EME 12.5 PG82-28 | 0.822                    | No                        | 0.956                    | No                        |
| SMA 12.5 PG70-28 | EME 12.5 PG82-28 | 0.002                    | Yes                       | 0.004                    | Yes                       |
| SMA 12.5 PG76-28 | EME 12.5 PG82-28 | 0.590                    | No                        | 0.940                    | No                        |
| SMA 12.5 PG82-28 | EME 12.5 PG82-28 | 0.384                    | No                        | 0.074                    | No                        |

Tukey's HSD test using Minitab© software was conducted to statistically rank the seven lab-produced asphalt mixes based on their FN values. The results were presented in Tables 5-4 to 5-6 for testing temperatures of 44°C, 50°C and 58°C respectively. The results showed that SMA 9.5-PG70-28 and SMA12.5-PG70-28 mixes were ranked lowest based on the Tukey analysis. The results also indicated that generally, asphalt mixes with 9.5mm NMAS ranked higher than 12.5mm NMAS when comparing asphalt mixes with the same PG binder.

**Table 5-4: Summarized Analysis of Tukey’s HSD Ranking Based on Average FN at 44°C Testing Temperature**

| <b>Factor</b>    | <b>FN Mean</b> | <b>Grouping</b> |  |   |
|------------------|----------------|-----------------|--|---|
| EME 12.5 PG82-28 | 10,000         | A               |  |   |
| SMA 12.5 PG82-28 | 10,000         | A               |  |   |
| SMA 12.5 PG76-28 | 10,000         | A               |  |   |
| SMA 9.5 PG82-28  | 10,000         | A               |  |   |
| SMA 9.5 PG76-28  | 10,000         | A               |  |   |
| SMA 9.5 PG70-28  | 4,637          |                 |  | B |
| SMA 12.5 PG70-28 | 3,472          |                 |  | B |

**Table 5-5: Summarized Analysis of Tukey’s HSD Ranking Based on Average FN at 50°C Testing Temperature**

| <b>Factor</b>    | <b>FN Mean</b> | <b>Grouping</b> |   |   |
|------------------|----------------|-----------------|---|---|
| SMA 9.5 PG82-28  | 6,686          | A               |   |   |
| EME 12.5 PG82-28 | 6,388          | A               | B |   |
| SMA 9.5 PG76-28  | 6,108          | A               | B |   |
| SMA 12.5 PG76-28 | 5,778          | A               | B | C |
| SMA 12.5 PG82-28 | 5,293          | A               | B | C |
| SMA 9.5 PG70-28  | 1,744          |                 | B | C |
| SMA 12.5 PG70-28 | 1,152          |                 |   | C |

*Note: A and C correspond to the highest and lowest ranks, respectively.*

**Table 5-6: Summarized Analysis of Tukey’s HSD Ranking Based on Average FN at 58°C Testing Temperature**

| <b>Factor</b>    | <b>FN Mean</b> | <b>Grouping</b> |   |   |
|------------------|----------------|-----------------|---|---|
| SMA 9.5 PG76-28  | 2,307          | A               |   |   |
| SMA 9.5 PG82-28  | 1,627          | A               | B |   |
| EME 12.5 PG82-28 | 1,607          | A               | B |   |
| SMA 12.5 PG76-28 | 1,582          | A               | B |   |
| SMA 12.5 PG82-28 | 900            |                 | B | C |
| SMA 9.5 PG70-28  | 102.7          |                 |   | C |
| SMA 12.5 PG70-28 | 66.3           |                 |   | C |

### 5.2.3. IDEAL-RT Test Results

The IDEAL-RT test was conducted on asphalt mixes to determine their resistance to shear and rutting. The test was performed at three different temperatures (44°C, 50°C, and 58°C) to assess the effect of temperature changes on the asphalt mixes. The results are presented in a bar chart

with the average IDEAL-RT Index, along with the standard deviation error bar and COV for each lab-produced asphalt mix at each temperature as illustrated in Figure 5-7.

The results shown in Figure 5-7 indicate that the IDEAL-RT Index decreases as the testing temperature increases for all asphalt mixes. The SMA mixes with 9.5mm NMAS tend to have higher IDEAL-RT Index values compared to the SMA mixes with 12.5mm NMAS, with the exception of the PG70-28 mix at 58°C. At this temperature, the 12.5mm NMAS mix provided a slightly higher IDEAL-RT Index. The SMA9.5-PG70-28 and SMA12.5-PG70-28 mixes had the lowest rutting resistance among all the mixes for all temperatures. On the other hand, the EME, SMA9.5-PG76-28, and SMA9.5-PG82-28 mixes provided the highest rutting resistance for all testing temperature, respectively.

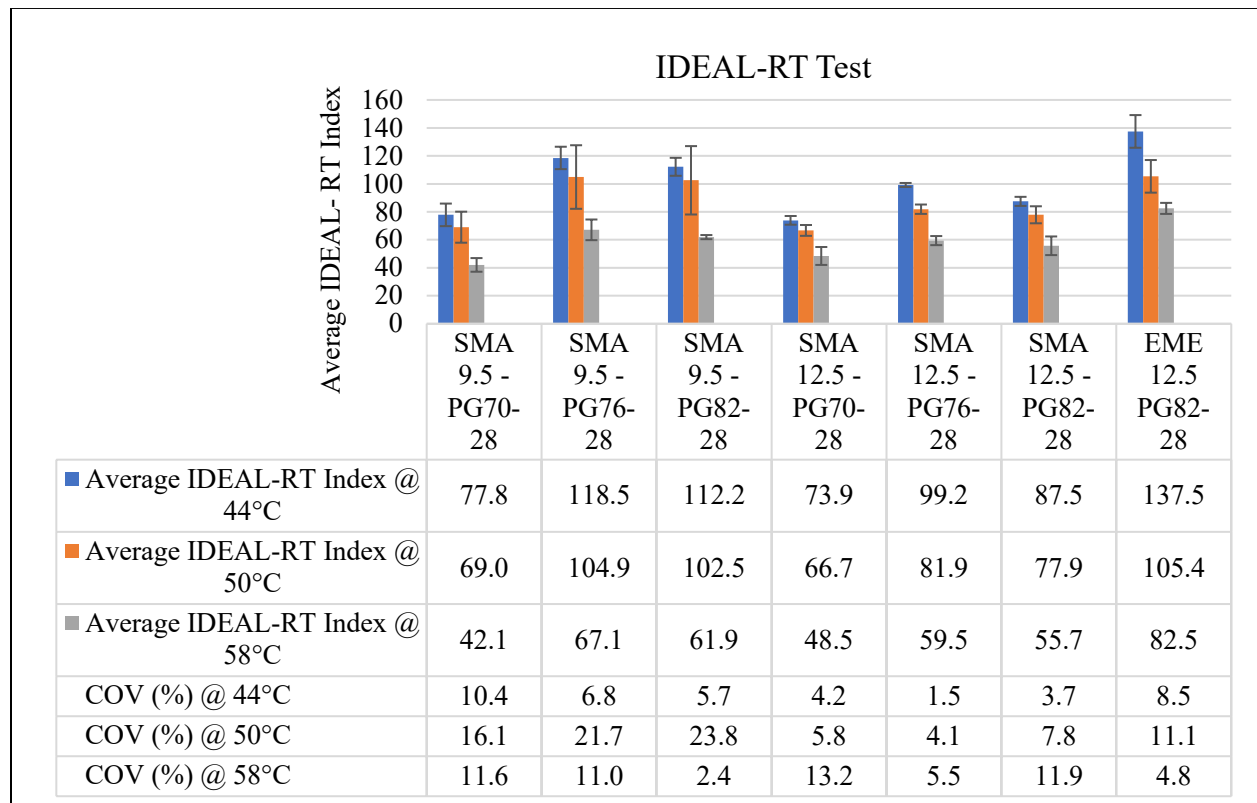


**Figure 5-7: IDEAL-RT Index Results at Three Testing Temperatures**

The results also showed that a 16.1% decrease in the IDEAL-RT Index value occurred when the testing temperature increased from 44°C to 50°C. The EME mix had the highest decrease followed by the SMA12.5-PG76-28, and SMA9.5-PG76-28 with drops of 30.5%, 21.1%, and 13.0%, respectively. When the temperature increased from 50°C to 58°C, the average IDEAL-RT Index value reduced by 45.8%. The SMA9.5-PG82-28 mix had the highest decrease at 65.6%, followed

by the SMA9.5-PG70-28 (64.1%) and SMA9.5-PG76-28 (56.2%). The EME mix had the least reduction in the IDEAL-RT Index value (27.8%).

As indicated in Figure 5-7, the COV for the average IDEAL-RT Index was found to be in the range of 1.5% to 23.8%, with an average COV of 9.1%. This is considered to be a low to medium level of COV. To see if there is a significant difference between the SMA mixes, the ANOVA analysis was conducted.

As presented in Table 5-7 and Figure 5-8, the results of the ANOVA showed that NMAS, PG binder, and test temperature were statistically significant factors affecting the IDEAL-RT Index value. Additionally, the interaction between NMAS and PG binder was found to be statistically significant.

**Table 5-7: Summarized Analysis of Variance (ANOVA) for IDEAL-RT Index for SMA Mixes**

| Source                | DF | Adj SS  | Adj MS  | F-Value | P-Value | Statistically Significant |
|-----------------------|----|---------|---------|---------|---------|---------------------------|
| NMAS                  | 1  | 1851.7  | 1851.72 | 19.97   | 0.000   | Yes                       |
| PG Binder             | 2  | 6477.2  | 3238.59 | 34.93   | 0.000   | Yes                       |
| Temperature           | 2  | 14597.3 | 7298.63 | 78.73   | 0.000   | Yes                       |
| NMAS*PG Binder        | 2  | 942.0   | 471.00  | 5.08    | 0.011   | Yes                       |
| NMAS*Temperature      | 2  | 573.9   | 286.95  | 3.10    | 0.057   | No                        |
| PG Binder*Temperature | 4  | 386.8   | 96.71   | 1.04    | 0.399   | No                        |
| Error                 | 36 | 3337.4  | 92.71   |         |         |                           |
| Total                 | 53 | 28218.0 |         |         |         |                           |

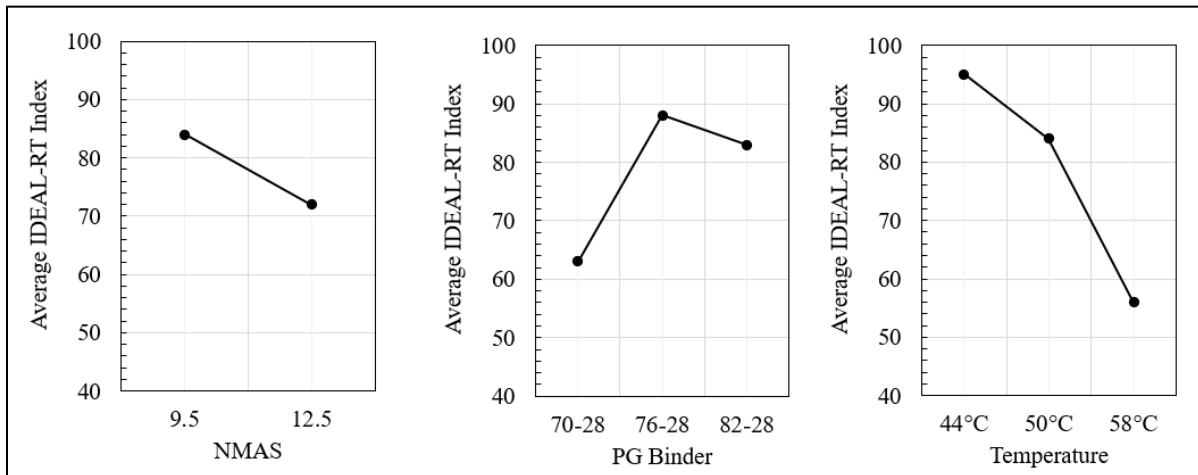


**Figure 5-8: Main Effects Plots for IDEAL-RT Index for SMA Mixes**



Figure 5-8 illustrates the main effect plots for the IDEAL-RT Index value using ANOVA analysis. The results show that 9.5mm NMAS has a higher rutting resistance compared to 12.5mm NMAS based on the average of 27 test specimens. Additionally, the PG76-28 asphalt binder had the highest average value of the IDEAL-RT Index, followed by PG82-28 and PG70-28 binders. Additionally, the results showed that a higher testing temperature led to a decrease in the resistance to rutting in SMA asphalt mixes.

A paired t-test was used to compare the IDEAL-RT Index values of SMA and EME asphalt mixes. As presented in Table 5-8, there were statistically significant differences between EME and all other SMA mixes except for SMA9.5-PG76-28 mix at 44°C testing temperature. The EME mix had similar resistance to rutting as the SMA9.5-PG76-28 and SMA9.5-PG82-28 mixes at 50°C, and had the highest IDEAL-RT Index value among all mixes at 58°C.

**Table 5-8: Statistical Analysis for IDEAL-RT Index (EME vs. SMA mixes)**

| Paired Mixes        |                     | Testing Temperature 44°C |                           | Testing Temperature 50°C |                           | Testing Temperature 58°C |                           |
|---------------------|---------------------|--------------------------|---------------------------|--------------------------|---------------------------|--------------------------|---------------------------|
|                     |                     | P-Value                  | Statistically Significant | P-Value                  | Statistically Significant | P-Value                  | Statistically Significant |
| SMA 9.5<br>PG70-28  | EME 12.5<br>PG82-28 | 0.002                    | Yes                       | 0.017                    | Yes                       | 0.000                    | Yes                       |
| SMA 9.5<br>PG76-28  | EME 12.5<br>PG82-28 | 0.081                    | No                        | 0.975                    | No                        | 0.034                    | Yes                       |
| SMA 9.5<br>PG82-28  | EME 12.5<br>PG82-28 | 0.030                    | Yes                       | 0.865                    | No                        | 0.001                    | Yes                       |
| SMA 12.5<br>PG70-28 | EME 12.5<br>PG82-28 | 0.001                    | Yes                       | 0.006                    | Yes                       | 0.001                    | Yes                       |
| SMA 12.5<br>PG76-28 | EME 12.5<br>PG82-28 | 0.005                    | Yes                       | 0.028                    | Yes                       | 0.001                    | Yes                       |
| SMA 12.5<br>PG82-28 | EME 12.5<br>PG82-28 | 0.002                    | Yes                       | 0.022                    | Yes                       | 0.004                    | Yes                       |

Tukey's HSD test was used to rank the asphalt mixes based on their IDEAL-RT Index values at a 5% confidence level. The results of the Tukey ranking, as shown in Tables 5-9 to 5-11, showed that the EME mix ranked first at all testing temperatures. However, as shown in Table 5-1, at 50°C testing temperature, all asphalt mixes were ranked the same, indicating that 50°C may not be an effective temperature for IDEAL-RT testing to differentiate between heavy-duty asphalt mixes. In general, the results showed that asphalt mixes with 9.5mm NMAS ranked higher than those with 12.5mm NMAS, when using the same PG binder, for both IDEAL-RT Index and FN test. This trend was consistent across both tests.

**Table 5-9: Summarized Analysis of Tukey’s HSD Ranking Based on Average IDEAL-RT Index at 44°C Testing Temperature**

| <b>Factor</b>    | <b>Mean</b> | <b>Grouping</b> |   |   |   |   |
|------------------|-------------|-----------------|---|---|---|---|
| EME 12.5 PG80-28 | 137.50      | A               |   |   |   |   |
| SMA 9.5 PG76-28  | 118.53      | A               | B |   |   |   |
| SMA 9.5 PG82-28  | 112.20      |                 | B | C |   |   |
| SMA 12.5 PG76-28 | 99.21       |                 |   | C | D |   |
| SMA 12.5 PG82-28 | 87.49       |                 |   |   | D | E |
| SMA 9.5 PG70-28  | 77.85       |                 |   |   |   | E |
| SMA 12.5 PG70-28 | 73.92       |                 |   |   |   | E |

**Table 5-10: Summarized Analysis of Tukey’s HSD Ranking Based on Average IDEAL-RT Index at 50°C Testing Temperature**

| <b>Factor</b>    | <b>Mean</b> | <b>Grouping</b> |
|------------------|-------------|-----------------|
| EME 12.5 PG82-28 | 105.37      | A               |
| SMA 9.5 PG76-28  | 104.9       | A               |
| SMA 9.5 PG82-28  | 102.5       | A               |
| SMA 12.5 PG76-28 | 81.89       | A               |
| SMA 12.5 PG82-28 | 77.90       | A               |
| SMA 9.5 PG70-28  | 69.03       | A               |
| SMA 12.5 PG70-28 | 66.73       | A               |

**Table 5-11: Summarized Analysis of Tukey’s HSD Ranking Based on Average IDEAL-RT Index at 58°C Testing Temperature**

| <b>Factor</b>    | <b>Mean</b> | <b>Grouping</b> |   |   |   |   |
|------------------|-------------|-----------------|---|---|---|---|
| EME 12.5 PG82-28 | 82.50       | A               |   |   |   |   |
| SMA 9.5 PG76-28  | 67.15       |                 | B |   |   |   |
| SMA 9.5 PG82-28  | 61.94       |                 | B | C |   |   |
| SMA 12.5 PG76-28 | 59.45       |                 | B | C |   |   |
| SMA 12.5 PG82-28 | 55.75       |                 | B | C | D |   |
| SMA 12.5 PG70-28 | 48.47       |                 |   | C | D |   |
| SMA 9.5 PG70-28  | 42.08       |                 |   |   |   | D |

### 5.2.4. Dynamic Modulus Test Results

The Dynamic Modulus test was carried out to evaluate the linear viscoelastic characteristics of the asphalt mixes using the AASHTO TP132 procedure. Two test samples of each mix were tested at five different temperatures (-10°C, 4.4°C, 21.1°C, 37.8°C, 54.4°C) and six frequencies (25, 10, 5, 1, 0.5, 0.1 Hz) by applying sinusoidal loading and measuring the dynamic modulus. The results are shown in Figures 5-9 to 5-13, which display the average measured  $|E^*|$  values for each asphalt mix at different temperatures for the six frequencies tested.

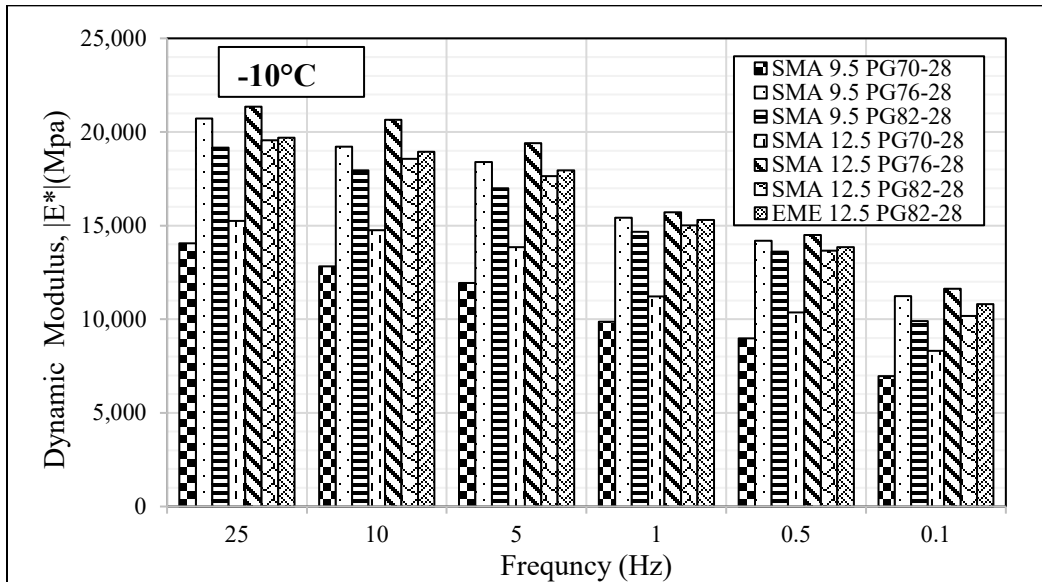


Figure 5-9: Dynamic Modulus Results at -10°C Testing Temperature

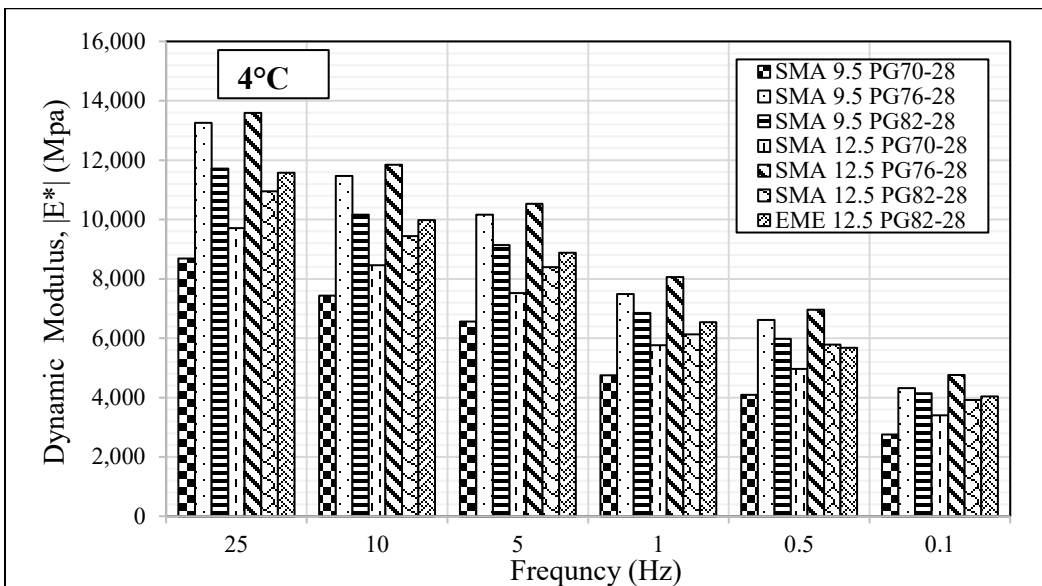


Figure 5-10: Dynamic Modulus Results at 4°C Testing Temperature

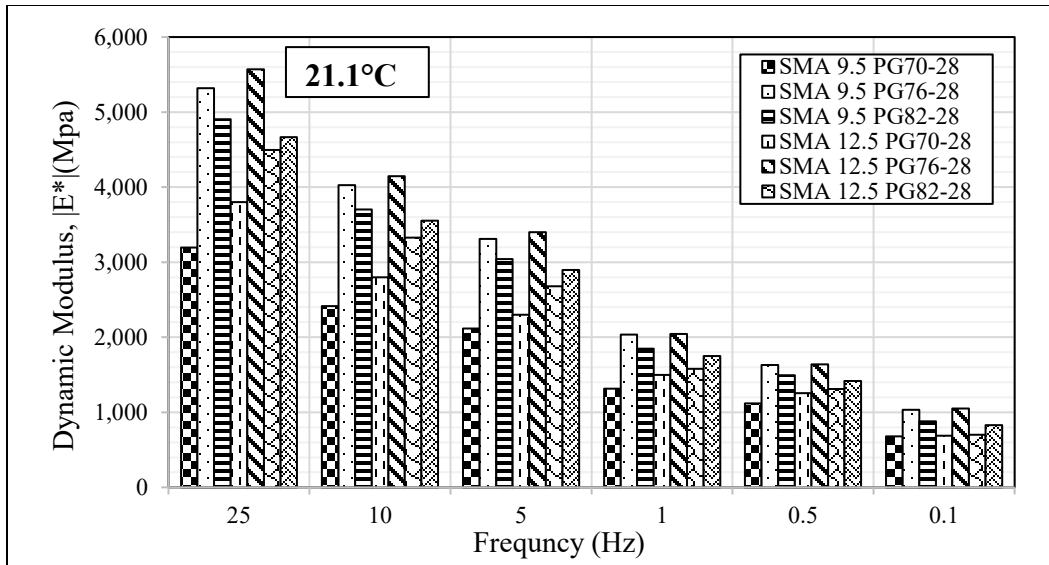


Figure 5-11: Dynamic Modulus Results at 21.1°C Testing Temperature

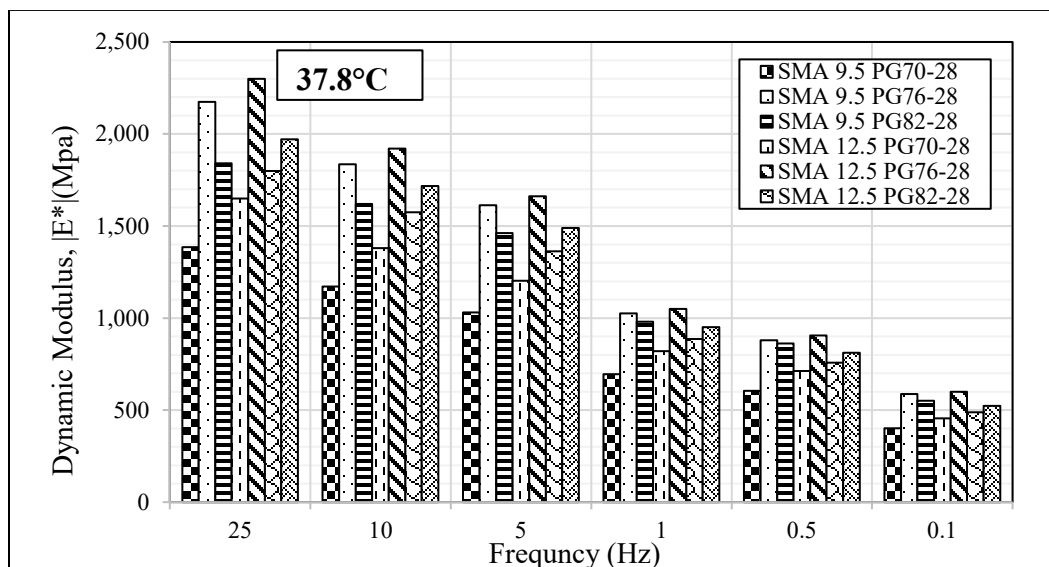


Figure 5-12: Dynamic Modulus Results at 37.8°C Testing Temperature

As shown in Figures 5-9 to 5-13, the  $|E^*|$  of all asphalt mixes decreases as the testing temperature increases and the load frequency decreases. This is in line with previous research findings which showed that low frequency loads result in higher stress levels and thus lower  $|E^*|$  values. The average reduction in  $|E^*|$  was 96.8% when testing temperature increased from  $-10^{\circ}\text{C}$  to  $54.4^{\circ}\text{C}$ . To evaluate the rutting resistance of the asphalt mixes, the average  $|E^*|$  at  $54.4^{\circ}\text{C}$  testing temperature was selected for further analysis.

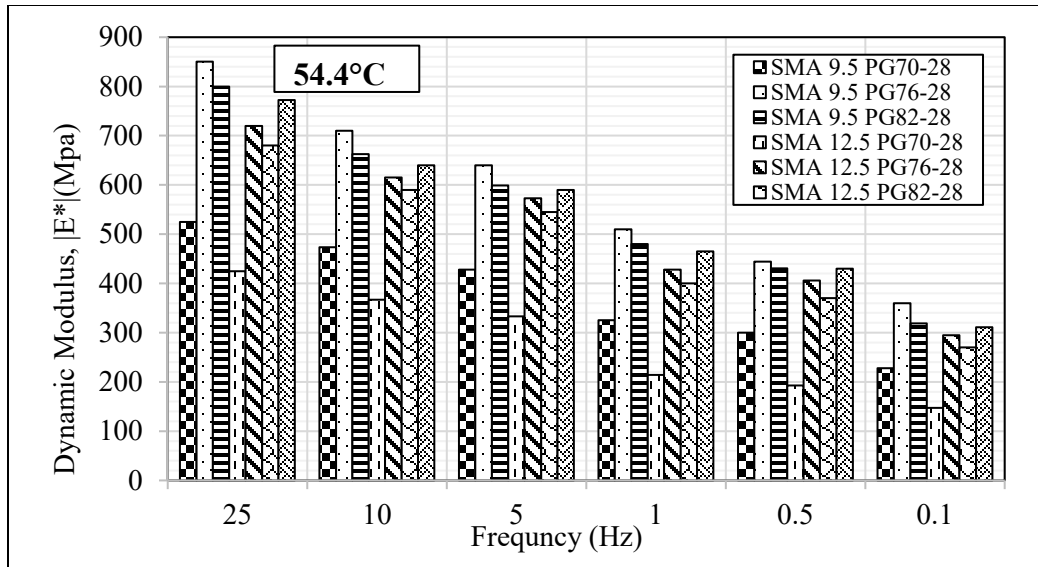


Figure 5-13: Dynamic Modulus Results at 54.4°C Testing Temperature

The Figure 5-13 shows that at 54.4°C testing temperature, SMA9.5-PG76-28 has the highest stiffness followed by SMA9.5-PG82-28, EME, SMA12.5-PG76-28, SMA12.5-PG82-28, SMA9.5-PG70-28, and SMA12.5-PG70-28, respectively. The results suggest that SMA mixes with 9.5mm NMAS have better rutting resistance compared to SMA mixes with 12.5mm NMAS and the same asphalt binder PG grade. The dynamic modulus results for SMA mixes are consistent with both FN test and IDEAL-RT test results.

In accordance with AASHTO PP62-09 procedure, the results obtained from Dynamic Modulus test were further combined to obtain a master curve for all asphalt mixes by merging the  $|E^*|$  measurement from different frequencies and temperatures at reference temperature of 21.1°C as shown in Figure 5-14. To better investigate the results, the previous studies at CPATT suggested that dividing the Master Curves into three zones (low, intermediate, and high frequencies) would potentially distinguish the asphalt mix behaviour for different types of distresses (Tighe & El-Hakim, 2010; Varamini, 2016). The results shown in Figure 5-15 indicate that the SMA12.5-PG70-28 and SMA9.5-PG70-28 asphalt mixes have a lower Dynamic Modulus compared to the other asphalt mixes, suggesting a lower level of resistance to rutting. This is likely due to the use of a softer grade of asphalt binder (PG70-28) in the mix design. Additionally, the results suggest that smaller NMAS (9.5mm) have a higher level of resistance to rutting compared to larger NMAS (12.5mm) with the same grade of asphalt binder, particularly at lower frequencies.

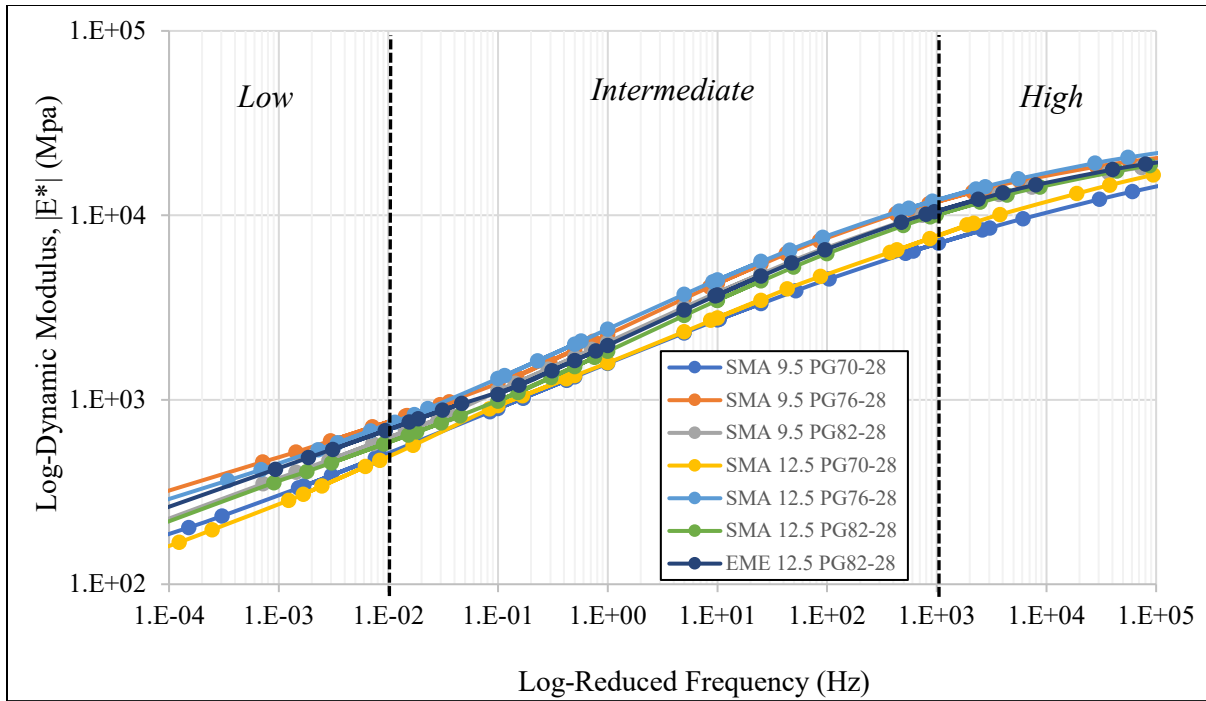


Figure 5-14: Master Curve Results for All Asphalt Mixes

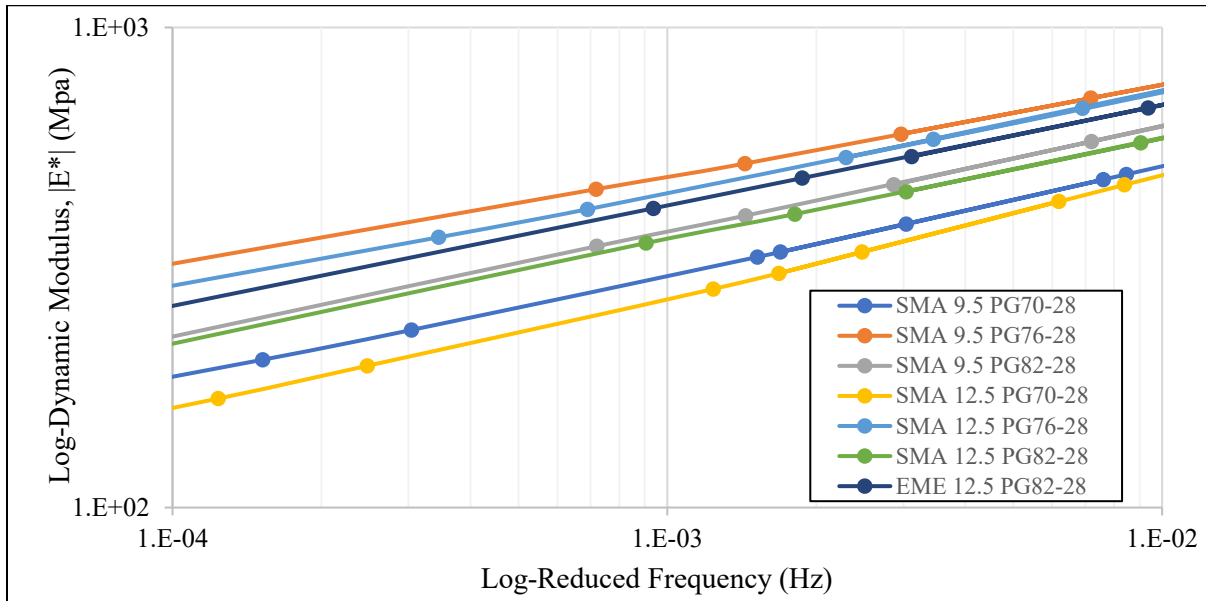


Figure 5-15: Low Frequency Zone Master Curve Results for All Asphalt Mixes

### 5.2.5. Relationship Between Test Results

In this research, the resistance of asphalt mixes to rutting was tested using HWTT, FN, and IDEAL-RT tests at three testing temperatures of 44°C, 50°C, and 58°C. The analysis was only conducted for 50°C and 58°C testing temperatures as most mixes did not fail at 44°C during FN test. For HWTT, the analysis was conducted on both 20,000 and 40,000 passes. The stiffness of

the asphalt mixes was evaluated using the Dynamic Modulus test at five temperatures (-10, 4.4, 21.1, 37.8, 54.4°C) and six frequencies (25, 10, 5, 1, 0.5, 0.1 Hz). In addition, the rutting resistance of asphalt mixes was investigated by conducting analyses at two frequencies, 1Hz and 0.1Hz, at a testing temperature of 54.4°C. The frequency of 1Hz was used to simulate one cycle per second, which is almost equivalent to the cycle time of both HWTT and FN tests. The more severe condition of repetitive traffic loading was represented by the frequency of 0.1Hz. The analysis was divided into two groups: A) all asphalt mixes and B) only SMA mixes.

Figures 5-16 to 5-21 present a subset of graphs that were used to determine the relationship between different rutting parameters. Figures 5-16 to 5-18 show the correlation between  $|E^*|$  at 54.4°C and a frequency of 1Hz with FN value, IDEAL-RT Index value, and HWTT rut depth at 20,000 passes and 50°C testing temperature, respectively, for all asphalt mixes. The remaining figures can be found in Appendix A. The results showed a high correlation between  $|E^*|$  at 54.4°C and 1Hz frequency with FN values ( $R^2=0.84$ ) and IDEAL-RT Index values ( $R^2=0.75$ ). The high correlation between  $|E^*|$  and FN values can be attributed to the similarity of testing specimens and sinusoidal loading. However, the correlation between  $|E^*|$  and HWTT rut depth at 20,000 passes was low ( $R^2=0.55$ ), indicating that not only the type of loading but also the testing conditions (such as the asphalt sample being submerged in water for HWTT) may influence the correlation. Similar trends were observed when comparing FN, IDEAL-RT Index, and HWTT for all asphalt mixes, as shown in Figures 5-19 to 5-21. As illustrated in Figure 5-19, there was a good correlation between FN and IDEAL-RT Index values at 50°C testing temperature ( $R^2=0.78$ ). It then followed by correlation between FN and HWTT ( $R^2=0.63$ ) and IDEAL-RT and HWTT ( $R^2=0.59$ ) as shown in Figures 5-20 and 5-21, respectively. This suggests that both the type of loading and testing conditions may influence the correlation between different methods of evaluating rutting resistance.

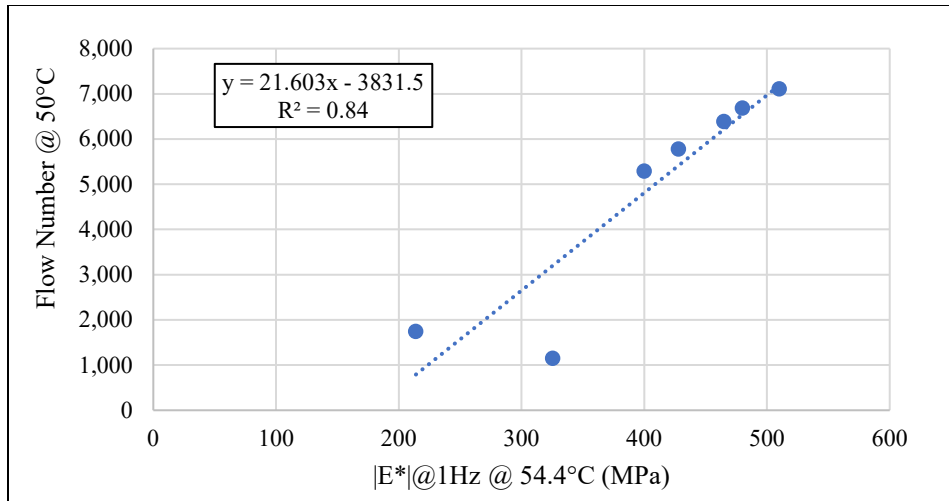


Figure 5-16: Flow Number at 50°C vs. Dynamic Modulus |E\*| at 54.4°C at 1Hz for Group A

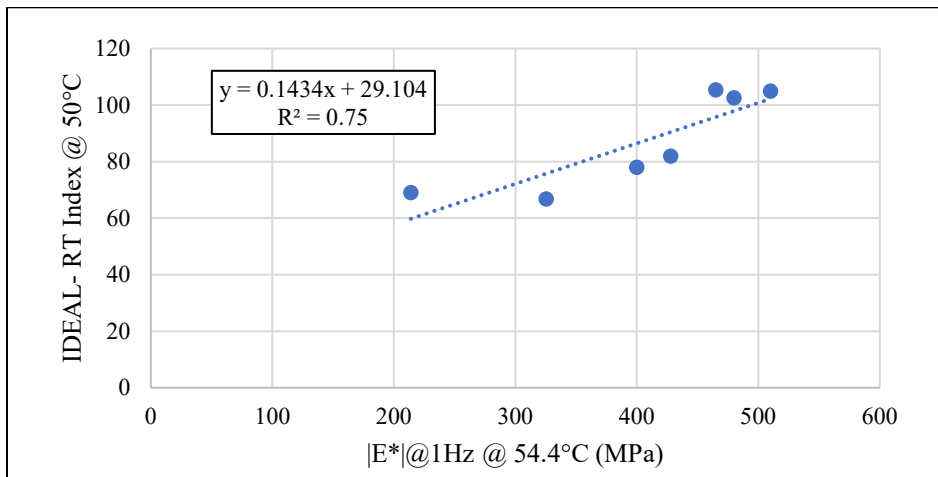


Figure 5-17: IDEAL-RT Index at 50°C vs. Dynamic Modulus |E\*| at 54.4°C at 1Hz for Group A

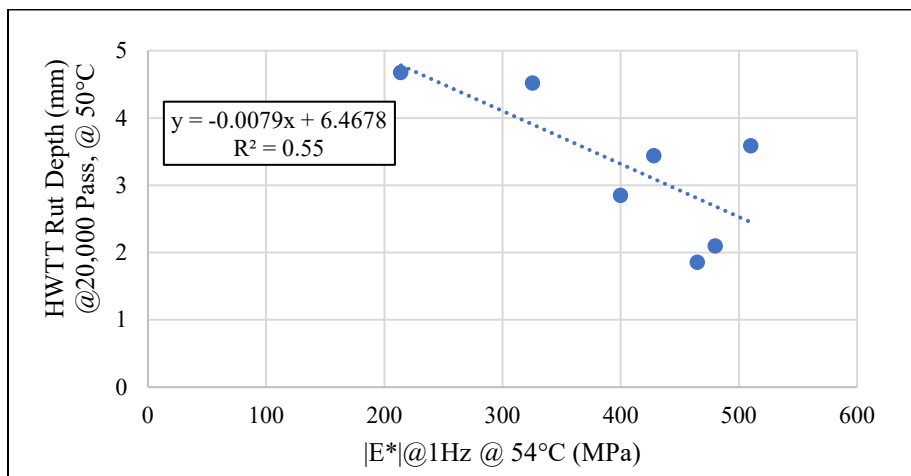


Figure 5-18: HWTT at 20,000 pass at 50°C vs. Dynamic Modulus |E\*| at 54.4°C at 1Hz for Group A



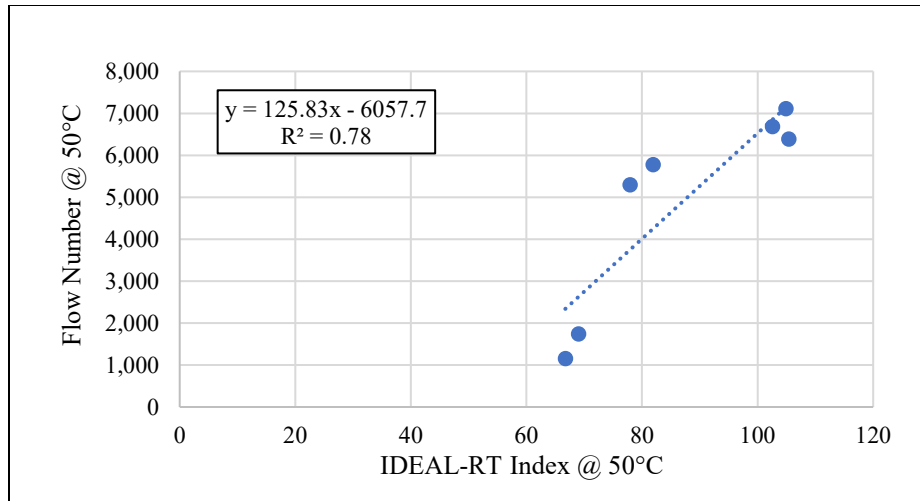


Figure 5-19: FN at 50°C vs. IDEAL-RT Index at 50°C for Group A

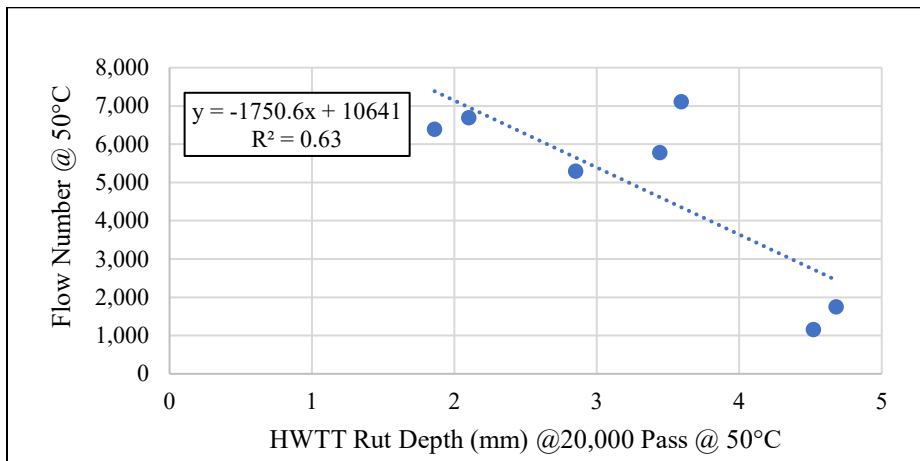


Figure 5-20: FN at 50°C vs. HWTT at 20,000 pass at 50°C for Group A

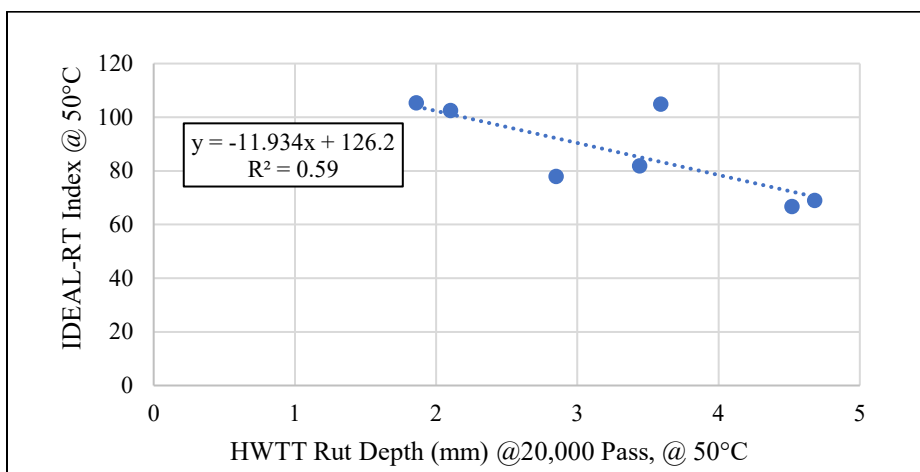


Figure 5-21: IDEAL-RT Index at 50°C vs. HWTT at 20,000 pass at 50°C for Group A

Table 5-12 summarizes the correlation between FN, IDEAL-RT Index, HWTT (20,000 and 40,000 passes), and Dynamic Modulus (54.4°C@ 1Hz and 0.1Hz) for both groups A and B at 50°C and 58°C testing temperatures. Generally, the results indicate that testing temperature of 50°C was not effective in differentiating between the SMA and EME mixes for both groups A and B. The IDEAL-RT Index and HWTT showed poor correlation with  $R^2$  values ranging from 0.40 to 0.59 at 50°C. The correlation between the  $|E^*|$  at 1Hz and 0.1Hz frequency and HWTT was also poor, with  $R^2$  values ranging from 0.45 to 0.64. However, the correlation between the parameters and  $|E^*|$  at 1Hz frequency was higher than that at 0.1Hz frequency for both groups A and B at 50°C. On the other hand, the results suggest that testing temperature at 58°C was more effective in distinguishing between the SMA and EME mixes for both groups A and B. As shown in Table 5-12, both FN and IDEAL-RT have a strong correlation with  $|E^*|$  ( $R^2$  ranging from 0.84 to 0.98) at a testing temperature of 58°C for group B at both 1Hz and 0.1Hz frequencies. Testing at 58°C results in higher correlation between FN/IDEAL-RT and  $|E^*|$  compared to testing at 50°C. There was a strong correlation between IDEAL-RT and FN ( $R^2=0.93$ ) for group B at 58°C. However, there was a very poor correlation between IDEAL-RT and HWTT at 40,000 ( $R^2=0.012$ ) and between FN and HWTT at 40,000 ( $R^2=0.13$ ) for group A at 58°C testing temperature. The results suggest that testing at 58°C temperature was effective in differentiating the rutting resistance of asphalt mixes containing SMA and EME. The higher correlation in the group B containing only SMA mixes compared to group A supports that 58°C is an appropriate temperature to evaluate rutting resistance of heavy-duty asphalt mixes.

**Table 5-12: Correlation Summary Between FN, IDEAL-RT Index, HWTT, and Dynamic Modulus (54.4°C@ 1Hz and 0.1Hz) for Both Groups A and B at 50°C and 58°C Testing Temperatures**

| Comparison Parameters   | Testing Temperature of 50°C ( $R^2$ ) |         | Testing Temperature of 58°C ( $R^2$ ) |         |
|---|---------------------------------------|---------|---------------------------------------|---------|
|   | Group A                               | Group B | Group A                               | Group B |
| Flow Number vs. Dynamic Modulus $ E^* $ at 54.4°C at 1Hz      | 0.84                                  | 0.83    | 0.85                                  | 0.84    |
| Flow Number vs. Dynamic Modulus $ E^* $ at 54.4°C at 0.1Hz    | 0.81                                  | 0.80    | 0.86                                  | 0.86    |
| IDEAL-RT Index vs. Dynamic Modulus $ E^* $ at 54.4°C at 1Hz   | 0.75                                  | 0.76    | 0.66                                  | 0.98    |
| IDEAL-RT Index vs. Dynamic Modulus $ E^* $ at 54.4°C at 0.1Hz | 0.72                                  | 0.75    | 0.62                                  | 0.98    |

| Comparison Parameters   | Testing Temperature of 50°C (R <sup>2</sup> ) |         | Testing Temperature of 58°C (R <sup>2</sup> ) |         |
|---|---|---------|---|---------|
|   | Group A                                       | Group B | Group A                                       | Group B |
| HWTT at 20,000 pass vs. Dynamic Modulus  E*  at 54.4°C at 1Hz   | 0.55  | 0.55    | 0.54  | 0.51    |
| HWTT at 20,000 pass vs. Dynamic Modulus  E*  at 54.4°C at 0.1Hz | 0.45  | 0.46    | 0.49  | 0.46    |
| HWTT at 40,000 pass vs. Dynamic Modulus  E*  at 54.4°C at 1Hz   | 0.64  | 0.64    | 0.32  | 0.55    |
| HWTT at 40,000 pass vs. Dynamic Modulus  E*  at 54.4°C at 0.1Hz | 0.55  | 0.56    | 0.32  | 0.52    |
| Flow Number vs. IDEAL-RT Index                                  | 0.78  | 0.80    | 0.60  | 0.93    |
| Flow Number vs. HWTT at 20,000 pass                             | 0.63  | 0.65    | 0.42  | 0.39    |
| Flow Number vs. HWTT at 40,000 pass                             | 0.56  | 0.55    | 0.13  | 0.26    |
| IDEAL-RT Index vs. HWTT at 20,000 pass                          | 0.59  | 0.47    | 0.49  | 0.48    |
| IDEAL-RT Index vs. HWTT at 40,000 pass                          | 0.53  | 0.40    | 0.012   | 0.46    |

**5.2.6. Asphalt Mixes Ranking**

The resistance of asphalt mixes to rutting was compared using a numerical ranking method based on three parameters: FN, IDEAL-RT Index, and rut depth at 40,000 passes for HWTT. The Tukey's HSD test was used to statistically rank the asphalt mixes based on their average FN and IDEAL-RT Index values with 95% confidence level. However, the grouping for Tukey's HSD was based on alphabetical orders; therefore, for ranking purposes the numerical values were assigned to the grouping where grouping A ranked as 1 (best asphalt mix) and the rest of the groups assigned in ascending numerical order. To compare the HWTT results, the asphalt mixes were ranked based on the measured rut depth at 40,000 passes, with the mix with the lowest rut depth ranked as 1 and the mix with the highest rut depth ranked as 7. The total rank for each asphalt mix was calculated by adding up the ranks from each test, referred to as the "Total Ranking". A lower Total Ranking value indicates a better rutting resistance. As discussed in section 5.2.5, the 58°C testing temperature was found to be appropriate for distinguishing between SMA mixes and EME mixes. Hence, for ranking purposes, only the test results at 58°C were considered. Table 5-13 presents the ranking of each asphalt mix based on FN, IDEAL-RT Index, and rut depth at 40,000 passes for HWTT values.

**Table 5-13: Rankings of Asphalt Mixes' Rutting Resistance Based on HWTT, FN, and IDEAL-RT Tests at 58°C Testing Temperature**

| Asphalt Mixes     | <i>HWTT</i>                  |         | <i>FN Test</i>           |                  |         | <i>IDEAL-RT Test</i>     |                  |         | <i>Total Ranking</i> |
|-------------------|------------------------------|---------|--------------------------|------------------|---------|--------------------------|------------------|---------|----------------------|
|                   | 58°C Testing Temperature     |         | 58°C Testing Temperature |                  |         | 58°C Testing Temperature |                  |         |                      |
|                   | Rut Depth (mm) @ 40,000 Pass | Ranking | Average FN               | Tukey's Grouping | Ranking | Average IDEAL-RT Index   | Tukey's Grouping | Ranking |                      |
| SMA 9.5 - PG70-28 | 22.0                         | 7       | 103                      | C                | 4       | 42.1                     | D                | 6       | 17                   |
| SMA 9.5-PG76-28   | 9.4                          | 4       | 2,307                    | A                | 1       | 67.2                     | B                | 2       | 7                    |
| SMA 9.5-PG82-28   | 7.4                          | 3       | 1,627                    | AB               | 2       | 61.9                     | BC               | 3       | 8                    |
| SMA 12.5-PG70-28  | 9.6                          | 5       | 66                       | C                | 4       | 48.5                     | CD               | 5       | 14                   |
| SMA 12.5-PG76-28  | 4.6                          | 2       | 1,582                    | AB               | 2       | 59.5                     | BC               | 3       | 7                    |
| SMA 12.5-PG82-28  | 4.1                          | 1       | 900                      | BC               | 3       | 55.8                     | BCD              | 4       | 8                    |
| EME 12.5-PG80-28  | 16.0                         | 6       | 1,607                    | AB               | 2       | 82.5                     | A                | 1       | 9                    |

Note: Lower the ranking, better the Rutting Resistance of Asphalt Mix

As shown in Table 5-13, SMA12.5-PG82-28, SMA9.5-PG76-28, and EME mix were ranked 1 (the best performed asphalt mix) with respect to HWTT, FN, and IDEAL-RT Index values, respectively. However, as per total ranking score both SMA9.5-PG76-28 and SMA12.5-PG76-28 received a ranking score of 7 which is the lowest score compared to rest of asphalt mixes. The results suggested that both SMA9.5-PG76-28 and SMA12.5-PG76-28 were relatively sound asphalt mixes in terms of rutting resistance.

### 5.3. Summary and Conclusions

In this chapter, HWTT, FN, and IDEAL-RT tests were employed to understand the rutting resistance of the seven lab-produced asphalt mixes including six SMA mixes and a EME mix. All tests were conducted at 44°C, 50 °C, and 58 °C to evaluate the sensitivity of the rutting resistance response of asphalt mixes to temperature change. In addition, different statistical analysis methods were employed for both FN and IDEAL-RT Index to analyze the results. Moreover, Dynamic Modulus test was conducted at five temperatures (-10, 4.4, 21.1, 37.8, 54.4°C) and six frequencies (25, 10, 5, 1, 0.5, 0.1 Hz) and master curve was developed by merging the |E\*| measurement from different frequencies and temperatures at reference temperature of 21.1°C. The results from the HWTT, FN, and IDEAL-RT tests were analyzed for their correlation with the |E\*| values at two frequencies (1Hz and 0.1Hz) at a temperature of 54.4°C. A ranking system was used to rank all

asphalt mixes based on their rutting resistance based on the results from the HWTT, FN, and IDEAL-RT tests.

The following conclusions could be drawn based on the experimental results and discussions provided in this chapter:

- In general, the 58°C testing temperature was selected as an appropriate test temperature to distinguish heavy-duty asphalt mixes. This was more prudent for HWTT as stripping inflection points were observed only at 58°C. In addition, it is recommended to increase wheel-track passes to 40,000 and set a maximum allowable pavement deformation of 6mm rut depth for high truck traffic intersections.
- Overall, considering the same asphalt binder, the results of the IDEAL-RT Index, FN, and  $|E^*|$  values indicated that SMA mixes with 9.5mm NMA provide better resistance to rutting than SMA mixes with 12.5mm NMA. However, the results of the HWTT tests showed the opposite trend, where SMA mixes with 12.5mm NMA provided better resistance to rutting than SMA mixes with 9.5mm NMA.
- Generally, the FN test showed higher variability compared to the IDEAL-RT test, with a COV ranging from 20.4% to 33.9% for FN values, and from 1.5% to 23.8% for IDEAL-RT Index values.
- The results of the t-test showed that there was a significant difference in FN values between EME mix and SMA9.5-PG70-28 and SMA12.5-PG70-28 mixes at 44°C, 50°C, and 58°C testing temperatures. There was also a significant difference between EME and all SMA mixes in IDEAL-RT Index values at 58°C testing temperature.
- The results indicated that NMA, PG binder, and testing temperatures were significant factors affecting the rutting resistance of SMA mixes, as they showed a significant impact on both FN and IDEAL-RT Index values
- The correlation results for the rutting parameters of SMA mixes at 58°C testing temperature showed a strong correlation ( $R^2=0.93$ ) between IDEAL-RT Index and FN values. Additionally, both IDEAL-RT Index and FN values showed a high correlation with  $|E^*|$  at 54.4°C and with the frequencies of 1Hz and 0.1Hz for both group A and B.

- Generally, HWTT test results were poorly correlated with all other rutting parameters obtained from IDEAL-RT, FN, and Dynamic Modulus tests.
- In general,  $|E^*|$  at a temperature of 54.4°C and a frequency of 1Hz showed a stronger relationship with the other rutting parameters, compared to the results from the same test at a temperature of 54.4°C and a frequency of 0.1Hz.
- The overall ranking score of asphalt mixes based on HWTT, IDEAL-RT, and FN tests, exhibited that both SMA9.5-PG76-28 and SMA12.5-PG76-28 performed better in terms of resistance to rutting compared to other asphalt mixes.

## **Chapter 6 Development of Performance-based Specifications for Heavy-Duty Asphalt Mixes in Southern Ontario**

*Parts of this chapter have been submitted to the Journal of Materials in Civil Engineering (Kafi Farashah, 2023b).*

Due to an increase in truck traffic volume and the impact of climate change, approach intersections experiencing more severe loading compared to other road sections. To address this, performance-related specifications can be used to produce asphalt mixes that perform well and reduce the need for maintenance and minimize user delays. In this case, six SMA mixes were produced in the laboratory, using three different types of PG asphalt binders (PG70-28, PG76-28, and PG82-28) and two different sizes of aggregates (9.5mm and 12.5mm). Additionally, an EME mix was also produced, using a 12.5mm aggregate size and a PG82-28 asphalt binder, under controlled conditions at CPATT.

Various asphalt tests were performed to evaluate the rheological properties of asphalt binders, including the Bending Beam Rheometer (BBR) to assess low-temperature cracking resistance, the Dynamic Shear Rheometer (DSR) to evaluate intermediate temperature cracking resistance, the Multiple Stress Creep and Recovery (MSCR) and DSR tests to measure shear resistance, and the Rotational Viscometer (RV) test to determine viscosity.

To evaluate the asphalt mixes various tests were performed, including the Disk-Shaped Compact Tension (DC(T)) test for low-temperature cracking resistance, the Indirect Tensile Asphalt Cracking Test (IDEAL-CT) and Illinois Flexibility Index Test (I-FIT) for intermediate temperature cracking resistance, the Hamburg Wheel Tracking Test (HWTT) for shear resistance, and the British Pendulum Friction Test (BPT) for surface friction.

Statistical analysis was performed to compare the low-temperature and intermediate temperature cracking resistance of the asphalt mixes using ANOVA and Tukey's HSD tests in Minitab© software. In addition, a t-test was used to determine any statistically significant differences between the EME mix and the six SMA mixes in terms of low and intermediate temperature cracking resistance.

A preliminary performance-based specification was developed to assess heavy-duty asphalt mixes and a life cycle cost analysis was performed to compare the potential benefits of using heavy-duty asphalt as a surface course versus a currently specified asphalt surface mix in York Region.

### **6.1. Asphalt Binder Characterization Results**

The DSR and MSCR tests were conducted to evaluate the shear resistance of three asphalt binders, according to AASHTO T315 and T350, respectively. The DSR test determined the  $|G^*|/\sin(\delta)$  parameter for unaged and short-term aged asphalt binders, with AASHTO 315 specifying lower limits of 1.0 kPa and 2.2 kPa unaged and RTFO aged asphalt binders, respectively. The MSCR test was used to determine the creep recovery behavior of RTFO-aged asphalt binders by considering the non-recoverable creep compliance ( $J_{nr}$ ) (upper limit of 4.5 1/kPa) and percent recovery (R) at 3.2 kPa shear stress. The Rotational Viscometer (RV) test was also performed according to AASHTO T316 to determine the viscosity of the asphalt binders.

The intermediate temperature cracking resistance of three asphalt binders was evaluated using the DSR test on Pressure Aging Vessel (PAV) aged binders. The DSR test determined the  $|G^*|. \sin(\delta)$  value, with AASHTO T315 specifying an upper limit of 5,000 MPa for the parameter. The lower the value of  $|G^*|. \sin(\delta)$ , the less stiff the asphalt binder is.

The low-temperature cracking resistance of three asphalt binders was evaluated using the Bending Beam Rheometer (BBR) test in accordance with AASHTO T313. The BBR test was conducted on PAV aged binders, measuring the creep stiffness (S) and creep rate (m-value) at testing temperatures of  $-18^{\circ}\text{C}$  to simulate the minimum pavement temperature of  $-28^{\circ}\text{C}$ . The AASHTO T313 specification sets an upper limit of 300 MPa for creep stiffness and a lower limit of 0.300 for the m-value. It should be noted that reducing creep stiffness (or increasing m-value) leads to a less stiff asphalt binder (more flexible), and thus able to deform without storing relatively large stresses. Table 6-1 presents the rheological properties of three asphalt binders used in this research.



**Table 6-1: Asphalt Binder Properties**

| <b>Tests on Original Asphalt Binders</b>     | <b>PG70-28</b>              | <b>PG76-28</b>              | <b>PG82-28</b>              | <b>Specification Limits</b> |
|--|-----------------------------|-----------------------------|-----------------------------|-----------------------------|
| Brookfield Viscosity (Pa.s) (135°C)          | 1.45                        | 1.805                       | 2.38                        | 3.0 max                     |
| Brookfield Viscosity (Pa.s) (165°C)          | 0.45                        | 0.56                        | 0.74                        | -                           |
| G*/sin( $\delta$ ) (kPa) (70°C)              | 1.870                       | 3.28                        | 6.98                        | 1.0 min                     |
| Ash Content (%)                              | 0.23                        | 0.2                         | 0.21                        | 0.6 max                     |
| <b>Tests on RTFO Residue Asphalt Binders</b> |                             |                             |                             |                             |
| G*/sin( $\delta$ ) (kPa) (70°C)              | 2.52 (70°C) and 1.26 (76°C) | 2.43 (76°C) and 1.21 (82°C) | 2.83 (82°C) and 1.41 (88°C) | 2.2 min                     |
| MSCR Jnr (1/kPa) (58°C and 3.2 kPa)          | 0.18                        | 0.09                        | 0.05                        | 4.5 max                     |
| MSCR Percent Recovery (%) (58°C and 3.2 kPa) | 83.50                       | 92.3                        | 81.5                        | -                           |
| <b>Tests on PAV Residue Asphalt Binders</b>  |                             |                             |                             |                             |
| G*.sin( $\delta$ ) (kPa) (25°C)              | 1,811                       | 2,150                       | 3,422                       | 5,000 max                   |
| BBR Creep Stiffness (Mpa) (-18°C)            | 156                         | 124                         | 135                         | 300 max                     |
| BBR m-value (-18°C)                          | 0.325                       | 0.361                       | 0.351                       | 0.300 min                   |
| Continuous PG Grade (°C)                     | 71.5-29.1                   | 77.1-33.4                   | 84.7-30.8                   | -                           |

## 6.2. Asphalt Mix Characterization Results

### 6.2.1. Disk-Shaped Compact Tension DC(T) Test

The DC(T) test was conducted on triplets in accordance with (ASTM D7313) to characterize the fracture behaviour of asphalt mixes at low temperatures. The DC(T) test was performed at testing temperatures of -18°C to simulate lowest pavement surface temperature of -28°C. Figure 6-1 presents the results of the DC(T) test conducted on the asphalt mixes, and it includes the average fracture energy along with the one standard deviation error bar, the COV, and the continuous low temperature grade of the virgin binder used in each mix.

As shown in Figure 6-1, the SMA mixes with PG76-28 asphalt binder showed higher DC(T) fracture energy compared to those with the same NMA. This could be attributed to the fact that the virgin PG76-28 asphalt binder had the lowest continuous low-temperature grade of -33.4°C, which is significantly below its corresponding low temperature PG of -28°C. On the other hand,

the continuous low temperature grades of PG82-28 and PG70-28 were -30.8°C and -29.1°C respectively. In addition, the m-value of PG76-28 asphalt binder (0.361) was higher than that of PG-82-28 (0.351) and PG-70-28 (0.325), which suggests that the SMA mixes containing PG76-28 binder have a better ability to relax thermal stresses. In addition, SMA mixes with 12.5mm NMA S provided slightly higher average DC(T) fracture energy compared to SMA mixes with 9.5mm NMA S. Moreover, SMA12.5-PG76-28 provided the highest average DC(T) fracture energy (1,091 J/m<sup>2</sup>) followed by SMA9.5-PG76-28 (1,045 J/m<sup>2</sup>) and EME (1,025 J/m<sup>2</sup>). Additionally, the average DC(T) fracture energy for all seven tested asphalt mixes was found to be 958 J/m<sup>2</sup>. As indicated in Figure 6-1, the COV values for the DC(T) fracture energy of the seven tested asphalt mixes varied from 2.9% to 17.9%, which shows that there is low to medium variability in the results of the DC(T) test.

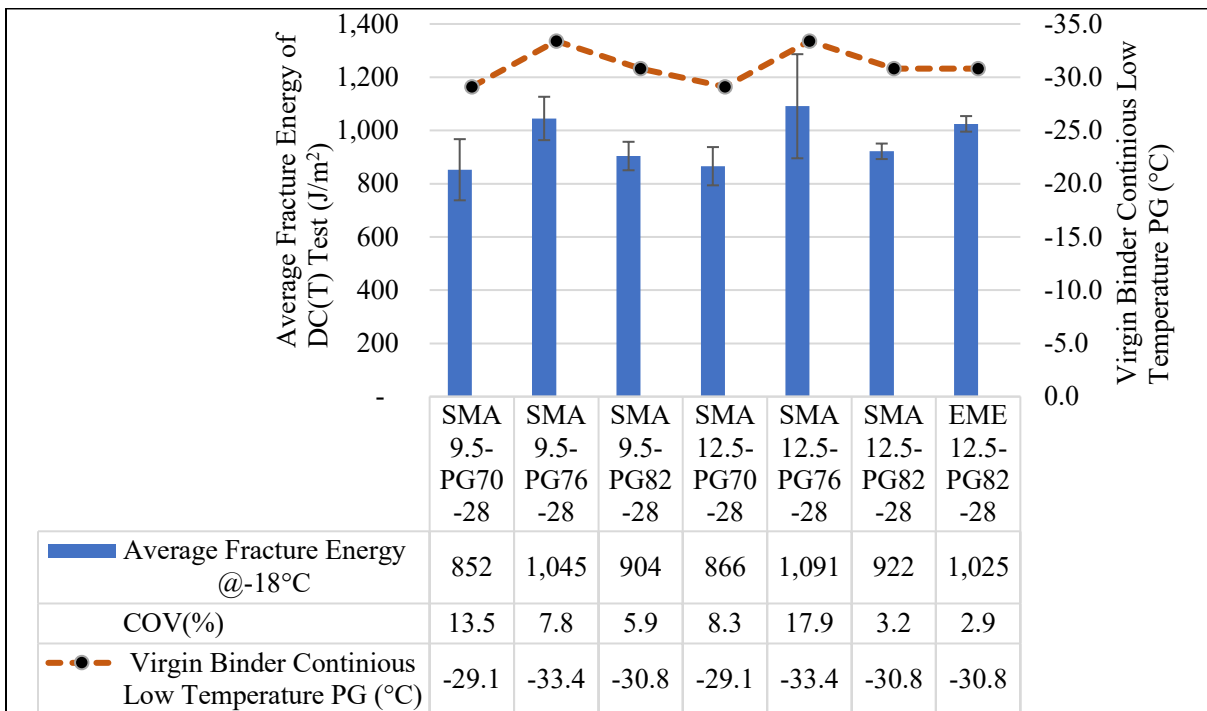


Figure 6-1: DC(T) Fracture Energy Results at -18°C Testing Temperatures

The ANOVA analysis was conducted to determine if there is any statistically significance difference between the SMA mixes. As presented in Table 6-2, the ANOVA analysis found that there is no significant difference between the different SMA mixes (NMA S, asphalt binder PG, and the combination of NMA S and PG binder) with regards to DC(T) fracture energy. However,

it is important to note that the P-value for the PG asphalt binder is close to 0.05 and has the highest F-value, indicating that it may be approaching statistical significance.

**Table 6-2: Summarized Analysis of Variance (ANOVA) for DC(T) Fracture Energy for SMA Mixes**

| Source         | DF | Adj SS | Adj MS  | F-Value | P-Value | Statistically Significant |
|----------------|----|--------|---------|---------|---------|---------------------------|
| NMAS           | 1  | 13604  | 13604.4 | 0.94    | 0.355   | No                        |
| PG Binder      | 2  | 112521 | 56260.6 | 3.89    | 0.056   | No                        |
| NMAS*PG Binder | 2  | 3928   | 1963.8  | 0.14    | 0.875   | No                        |
| Error          | 10 | 144615 | 14461.5 |         |         |                           |
| Total          | 17 | 274810 |         |         |         |                           |

Figure 6-2 confirms that based on the average of 9 test specimens, the 12.5mm NMAS mix showed better resistance to low-temperature cracking compared to the 9.5mm NMAS mix. Additionally, the average of 6 test specimens showed that the PG76-28 asphalt binder had a higher average DC(T) fracture energy compared to the PG82-28 and PG70-28 asphalt binders.

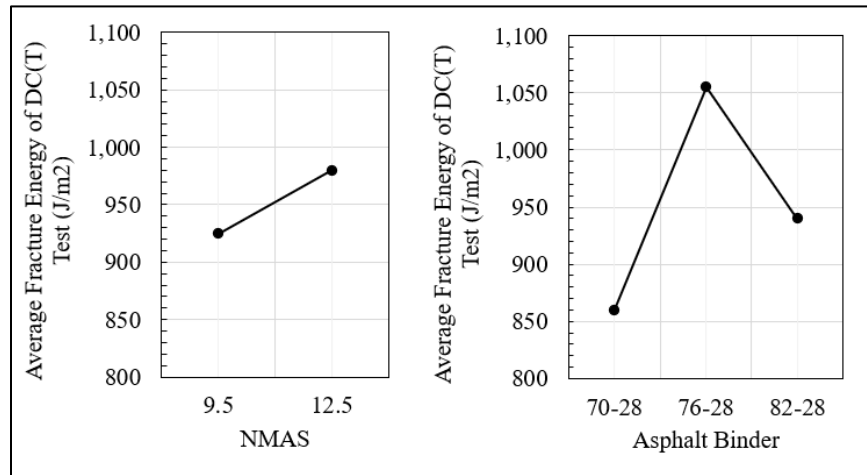


**Figure 6-2: Main Effects Plots for Average DC(T) Fracture Energy for SMA Mixes**

The effect of PG asphalt binder on DC(T) fracture energy was investigated by conducting a t-test on the fracture energy values of asphalt mixes containing PG70-28, PG76-28, and PG82-28 (Table 6-3). The results showed a significant difference between the mixes containing PG70-28 and PG76-28 (P-value = 0.010 < 0.05) and between PG76-28 and PG82-28 (P-value = 0.020 < 0.05). However, the t-test indicated no significant difference between the mixes containing PG70-28 and PG82-28 (P-value = 0.190 > 0.05).

**Table 6-3: Statistical Analysis for Average DC(T) Fracture Energy for PG Asphalt Binder**

| Testing Temperature at -18°C |         |         |                           |
|------------------------------|---------|---------|---------------------------|
| Paired Mixes                 |         | P-Value | Statistically Significant |
| PG70-28                      | PG76-28 | 0.010   | Yes                       |
| PG76-28                      | PG82-28 | 0.020   | Yes                       |
| PG70-28                      | PG82-28 | 0.190   | No                        |

A paired t-test was used to compare the average DC(T) fracture energy values of SMA and EME asphalt mixes. The results in Table 6-4 showed that there were significant differences between EME and the three SMA mixes (SMA9.5-PG82-28, SMA12.5-PG70-28, and SMA 12.5-PG82-28).

**Table 6-4: Statistical Analysis for Average DC(T) Fracture Energy (EME vs. SMA mixes)**

| Testing Temperature at -18°C |                  |         |                           |
|------------------------------|------------------|---------|---------------------------|
| Paired Mixes                 |                  | P-Value | Statistically Significant |
| SMA 9.5 PG70-28              | EME 12.5 PG82-28 | 0.065   | No                        |
| SMA 9.5 PG76-28              | EME 12.5 PG82-28 | 0.705   | No                        |
| SMA 9.5 PG82-28              | EME 12.5 PG82-28 | 0.026   | Yes                       |
| SMA 12.5 PG70-28             | EME 12.5 PG82-28 | 0.024   | Yes                       |
| SMA 12.5 PG76-28             | EME 12.5 PG82-28 | 0.593   | No                        |
| SMA 12.5 PG82-28             | EME 12.5 PG82-28 | 0.012   | Yes                       |

The Tukey's HSD test was used to rank all the asphalt mixes based on average DC(T) fracture energy values at a 95% confidence level. The results, shown in Table 6-5, ranked SMA12.5-PG76-28 as the highest, followed by SMA9.5-PG76-28 and EME, respectively. Both SMA9.5-PG82-28 and SMA9.5-PG70-28 ranked the lowest according to average DC(T) fracture energy values at a testing temperature of -18°C.

**Table 6-5: Summarized Analysis of Tukey's HSD Ranking Based on Average DC(T) Fracture Energy**

| Factor           | Mean  | Grouping |   |   |
|------------------|-------|----------|---|---|
| SMA 12.5 PG76-28 | 1,091 | A        |   |   |
| SMA 9.5 PG76-28  | 1,045 | A        | B |   |
| EME 12.5 PG82-28 | 1,025 | A        | B | C |
| SMA 12.5 PG82-28 | 922   |          | B | C |
| SMA 12.5 PG70-28 | 904   |          | B | C |
| SMA 9.5 PG82-28  | 866   |          |   | C |
| SMA 9.5 PG70-28  | 852   |          |   | C |

### 6.2.2. Indirect Tensile Asphalt Cracking Test (IDEAL-CT)

The IDEAL-CT test was conducted to evaluate the intermediate temperature cracking resistance of asphalt mixes, following the ASTM D8225 standard, at a testing temperature of 25°C. The results of the IDEAL-CT test for the seven laboratory-produced asphalt mixes are shown in Figure 6-3 as the CT Index values. According to the figure, SMA12.5-PG82-28 had the highest intermediate temperature cracking resistance with an average CT Index of 907, followed by SMA12.5-PG76-28 (CT Index = 799) and SMA12.5-PG70-28 (CT Index = 699). The EME mix had the lowest average CT Index value of 119. The results may suggest that the IDEAL-CT test is highly dependent on the gradation of the asphalt mix. The SMA mix with the same NMAS and PG grade (SMA12.5-PG-82-28) as the EME mix showed a CT Index value that was approximately 760% higher than the dense-graded EME12.5-PG82-28 mix. In general, the results of the study suggest that SMA mixes with a 12.5 NMAS have better intermediate temperature cracking resistance compared to SMA mixes with a 9.5 NMAS with similar asphalt binder PG grades. Additionally, the average CT Index value for all seven tested asphalt mixes was 521. Moreover, the COV for the CT Index values of the seven asphalt mixes in this study ranged from 14.9% to 32%, indicating medium to high variability in the results obtained from the IDEAL-CT test.

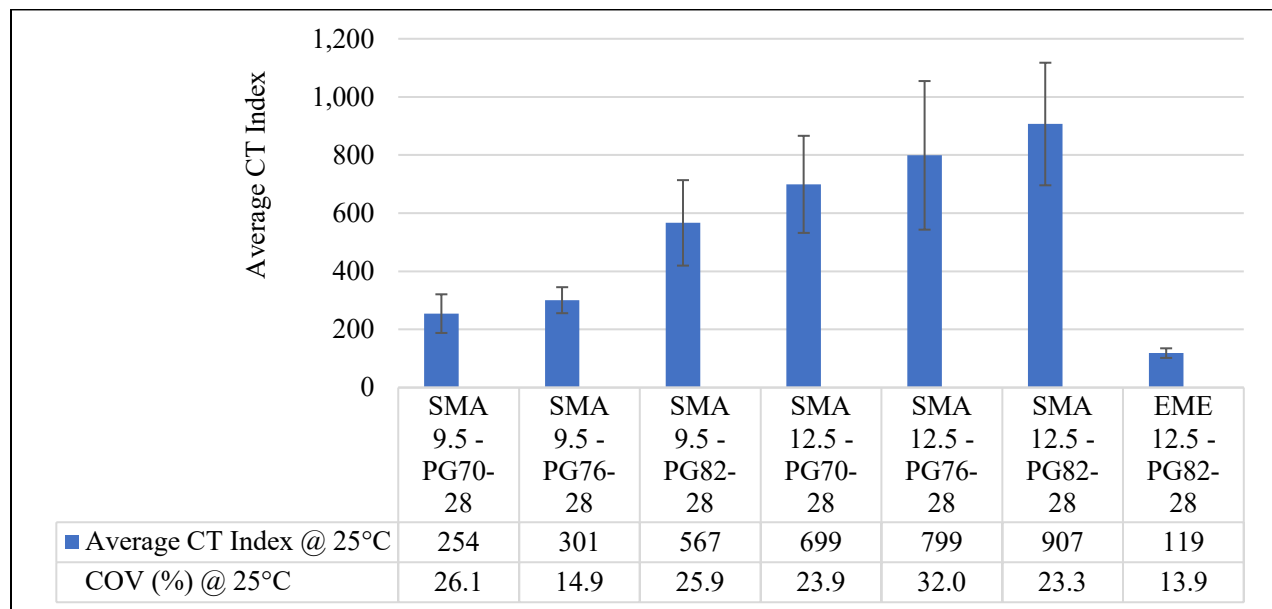


Figure 6-3: Average CT Index Results at 25°C Testing Temperatures

The results of the ANOVA analysis showed that both asphalt binder PG and NMAS are significant parameters in affecting the CT Index. However, NMAS had a higher impact with a higher F value

of 35.55 compared to PG binder with 5.82. The results also indicated that there was no significant interaction between NMAS and PG binder. These findings are summarized in Table 6-6.

**Table 6-6: Summarized Analysis of Variance (ANOVA) for CT Index for SMA Mixes**

| Source         | DF | Adj SS  | Adj MS | F-Value | P-Value | Statistically Significant |
|----------------|----|---------|--------|---------|---------|---------------------------|
| NMAS           | 1  | 782855  | 782855 | 35.55   | 0.000   | Yes                       |
| PG Binder      | 2  | 256294  | 128147 | 5.82    | 0.017   | Yes                       |
| NMAS*PG Binder | 2  | 6086    | 3043   | 0.14    | 0.872   | No                        |
| Error          | 12 | 264226  | 22019  |         |         |                           |
| Total          | 17 | 1309461 |        |         |         |                           |

The main effect plots from the ANOVA analysis, shown in Figure 6-4, indicate that the 12.5mm NMAS produced greater intermediate temperature cracking resistance than the 9.5mm NMAS, based on the average of 9 test specimens. Additionally, the average CT Index was higher for the PG82-28 asphalt binder compared to the PG76-28 and PG70-28 asphalt binders, based on the average of 6 test specimens.

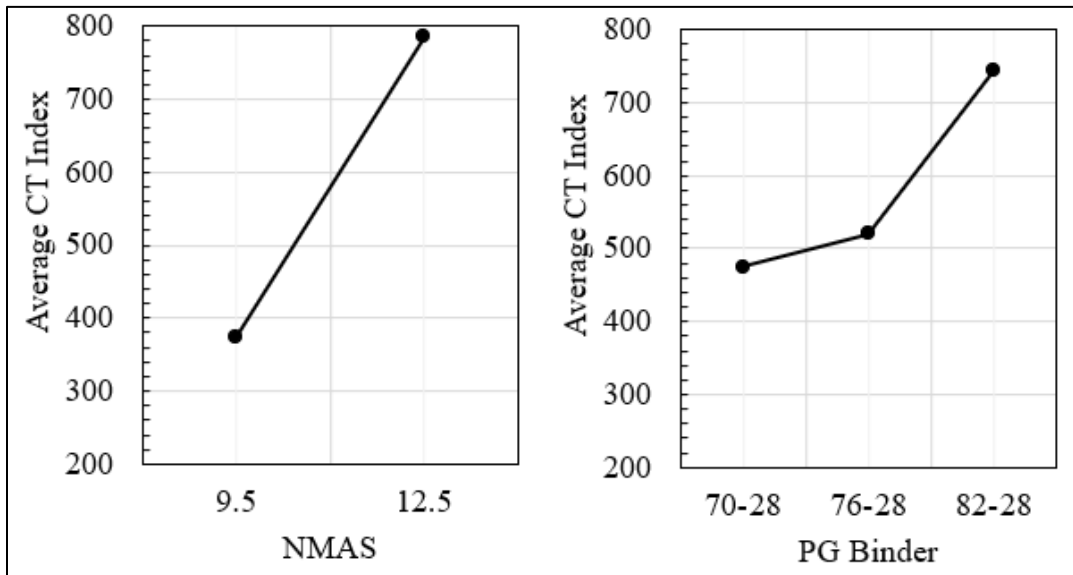


**Figure 6-4: Main Effects Plots for Average CT Index for SMA Mixes**

As shown in Table 6-7, there was a statistically significant difference between the CT Index values of all the SMA mixes and the EME mix, indicating that the IDEAL-CT test is sensitive to the gradation of the asphalt mix.

**Table 6-7: Statistical Analysis for CT Index (EME vs. SMA mixes)**

| Testing Temperature 25°C |                  |         |                           |
|--------------------------|------------------|---------|---------------------------|
| Paired Mixes             |                  | P-Value | Statistically Significant |
| SMA 9.5 PG70-28          | EME 12.5 PG82-28 | 0.026   | Yes                       |
| SMA 9.5 PG76-28          | EME 12.5 PG82-28 | 0.003   | Yes                       |
| SMA 9.5 PG82-28          | EME 12.5 PG82-28 | 0.006   | Yes                       |
| SMA 12.5 PG70-28         | EME 12.5 PG82-28 | 0.004   | Yes                       |
| SMA 12.5 PG76-28         | EME 12.5 PG82-28 | 0.010   | Yes                       |
| SMA 12.5 PG82-28         | EME 12.5 PG82-28 | 0.003   | Yes                       |

The Tukey's HSD test was used to rank 7 lab-produced asphalt mixes based on their average CT-Index using Minitab software at 95% confidence level. As presented in Table 6-8, SMA12.5-PG82-28 and SMA12.5-PG76-28 statistically had higher average CT Index than other asphalt mixes. On the other hand, EME12.5-PG82-28 mix ranked lowest among all other asphalt mixes. The results indicated that CT Index was able to distinguish intermediate cracking resistance of asphalt mixes.

**Table 6-8: Summarized Analysis of Tukey's HSD Ranking Based on Average CT-Index**

| Factor           | Mean | Grouping |   |   |   |
|------------------|------|----------|---|---|---|
| SMA 12.5-PG82-28 | 907  | A        |   |   |   |
| SMA 12.5-PG76-28 | 799  | A        |   |   |   |
| SMA 12.5-PG70-28 | 699  | A        | B |   |   |
| SMA 9.5-PG82-28  | 567  | A        | B | C |   |
| SMA 9.5-PG76-28  | 301  |          | B | C | D |
| SMA 9.5-PG70-28  | 254  |          |   | C | D |
| EME 12.5-PG82-28 | 119  |          |   |   | D |

### 6.2.3. Illinois Flexibility Index Test (I-FIT)

The I-FIT test was used as a second method to evaluate the intermediate temperature cracking resistance of asphalt mixes. The test followed the guidelines of AASHTO TP-124 and was performed on three replicates at a testing temperature of 25°C. The intermediate temperature cracking resistance was evaluated using the Flexibility Index (FI). The results of the I-FIT test, in terms FI, are presented in Figure 6-5. The SMA mixes with the same NMAS showed similar average FI values. The SMA12.5-PG76-28 mix showed the highest intermediate temperature cracking resistance, with an average FI value of 27.2, followed by SMA12.5-PG82-28 (FI=26.7) and SMA12.5-PG70-28 (FI=24.8). The SMA9.5-PG70-28 mix had the lowest intermediate temperature cracking resistance, with an average FI value of 20.9, as shown in Figure 6-5. In addition, the COV for the Flexibility Index (FI) values of the seven asphalt mixes ranged from

3.6% to 17.5%, indicating low to medium variability in the results of the I-FIT test. Moreover, the results showed a trend where SMA mixes with 12.5 NMAS tended to have higher FI values compared to SMA mixes with 9.5 NMAS with the same PG binder. This suggests that the NMAS might have minimal impact on the intermediate temperature cracking resistance when evaluated using the I-FIT test.

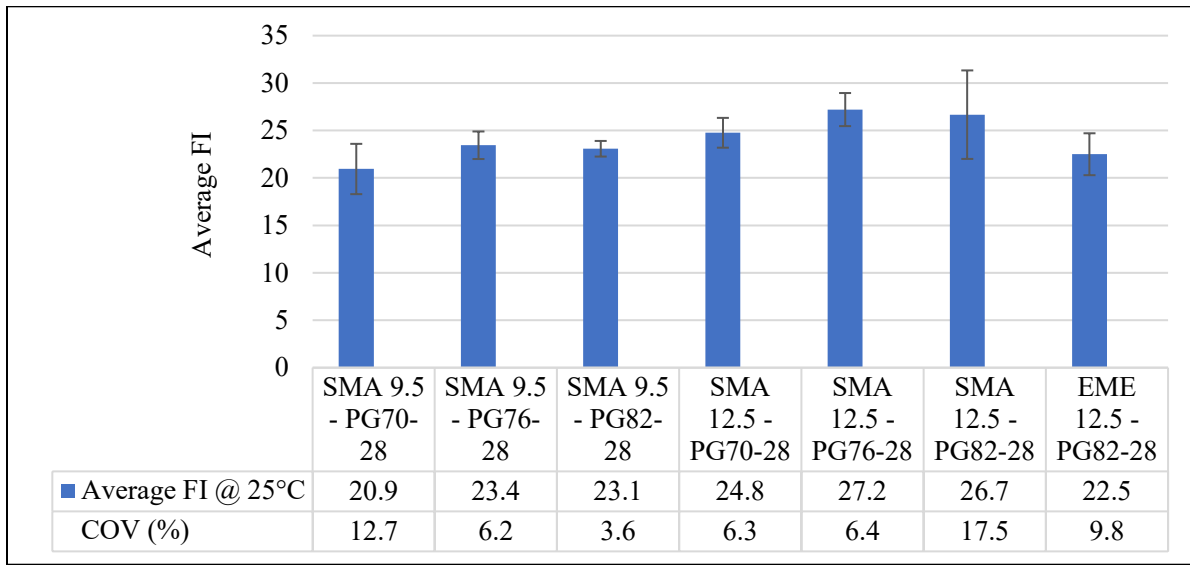


**Figure 6-5: Average FI Results at 25°C Testing Temperatures**

To determine if the NMAS and asphalt binder PG were statistically significant factors affecting the FI values, the ANOVA was performed. Table 6-9 illustrates the results of the ANOVA, which indicates that the NMAS ( $P=0.066>0.05$ ), the asphalt binder PG ( $P=0.401>0.05$ ), and the interaction between NMAS and asphalt binder PG ( $P=0.696>0.05$ ) were not significant factors affecting the FI values when evaluating SMA mixes.

The main effect plots for the ANOVA analysis, shown in Figure 6-6, confirm that based on the average of 9 test specimens, a 12.5mm NMAS produced greater intermediate temperature cracking resistance compared to a 9.5mm NMAS. Additionally, based on the average of 6 test specimens, the PG82-28 asphalt binder produced a higher average FI compared to the PG76-28 and PG70-28 asphalt binders, respectively. However, as shown in Figure 6-6, the average FI values were very close to each other for each main effect.



**Table 6-9: Summarized Analysis of Variance (ANOVA) for FI for SMA Mixes**

| Source         | DF | Adj SS | Adj MS | F-Value | P-Value | Statistically Significant |
|----------------|----|--------|--------|---------|---------|---------------------------|
| NMAS           | 1  | 130.47 | 130.47 | 4.27    | 0.066   | No                        |
| PG Binder      | 2  | 61.3   | 30.65  | 1       | 0.401   | No                        |
| NMAS*PG Binder | 2  | 22.93  | 11.47  | 0.38    | 0.696   | No                        |
| Error          | 10 | 305.38 | 30.54  |         |         |                           |
| Total          | 17 | 598.72 |        |         |         |                           |

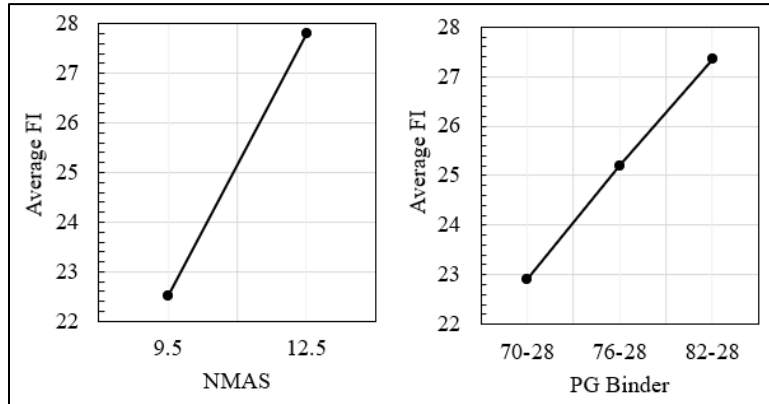


**Figure 6-6: Main Effects Plots for Average FI for SMA Mixes**

To determine if there was a statistically significant difference in the FI values between the EME mix and each of the SMA mixes, a t-test was performed. The results of the t-test, as shown in Table 6-10, indicated that there was no statistically significant difference between all SMA mixes and the EME mix except for the SMA12.5-PG76-28 mix, which was found to be significantly different from the EME mix ( $P=0.044 < 0.05$ ).

**Table 6-10: Statistical Analysis for FI Index (EME vs. SMA mixes)**

| Testing Temperature 25°C |                  |         |                           |
|--------------------------|------------------|---------|---------------------------|
| Paired Mixes             |                  | P-Value | Statistically Significant |
| SMA 9.5 PG70-28          | EME 12.5 PG82-28 | 0.478   | No                        |
| SMA 9.5 PG76-28          | EME 12.5 PG82-28 | 0.568   | No                        |
| SMA 9.5 PG82-28          | EME 12.5 PG82-28 | 0.693   | No                        |
| SMA 12.5 PG70-28         | EME 12.5 PG82-28 | 0.222   | No                        |
| SMA 12.5 PG76-28         | EME 12.5 PG82-28 | 0.044   | Yes                       |
| SMA 12.5 PG82-28         | EME 12.5 PG82-28 | 0.234   | No                        |

To statistically rank all of the asphalt mixes based on their average FI values, the Tukey's HSD test was performed using Minitab© software at a 95% confidence level. The results, as shown in Table 6-11, indicated that all of the asphalt mixes were grouped in the same category, meaning

that the I-FIT test was not able to distinguish the intermediate temperature cracking resistance of the heavy-duty asphalt mixes.

**Table 6-11: Summarized Analysis of Tukey’s HSD Ranking Based on Average FI**

| <b>Factor</b>    | <b>Mean</b> | <b>Grouping</b> |
|------------------|-------------|-----------------|
| SMA 12.5 PG76-28 | 27.2        | A               |
| SMA 12.5 PG82-28 | 26.7        | A               |
| SMA 12.5 PG70-28 | 24.8        | A               |
| SMA 9.5 PG76-28  | 23.4        | A               |
| SMA 9.5 PG82-28  | 23.1        | A               |
| EME 12.5 PG82-28 | 22.5        | A               |
| SMA 9.5 PG70-28  | 20.9        | A               |

#### **6.2.4. Hamburg Wheel Tracking Test (HWTT) Results**

The HWTT was performed to evaluate the rutting resistance and moisture susceptibility of the laboratory-produced asphalt mixes. As explained previously in Chapter 5.0, the HWTT test was carried out in accordance with AASHTO T324 standards and the test conditions, such as testing temperature (50°C), number of passes (20,000), and rut depth trigger level (12.5mm), were adjusted to better understand the behavior of the asphalt mixes under harsh conditions and to distinguish the most rut-resistant mix. HWTT was conducted at three different temperatures (44°C, 50°C, and 58°C) and the number of wheel-track passes was increased to 40,000. Also, a trigger level of 6mm total rut depth was chosen for the testing procedure. This decision was based on a recommendation from ASTM 1989, which states that a rut depth below 6mm does not necessitate pavement treatment ASTM 1989. Overall, the 58°C testing temperature was selected as appropriate to distinguish between heavy-duty asphalt mixes. During the test, stripping points were observed in two of the mixes (EME and SMA9.5-PG70-28). The results showed that in general, SMA mixes with a NMA of 12.5mm had higher rut resistance compared to SMA mixes with a 9.5mm NMA and the same PG asphalt binder. Additionally, the SMA12.5-PG-82-28 mix was found to have the highest shear resistance of all the mixes tested, with a resistance of 4.1mm after 40,000 wheel-track passes at a testing temperature of 58°C followed by SMA12.5-PG-76-28 (4.6mm).

#### **6.2.5. British Pendulum Friction Test**

The British Pendulum Tester (BPT) was conducted to evaluate the surface frictional characteristics of asphalt mixes. The BPT works by measuring the loss in kinetic energy of a sliding pendulum

when it comes into contact with the surface of the asphalt mix samples. This measurement is expressed in terms of the British Pendulum Number (BPN) and is done according to ASTM E 303-93. The pendulum's swing is reduced and the BPN reading increases with the increase in friction between the pendulum and the surface of the asphalt mix sample. The test was performed in both dry and wet conditions at five temperatures (0, 10, 23, 37, 58°C). Figures 6-7 and 6-8 show the average BPN results for each asphalt mix at different temperatures, along with the standard deviation error bars and COV, in both dry and wet conditions, respectively. Based on the results from both dry and wet conditions, it can be concluded that the BPN values increase with an increase in testing temperature for all asphalt mixes. This can be attributed to the fact that at higher temperatures, the asphalt binder becomes softer and more viscous, leading to an increase in friction between the pendulum and the asphalt mix. Furthermore, the EME mix showed higher BPN values compared to the SMA mixes. Additionally, the COV for BPN results was between 0.9% and 8.2%, indicating that the BPT provides results with low variability.

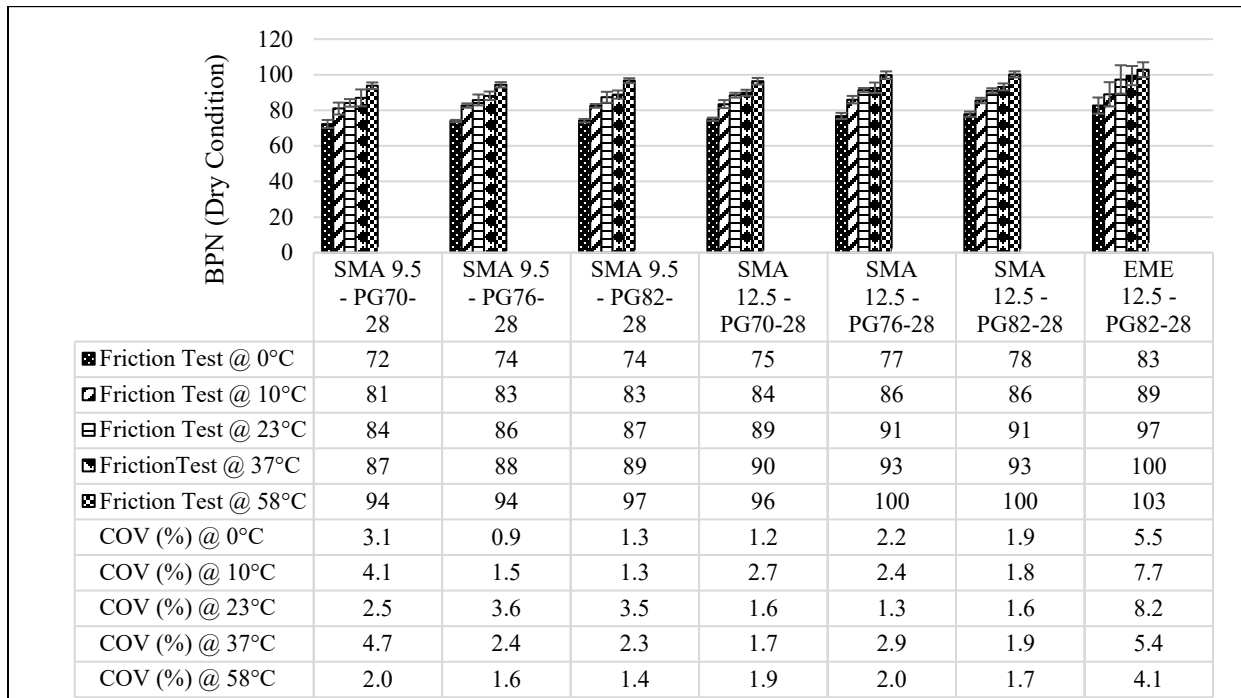


**Figure 6-7: Average BPN Results at Various Testing Temperatures in Dry Condition**

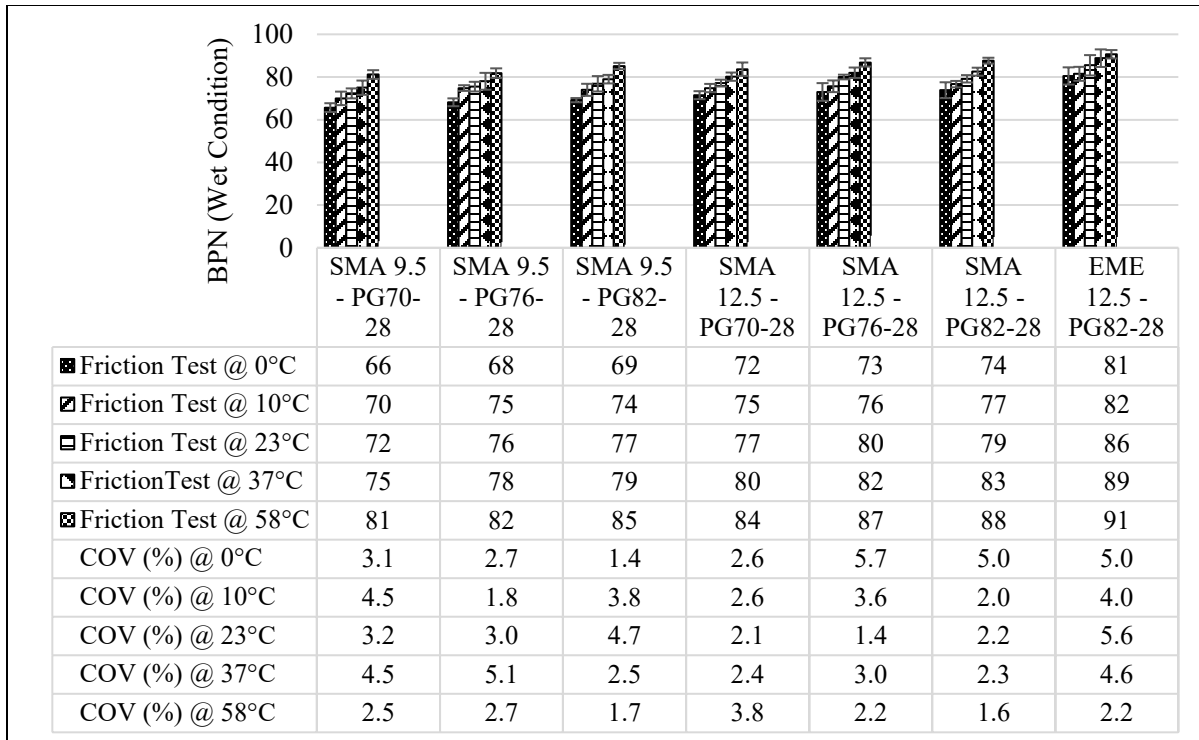


**Figure 6-8: Average BPN Results at Various Testing Temperatures in Wet Condition**

The ANOVA analysis was conducted to assess the statistical significance of the friction values between the SMA mixes. The results, as shown in Table 6-12, indicate a statistically significant difference between the NMA, PG of the asphalt binder, testing temperature, testing condition (dry/wet), and the interaction between testing temperature and testing condition, with a P-value less than 0.05.

The ANOVA analysis, as shown in Figure 6-9, illustrated that 12.5mm NMA produced higher friction compared to 9.5mm NMA, based on an average of 180 tests. The results also indicated that PG82-28 asphalt binder produced higher BPN values than PG76-28 and PG70-28 asphalt binders, based on an average of 120 tests. The results of 72 tests showed that higher temperatures resulted in higher friction in asphalt mixes. Finally, based on 180 tests, the results showed that wet conditions resulted in lower friction values as indicated by the BPN results.

**Table 6-12: Summarized Analysis of Variance (ANOVA) for BPN for SMA Mixes**

| Source                             | DF  | Adj SS  | Adj MS  | F-Value | P-Value | Statistically Significant |
|------------------------------------|-----|---------|---------|---------|---------|---------------------------|
| NMAS                               | 1   | 1254.4  | 1254.4  | 242.47  | 0.000   | Yes                       |
| PG Binder                          | 2   | 559.2   | 279.62  | 54.05   | 0.000   | Yes                       |
| Temperature                        | 4   | 12818   | 3204.5  | 619.43  | 0.000   | Yes                       |
| Dry/Wet                            | 1   | 8313.6  | 8313.61 | 1607.01 | 0.000   | Yes                       |
| NMAS*PG Binder                     | 2   | 6.2     | 3.11    | 0.6     | 0.549   | No                        |
| NMAS*Temperature                   | 4   | 20.8    | 5.21    | 1.01    | 0.404   | No                        |
| NMAS*Dry/Wet                       | 1   | 0.7     | 0.71    | 0.14    | 0.711   | No                        |
| PG Binder*Temperature              | 8   | 24.8    | 3.1     | 0.6     | 0.779   | No                        |
| PG Binder*Dry/Wet                  | 2   | 7.4     | 3.7     | 0.72    | 0.490   | No                        |
| Temperature*Dry/Wet                | 4   | 644.9   | 161.24  | 31.17   | 0.000   | Yes                       |
| NMAS*PG Binder*Temperature         | 8   | 42.8    | 5.35    | 1.03    | 0.410   | No                        |
| NMAS*PG Binder*Dry/Wet             | 2   | 25      | 12.5    | 2.42    | 0.091   | No                        |
| NMAS*Temperature*Dry/Wet           | 4   | 17.8    | 4.46    | 0.86    | 0.487   | No                        |
| PG Binder*Temperature*Dry/Wet      | 8   | 3       | 0.37    | 0.07    | 1.000   | No                        |
| NMAS*PG Binder*Temperature*Dry/Wet | 8   | 9.4     | 1.17    | 0.23    | 0.986   | No                        |
| Error                              | 300 | 1552    | 5.17    |         |         |                           |
| Total                              | 359 | 25300.1 |         |         |         |                           |

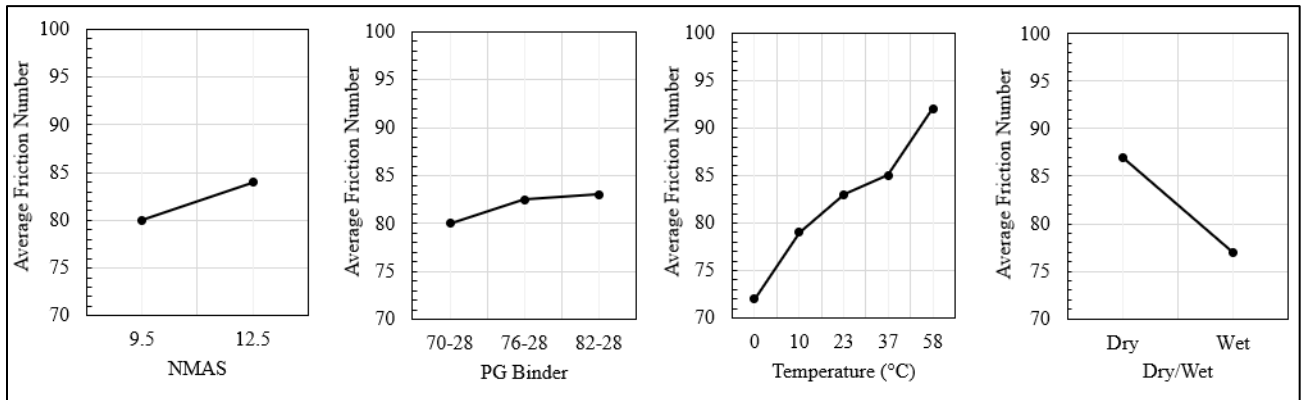


**Figure 6-9: Main Effects Plots for BPN Values for SMA Mixes**

### 6.2.6. Relationship Between Cracking Resistance Test Results

In this research DC(T) was employed to DC(T) to assess the low-temperature cracking resistance of the asphalt mixes at a testing temperature of  $-18^{\circ}\text{C}$ . To evaluate the intermediate temperature cracking resistance, both I-FIT and IDEAL CT were performed at a testing temperature of  $25^{\circ}\text{C}$ . Overall, analysis was divided into two groups: A) all asphalt mixes and B) only SMA mixes. Figures 6-10 and 6-11 show the correlation between FI and CT Index for group A and group B asphalt mixes, respectively.

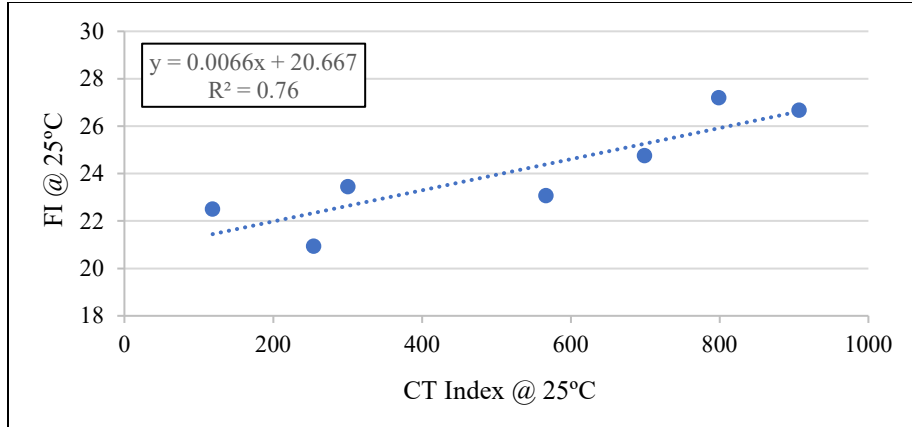


**Figure 6-10: FI vs. CT Index for Group A**

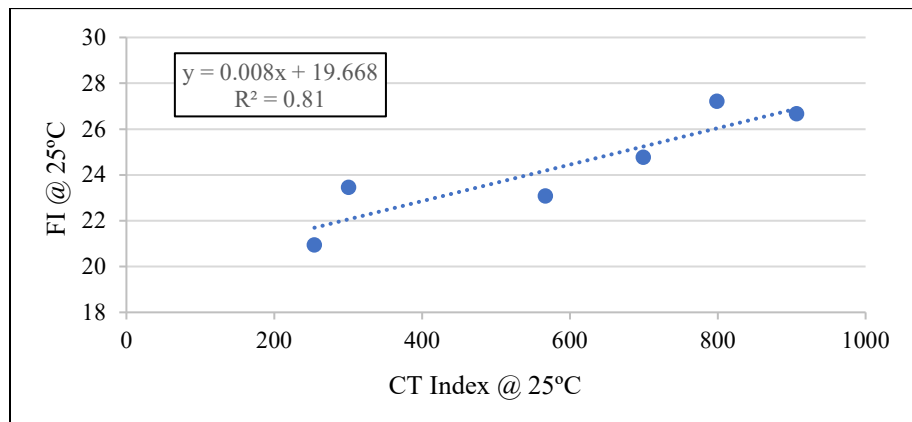


**Figure 6-11: FI vs. CT Index for Group B**

As shown in Figures 6-10 and 6-11, there was a relatively high correlation between FI and CT Index for both group A ( $R^2=0.76$ ) and group B ( $R^2=0.81$ ), respectively. However, there was a very poor correlation between both CT Index and FI with DC(T) fracture energy as illustrated in Figures 6-12 and 6-13. The Figures 6-12 and 6-13 showed that there was no correlation between DC(T) fracture energy and CT Index for both groups A and B, as indicated by the  $R^2$  values of 0.003 and 0.03, respectively. There was also a poor correlation between DC(T) fracture energy and FI for both groups A ( $R^2=0.18$ ) and B ( $R^2=0.34$ ), as shown in Figures 6-14 and 6-15, respectively.

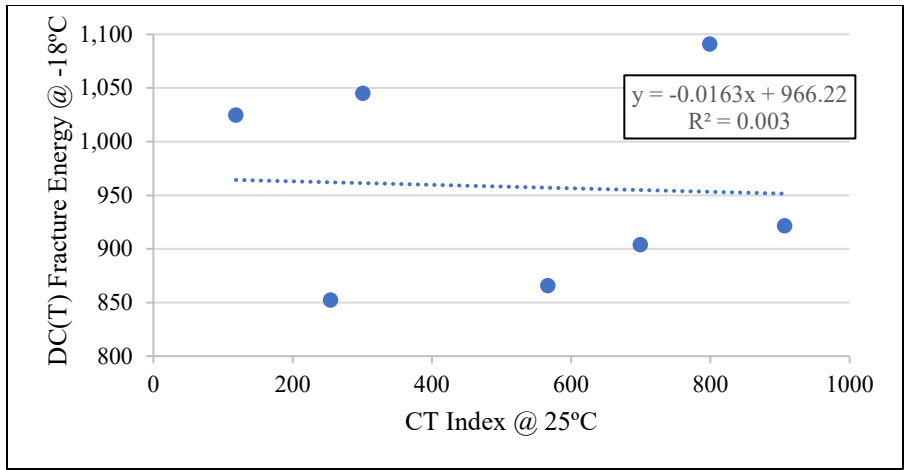


**Figure 6-12: DC(T) Fracture Energy vs. CT Index for Group A**

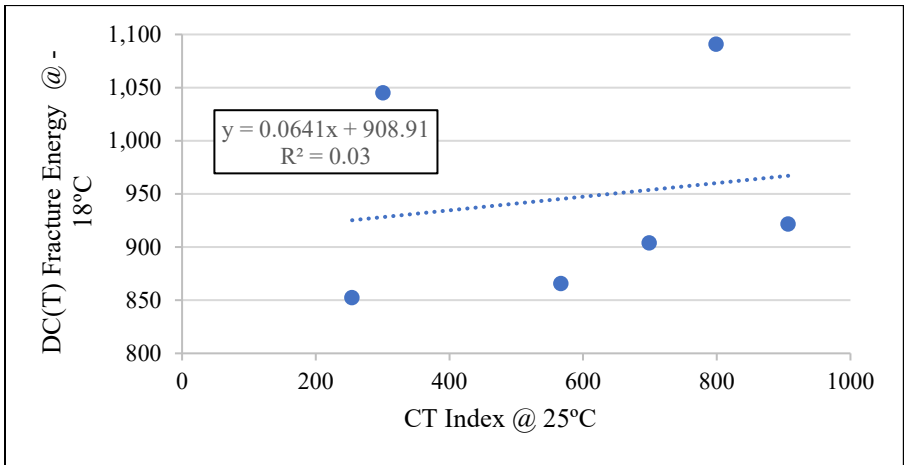


**Figure 6-13: DC(T) Fracture Energy vs. CT Index for Group B**

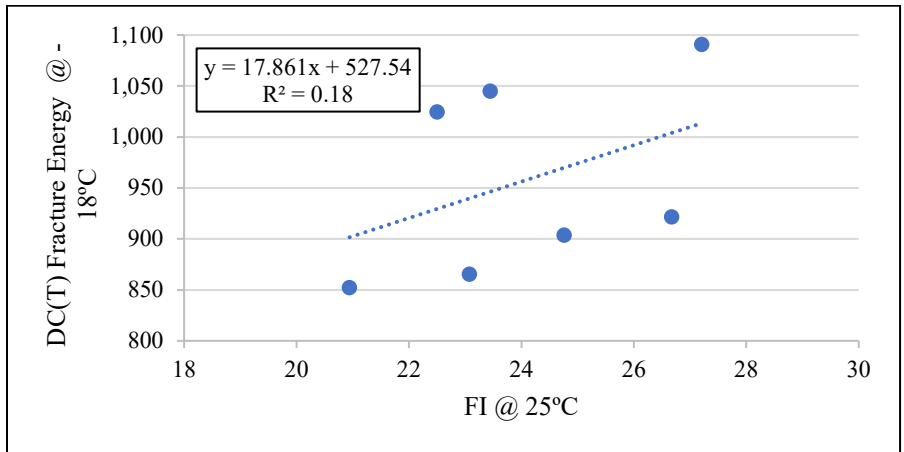


**Figure 6-14: DC(T) Fracture Energy vs. FI for Group A**

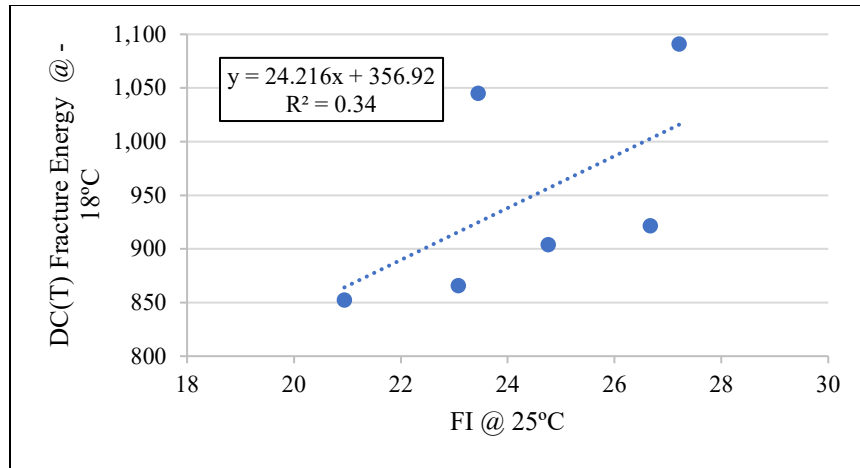


**Figure 6-15: DC(T) Fracture Energy vs. FI for Group B**

Overall, the results indicated that there was a very poor correlation between low-temperature cracking resistance and intermediate temperature cracking resistance parameters. In general, the parameters in group B, which only contained SMA mixes, had a higher correlation compared to group A.

### 6.2.7. Asphalt Mixes Ranking

To evaluate the resistance of seven lab-produced asphalt mixes to low-temperature cracking, intermediate cracking, and rutting, a numerical ranking method was used on DC(T) fracture energy, CT Index, FI, and rut depth at 40,000 passes for HWTT at a testing temperature of 58°C. Tukey's HSD test was used to statistically rank all the asphalt mixes based on the average DC(T) fracture energy, CT Index, and FI values at a 95% confidence level. However, the groups for Tukey's HSD were based on alphabetical orders, so to rank the asphalt mixes, numerical values were assigned to the groups. Group A was ranked as 1, which represents the best asphalt mix, and the rest of the groups were assigned numerical values in ascending order. Furthermore, to compare the results of the HWTT, the asphalt mixes were ranked based on the measured rut depth at 40,000 passes in an ascending numerical order. The asphalt mix with the lowest rut depth was ranked as 1, and the asphalt mix with the highest rut depth was ranked as 7. It's worth noting that friction is considered a functional performance of asphalt mixes, so BPT test values were excluded from the ranking method. Table 6-13 presents the ranking of each asphalt mix based on DC(T) fracture energy, CT Index, FI, and rut depth at 40,000 pass for HWTT values. The total rank for each asphalt mix was calculated by adding up the ranks from each test, referred to as the "Total Ranking". A lower Total Ranking value indicates a better rutting resistance.



**Table 6-13: Rankings of Asphalt Mixes' Cracking and Rutting Resistance Based on HWTT, IDEAL-CT, I-FIT, and DC(T) Tests**

| Asphalt Mixes    | HWTT                         |         | IDEAL-CT Test            |                  |         | Illinois Flexibility Index Test |                  |         | DCT Test                    |                  |         | Total Ranking |
|------------------|------------------------------|---------|--------------------------|------------------|---------|---------------------------------|------------------|---------|-----------------------------|------------------|---------|---------------|
|                  | 58°C Testing Temperature     |         | 25°C Testing Temperature |                  |         | 25°C Testing Temperature        |                  |         | (-18)°C Testing Temperature |                  |         |               |
|                  | Rut Depth (mm) @ 40,000 Pass | Ranking | Average CT-Index         | Tukey's Grouping | Ranking | Average FI                      | Tukey's Grouping | Ranking | Average Fracture Energy     | Tukey's Grouping | Ranking |               |
| SMA 9.5-PG70-28  | 22.0                         | 7       | 254                      | CD               | 5       | 20.9                            | A                | 1       | 852                         | C                | 5       | 18            |
| SMA 9.5-PG76-28  | 9.4                          | 4       | 301                      | BCD              | 4       | 23.4                            | A                | 1       | 1045                        | AB               | 2       | 11            |
| SMA 9.5-PG82-28  | 7.4                          | 3       | 567                      | ABC              | 3       | 23.1                            | A                | 1       | 866                         | BC               | 4       | 11            |
| SMA 12.5-PG70-28 | 9.6                          | 5       | 699                      | AB               | 2       | 24.8                            | A                | 1       | 904                         | C                | 5       | 13            |
| SMA 12.5-PG76-28 | 4.6                          | 2       | 799                      | A                | 1       | 27.2                            | A                | 1       | 1091                        | A                | 1       | 5             |
| SMA 12.5-PG82-28 | 4.1                          | 1       | 907                      | A                | 1       | 26.7                            | A                | 1       | 922                         | BC               | 4       | 7             |
| EME 12.5-PG80-28 | 16.0                         | 6       | 119                      | D                | 6       | 22.5                            | A                | 1       | 1025                        | ABC              | 3       | 16            |

Note: Lower the ranking, better the Cracking and Rutting Resistance of Asphalt Mix

Table 6-13 shows that the SMA12.5-PG82-28 mix performed the best in the HWTT test and was ranked number 1. Both SMA12.5-PG82-28 and SMA12.5-PG76-28 were also ranked number 1 in the IDEAL-CT test. SMA12.5-PG76-28 received a ranking of number 1 in the DC(T) test. In the I-FIT test, all asphalt mixes received the same ranking and were categorized into group A according to Tukey's HSD. The total ranking score of SMA12.5-PG76-28 was 5, which was the lowest among all the asphalt mixes. This indicated that SMA12.5-PG76-28 was a relatively strong mix as it showed high resistance to low-temperature cracking, intermediate temperature cracking, and rutting.

### 6.2.8. Interaction Plots Between HWTT Rut Depth, DC(T) Fracture Energy, CT Index, and FI

To produce high-performing asphalt mixes, it is important to establish performance-related specifications for the three main asphalt mix performance criteria, namely low and intermediate temperatures, and shear resistance. Asphalt mixes with high stiffness tend to perform better in

rutting resistance, while softer mixes are better able to withstand low and intermediate cracking. Developing asphalt mix performance criteria is crucial in understanding the durability of each mix and ensuring the production of high-performing asphalt mixes. To better understand the cracking and rutting resistance of the seven laboratory-produced asphalt mixes, individual performance space diagrams were developed. These diagrams plotted the HWTT rut depth at 58°C after 40,000 passes against the DC(T) fracture energy, CT Index, and FI. This helped to characterize the cracking and rutting resistance of the different mixes. The performance space diagrams were divided into four individual quadrants using recommended preliminary thresholds for cracking and shear resistance of high-performance asphalt mixes for use in Southern Ontario's approach intersections. Only the top left quadrant was considered as passing, meaning that the mix had high resistance to both rutting and cracking. The other quadrants were considered as failing as they either failed to meet the minimum trigger level for cracking or rutting, or both.

Previous research conducted at CPATT in 2019 suggested a threshold value of 700 J/m<sup>2</sup>, 15, and 6mm rut depth at a testing temperature of 50°C and 20,000 wheel-track passes, for DC(T) fracture energy, FI, and rut depth, respectively (Salehi-Ashani, 2019; Bashir et al., 2020). These values were used as the minimum trigger levels for cracking and shear resistance in the performance space diagrams. The threshold values in the study conducted at CPATT in 2019 were based on sixteen asphalt mixes with asphalt binder ranging from PG-52-40 to PG-70-28, including four mixes that contained 20% reclaimed asphalt pavement (RAP). Therefore, for the purpose of this study, the minimum acceptable level for DC(T) and FI has been raised to 900 J/m<sup>2</sup> and 20, respectively. The 900 J/m<sup>2</sup> threshold for DC(T) fracture energy was chosen because five out of seven lab-produced asphalt mixes had an average value above this threshold and the average DC(T) fracture energy of all seven mixes was 958 J/m<sup>2</sup>. The minimum acceptable level of 20 for FI was chosen as all asphalt mixes had a higher average value. The minimum acceptable level of 500 for CT Index was selected as it was slightly lower than the average CT Index of all seven lab-produced mixes, which was 521. The rut depth of 6mm was chosen as a trigger value for the HWTT at 40,000 passes and a testing temperature of 58°C. The testing temperature and number of wheel-track passes for the rut depth trigger level were different from a study conducted by CPATT in 2019 as the focus of this research is to develop asphalt mixes for approach intersections that experience significant shear stresses. Figures 6-16 to Figure 6-18 illustrate performance space diagrams showing the

relationship between DC(T) fracture energy and rut depth, FI and rut depth, and CT Index and rut depth, respectively.

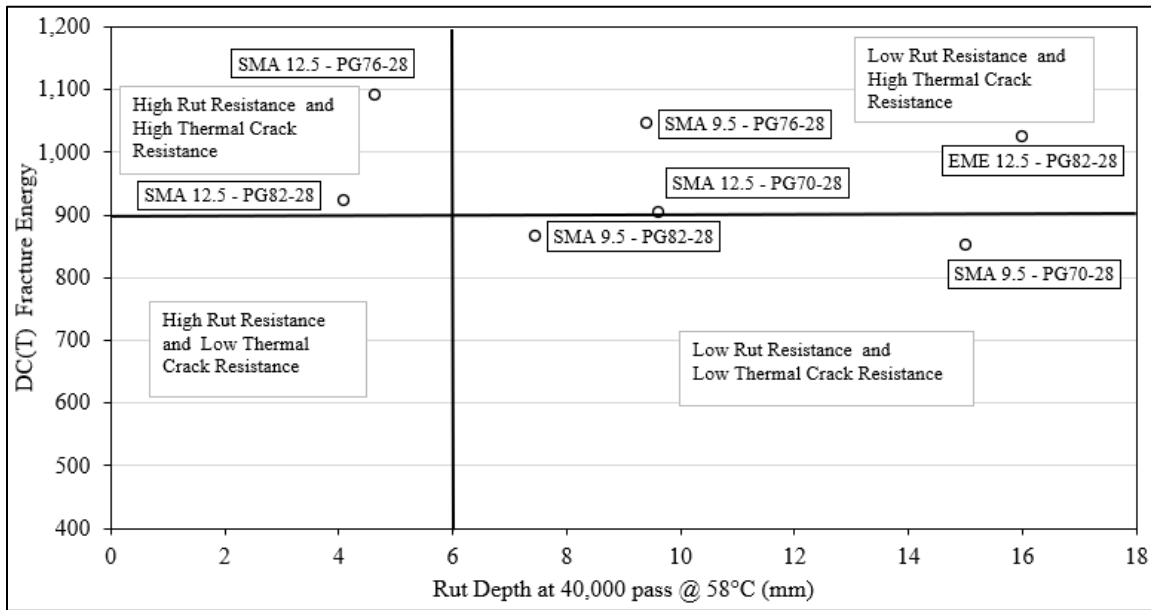


Figure 6-16: Performance Space Diagram of DC(T) Fracture Energy vs. Rut Depth with Preliminary Threshold Criteria

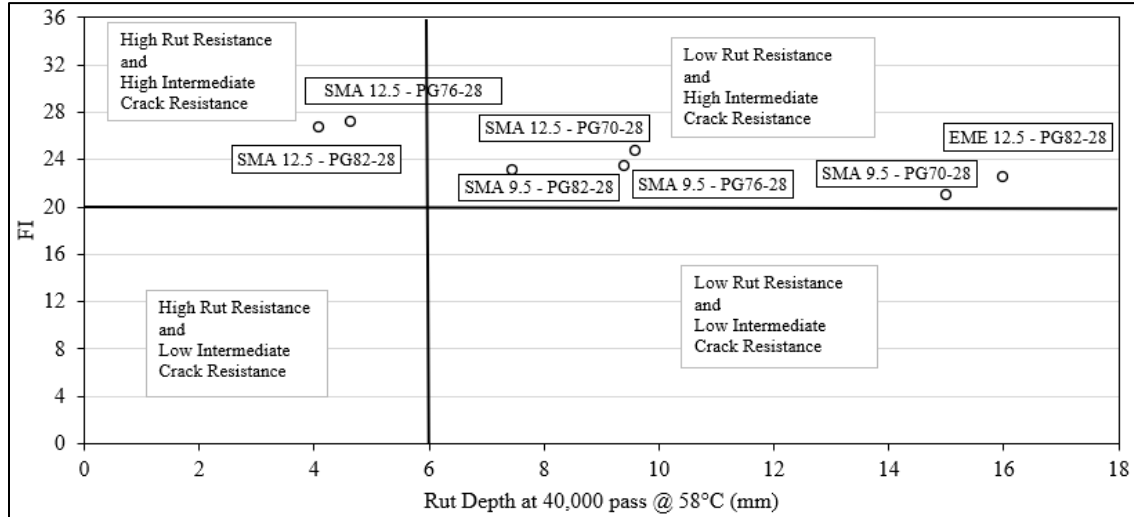
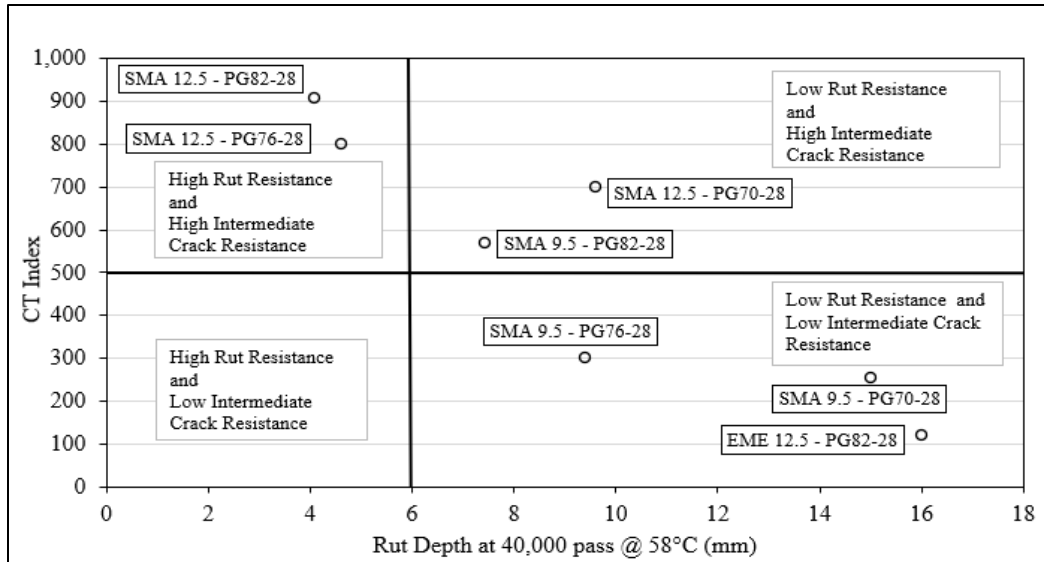


Figure 6-17: Performance Space Diagram of FI vs. Rut Depth with Preliminary Threshold Criteria



**Figure 6-18: Performance Space Diagram of IDEAL-CT vs. Rut Depth with Preliminary Threshold Criteria**

Figures 6-16 to 6-18 show that the asphalt mixes SMA12.5-PG76-28 and SMA12.5-PG82-28 performed well in all three performance space diagrams, displaying high resistance to rutting as well as good resistance to low and intermediate cracking. This indicates that these mixes have desirable characteristics for a well-performing asphalt mix. Figure 6-16 indicates that SMA9.5-PG70-28 and SMA9.5-PG82-28 mixes showed poor resistance to both rutting and low-temperature cracking resistance. Comparing results in Figure 6-17 indicated that all asphalt mixes illustrated high intermediate temperature cracking resistance considering FI values. As shown in Figure 6-18, SMA9.5-PG70-28, SMA9.5-PG76-28, and EME mixes showed low resistance in both rutting and intermediate temperature cracking. In addition, SMA9.5-PG82-28, SMA12.5-PG70-28 showed high intermediate temperature cracking resistance considering CT Index values. Figure 6-16 indicates that the SMA9.5-PG70-28 and SMA9.5-PG82-28 mixes performed poorly in terms of resistance to rutting and low-temperature cracking. The results in 6-17 imply that all asphalt mixes had high intermediate temperature cracking resistance, as indicated by their FI values. Figure 6-18 shows that the SMA9.5-PG70-28, SMA9.5-PG76-28, and EME mixes had low resistance to both rutting and intermediate temperature cracking. In addition, the SMA9.5-PG82-28 and SMA12.5-PG70-28 mixes had high intermediate temperature cracking resistance, as indicated by their CT Index values. Overall, the results suggest that performance space diagrams can be used as a tool in the asphalt mix design process to achieve a balanced mix that is resistant to both cracking and rutting based on laboratory performance tests.

### 6.2.9. Predicted Life Cycle Cost Analysis

The aim of the life cycle cost assessment was to determine the financial requirements for constructing and maintaining an asphalt pavement at an approach intersection, using the SMA12.5-PG76-28 surface course asphalt mix, over its service life while meeting a specified minimum acceptable level. The results of the comparison were made between two asphalt mixes: the currently specified asphalt surface mix (SP12.5 FC2-PG70-28) used in York Region and the proposed asphalt surface mix (SMA12.5-PG76-28). The properties of the plant-produced SP12.5 FC2-PG70-28 were explained in Chapter 4. The comparison was done to determine the potential benefits of using the proposed asphalt mix SMA12.5-PG76-28.

Prior to conducting a life cycle assessment, four steps were taken. Firstly, the DC(T) fracture energy, I-FIT, and HWTT (at 58°C testing temperature) test results of the two asphalt mixes (SP12.5 FC2-PG70-28 and SMA12.5-PG76-28) were compared to evaluate the benefits in cracking and rutting resistance when using SMA12.5-PG76-28. Secondly, the benefits determined in step 1 applied to the current asphalt pavement deterioration curve used for high-traffic volume urban roads in York Region. Thirdly, the appropriate pavement treatments and timing were selected to extend the average service life of the approach intersection to 50 years, which matches York Region's roads asset management plan. And lastly, the Net Present Worth (NPW) method was employed to compute the life cycle cost. Figure 6-19 presents both the DC(T) and FI values obtained for the plant-produced asphalt mix SP12.5 FC2-PG70-28.

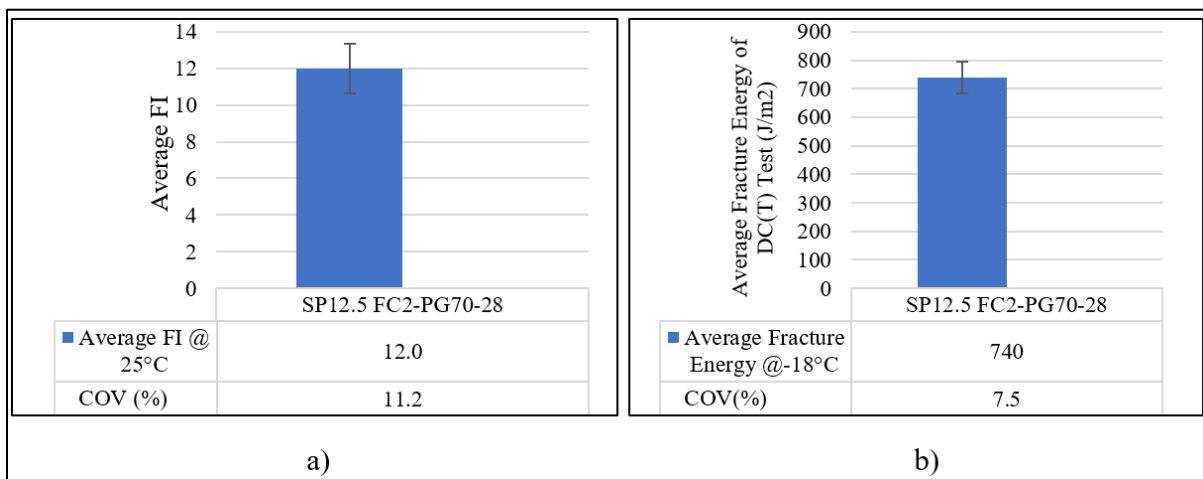


Figure 6-19: Results for SP12.5 FC2-PG70-28 for both a) Average FI and b) Average DC(T) Fracture Energy

Table 6-14 presents the performance results of both SMA12.5-PG76-28 and SP12.5 FC2-PG70-28 asphalt mixes in terms of fracture energy, FI, and the number of passes required for each mix to reach 6mm deformation during the HWTT at a temperature of 58°C. It should be noted that for SMA12.5-PG76-28, the rutting depth was assumed to reach 6mm after 40,000 passes as there was no data beyond this point.

Table 6-14 demonstrates the improvement in low and intermediate temperature cracking resistance, as well as rutting resistance, when using SMA12.5-PG76-28 asphalt mix compared to the currently specified asphalt mix (SP12.5 FC2-PG70-28) for approach interstation applications. In addition, Table 6-14 highlights that the highest importance factor (0.5) was assigned to rutting resistance due to its significance in terms of safety concerns at approach intersections. The intermediate temperature cracking resistance received a factor of 0.3, while the low-temperature cracking resistance received a factor of 0.2. The overall result was an improvement of 171% in asphalt mix performance when using SMA12.5-PG76-28 compared to SP12.5 FC2-PG70-28.

**Table 6-14: Performance Comparison SMA12.5-PG76-28 vs. SP12.5FC2-PG70-28**

| Testing Parameters                                     | Asphalt Mixes       |                    | Performance Improvement (%)<br>$C=(A-B/B)*100$ | Importance Factor (D) | Weighted Performance Improvement (%) (E = C x D) | Sum of Weighted Performance Improvement (%) |
|--|---------------------|--------------------|--|-----------------------|--|---|
|  | SMA12.5-PG76-28 (A) | SP12.5-PG70-28 (B) |  |                       |  |   |
| (HWTT) Number of Passes reached 6mm Deformation @ 58°C | 40,000              | 11,500             | 248  | 0.5                   | 124  | 171   |
| FI @ 25°C  | 27.2                | 12                 | 127  | 0.3                   | 38   |   |
| DC(T) Fracture Energy @ -18°C                          | 1,091               | 740                | 47   | 0.2                   | 9  |   |

To assess the condition of road segments, municipalities conduct a detailed pavement condition assessment survey and compile the data to generate an overall pavement condition index (PCI), which ranges from 0 to 100. A PCI score of 100 represents a newly constructed or rehabilitated pavement, while a score of 0 indicates the poorest or failed condition.

Figure 6-20 illustrate the estimated asphalt pavement deterioration curve used in York Region for high traffic volume roads with a strong subbase and medium total asphalt layer thickness. Additionally, the estimated deterioration curve for SMA12.5-PG76-28 was developed considering the 171% performance improvement. Furthermore, a PCI value of 50 was used as the minimum

acceptable level, indicating that the SP12.5FC2-PG70-28 and SMA12.5-PG76-28 mixes would reach the trigger level at ages 21 and 36, respectively. Table 6-15 presents the typical asphalt pavement life cycle activities, including preservation and rehabilitation works, used in York Region to extend the life of heavy traffic volume roads to 50 years.

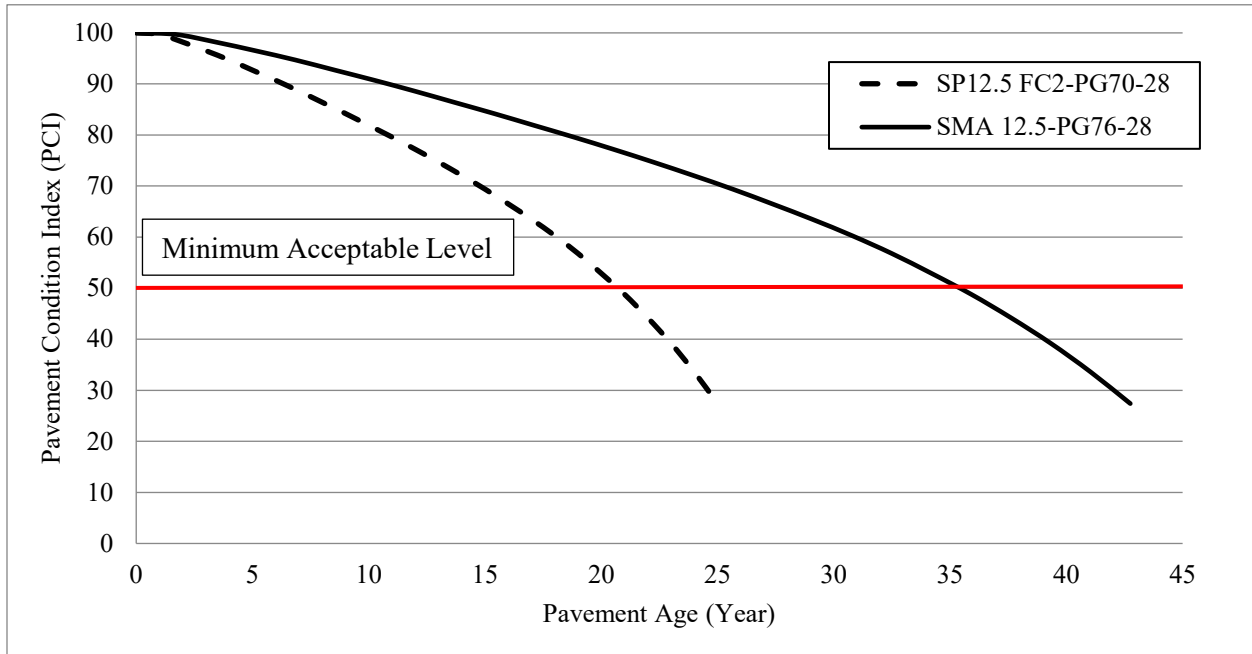


**Figure 6-20: Deterioration Curves for SP12.5 FC2-PG70-28 and SMA 12.5-PG76-28 Asphalt Mixes with No Life Cycle Treatment**

**Table 6-15: Typical Life Cycle Activities for Heavy Traffic Volume Roads in York Region**

| Pavement Age (Year) | Life Cycle Activities     |
|---------------------|---------------------------|
| 0                   | Initial Construction      |
| 4                   | Crack Seal (20%)          |
| 8                   | Surface Treatment         |
| 12                  | Crack Seal (20%)          |
| 17                  | Mill and Pave 50mm (100%) |
| 21                  | Crack Seal (20%)          |
| 25                  | Crack Seal (20%)          |
| 30                  | Pavement Rehabilitation   |
| 34                  | Crack Seal (20%)          |
| 40                  | Surface Treatment         |
| 44                  | Crack Seal (20%)          |
| 48                  | Grind and Patch (20%)     |

The information from Figure 6-20 and Table 6-15 was used to develop 50-year life cycle asphalt performance deterioration curves for the SP12.5 FC2-PG-70-28 and SMA 12.5-PG76-28 asphalt mixes, which are presented in Figures 6-21 and 6-22, respectively.

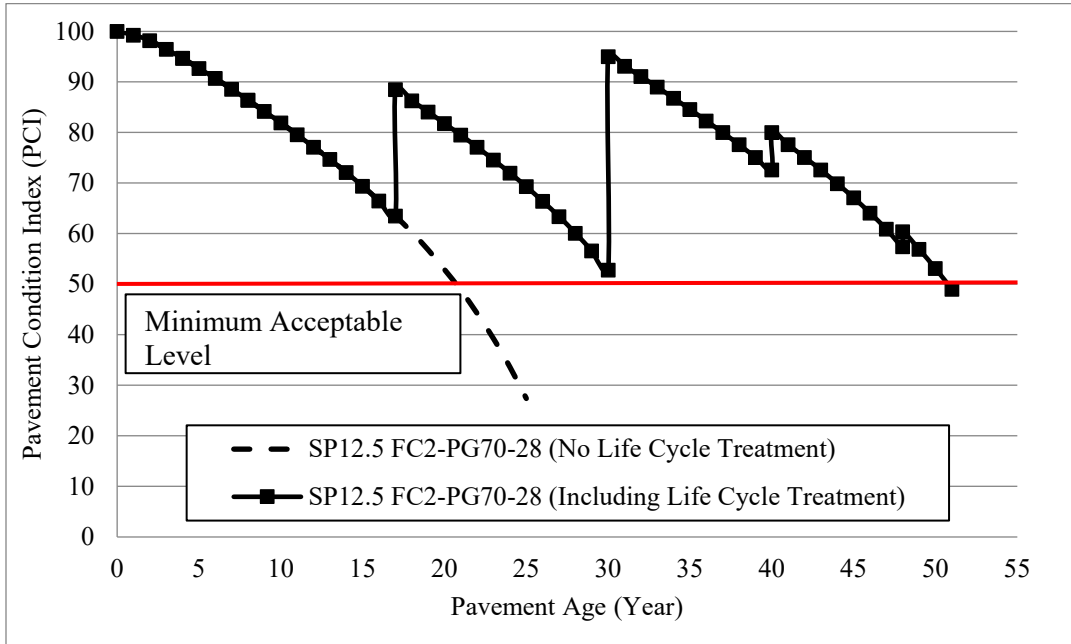


**Figure 6-21: Deterioration Curves for SP12.5 FC2-PG70-28 Asphalt Mix (No Life Cycle Treatment vs. Including Life Cycle Treatment)**

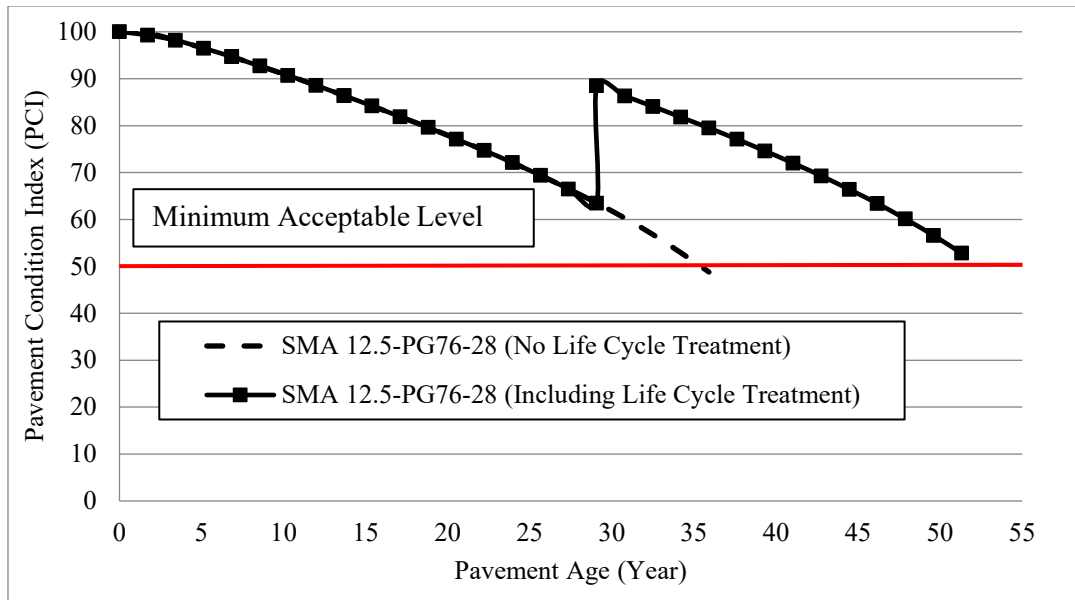


**Figure 6-22: Deterioration Curves for SMA 12.5-PG76-28 Asphalt Mix (No Life Cycle Treatment vs. Including Life Cycle Treatment)**



The Net Present Worth (NPW) method was used to determine the life cycle cost for both the SP12.5 FC2-PG70-28 and SMA 12.5-PG76-28 asphalt mixes over a 50-year period, as presented in Equation 6-1. The comparison of the life cycle cost was performed using discount rates of 0%, 2%, and 4%. It is important to note that all costs are per 1-lane.km (3,500m<sup>2</sup>) and the initial construction cost unit rate is the average cost of constructing 4-lane roads in an urban setting.

Where:

$$NPW = IC + \sum_{j=1}^k (M\&R_j \times \left( \frac{1}{1 + i_{Discount}} \right)^{n_j}) \quad (6-1)$$

- NPW = Net Present Worth (\$),
- IC = Initial Cost (\$),
- K = Number of future maintenance, preservation, and rehabilitation
- M&R<sub>j</sub> = Cost of j<sup>th</sup> future maintenance, preservation and rehabilitation activity (\$)
- i<sub>Discount</sub> = Discount Rate,
- n<sub>j</sub> = Number of years from presents of the j<sup>th</sup> future maintenance, preservation and rehabilitation activity

Tables 6-16 and 6-17 presents the calculated NPW values for maintaining roads constructed with SMA 12.5-PG76-28 and SP12.5 FC2-PG-70-28 asphalt mix surface course over a 50-year lifespan, considering different discount rate values, respectively.

The conclusion from the results showed that even though the initial construction cost of a 1-lane.km road with SMA 12.5-PG76-28 surface course was \$105,000 more, the overall 50-year life cycle cost was \$218,400 less at a 0% discount rate. Moreover, the difference was decreased to \$72,975 and \$3,391 at 2% and 4%, respectively. This indicates that at higher discount rate the difference is not significant, and two alternatives have very similar costs. Additionally, the results indicated that the number of life cycle activities required to maintain a road constructed with SMA 12.5-PG76-28 was less than that of SP12.5-PG70-28, potentially reducing the material production and hauling and resulting in less fuel usage and fewer greenhouse gas emissions.

**Table 6-16: Life Cycle Net Present Worth for Maintaining Heavy Traffic Roads with SMA 12.5-PG76-28 Asphalt Mix Surface Course**

| Year                                      | Life Cycle Activities     | Unit           | Unit Cost (\$/m <sup>2</sup> ) | Cost Per Lane.km (lane.km = 3,500m <sup>2</sup> ) | 0% Discount Rate   | 2% Discount Rate   | 4% Discount Rate   |
|---|---------------------------|----------------|--------------------------------|---|--------------------|--------------------|--------------------|
| 0   | Initial Construction      | m <sup>2</sup> | 290                            | \$ 1,015,000                                      | \$1,015,000        | \$1,015,000        | \$1,015,000        |
| 7   | Crack Seal (20%)          | m <sup>2</sup> | 0.2                            | \$700   | \$700              | \$609              | \$532              |
| 14  | Surface Treatment         | m <sup>2</sup> | 15                             | \$52,500  | \$52,500           | \$39,788           | \$30,317           |
| 21  | Crack Seal (20%)          | m <sup>2</sup> | 0.2                            | \$700   | \$700              | \$462              | \$307              |
| 29  | Mill and Pave 50mm (100%) | m <sup>2</sup> | 65                             | \$227,500   | \$227,500          | \$128,108          | \$72,948           |
| 36  | Crack Seal (20%)          | m <sup>2</sup> | 0.2                            | \$700   | \$700              | \$343              | \$171              |
| 43  | Crack Seal (20%)          | m <sup>2</sup> | 0.2                            | \$700   | \$700              | \$299              | \$130              |
| <b>Total 50-Year Life Cycle Cost (\$)</b> |                           |                |                                | <i>\$1,297,800</i>                                | <i>\$1,297,800</i> | <i>\$1,184,610</i> | <i>\$1,119,405</i> |
| <b>Average Cost (\$)/Year</b>             |                           |                |                                | <i>\$25,956</i>                                   | <i>\$25,956</i>    | <i>\$23,692</i>    | <i>\$ 22,388</i>   |

**Table 6-17: Life Cycle Net Present Worth for Maintaining Heavy Traffic Roads with SP12.5 FC2-PG70-28 Asphalt Mix Surface Course**

| Year                                      | Life Cycle Activities     | Unit           | Unit Cost (\$/m <sup>2</sup> ) | Cost Per Lane.km (lane.km = 3,500m <sup>2</sup> ) | 0% Discount Rate   | 2% Discount Rate   | 4% Discount Rate   |
|---|---------------------------|----------------|--------------------------------|---|--------------------|--------------------|--------------------|
| 0   | Initial Construction      | m <sup>2</sup> | 260                            | \$910,000   | \$910,000          | \$910,000          | \$910,000          |
| 4   | Crack Seal (20%)          | m <sup>2</sup> | 0.2                            | \$700   | \$700              | \$647              | \$598              |
| 8   | Surface Treatment         | m <sup>2</sup> | 15                             | \$52,500  | \$52,500           | \$44,808           | \$38,361           |
| 12  | Crack Seal (20%)          | m <sup>2</sup> | 0.2                            | \$700   | \$700              | \$552              | \$437              |
| 17  | Mill and Pave 50mm (100%) | m <sup>2</sup> | 36                             | \$126,000   | \$126,000          | \$89,984           | \$64,685           |
| 21  | Crack Seal (20%)          | m <sup>2</sup> | 0.2                            | \$700   | \$700              | \$462              | \$307              |
| 25  | Crack Seal (20%)          | m <sup>2</sup> | 0.2                            | \$700   | \$700              | \$427              | \$263              |
| 30  | Pavement Rehabilitation   | m <sup>2</sup> | 74                             | \$259,000   | \$259,000          | \$142,986          | \$79,855           |
| 34  | Crack Seal (20%)          | m <sup>2</sup> | 0.2                            | \$700   | \$700              | \$357              | \$184              |
| 40  | Surface Treatment         | m <sup>2</sup> | 15                             | \$52,500  | \$52,500           | \$23,777           | \$10,935           |
| 44  | Crack Seal (20%)          | m <sup>2</sup> | 0.2                            | \$700   | \$700              | \$293              | \$125              |
| 48  | Grind and Patch (20%)     | m <sup>2</sup> | 32                             | \$112,000   | \$112,000          | \$43,292           | \$17,046           |
| <b>Total 50-Year Life Cycle Cost (\$)</b> |                           |                |                                | <i>\$1,516,200</i>                                | <i>\$1,516,200</i> | <i>\$1,257,585</i> | <i>\$1,122,796</i> |
| <b>Average Cost (\$)/Year</b>             |                           |                |                                | <i>\$30,324</i>                                   | <i>\$30,324</i>    | <i>\$25,152</i>    | <i>\$22,456</i>    |

### 6.3. Summary and Conclusions

This chapter investigated the low-temperature cracking and shear resistance of 7 lab-made asphalt mixes, including six SMA and one EME mix, using DC(T) and HWTT tests, respectively. The intermediate temperature cracking resistance was determined using I-FIT and IDEAL-CT tests. A ranking system was used to rank the mixes based on their resistance to cracking and rutting. A minimum acceptable level value was also recommended for each performance test to construct performance space diagrams.

The following conclusions can be drawn based on the experimental results and the discussions provided in this chapter:

- The study found that SMA mixes with 12.5mm NMAAS showed higher DC(T) fracture energy compared to SMA mixes with 9.5mm NMAAS with the same asphalt binder PG. The results also suggest that lower continuous low-temperature grade and m-value of asphalt binder results in higher DC(T) fracture energy. On average, all seven tested asphalt mixes had a DC(T) fracture energy of 958 J/m<sup>2</sup>. The ANOVA analysis showed no significant difference between NMAAS and asphalt binder PG. The highest ranking was given to SMA12.5-PG76-28, followed by SMA9.5-PG76-28 and EME based on Tukey analysis. The DC(T) fracture energy results concluded that the DC(T) test has low to medium variability
- The CT Index results indicated that the IDEAL-CT test may be sensitive to asphalt mix gradation, as the CT Index value for EME mix was low compared to SMA mixes. Bigger NMAAS was found to result in higher CT Index values. On average, the seven tested asphalt mixes had a CT Index value of 521. The ANOVA analysis found that both NMAAS and asphalt binder PG had a significant impact on CT Index values. The Tukey analysis showed that SMA12.5-PG82-28 and SMA12.5-PG76-28 had statistically higher average CT Index. In conclusion, the CT Index results showed that the IDEAL-CT test has medium to high variability.
- The results of the I-FIT test on different heavy-duty asphalt mixes suggest that the test has limited ability to distinguish differences in intermediate temperature cracking resistance. The ANOVA analysis showed no significant difference between the SMA mixes and all

were ranked as "A" in the Tukey analysis. The I-FIT test has low to medium variability. The average fracture index (FI) value was highest for the SMA12.5-PG-76-28 mix.

- The results indicate that the EME mix provided higher friction compared to the SMA mixes based on the average BPN values. Higher testing temperature, larger NMAS, dry conditions, and greater asphalt binder PG led to higher BPN values when comparing SMA mixes.
- The results from the HWTT, I-FIT, DC(T), and IDEAL-CT tests suggest that the SMA12.5-PG76-28 mix was the best performing asphalt mix based on the overall ranking.
- The following threshold values were recommended for the heavy-duty asphalt mix performance test based on the results of this study and previous CPATT study in 2019:
  - DC(T) fracture energy: 900J/m<sup>2</sup>
  - FI: 20
  - CT Index: 500
  - HWTT: 6mm rut depth at 40,000 passes and 58°C testing temperature
- The results showed a very poor correlation between DC(T) fracture energy and both CT Index and FI, indicating that mixes with high DC(T) fracture energy might not necessarily have high intermediate temperature cracking resistance. Therefore, both low and intermediate temperature cracking resistance tests are necessary to accurately distinguish the durability of asphalt mixes.
- The results showed that performance space diagrams can be a useful tool in the asphalt mix design process to achieve a balanced mix design and to ensure resistance to both cracking and rutting based on laboratory tests. It is recommended to use the HWTT, DC(T), I-FIT, and IDEAL-CT tests, along with current volumetric mix attributes, to evaluate the resistance of asphalt mixes to both low and intermediate temperature cracking and rutting to produce a durable mix.
- The life cycle cost analysis showed that using SMA12.5-PG76-28 as a surface course for roads in York Region could increase the road service life by 171% and result in lower costs over a 50-year lifespan, despite its higher initial cost.

## **Chapter 7 Conclusions, Recommendations, and Future research**

### **7.1. General Summary**

This research was conducted to fulfill the following objectives: (1) To propose a sustainable asphalt surface mix for approach intersections in Southern Ontario to improve resistance to rutting and cracking by means of performance testing, (2) To identify suitable and practical performance tests to be used in quality assurance and control activities for evaluating the resistance of asphalt mixes to rutting and cracking in Southern Ontario, (3) To implement performance specifications for evaluating the rutting and cracking resistance of surface asphalt mixes used in heavy traffic volume approach intersections in Southern Ontario, and (4) To predict the service life and associated life cycle costs of the proposed asphalt surface mix for use in approach intersections.

To achieve the first objective, a total of seven lab-produced asphalt surface mixes including six SMA and one EME asphalt mixes were investigated. The SMA mixes were produced using two different NMAAS (9.5mm and 12.5mm) and three different polymer-modified asphalt binders (PG70-28, PG76-28, and PG82-28). The EME mix was made using 12.5mm aggregate size and PG82-28 asphalt binder. The second objective was fulfilled by conducting several tests on the asphalt mixes. The tests were selected based on a literature review and the availability of testing equipment. HWTT, IDEAL-RT, Flow Number, and Dynamic Modulus tests were conducted to evaluate the shear resistance of asphalt mixes. In addition, I-FIT and IDEAL-CT tests were applied to determine the intermediate temperature cracking resistance, while the DC(T) test was employed to evaluate the low-temperature cracking resistance. Furthermore, BPT and TSR tests were conducted to investigate the friction and moisture susceptibility of asphalt mixes, respectively. The third objective was achieved through analyzing laboratory results of four tests (HWTT, IDEAL-CT, I-FIT, and DC(T)) performed on seven heavy-duty asphalt mixes. Based on the analysis, preliminary specifications were recommended as quality assurance criteria for these tests. The fourth objective was fulfilled by using the laboratory results of three tests (HWTT, I-FIT, and DC(T) tests) performed on two asphalt mixes (SMA12.5-PG76-28 and SP12.5-PG70-28) to perform a life cycle cost analysis.

## 7.2. Major Findings and Conclusions

The findings from the field investigation revealed that the rutting damage was confined solely to the asphalt surface layer, suggesting that the pavement structure was structurally sound. The root cause of the rutting could be attributed to the insufficient stability of the asphalt mixture. It appears that the volumetric design method may not provide a comprehensive understanding of how the asphalt mixture will perform under heavy traffic loads.

The results from the HWTT tests at 58°C for the three plant-made mixes showed that all three mixes experienced excessive rutting before 20,000 wheel-track passes. It was concluded that the current asphalt mixes used in York Region are unsuitable for heavy truck traffic areas like approach intersections, as they have low resistance to rutting. The study concluded that a testing temperature of 58°C was an appropriate method to differentiate heavy-duty asphalt mixes. The study also suggested that increasing the number of wheel-track passes to 40,000 during the HWTT test would provide a clearer distinction between heavy-duty asphalt mixes.

The overall analysis showed that for the same asphalt binder, mixes with a 9.5mm NMA had better rutting resistance as indicated by the IDEAL-RT Index, FN, and  $|E^*|$  values. However, the results from the HWTT tests did not align with this trend, as mixes with a 12.5mm NMA exhibited higher rutting resistance than those with a 9.5mm NMA. Moreover, the analysis showed that NMA, PG binder, and testing temperature were important factors that affected FN and IDEAL-RT values for SMA mixes. The FN test showed higher variability compared to the IDEAL-RT test. Additionally, the results showed that the  $|E^*|$  values at a temperature of 54.4°C and a frequency of 1Hz had a stronger correlation with other rutting parameters compared to the values at 54.4°C and a frequency of 0.1Hz. Furthermore, the correlation analysis of rutting parameters for SMA mixes revealed a strong relationship between IDEAL-RT Index and FN values when tested at 58°C. Additionally, both IDEAL-RT Index and FN values were highly correlated with  $|E^*|$  at 54.4°C and two frequencies (1Hz and 0.1Hz) for all groups. Furthermore, the results from the HWTT tests had poor correlations with other rutting parameters determined through IDEAL-RT, FN, and Dynamic Modulus tests. The overall ranking of the asphalt mixes, based on the HWTT, IDEAL-RT, and FN tests, showed that both SMA9.5-PG76-28 and SMA12.5-PG76-28 had strong resistance to rutting compared to the other asphalt mixes.

The DC(T) fracture energy results showed that SMA mixes with a 12.5mm NMAAS had higher fracture energy values compared to those with 9.5mm NMAAS when using the same PG asphalt binder. Additionally, the study suggested that mixes with asphalt binders that have a lower continuous low-temperature grade and lower m-value tend to have higher DC(T) fracture energy. Additionally, the statistical analysis using ANOVA showed that both NMAAS and PG binder had no significant effect on the DC(T) fracture values. However, the t-test results indicated a significant difference between the asphalt mixes containing PG70-28 and PG76-28, and between PG76-28 and PG82-28. In conclusion, the results of the DC(T) fracture energy test demonstrated that the variability of the results was low to medium.

The results from the I-FIT test (FI values) indicated that the test was not effective in differentiating the intermediate temperature cracking resistance of heavy-duty asphalt mixes, as the values were relatively similar. The findings from the FN test suggested that the I-FIT test had low to medium variability. The CT Index values showed that the IDEAL-CT test may be influenced by the gradation of the asphalt mix, as the EME mix had much lower CT Index value compared to the SMA mixes. The ANOVA analysis showed that both the size of the NMAAS and the asphalt binder PG had a significant impact on the CT Index values. The CT Index results indicated that larger NMAAS led to higher CT Index values. The conclusion drawn from the CT Index results was that the variability of the IDEAL-CT test was moderate to high.

The results showed that there was generally a very poor correlation between the DC(T) fracture energy and both the CT Index and FI. This implies that asphalt mixes that have good resistance to low-temperature cracking might not necessarily have good resistance to intermediate temperature cracking. Thus, it is important to conduct both low and intermediate temperature cracking resistance tests to accurately assess the durability of asphalt mixes.

The overall results suggested that performance space diagrams can be used as a tool in the asphalt mix design process to achieve a balanced design and to ensure that the asphalt mix has resistance to both cracking and rutting, based on the results of performance laboratory tests. In addition, the results indicated that the HWTT, DC(T), I-FIT, and IDEAL-CT tests could be used in conjunction with the current volumetric mix attributes to assess the resistance of asphalt mixes to low temperature cracking, intermediate temperature cracking, and rutting, in order to produce a durable asphalt mix.

The overall ranking, based on the results of the HWTT, I-FIT, DC(T), and IDEAL-CT tests, showed that the SMA12.5-PG76-28 asphalt mix was the best performing of the lab-produced mixes. The life cycle cost analysis demonstrated that using the SMA12.5-PG76-28 asphalt mix instead of the current asphalt mix used in York Region resulted in a significant increase in pavement service life, leading to material and cost savings.

### **7.3. Contributions**

The study found that the volumetric-based approach to asphalt mix design has been inadequate for approach intersections in York Region. As a result, the research suggested incorporating the HWTT, IDEAL-CT, I-FIT, and DC(T) tests into the asphalt mix design and quality assurance process, in order to create a sustainable asphalt mix for heavy truck traffic approach intersections in Southern Ontario.

The temperature sensitivity analysis of the rutting resistance tests revealed that a testing temperature of 58°C is appropriate for differentiating between heavy-duty asphalt mixes. For the HWTT, it was recommended to not only increase the testing temperature from 50°C to 58°C, but also to increase the number of wheel-track passes from 20,000 to 40,000 to more accurately reflect harsh conditions. To address safety concerns at approach intersections, it was also recommended to reduce the rut depth acceptance threshold from 12.5mm to 6mm.

The study proposed the following preliminary low and intermediate temperature cracking resistance thresholds for the development and selection of heavy-duty asphalt mixes in Southern Ontario: DC(T) fracture energy value of 900 J/m<sup>2</sup>, a FN value of 20, and a CT Index value of 500.

### **7.4. Future Research Opportunities**

Based on the research presented in this thesis, the following are possible areas for future research on heavy-duty asphalt mixes:

- Future research is needed to assess the impact of both short-term aging and long-term aging on the performance of heavy-duty asphalt mixes.



- This research evaluated the preliminary performance specifications of laboratory-made asphalt mixes. However, it is recommended that a field trial be conducted to assess the in-service performance of a heavy-duty asphalt mix.
- It is recommended to design and construct an instrumented trial section that includes various instrumentation tools, such as strain gauges, pressure cells, temperature probes, and moisture gauges, to better predict the service life of a heavy-duty asphalt mix and to gather data on field responses.
- Future research should be carried out to examine to investigate the feasibility of producing fibre-free SMA using different types of asphalt binder modifiers, with the aim of reducing the usage of raw materials, lowering costs, and streamlining plant operations.
- Further research should be conducted to examine the impact of asphalt mix gradation on the IDEAL-CT test, as the CT Index results indicated that the IDEAL-CT test might be sensitive to the gradation of the asphalt mix, as the CT index value for the EME mix was significantly lower compared to the SMA mixes.
- A future study should be performed to evaluate the effect of temperature on the I-FIT test results, as the test failed to distinguish between heavy-duty asphalt mixes at a 25°C testing temperature in this study.
- Future research should explore the possibility of incorporating recycled materials, such as recycled plastic, into SMA mixes.

## Bibliography

- Albayati, A. H. (2006). *Permanent Deformation Prediction of Asphalt Concrete Under Repeated Loading*. University of Baghdad, Iraq.
- Al-Mosawe, H. (2016). *Prediction of Permanent Deformation in Asphalt Mixtures*. University of Nottingham.
- American Association of State and Highway Transportation Officials. (1993). *Guide for Design of Pavement Structures*. Washington, D.C.
- American Association of State and Highway Transportation Officials M320. (2010). *Standard Specification for Performance-Graded Asphalt Binder*. Standard Specifications for Transportation Materials and Methods of Sampling and Testing, Part 1B. Washington, DC.
- American Association of State and Highway Transportation Officials PP62. (2009). *Standard Practice for Developing Dynamic Modulus Master Curves for Hot Mix Asphalt (HMA)*. Standard Specifications for Transportation Materials and Methods of Sampling and Testing. Washington, DC.
- American Association of State and Highway Transportation Officials T19. (2014). *Standard Method of Test for Bulk Density ("Unit Weight") and Voids in Aggregate*. Washington, D.C.
- American Association of State and Highway Transportation Officials T240. (2009). *Effect of Heat and Air on a Moving Film of Asphalt Binder (Rolling Thin-Film Oven Test)*. Standard Specifications for Transportation Materials and Methods of Sampling and Testing. Washington, D.C.
- American Association of State and Highway Transportation Officials T305. (2005). *Draindown Characteristics In Uncompacted Asphalt Mixtures*. Washington, D.C.
- American Association of State and Highway Transportation Officials T315. (2012). *Determining the Rheological Properties of Asphalt Binder Using a Dynamic Shear Rheometer (DSR)*. Standard Specifications for Transportation Materials and Methods of Sampling and Testing. Washington, D.C.
- American Association of State and Highway Transportation Officials T320-07. (2011). *Standard method of test for determining the permanent shear strain and stiffness of asphalt mixtures using the Superpave shear tester (SST)*. Washington, D.C.
- American Association of State and Highway Transportation Officials T324. (2016). *Standard Method of Test for Hamburg Wheel-Track Testing of Compacted Hot Mix Asphalt (HMA)*. Standard Specifications for Transportation Materials and Methods of Sampling and Testing. Washington, D.C.

- American Association of State and Highway Transportation Officials T378. (2017). *Standard Method of Test for Determining the Dynamic Modulus and Flow Number for Asphalt Mixtures Using the Asphalt Performance Tester (AMPT)*. Standard Specifications for Transportation Materials and Methods of Sampling and Testing. Washington, D.C.
- American Society for Testing and Materials ASTM WK71466. (2021). *Standard Test Method for Determination of Rutting Tolerance Index of Asphalt Mixture Using the Rapid Rutting Test*.
- Asphalt Institute, (2014). *MS-2 Asphalt Mix Design Methods*. 7th Edition, USA
- Auld, Ed. (2007). *Weathering of building infrastructure and the changing climate: adaptation options*. Environment Canada
- Baghaee Moghaddam, T., Karim, M. R. & Abdelaziz, M. (2011). A review on fatigue and rutting performance of asphalt mixes. *Scientific Research and Essays*, 6, 670-682
- Baghaee Moghaddam, T. & Baaj, H. (2018). Application of compressible packing model for optimization of asphalt concrete mix design. *Construction and Building Materials*, 159, 530-539.
- Baghaee Moghaddam, T. (2019). *Development of High Modulus Asphalt Concrete Mix Design Technology for Use on Ontario's Highways*. [Doctoral thesis, University of Waterloo]. UWSpace. <http://hdl.handle.net/10012/14323>
- Bashir, I., Salehi-Ashani, S., Ahmed, D., Tabib, S., & Vasiliu, G. (2020). MTO's Experience with Post-Production Asphalt Mixture Performance Testing. *Proceedings Canadian Technical Asphalt Association*, 60, pp. 315-344.
- Bassett, C. E. (1990). Effects of maximum aggregate size on rutting potential and other properties of asphalt-aggregate mixtures. *Transportation Research Record*, 1259, 107–119.
- Bennert, T. (2018). Innovations in Asphalt Mixture Design Procedure. *Transportation Research Circular, E-C237*. Transportation Research Board.
- Blazejowski, K. (2011). *Stone Matrix Asphalt Theory and Practice*. CRC Press Taylor & Francis Group Boca, Raton, Fl.
- Bonaquist, R. (2014). Enhancing the Durability of Asphalt Pavements. *Transportation Research Circular, E-C186*. Transportation Research Board.
- Brosseaud, J.L. Delmore & R. Hiernaux, (1993). *Study of permanent deformations in asphalt pavements with the use of the LCPC wheel tracking rutting tester, Evaluation of future prospects*. 72th Annual Meeting Transportation Research Board.
- Brown, R.R., & Bassett, C.E. (1990). Effects of Maximum Aggregate Size on Rutting Potential

- and Other Properties of Asphalt –Aggregate Mixtures. *Transportation Research Record*, 1259, pp. 107-119.
- Brown, E. R., & Bassett, C. E. (1989). *The effects of maximum aggregates size on properties of asphalt aggregate mixes*. ER-89-03, Highway Research Center, Harbert Engineering Center, Auburn Univ., Auburn, AL.
- Brown, E. R., Kandhal, P. S., Roberts, F. L., Kim, Y. R., Lee, D.-Y., & Kennedy, T. W. (2009). *Hot mix asphalt materials, mixture design, and construction*. NAPA Research and Education Foundation. 3rd edition, Lanham, Maryland, 318-321.
- Button, J.W., Perdomo, D., & Lytton, R.L. (1990). Influence of Aggregate on Rutting in Asphalt Concrete Pavements. *Transportation Research Record*, 1259, pp.141-152.
- Chen, J., & Liao, M. (2002). Evaluation of internal resistance in hot mix asphalt (HMA) concrete. *Construction and Building Materials*, 16(6), 313–319.
- Chen, H., Zhang, Y., & Bahia, H. (2021). The role of binders in mixture cracking resistance measured by ideal-CT test. *International Journal of Fatigue*, Vol 142. Elsevier. <https://doi.org/10.1016/j.ijfatigue.2020.105947>.
- Crawford, C. (1989). *Tender Mixes: Probable Causes, Possible Remedies*. Quality Improvement Series 108-3186. National Asphalt Pavement Association, Lanham, MD.
- Cooper, A. (2021). *Rutting and IDEAL RT Testing*. *Balance Mix Designs News*. Retrieved on March 04, 2021 from <https://www.balancedmixdesign.com/news/rutting-and-ideal-rt-testing.html>
- Cooper, S. B., & Mohammad, L. N. (2018). Innovations in Asphalt Mixture Design Procedure. *Transportation Research Circular E-C237*. Transportation Research Board.
- Das, P. K., Jelagin, D. & Birgisson, B. (2013). Evaluation of the low temperature cracking performance of asphalt mixtures utilizing HMA fracture mechanics. *Construction and Building Materials*, 47, 594-600.
- Dore G & Zubeck H. (2009). Cold Regions Pavement Engineering. *American Society of Civil Engineers (ASCE) Press*, Reston, VA.
- Du, Y., Chen, J., Han, Z., & Liu, W. (2018). A Review on Solutions for Improving Rutting Resistance of Asphalt Pavement and Test Methods. *Construction and Building Materials*, 168, 893–905.
- El-Hakim, M. & Tighe, S. (2013). Evaluation of Perpetual Pavement Design Philosophy for Three Traffic Volume Scenarios. *Transportation Research Board*. Annual Meeting, Washington, D.C.
- EvothermWMA (2020), *The Ideal Rutting Test with Dr. Fujie Zhou*. <https://www.youtube.com/watch?v=u6l0ka6uf34> (Accessed: March 03-2021)

- Faruk, A. (2015). Measurement of HMA shear resistance potential in the lab: the simple punching shear test. *Construction and Building Materials*, 99, 62-72.
- Federal Highway Administration FHWA-HIF-11-038. (2011). *The Multiple Stress Creep Recovery (MSCR) Procedure*. Office of Pavement Technology
- Francken, L. (1998). *Bituminous Binders and Mixes, State of the Art and Interlaboratory Tests on Mechanical Behaviour and Mix Design*.
- Government of Canada. (2019). *Canada's changing climate report-headline statements*. Accessed: June 14-2021: [https://changingclimate.ca/site/assets/uploads/sites/2/2019/03/CCCR\\_HeadlineStatements.pdf](https://changingclimate.ca/site/assets/uploads/sites/2/2019/03/CCCR_HeadlineStatements.pdf)
- Grobler, J., Rebbechi, J., & Denneman, E. (2018). *National Performance-based Asphalt Specification Framework*, Austroads.
- Haug Y.H., (2004). *Pavement Analysis and design*. 2nd Edition, Upper Saddle River, Pearson Prentice Hall, NJ.
- Gouvernement du Québec. (2003). *Hot mix asphalt: LC method of mix design*. Bibliothèque Nationale du Québec, National Library of Canada. ISBN 2-551-22896-4, 2003.
- Huber, G. (2017). *History of Mix Design in North America*. Accessed: Jan 31-2021 <http://asphaltmagazine.com/history-of-asphalt-mix-design-in-north-america-part-1/> and <http://asphaltmagazine.com/history-of-asphalt-mix-design-in-north-america-part-2/>
- Hunter, N. R. (2000). Asphalt in roads construction. *American Society of Civil Engineering*. Thomas Telford Publications, pp 75, London.
- Intergovernmental Panel on Climate Change. (2014). *Climate change 2014: synthesis report*. Contribution of Working Groups I, II and III to the fifth assessment report of the Intergovernmental Panel on Climate Change. Ipcc.
- Kafi Farashah, M. Salehiashiani, S. Varamini, S. & Tighe, S. (2021). *Best Practices in Measuring Rutting and Shoving on Asphalt Pavements*. Transportation Association of Canada (TAC) 2021 Conference and Exhibition - Recovery and Resilience: Transportation after COVID-19.
- Kafi Farashah, M., Varamini, S. & Tighe, S. (2021). Field Performance Evaluation of Asphalt Mixes at Approach Intersections: A Municipal Perspective. *Proceedings of the Canadian Society of Civil Engineering (CSCE) Annual Conference 2021*. Lecture Notes in Civil Engineering, vol 239 (pp. 531-545). Springer, Singapore. [https://doi.org/10.1007/978-981-19-0503-2\\_43](https://doi.org/10.1007/978-981-19-0503-2_43)
- Kafi Farashah, M. Salehiashiani, S. Baghaee Moghaddam, T. Varamini, S. & Tighe, S. (2021).

- Field and Laboratory Methods of Evaluating Rutting and Shoving. *Proceedings of the Sixty-Sixth Annual Conference of the Canadian Technical Asphalt Association (CTAA): Cyberspace*, 175-194. <https://trid.trb.org/view/1930562>
- Kalcheff, I. V. & Tunnicliff, D. G. (1982). Effects of crushed stone aggregate size and shape on properties of asphalt concrete. *Proceedings of Association of Asphalt Paving Technologists, Vol. 51*, pp. 453–483.
- Kandhal, S. P., Mallick B. R. & Brown R. E. (1998). *Hot Mix Asphalt for Intersections in Hot Climates*. National Center for Asphalt Technology, NCAT Report No. 98-06, Auburn, Alabama.
- Kennedy, T.W., P. S. Kandhal, S. F. Brown, D. Y. Lee, & F. L. Roberts. (1996). *Hot Mix Asphalt Materials, Mixture Design and Procedure*. NAPA Research and Education Foundation, Lanham, MD.
- Kim, Y. R., N. Yim, & N. P. Khosla. (1992). *Effects of Aggregate Type and Gradation on Fatigue and Permanent Deformation of Asphalt Concrete*. In American Society for Testing and Materials, STP 1147, West Conshohocken, PA.
- Mahboub, K. & Little, D. N. (1988). *Improved Asphalt Concrete Design Procedure*. Research Report 474-1F. Texas Transportation Institute.
- Mills, B.N, S. L. Tighe, J. Andrey, J. T. Smith, S. Parm & K. Huen. (2007). *The Road Well-Traveled: Implications of Climate Change for Pavement Infrastructure in Southern Canada*. Waterloo, Ontario, Canada.
- Ministry of Transportation Ontario (MTO). (2013). *Pavement Design and Rehabilitation Manual*. Second Edition. Toronto, Canada
- Monismith, C. L., & Tayebali, A. A. (1988). *Permanent Deformation (Rutting) Considerations in Asphalt Concrete Pavement Sections*. The Association of Asphalt Paving Technologists v.57, Williamsburg, Virginia.
- National Asphalt Pavement Association (NAPA) Quality Improvement Series 122. (2002). *Designing and Constructing SMA Mixtures-State-of-the-Practice*. U.S. Department of Transportation. Federal Highway Administration, Lanham, Maryland.
- National Center for Asphalt Technology (NCAT). (1998). *Hot Mix Asphalt for Intersections in Hot Climates*. Auburn, AL: NCAT Report 98-06.
- National Cooperative Highway Research Program (NCHRP). (2004). *Guide for Mechanistic Empirical-design of New and Rehabilitated Pavement Structures*. Transportation Research Board, National Research Council, Washington, D.C. (2004).
- National Cooperative Highway Research Program (NCHRP) 20-07/Task 406. (2016). *Development of a Framework for Balanced Mix Design*. Transportation Research Board, National Research Council, Washington, D.C.

- National Cooperative Highway Research Program (NCHRP) 9-57. (2016). *Experimental Design for Field Validation of Laboratory Tests to Assess Cracking Resistance of Asphalt Mixtures*. Transportation Research Board, National Research Council, Washington, D.C.
- National Cooperative Highway Research Program (NCHRP). (2011). *A Manual for Design of Hot-Mix Asphalt with Commentary*. Report No. 763. Transportation Research Board, National Research Council, Washington, D.C.
- Newcomb, D., & Zhou, F. (2018). *Balanced Design of Asphalt Mixtures Research Project*. Texas A&M Transportation Institute. Retrieved from <https://www.dot.state.mn.us/research/reports/2018/201822.pdf>
- Ozer, H., & Al-Qadi, I. L. (2018). Innovations in Asphalt Mixture Design Procedure. *Transportation Research Circular E-C237*. Transportation Research Board (TRB).
- Pavement Interactive. (2020). *Dynamic Shear Rheometer*, Retrieved on May 20-2020 from: <https://pavementinteractive.org/reference-desk/testing/binder-tests/dynamic-shear-rheometer/>
- Politano, L. (2012). *Warm Mix Asphalt - A Greener Alternative to Hot Mix Asphalt*. Presented at the Fredericton, New Brunswick Conference, Transportation Association of Canada.
- Roberts, F. L., Kandhal, P. S., Brown, E. R., Lee, D.Y. & Kennedy, T. W. (1991). *Hot mix asphalt materials, mixture design and construction*. NAPA Education Foundation, 603.
- Said, S. F., Ahmed, A. W. & Carlsson, H. (2016). *Evaluation of rutting of asphalt concrete pavement under field-like conditions*. Prague, 6th Eurasphalt & Eurobitume Congress.
- Salehi-Ashani, S. (2019). *Development of Performance-Related Specification for Asphalt Mixtures in Ontario*. [Doctoral thesis, University of Waterloo].
- Strategic Highway Research Program (SHRP) (1990). *The Asphalt Research Program: 1990 Strategic Planning Document*. Washington, DC.
- Superpave Fundamentals. (2000). *Superpave Fundamentals Reference Manual*. Federal Highway Administration, National Highway Institute: NHI (National Highway Institute)
- Superpave Asphalt Mixture Design and Analysis. Report SA-95-003. Federal Highway Administration, U.S. Department of Transportation.
- Sybilski, H. Soenen, M. Gajewski, E. Chailleux, & Bankowski, W. (2013). Binder testing In: *Advances in interlaboratory testing and evaluation of bituminous materials*. Springer, Dordrecht, pp. 15–83
- Thiessen, M. Shalaby, A. & Kavanagh, L. (2000). Strength Testing of In-Service Asphalt Pavements in Manitoba and Correlation on Rutting. *Canadian Technical Asphalt Association 45*, 203-227.

- Transportation Association of Canada (TAC). (2013). *Pavement Asset Design and Management Guide*. Transportation Association of Canada, Ottawa, ON.
- Transportation Association of Canada (TAC). (2014). *Pavement Asset Design and Management Guide*. Transportation Association of Canada, Ottawa, ON.
- Varamini, Sina. (2013). *Utilization of Recycled Plastics as Binder Modifiers for Use in Hot-Mix Asphalt Pavement*. Halifax, Nova Scotia, Canada.
- Varamini, Sina. (2016). *Evaluation of Innovative and Sustainable Technologies for Use in Hot-Mix Asphalt Pavements*. [Doctoral thesis, University of Waterloo]. UWSpace. <http://hdl.handle.net/10012/11112>
- West, R. R. (2018). *Development of a Framework for Balanced Mix Design*. National Cooperative Highway Research Program.
- Witczak M. (2005). *Simple Performance Tests: Summary of Recommended Methods and Database*. National Cooperative Highway Research Program (NCHRP) No. 547, Transportation Research Board, National Research Council, National Academies, Washington, D.C. (2005).
- Witczak, M., Kaloush, k . Pellinen, T., & Quintus, H. (2002) *Simple performance test for Superpave mix design*, NCHRP Report 465, D.C., National Academy Press, Washington
- Zak, J. Monismith, C.L. Coleri, E & Harvey. J. (2017). *Uniaxial Shear Tester – new test method to determine shear properties of asphalt mixtures, Road Materials and Pavement Design*. 18:sup1, 87-103, DOI: [10.1080/14680629.2016.1266747](https://doi.org/10.1080/14680629.2016.1266747).
- Zhang, A.E. Alvarez, I.L. Sang, A. Torres, & Walubita, L.F. (2013). Comparison of flow number, dynamic modulus, and repeated load tests for evaluation of HMA permanent deformation. *Construction and Building Materials*, 44 (7), 391–398 (2013).
- Zhou, F. (2017). *Development of an IDEAL Cracking Test for Asphalt Mix Design and QC/QA*. The Association of Asphalt Pavement Technologists, 86, 549-578.
- Zhou, F. Steger, R. & Mogawer, W. (2021). Development of a Coherent Framework for Balanced Mix Design and Production Quality Control and Quality Acceptance. *Construction and Building Materials*, Volume 28. <https://doi.org/10.1016/j.conbuildmat.2021.123020>



## Appendix A

### Group A – All Mixes

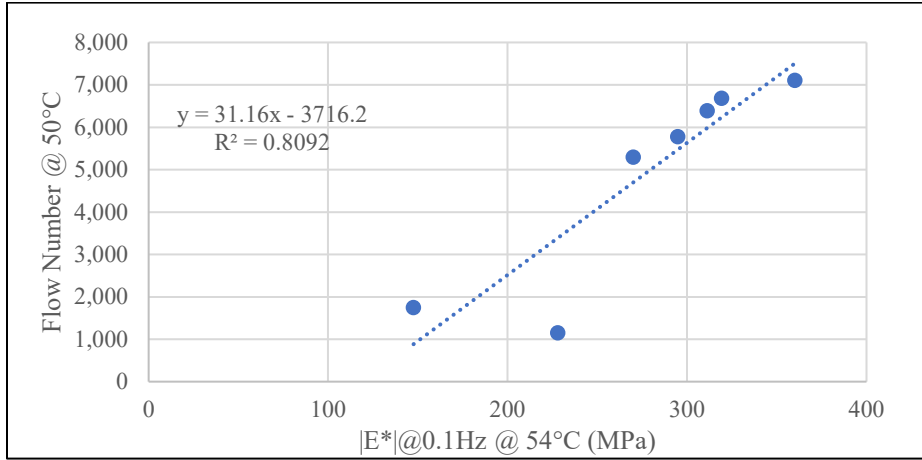


Figure A-1: Flow Number at 50°C vs. Dynamic Modulus  $|E^*|$  at 54.4°C at 0.1Hz for Group A

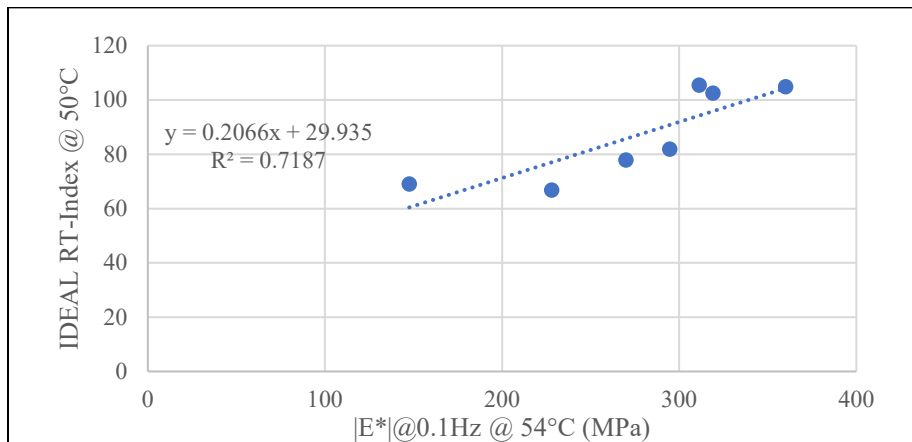


Figure A-2: IDEAL-RT Index at 50°C vs. Dynamic Modulus  $|E^*|$  at 54.4°C at 0.1Hz for Group A

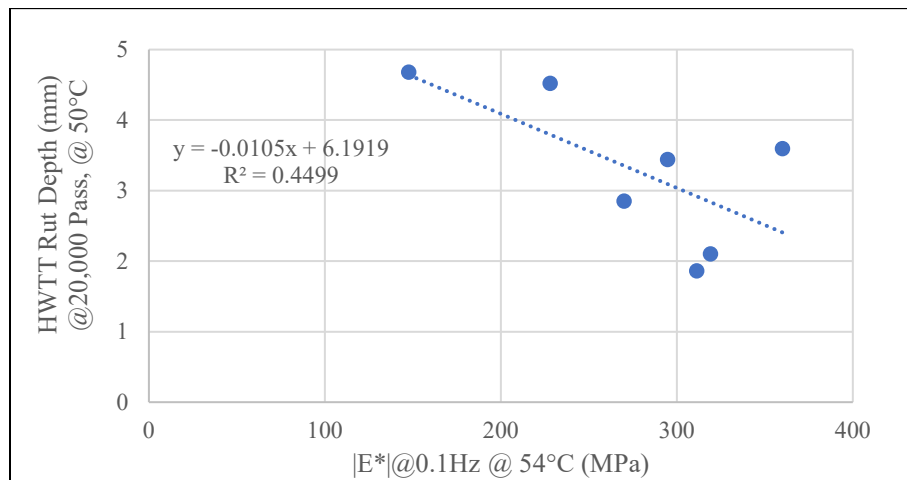


Figure A-3: HWTT at 20,000 pass at 50°C vs. Dynamic Modulus  $|E^*|$  at 54.4°C at 0.1Hz for Group A

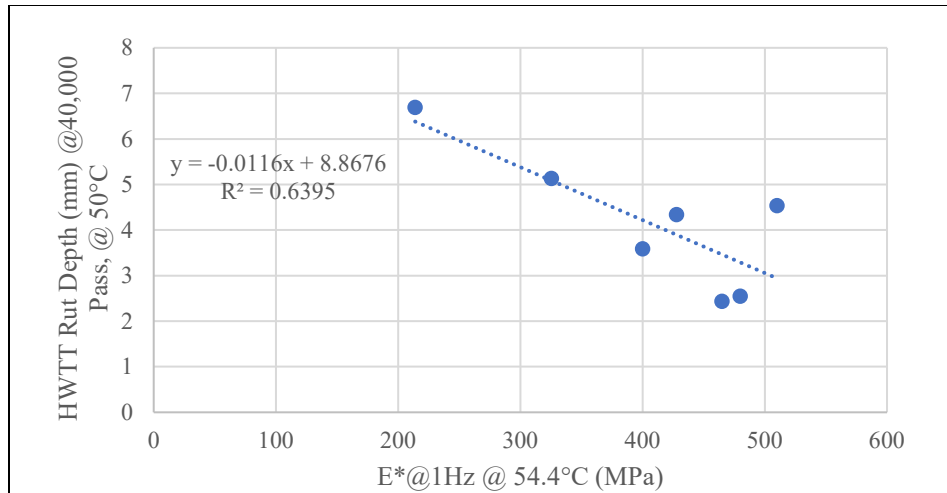


Figure A-4: HWTT at 40,000 pass at 50°C vs. Dynamic Modulus  $|E^*|$  at 54.4°C at 1Hz for Group A

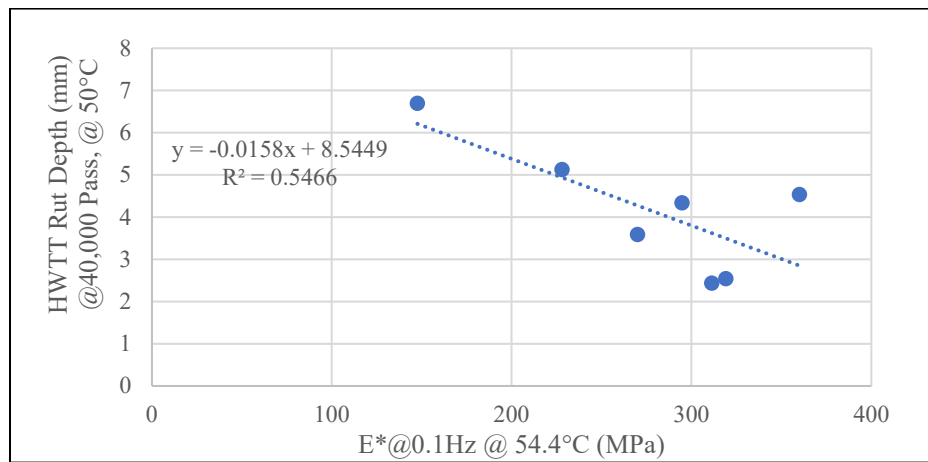


Figure A-5: HWTT at 40,000 pass at 50°C vs. Dynamic Modulus  $|E^*|$  at 54.4°C at 0.1Hz for Group A

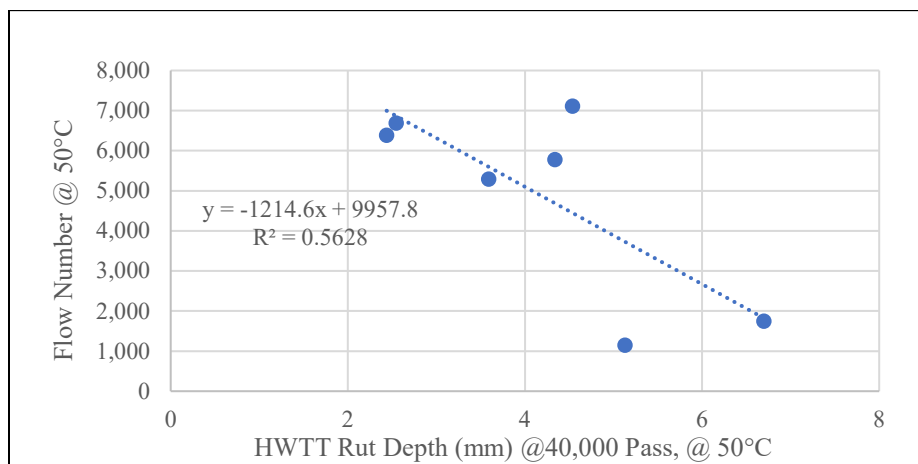


Figure A-6: FN at 50°C vs. HWTT at 40,000 pass at 50°C for Group A

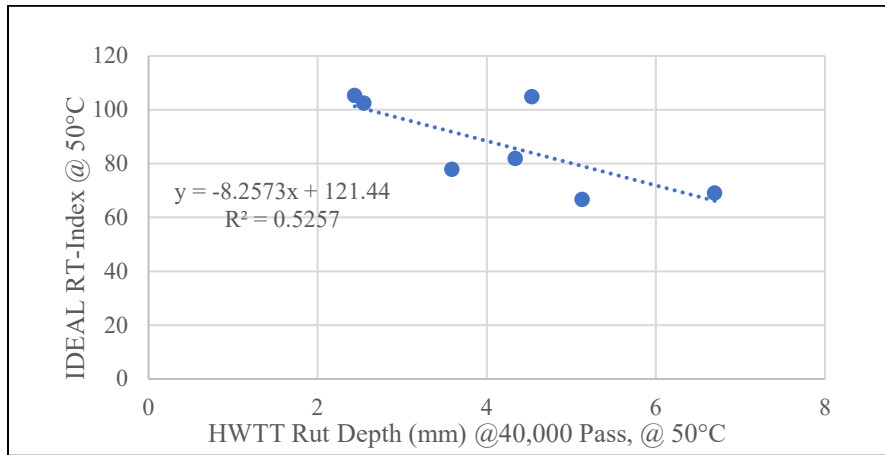


Figure A-7: IDEAL-RT Index at 50°C vs. HWTT at 40,000 pass at 50°C for Group A

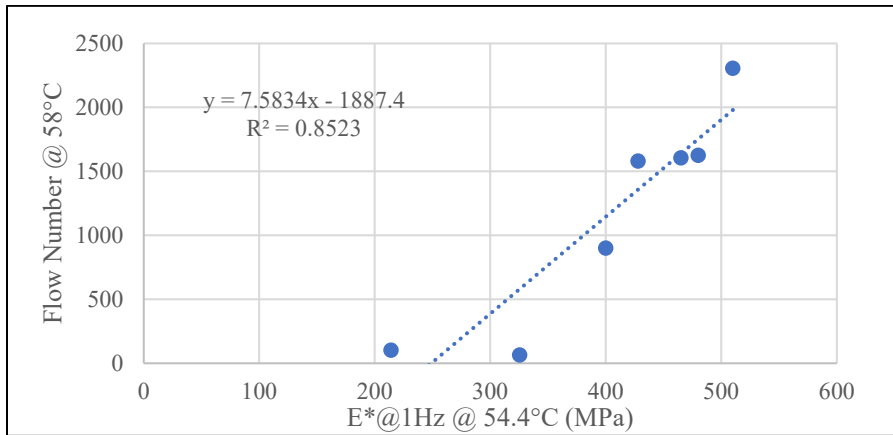


Figure A-8: Flow Number at 58°C vs. Dynamic Modulus |E\*| at 54.4°C at 1Hz for Group A

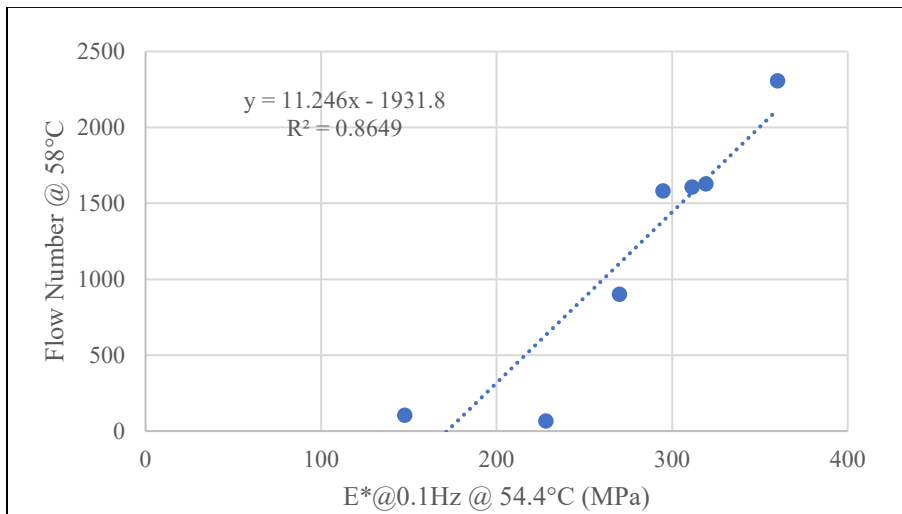


Figure A-9: Flow Number at 58°C vs. Dynamic Modulus |E\*| at 54.4°C at 0.1Hz for Group A

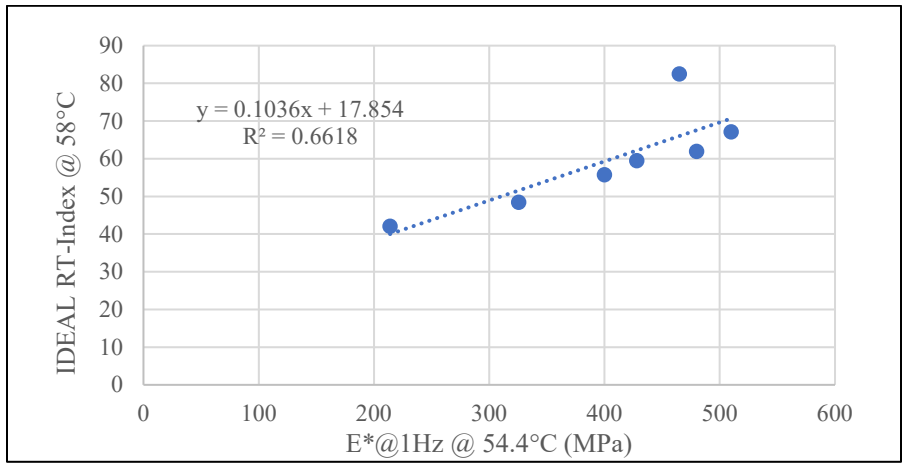


Figure A-10: IDEAL-RT Index at 58°C vs. Dynamic Modulus  $|E^*|$  at 54.4°C at 1Hz for Group A

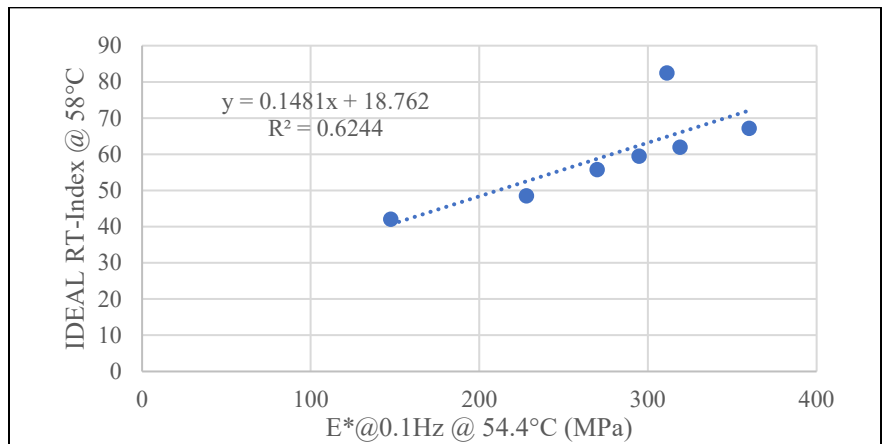


Figure A-11: IDEAL-RT Index at 58°C vs. Dynamic Modulus  $|E^*|$  at 54.4°C at 0.1Hz for Group A

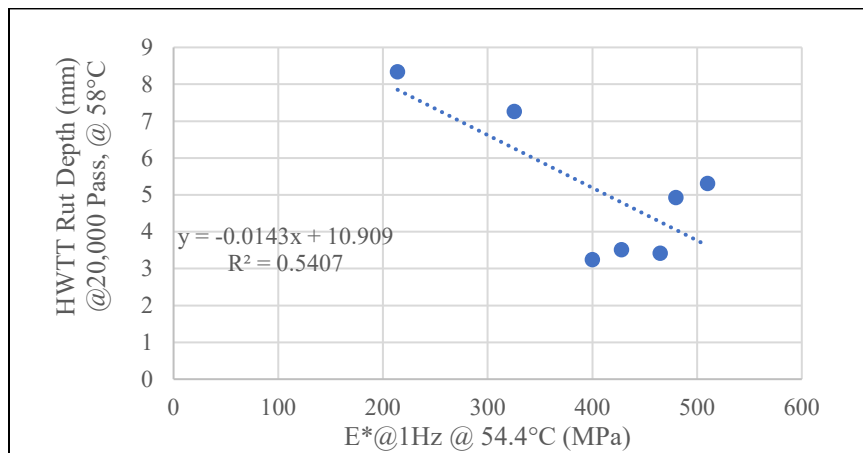


Figure A-12: HWTT at 20,000 pass at 58°C vs. Dynamic Modulus  $|E^*|$  at 54.4°C at 1Hz for Group A

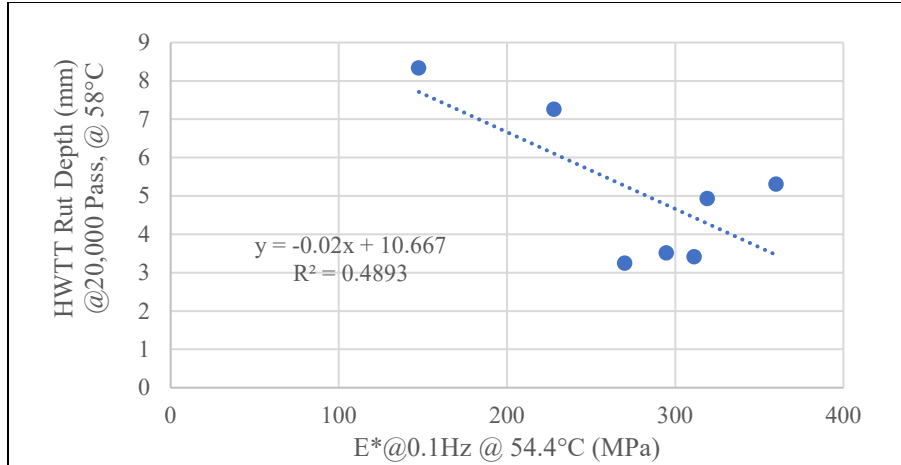


Figure A-13: HWTT at 20,000 pass at 58°C vs. Dynamic Modulus  $|E^*|$  at 54.4°C at 0.1Hz for Group A

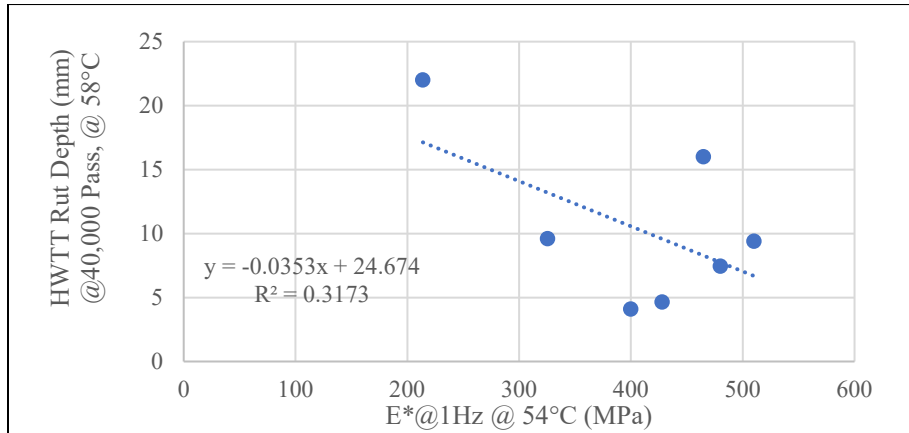


Figure A-14: HWTT at 40,000 pass at 58°C vs. Dynamic Modulus  $|E^*|$  at 54.4°C at 1Hz for Group A

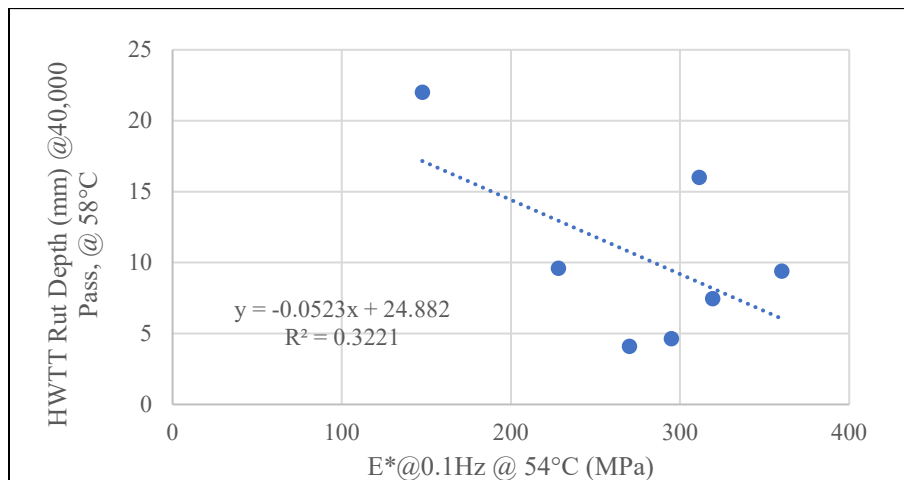


Figure A-15: HWTT at 40,000 pass at 58°C vs. Dynamic Modulus  $|E^*|$  at 54.4°C at 0.1Hz for Group A

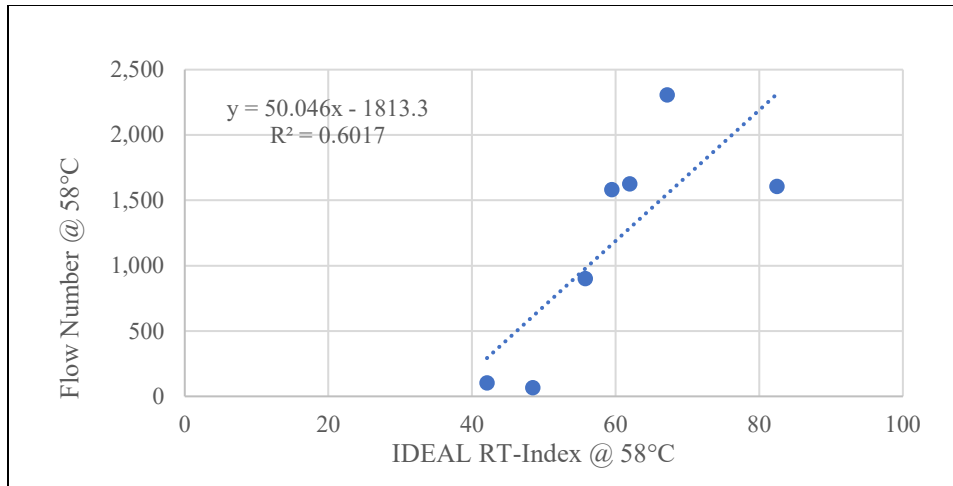


Figure A-16: FN at 58°C vs. IDEAL-RT Index at 58°C for Group A

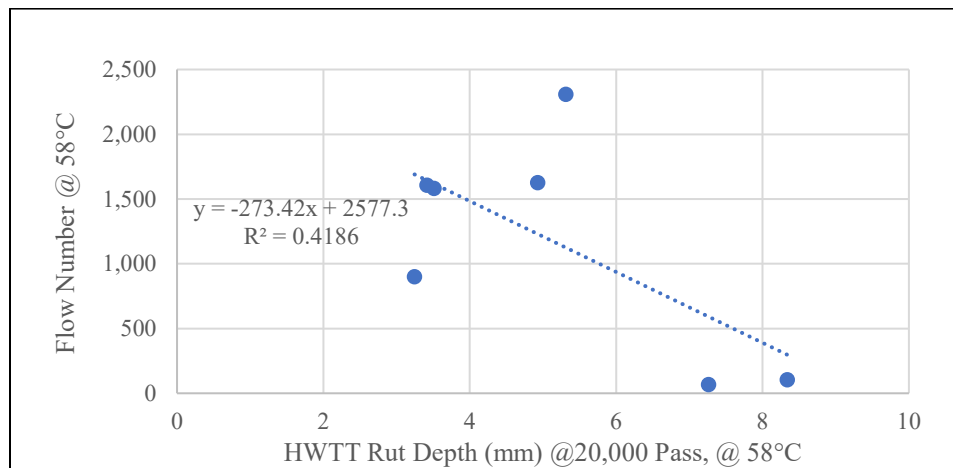


Figure A-17: FN at 58°C vs. HWTT at 20,000 pass at 58°C for Group A

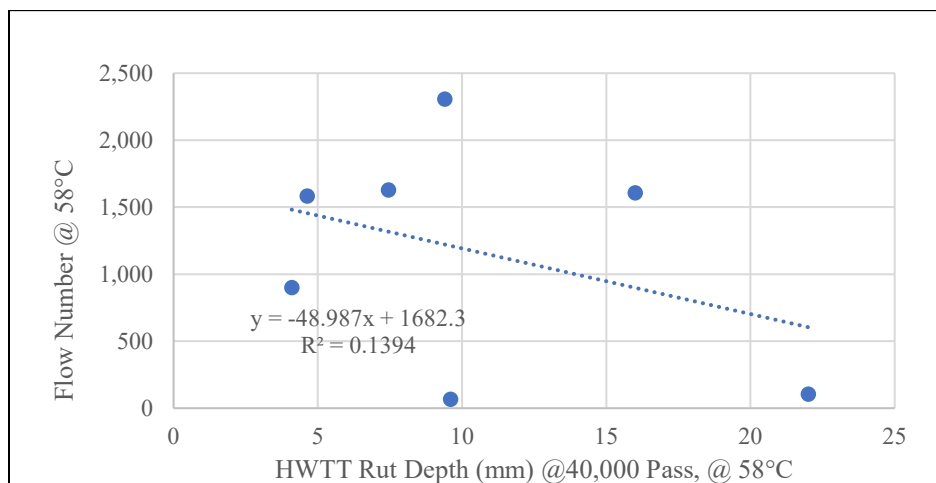


Figure A-18: FN at 58°C vs. HWTT at 40,000 pass at 58°C for Group A

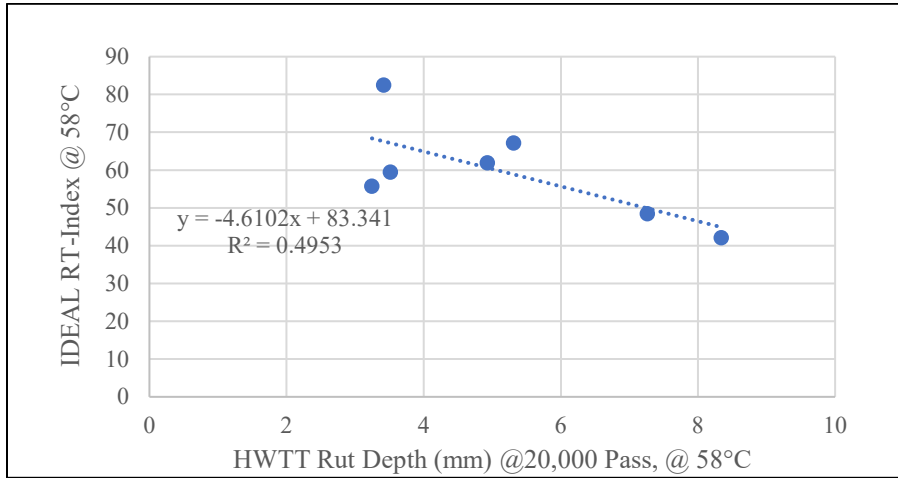


Figure A-19: IDEAL-RT Index at 58°C vs. HWTT at 20,000 pass at 58°C for Group A

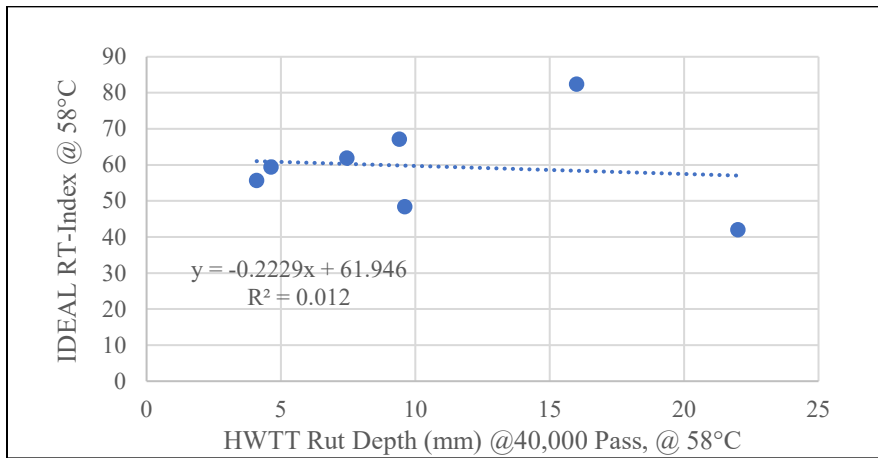


Figure A-20: IDEAL-RT Index at 58°C vs. HWTT at 40,000 pass at 58°C for Group A



### Group B – Only SMA Mixes

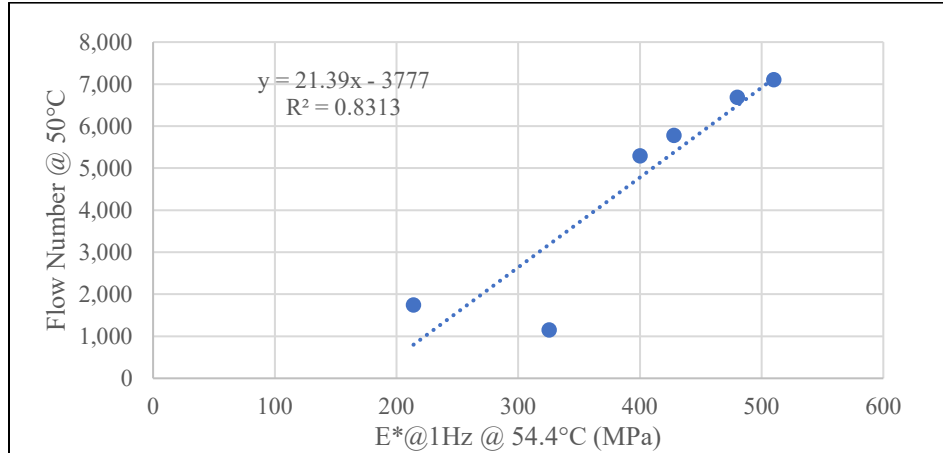


Figure B-1: Flow Number at 50°C vs. Dynamic Modulus  $|E^*|$  at 54.4°C at 1Hz for Group B

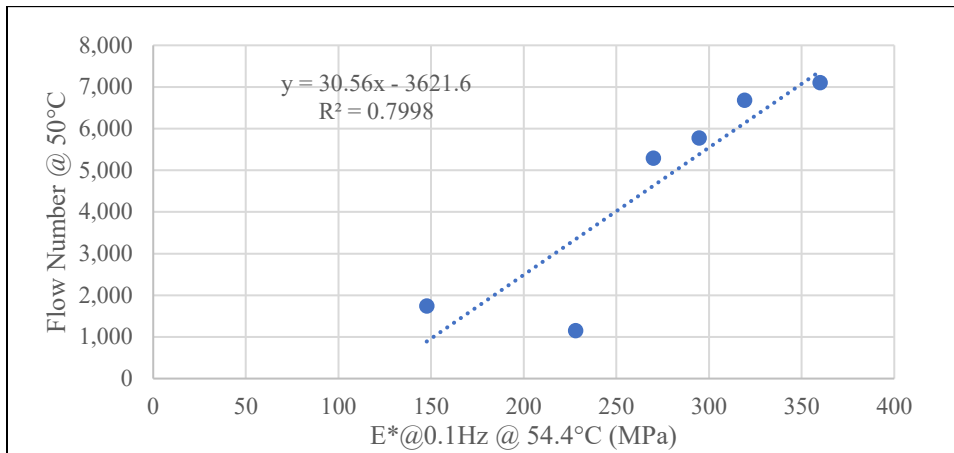


Figure B-2: Flow Number at 50°C vs. Dynamic Modulus  $|E^*|$  at 54.4°C at 0.1Hz for Group B

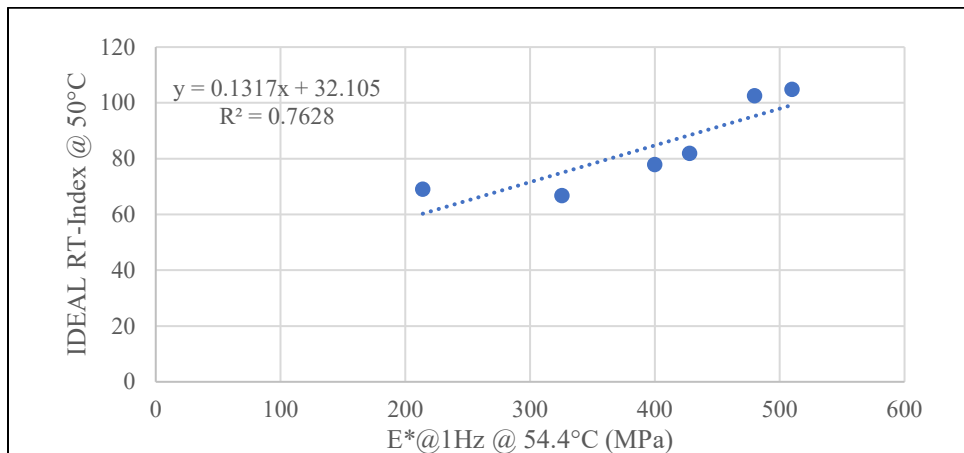


Figure B-3: IDEAL-RT Index at 50°C vs. Dynamic Modulus  $|E^*|$  at 54.4°C at 1Hz for Group B

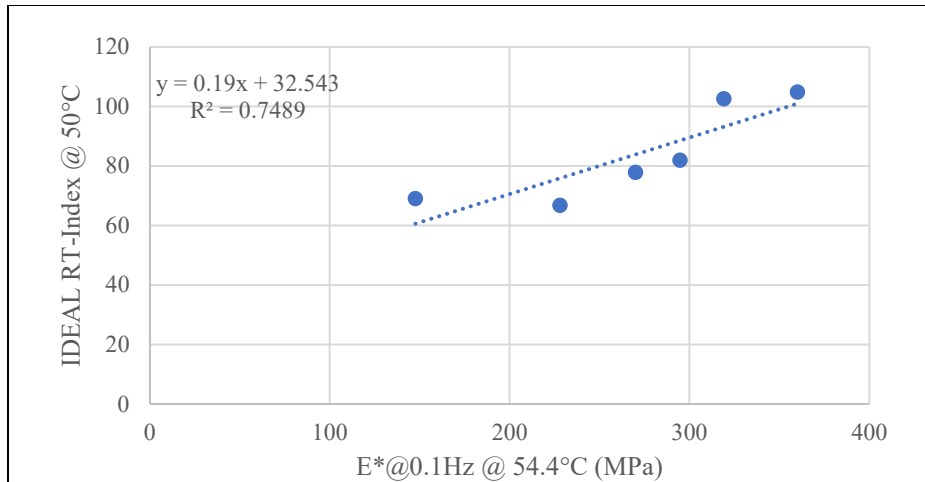


Figure B-4: IDEAL-RT Index at 50°C vs. Dynamic Modulus  $|E^*|$  at 54.4°C at 0.1Hz for Group B

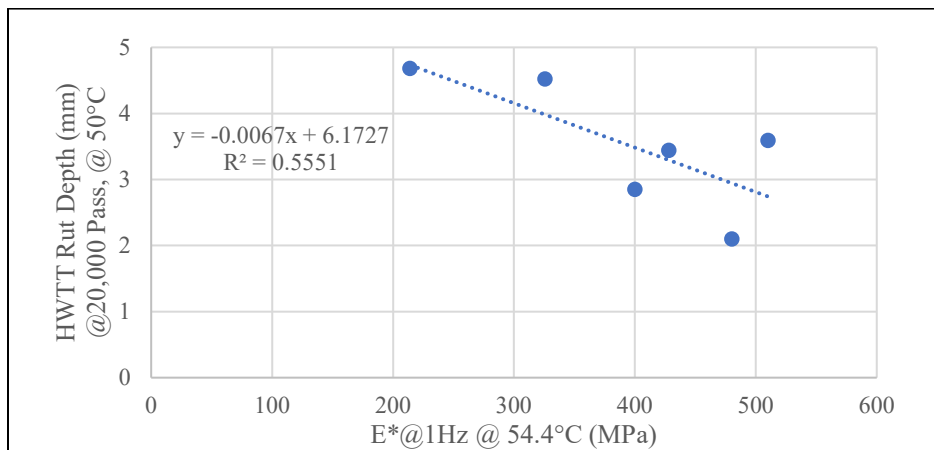


Figure B-5: HWTT at 20,000 pass at 50°C vs. Dynamic Modulus  $|E^*|$  at 54.4°C at 1Hz for Group B

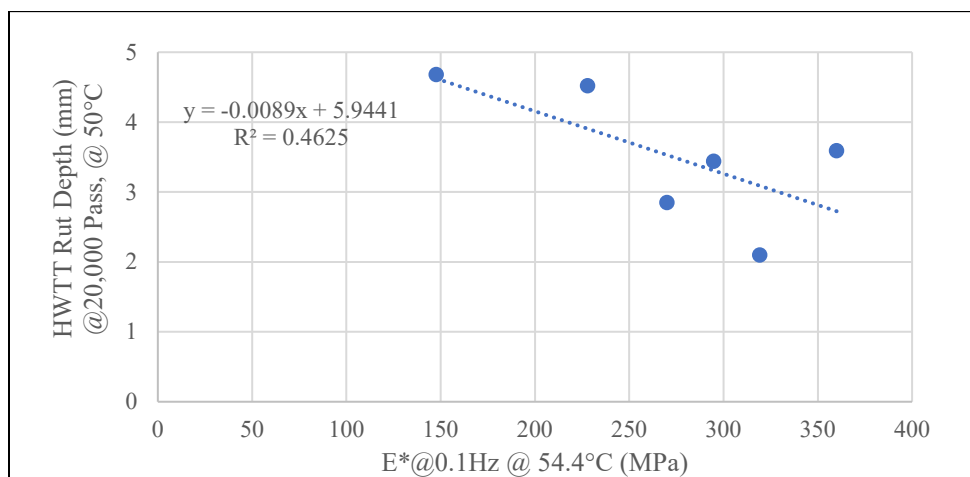


Figure B-6: HWTT at 20,000 pass at 50°C vs. Dynamic Modulus  $|E^*|$  at 54.4°C at 0.1Hz for Group B

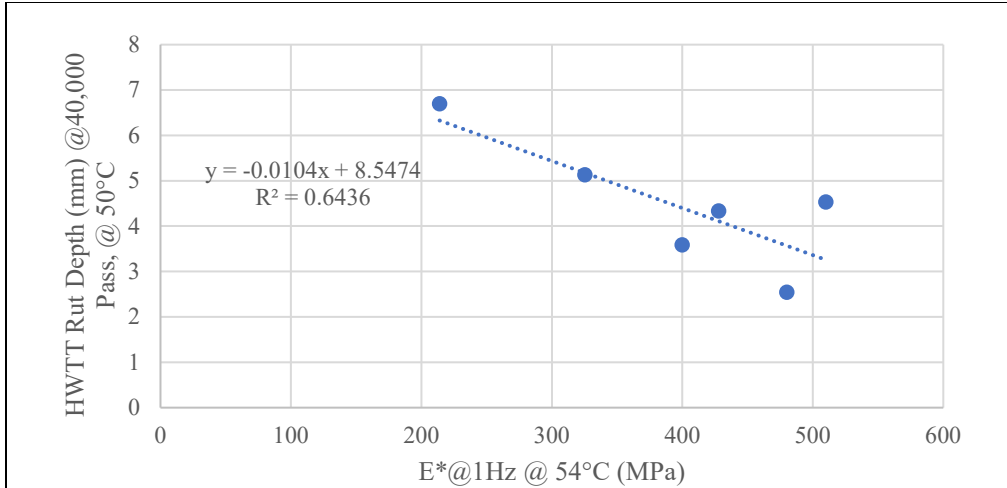


Figure B-7: HWTT at 40,000 pass at 50°C vs. Dynamic Modulus  $|E^*|$  at 54.4°C at 1Hz for Group B

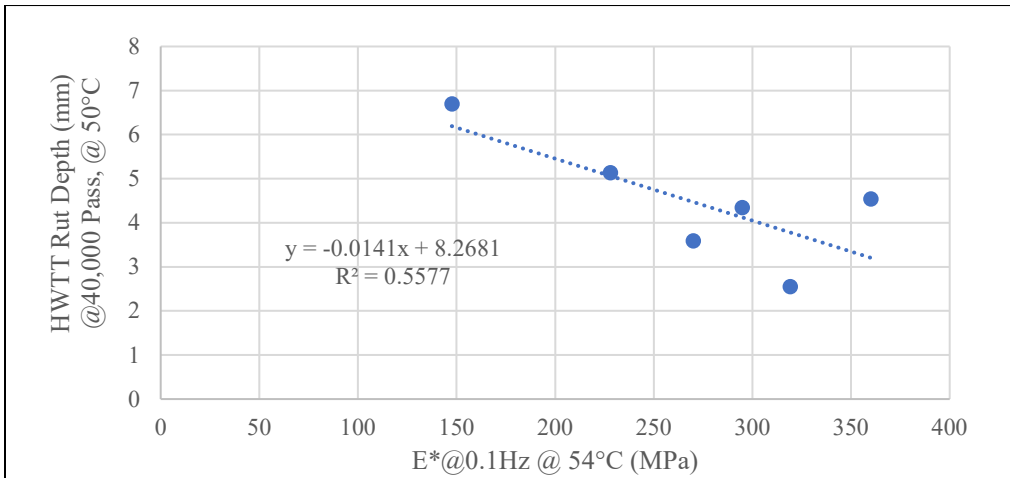


Figure B-8: HWTT at 40,000 pass at 50°C vs. Dynamic Modulus  $|E^*|$  at 54.4°C at 0.1Hz for Group B

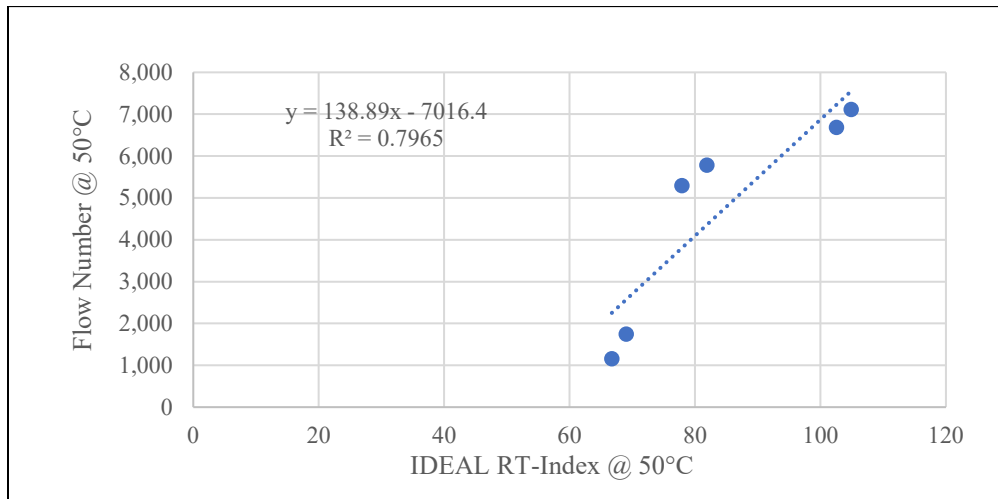


Figure B-9: Flow Number at 50°C vs. IDEAL-RT Index at 50°C for Group B

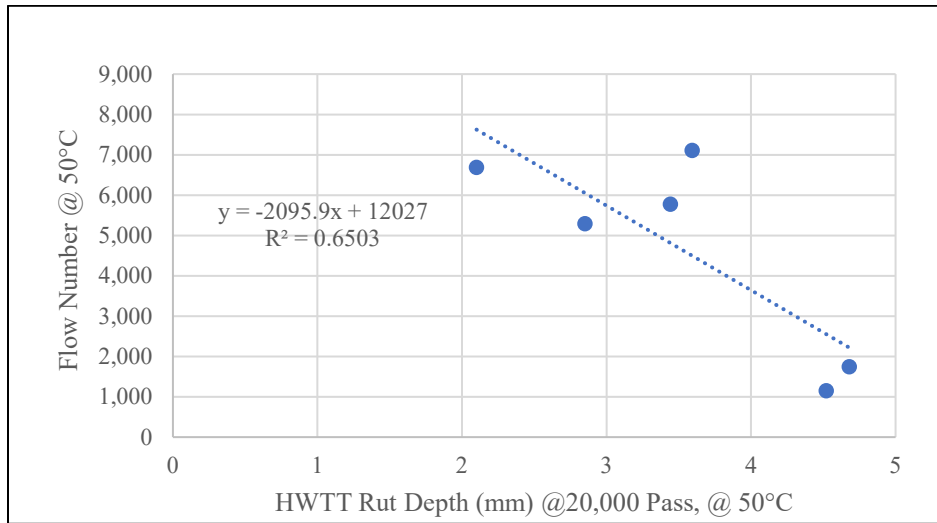


Figure B-10: FN at 50°C vs. HWTT at 20,000 pass at 50°C for Group B

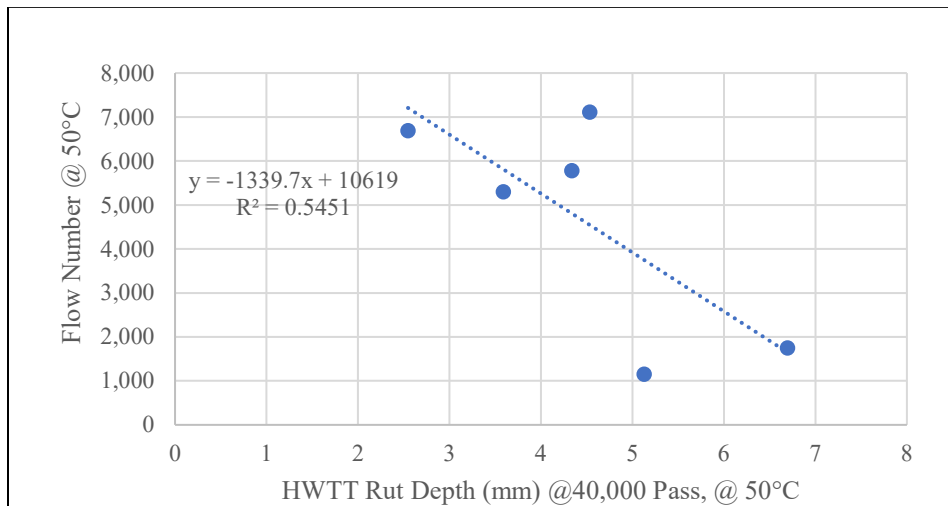


Figure B-11: FN at 50°C vs. HWTT at 40,000 pass at 50°C for Group B

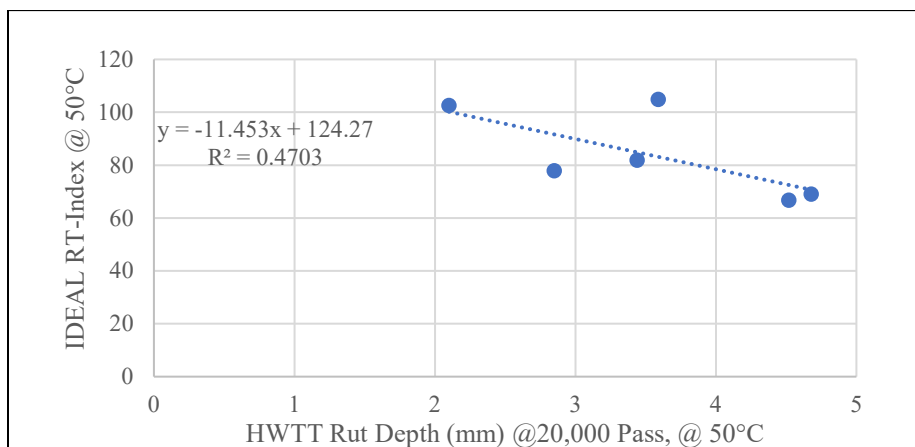


Figure B-12: IDEAL-RT Index at 50°C vs. HWTT at 20,000 pass at 50°C for Group B

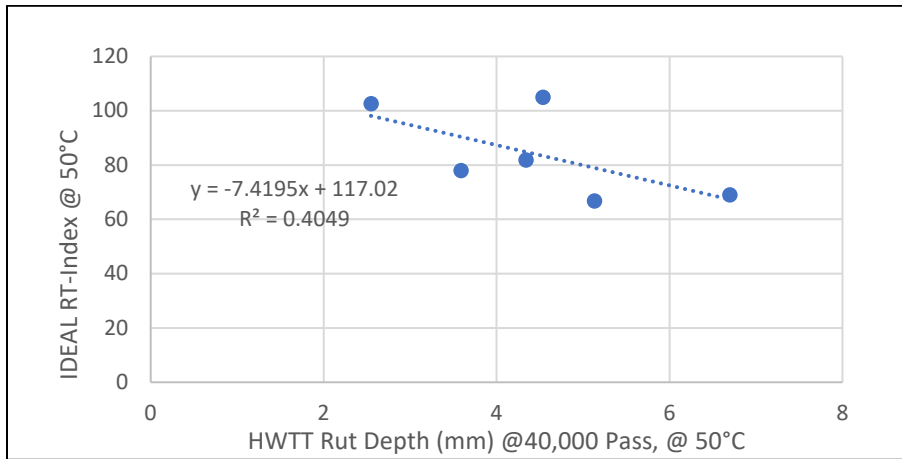


Figure B-13: IDEAL-RT Index at 50°C vs. HWTT at 40,000 pass at 50°C for Group B

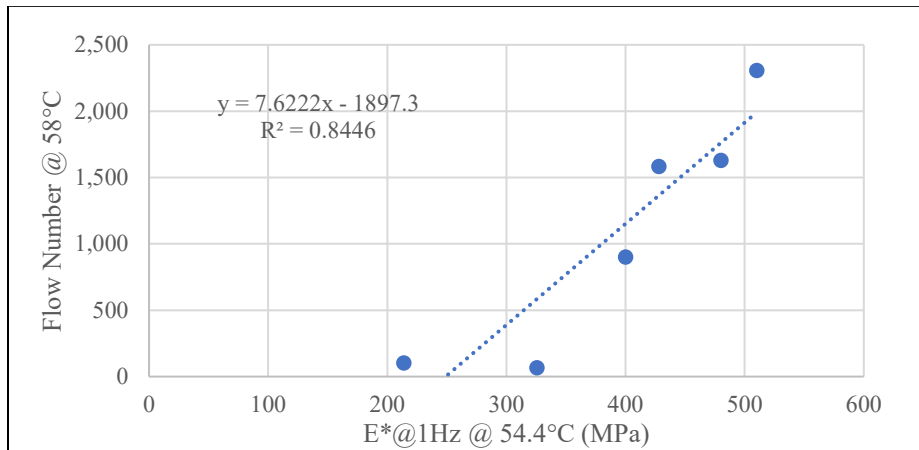


Figure B-14: Flow Number at 58°C vs. Dynamic Modulus  $|E^*|$  at 54.4°C at 1Hz for Group B

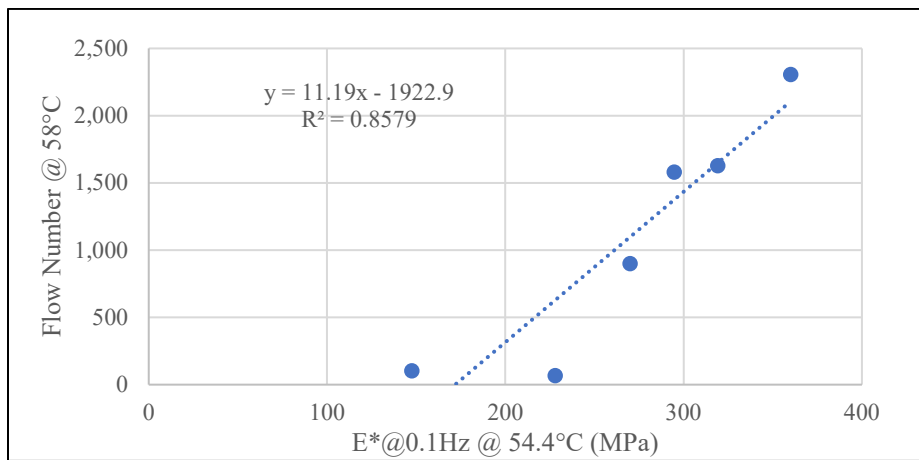


Figure B-15: Flow Number at 58°C vs. Dynamic Modulus  $|E^*|$  at 54.4°C at 0.1Hz for Group B

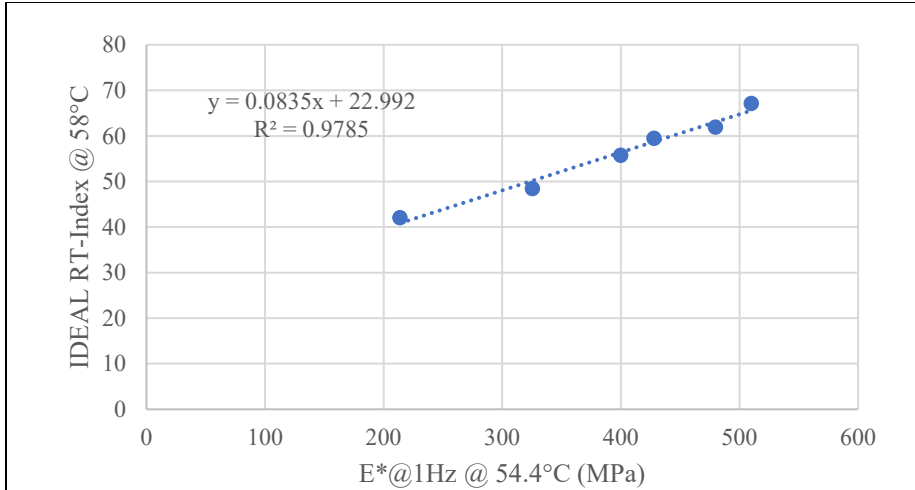


Figure B-16: IDEAL-RT Index at 58°C vs. Dynamic Modulus |E\*| at 54.4°C at 1Hz for Group B

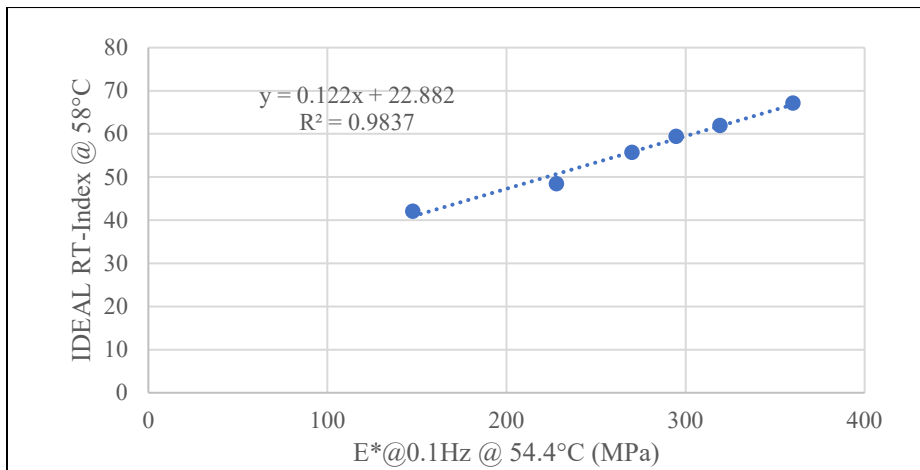


Figure B-17: IDEAL-RT Index at 58°C vs. Dynamic Modulus |E\*| at 54.4°C at 0.1Hz for Group B

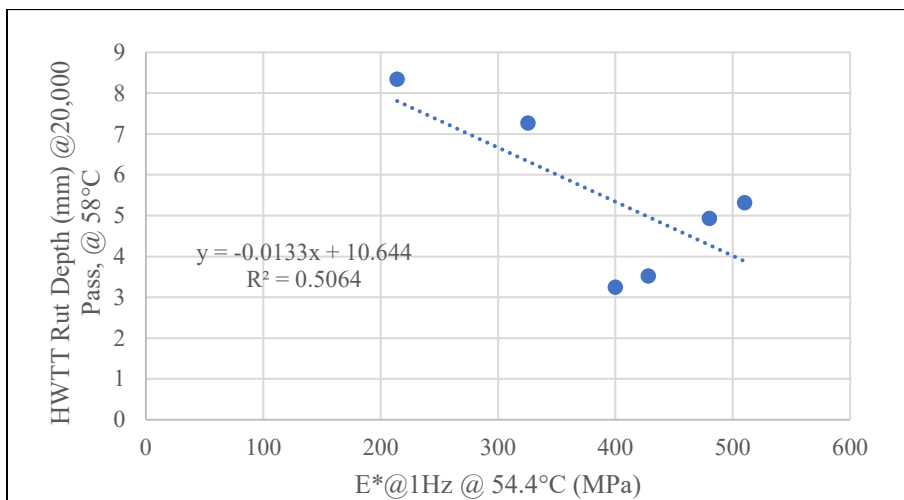


Figure B-18: HWTT at 20,000 pass at 58°C vs. Dynamic Modulus |E\*| at 54.4°C at 1Hz for Group B

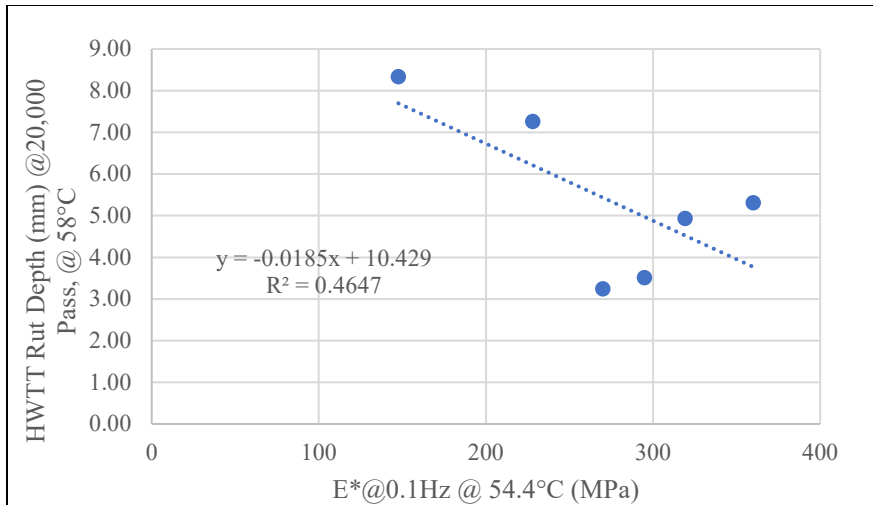


Figure B-19: HWTT at 20,000 pass at 58°C vs. Dynamic Modulus  $|E^*|$  at 54.4°C at 0.1Hz for Group B

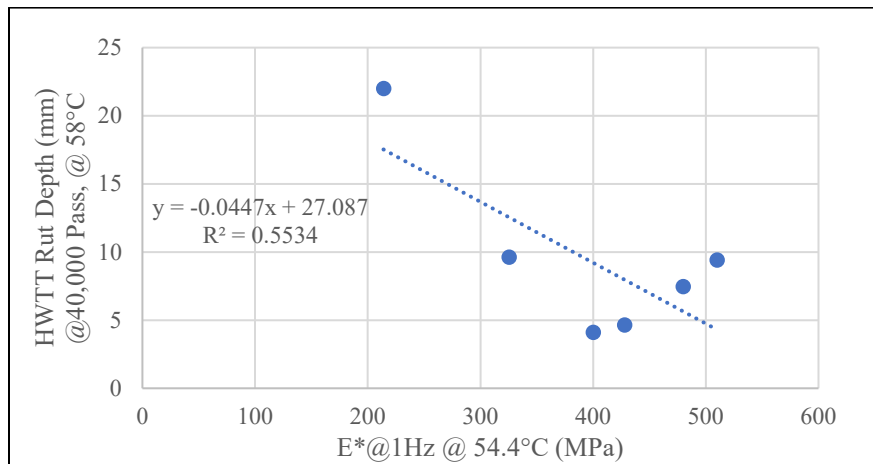


Figure B-20: HWTT at 40,000 pass at 58°C vs. Dynamic Modulus  $|E^*|$  at 54.4°C at 1Hz for Group B

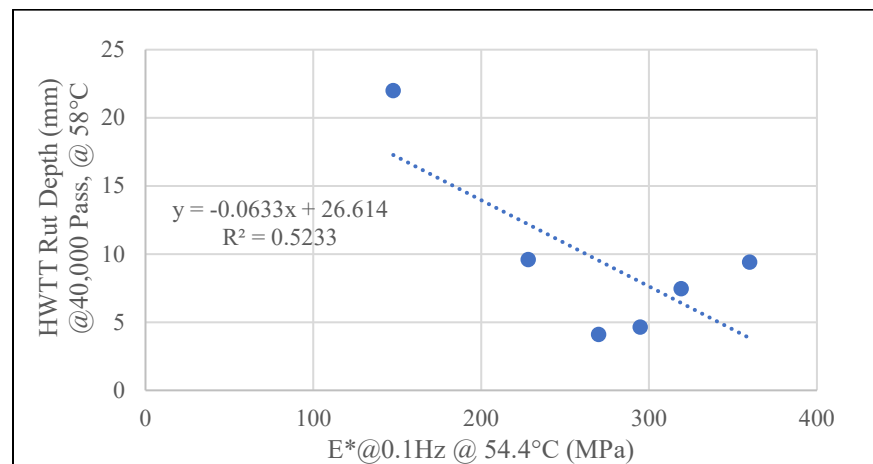


Figure B-21: HWTT at 40,000 pass at 58°C vs. Dynamic Modulus  $|E^*|$  at 54.4°C at 0.1Hz for Group B

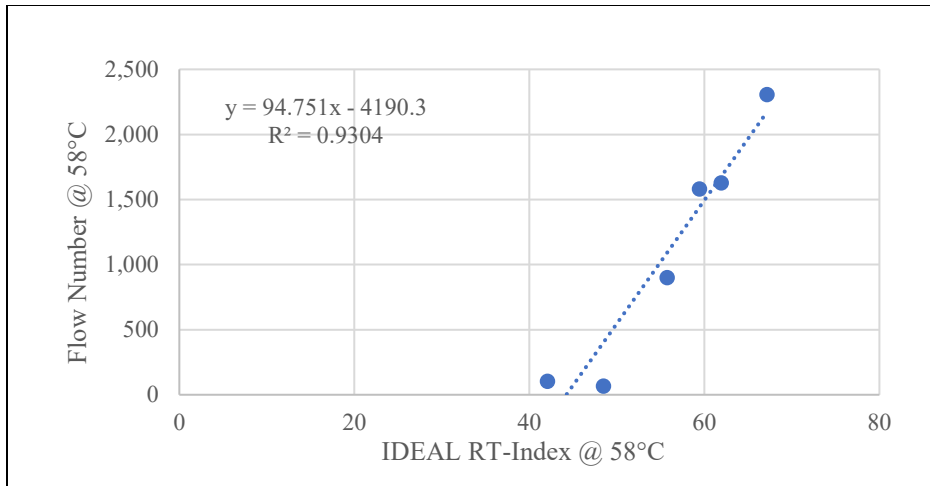


Figure B-22: FN at 58°C vs. HWTT at IDEAL-RT at 58°C for Group B

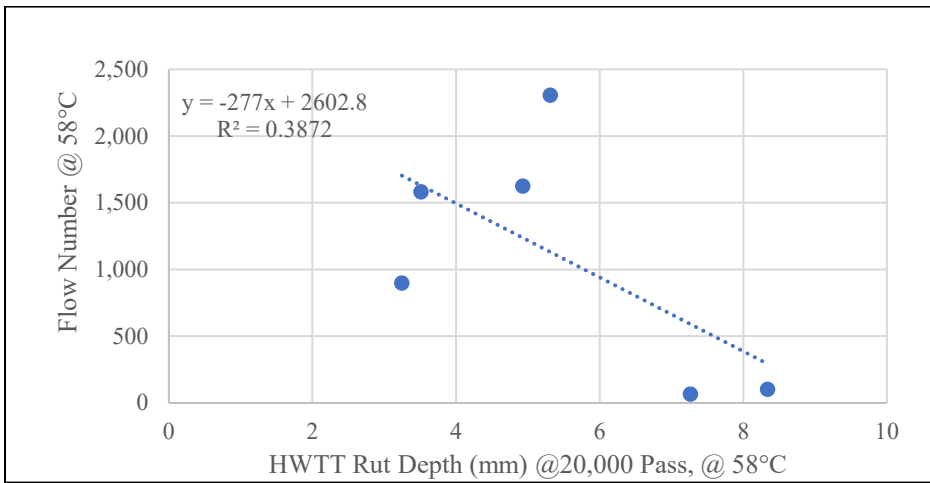


Figure B-23: FN at 58°C vs. HWTT at 20,000 pass at 58°C for Group B

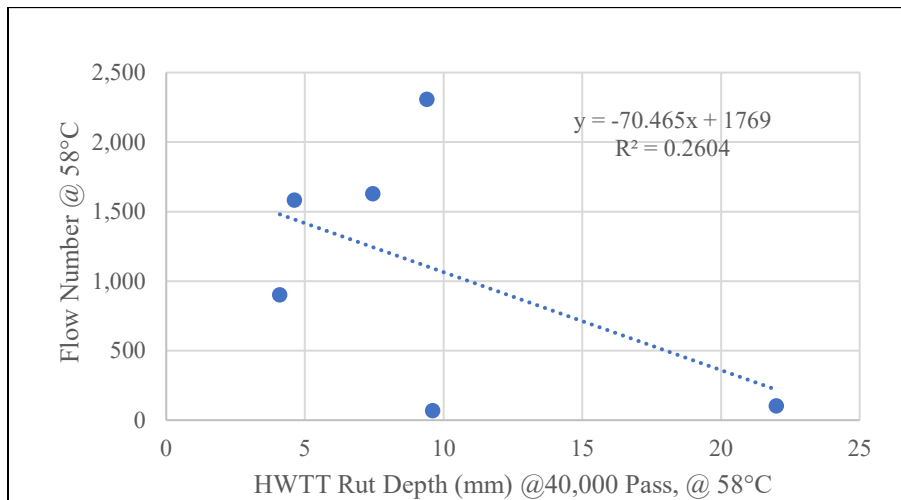


Figure B-24: FN at 58°C vs. HWTT at 40,000 pass at 58°C for Group B



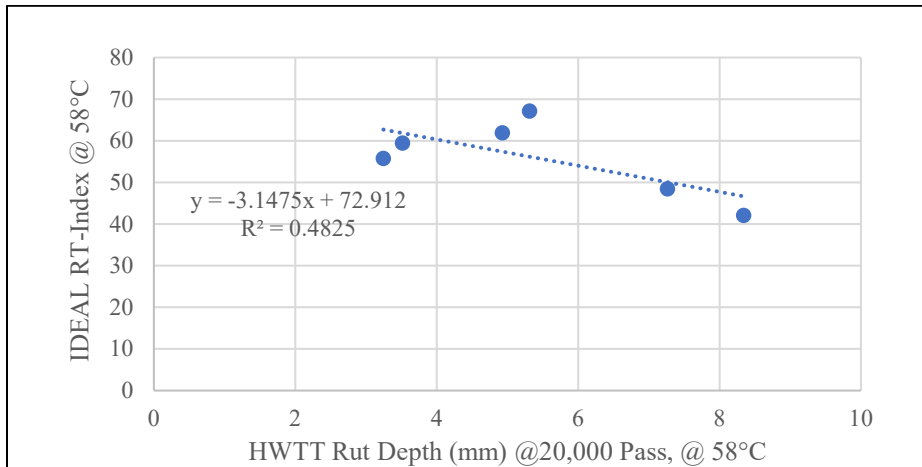


Figure B-25: IDEAL-RT Index at 58°C vs. HWTT at 20,000 pass at 58°C for Group B

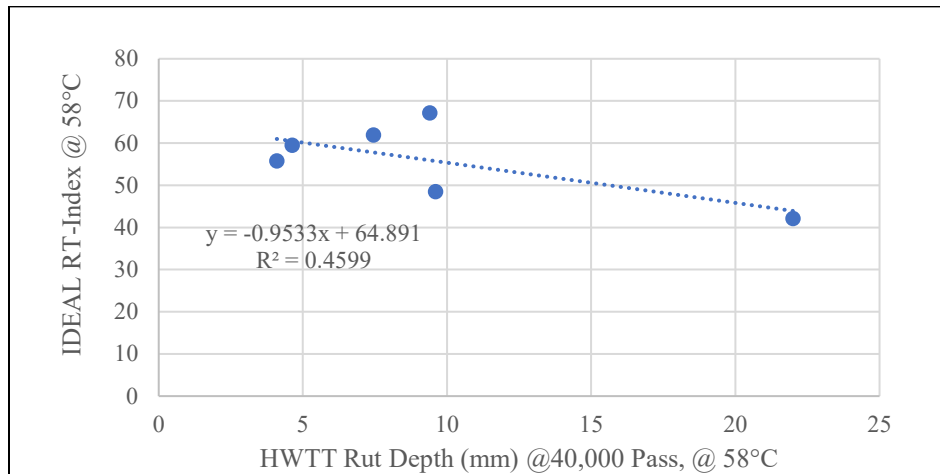


Figure B-26: IDEAL-RT Index at 58°C vs. HWTT at 40,000 pass at 58°C for Group B